

**CORRELATING AND PREDICTING
THERMAL CONDUCTIVITY
AND SELF-DIFFUSION
FROM ENTROPY SCALING
USING PCP-SAFT**

Von der Fakultät Energie-, Verfahrens- und Biotechnik
der Universität Stuttgart
zur Erlangung der Würde eines Doktors
der Ingenieurwissenschaft (Dr.-Ing.) genehmigte Abhandlung

Vorgelegt von
Madlen Hopp
geboren in Frankfurt (Oder)

Hauptberichter: Prof. Dr.-Ing. Joachim Groß
Mitberichter: Prof. Dr.-Ing. André Bardow

Tag der mündlichen Prüfung: 11.07.2022

Institut für Technische Thermodynamik und Thermische
Verfahrenstechnik der Universität Stuttgart

2022

Zusammenfassung

Zur vollständigen Beschreibung und Auslegung thermodynamischer Prozesse ist die Kenntnis der Stoffeigenschaften aller beteiligter Substanzen unbedingt notwendig. Während die Gleichgewichtseigenschaften bereits gut verstanden sind, fehlt es immer noch an einer handlichen Beschreibung der Transportgrößen.

Hier kann die Entropieskalierung Abhilfe schaffen, welche eine vielversprechend einfach erscheinende Methode zur Korrelation und Vorhersage von Transportgrößen realer Reinstoffe und Mischungen ist. In der Literatur ist die Entropieskalierung bereits als stabiles Konzept für die Viskosität η realer Stoffe bekannt, auch für stark nichtsphärische oder wasserstoffbrückenbildende Moleküle. In dieser Arbeit wird untersucht, ob die Methode auch auf Wärmeleitfähigkeit λ und Selbstdiffusion D^s von Reinstoffen Anwendung finden kann. In Übereinstimmung mit dem Ansatz von Y. Rosenfeld [Phys. Rev. A 1977, 15, 2545-2549], zeigt sich eine monovariablen Abhängigkeit von λ und D^s realer Stoffe von der residuellen Entropie, nachdem beide in geeigneter Weise dimensionslos gemacht wurden. In dieser Arbeit werden geeignete Referenzgrößen für beide Transporteigenschaften vorgeschlagen, um die Transportkoeffizienten von Reinstoffen mit Hilfe der *Perturbed-Chain Polar Statistical Associating Fluid Theory (PCP-SAFT)* Zustandsgleichung zu berechnen. Wir zeigen gutes Korrelationsverhalten für Wasser und mehr als 130 organische Reinstoffe diverser chemischer Familien, darunter lineare und verzweigte Alkane, Alkene, Aldehyde, Aromaten, Ether, Ester, Ketone, Alkohole und Säuren. Beide Modelle (λ und D^s) zeigen eine zufriedenstellende Robustheit gegenüber Extrapolation zu Zustandspunkten mit einem größeren Abstand zu experimentell vorhandenen Daten.

Darauf aufbauend entwickelten wir einen gruppenbeitragsbasierten Ansatz zur prädiktiven Berechnung von Wärmeleitfähigkeiten. Die residuelle Entropie stammt hier aus der gruppenbeitragsbasierten PCP-SAFT Zustandsgleichung. Der entwickelte Ansatz ist für alle fluiden Zustände organischer Substanzen in weiten Temperatur- und Druckbereichen geeignet. Wir schlagen Parameter für 29 chemische Gruppen vor, für die experimentelle Daten zu 231 Stoffen mit mehr als 50.000 Datenpunkte ausgewertet wurden.

Abstract

For a complete description and design of thermodynamic processes, knowledge of the properties of all substances involved is absolutely necessary. While the equilibrium properties are already well understood, there is still a lack of a handy description of the transport properties.

Entropy scaling is an intriguingly simple approach for correlating and predicting transport properties of real substances and mixtures. As convincingly documented in the literature entropy scaling is indeed a firm concept for the shear viscosity of real substances, including hydrogen-bonding species and strongly non-spherical species and for mixtures. In this thesis, we investigate whether the entropy scaling approach is applicable for the thermal conductivity as well as the self-diffusion coefficients of pure substances. In accordance with the entropy scaling approach proposed by Y. Rosenfeld [Phys. Rev. A 1977, 15, 2545-2549], we observe that the thermal conductivity λ and the self-diffusion coefficient D^s of real substances, once made dimensionless with an appropriate reference expression, only depend on residual entropy. We propose suitable reference expressions for both properties (λ and D^s), to calculate the coefficients of pure substances from entropy scaling using the Perturbed-Chain Polar Statistical Associating Fluid Theory (PCP-SAFT) equation of state. Good entropy scaling behavior is found for the entire fluid region for water and more than 130 organic substances from various chemical families: linear and branched alkanes, alkenes, aldehydes, aromatics, ethers, esters, ketones, alcohols and acids. Models for both, thermal conductivity and self diffusion coefficient, show satisfying robustness for extrapolating the coefficients to conditions rather distant from state points where experimental data is available.

Additionally, I derived a predictive group-contribution method for thermal conductivity based on entropy scaling. The excess entropy for this approach is calculated using the group-contribution PCP-SAFT equation of state. The model is applicable for gaseous phases and for liquid-phase conditions covering wide ranges of temperature and pressure. By considering 231 substances with more than 50,000 experimental data points I propose parameters of 29 chemical groups, resulting in 6.17% average absolute deviation for all considered data points.

Journal publications

This thesis led to the following publications:

- Chapter 2: Hopp, Gross: Thermal Conductivity of Real Substances from Excess Entropy Scaling Using PCP-SAFT, *Industrial & Engineering Chemistry Research*, 2017, 56, 15, 4527–4538, DOI:10.1021/acs.iecr.6b04289
- Chapter 3: Hopp, Mele, Gross: Self-Diffusion Coefficients from Entropy Scaling Using the PCP-SAFT Equation of State, *Industrial & Engineering Chemistry Research*, 2018, 57, 38, 12942–12950, DOI:10.1021/acs.iecr.8b02406
- Chapter 4: Hopp, Mele, Hellmann, Gross: Thermal Conductivity via Entropy Scaling: An Approach That Captures the Effect of Intramolecular Degrees of Freedom, *Industrial & Engineering Chemistry Research*, 2019, 58, 39, 18432–18438, DOI:10.1021/acs.iecr.9b03998
- Chapter 5: Hopp, Gross: Thermal Conductivity from Entropy Scaling: A Group-Contribution Method, *Industrial & Engineering Chemistry Research*, 2019, 58, 44, 20441–20449, DOI:10.1021/acs.iecr.9b04289

The chapters 2 to 5 present literal quotes of the published work. The Supporting Informations to the single chapters are presented in the Appendix of this thesis.

Contents

Zusammenfassung	iii
Abstract	v
Journal publications	vii
1 Introduction	1
1.1 State of the art in transport coefficient modeling	2
1.2 Outline	5
Bibliography	6
2 Thermal Conductivity of Real Substances from Excess Entropy Scaling Using PCP-SAFT	15
2.1 Rosenfeld's Entropy Scaling	15
2.2 Evaluation of Reference Thermal Conductivities	17
2.2.1 Chapman Enskog	17
2.2.2 Chapman Enskog with Eucken correction	18
2.2.3 LTST Approach	19
2.3 A new approach for the reference thermal conductivity	21
2.3.1 A new expression for Ideal Gas Limit	22
2.3.2 Correlation Function for Thermal Conductivity	24
2.4 Results and Discussion	27
2.4.1 Data Analysis	27
2.4.2 Substances with experimental data of λ in gas phase . .	28
2.4.3 Comprehensive correlation of pure substance thermal conductivity	31
2.4.4 Robustness to Extrapolation	32
2.5 Conclusions	33
2.5.1 Supporting Information	34
Appendix	34
Bibliography	36
3 Self-Diffusion Coefficients from Entropy Scaling using the PCP- SAFT equation of state	43
3.1 Entropy Scaling and Reference Self-Diffusion Coefficients	44
3.2 Ansatz Function for Correlating Self-Diffusion Coefficients . . .	47
3.2.1 Robustness of Parameterizing the Entropy Scaling Model	49
3.2.2 Subcooled Liquids	51
3.3 Results and Discussion	52
	ix

3.4	Conclusion	56
	Bibliography	58
4	Thermal Conductivity via Entropy Scaling: An Approach that Captures the Effect of Intramolecular Degrees of Freedom	61
4.1	Introduction	62
4.2	Entropy Scaling	62
4.3	Improved Reference Thermal Conductivity	65
4.4	Results	67
4.4.1	Fluids with a Low Number of Intramolecular Degrees of Freedom: Simple Fluids	67
4.4.2	Fluids with Higher Number of Intramolecular Degrees of Freedom	68
4.5	Conclusion	69
4.5.1	Supporting Information	69
	Bibliography	69
5	Thermal Conductivity from Entropy Scaling: A Group-Contribution Method	81
5.1	Introduction	81
5.2	Theoretical Background	83
5.2.1	Group-Contribution EoS	83
5.2.2	Transport Properties from Entropy Scaling	84
5.2.3	Group-Contribution Model for Thermal Conductivity	87
5.3	Results and Discussion	89
5.3.1	Model assessment	90
5.3.2	Transferability of group-contribution parameters	93
5.3.3	Overall correlation results	96
5.4	Conclusion	96
	Appendices	98
5.A	Mixing rules	98
5.B	Multi-functional alcohols	99
	Bibliography	100
6	Thermal Conductivity from Entropy Scaling: Mixtures	109
6.1	Introduction	109
6.2	Theoretical Background	110
6.2.1	Approach A - Trivial Mixing Rules	111
6.2.2	Approach B - Mixture Reference	112
6.2.3	Approach B.1 - Mixing Rules for Pure Polynomials	115
6.2.4	Approach B.2 - Mix the Parameters	115
6.2.5	Combinational Possibilities	116

6.3	Results and Discussion	117
6.3.1	Definition of Datasets	117
6.3.2	First Elimination-round for Candidate Models	118
6.3.3	Further investigation of Approach B.2	122
6.4	Conclusion	130
	Bibliography	130
7	Conclusions	133
	Appendices	135
A	Supporting Information for Chapter 2: Thermal Conductivity of real Substances from Excess Entropy Scaling using PCP-SAFT	137
A.1	PCP-SAFT Parameters	138
A.2	Parameters (<i>A-D</i>) and Absolute Average Deviations	145
A.2.1	proposed scaling approach $\lambda_{\alpha, scale}^{ref}$	146
A.2.2	α -Eucken approach $\lambda_{\alpha, Eu}^{ref}$	153
A.2.3	α -LTST approach $\lambda_{\alpha, LTST}^{ref}$	159
A.2.4	α -CCE approach $\lambda_{\alpha, CCE}^{ref}$	165
A.3	Full Legend of Fig.2.6	171
A.4	Entropy Scaling of Water	171
A.5	Entropy Scaling of Lennard-Jones Chains	173
	Bibliography	175
B	Supporting Information for Chapter 3: Self-Diffusion Coefficients from Entropy Scaling using the PCP-SAFT equation of state	177
B.1	PCP-SAFT Parameters	178
B.2	Correlation Parameters (<i>a-c</i>) and Absolute Average Deviations	184
B.3	Diagram for reference self-diffusion coefficients	192
	Bibliography	193
C	Supporting Information for Chapter 4: Thermal Conductivity via Entropy Scaling: An Approach that Captures the Effect of Intramolecular Degrees of Freedom	201
C.1	Comparison of Averaged Absolute Deviations	202
C.2	Correlation Parameters (<i>A-D</i>) using λ^{CE}	208
C.3	Correlation Parameters (<i>A-D</i>) using λ^{ref, ρ^D}	208
C.4	Correlation Parameters (<i>A-D</i>) using $\lambda^{ref, \alpha}$	212
D	Supporting Information for Chapter 5: Thermal Conductivity from Entropy Scaling: A Group-Contribution Method	215
D.1	Definition of AAD	215
D.2	resulting gc parameters $A_{\alpha} - C_{\alpha}$	215
D.3	Full Legend of Fig. 5.1	218

D.4	Additions to Fig. 5.3	219
D.5	Components of Fig. 5.6	220
D.6	Substances with different functional groups	222
D.7	Averaged Absolute Deviations	223
D.8	Parameters (<i>A-D</i>) for individual Entropy-Scaling with PCP- SAFT	241
D.9	PCP-SAFT Parameters	245
D.10	Group Decomposition	251

1 Introduction

In process engineering, knowledge about transport of mass, momentum and energy is essential to design process equipment and to predict and optimize processes. As an industry with high energy and material costs, there is a drive to continuous optimization for reducing energy conversion and for maximizing yield and selectivity. It is costly to experimentally optimize the processes because of the high number of degrees of freedom, e.g. in process conditions. In the last decades, numerical investigation of processes and design of process equipment gained importance and nowadays are equally important in the development and optimization process in process engineering [1].

The basis of numerical investigation of processes are the balances of mass, momentum and energy. They are used to investigate the transport of mass, momentum and energy. Within these balances, it is required to use constitutive equations, e.g. linear relations between fluxes and driving forces. The linear driving force approaches consist of a conduction coefficient and a linear driving force [2]. The coefficients of conduction or transport coefficients, respectively, are the diffusion coefficients, shear viscosity and thermal conductivity. The corresponding linear driving forces are the gradients of chemical potential, velocity and temperature. For numerical or analytic investigation of transport, it is fundamental to know the transport coefficients to understand and to model relevant transport processes, e.g. heat conduction in separation units or chemical reactors.

The transport coefficient viscosity is associated with the transport of momentum. The viscosity represents the effective conduction of the dissipative part of momentum transport [3]. The macroscopic effect of the viscosity is present in many examples in process engineering, e.g. where pumps with different power are needed to transport water, crude oil or a polymer melt through a pipe.

Thermal conductivity is the transport coefficient corresponding to the transport of energy, describing the ability of matter to transport thermal energy ("heat") along a negative temperature gradient. In process engineering, the size of heat exchange areas strongly depend on this property.

In the transport of matter, the diffusion coefficient is the corresponding transport coefficient [4]. In process engineering, the diffusive behavior of a substance must be known to design the interior of columns to create the necessary amount of contacting surface e.g. in an absorption process. Three different types of diffusion coefficients are usually distinguished: the self-diffusion coefficient, the diffusion coefficient in infinitely diluted solutions and the binary diffusion coefficient. While the first two listed diffusion coefficients origin

from a stochastic motion of a molecule in a fluid system, the binary transport diffusion coefficient is driven by gradients in the chemical potential. The self-diffusion coefficient describes the stochastic motion of a molecule surrounded by molecules of the same substance without an external driving force. It can be measured as the time correlation of the velocity of the molecule of interest. The diffusion coefficient in infinitely diluted solutions describes the stochastic motion of a single molecule of substance A in a volume consisting of molecules of substance B without external driving force. The diffusion coefficients at infinite dilution represent the limits of the binary diffusion coefficient. The self-diffusion coefficient of a pure substance can be used to estimate binary (transport) diffusion coefficients [5–9] and is therefore of major practical importance.

1.1 State of the art in transport coefficient modeling

To reduce duplication, this section quotes and combines the introductions of: M. Hopp, J. Gross: Thermal Conductivity of Real Substances from Excess Entropy Scaling Using PCP-SAFT, Ind.Eng.Chem.Res., 2017, 56, 15, 4527–4538.

M. Hopp, J. Mele, J. Gross: Self-Diffusion Coefficients from Entropy Scaling Using the PCP-SAFT Equation of State, Ind.Eng.Chem.Res., 2018, 57, 38, 12942–12950.

There[†] are several routes for calculating the thermal conductivity λ of real substances. Popular approaches for correlating or predicting thermal conductivities are developed for a certain range of conditions [9]. They are useful for defined phases, i.e. certain ranges of thermodynamic conditions, and are particularly suited for non-polar or moderately polar substances. Predicting the transport properties of polar or associating substances remains difficult. We can distinguish three methods for analytically estimating thermal conductivities: corresponding states approaches [10, 11]; description of the reduced transport coefficients through another characteristic property, e.g. a characteristic volume [12–18]; and approaches that achieve a collapse of experimental values to universal lines for certain ranges [19–21].

Corresponding states approaches rely on a well described reference fluid. They relate the thermal conductivity of the target substance to the properties of the reference fluid. Models for the thermal conductivity often rely on the viscosity η of the dilute-gas state of the target substance and on λ of a reference fluid [10]. Additional properties, such as the acentric factor of the target substance may also be included. The reference fluid is not necessarily a real

[†]The following paragraphs literally quote M. Hopp, J. Gross: Thermal Conductivity of Real Substances from Excess Entropy Scaling Using PCP-SAFT, Ind.Eng.Chem.Res., 2017, 56, 15, 4527–4538.

fluid - simple model fluids such as Lennard-Jones (LJ) fluids have also been used [11].

Another approach is the rough-hard-sphere theory by Assael and Dymond [12–18, 22]. These authors describe λ as a function of temperature, the number of carbon-atoms in the homologous series of n-alkanes, and the characteristic volume of the substance. Their approach relies on the individual adjustment of the characteristic volume for each group of substances. The characteristic volume is expressed as a polynomial depending on the number of carbon atoms. The rough-hard-sphere theory was shown to give accurate results for pure dense fluids and some mixtures [12–18, 22].

Further approaches aim at establishing and using quasi-universal relationships f . For these relationships f , a collapse of experimental data to a 'universal' behavior is necessary. The collapse is achieved through an empirical scaling in the general form $\alpha\lambda = f(\beta)$, where α and β are functions of temperature, density, molecular mass, and critical point properties. Definition of α and β vary between different authors [19–21]. The resulting quasi-universal relationships f can easily be described through polynomials and lead to good descriptions for a certain phase and for certain classes of substances, e.g. for non-polar substances in gaseous phase at atmospheric pressure [19].

Beyond these three methods for devising models, highly accurate many-parameter equations are available for selected pure substances [23, 24]. Such components are usually chosen as reference fluids for corresponding states methods and provide reliable results for the given substance in wide ranges of temperature and pressure.

Other approaches adopt a molecular viewpoint, using the Green-Kubo equations or the kinetic gas theory. The Green-Kubo formalism formulates transport properties as time integrals of autocorrelation functions [25–27]. The thermal conductivity can be obtained by observing the autocorrelation of a system's instantaneous energy current. This is done in equilibrium molecular dynamics simulations, which get more reliable and accessible due to the development of better force fields [28–32]. In non-equilibrium simulations, the thermal conductivity is calculated via Fourier's law by measuring the temperature gradient evolving due to an heat flux applied to the system [33, 34].

The kinetic gas theory provides a strong framework for developing predictive methods for gaseous phases [35–38]. The full kinetic theory can approximately be solved e.g. by using substance-specific accurate (angle-dependent) intermolecular potentials and so-called generalized cross-sections [35–37].

The[‡] self-diffusion coefficient of a pure substance is a transport property not widely known, but is useful for estimating mutual (transport) diffusion coefficients [6–9, 39]. The transport behavior of ions in ionic liquids was investi-

[‡]The following paragraphs literally quote M. Hopp, J. Mele, J. Gross: Self-Diffusion Coefficients from Entropy Scaling Using the PCP-SAFT Equation of State, Ind.Eng.Chem.Res., 2018, 57, 38, 12942–12950.

gated through self-diffusion by calculating the so-called haven ratio, a measure for ionicity of ionic liquids [40]. Self-diffusion coefficients can also be useful for correlating other properties, like for polymers, where a correlation between the bulk self-diffusion coefficient and their glass transition temperature exists [41, 42].

Self-diffusion describes the average displacement of a marked molecule at time t , from its initial position at time $t = 0$. The displacement of molecules is caused by thermal molecular motion in absence of external driving forces, i.e. for a system in equilibrium. The self-diffusion coefficient of a pure substance shows a rather complicated behavior concerning temperature and pressure that makes it non-trivial to correlate or predict self-diffusion coefficients over a wide range of conditions. The self-diffusion coefficient of a substance in a mixture is often also referred to as tracer-diffusion coefficient. Pure substance self-diffusion is the limit of tracer-diffusion when all but one component vanish. Several routes can be taken for estimating self-diffusion coefficients. All approaches, however, are restricted to defined ranges in state space. One option for calculating transport properties for low densities is the kinetic gas theory, with the theory of Chapman and Enskog [43, 44] as the most prominent approach. Longuet-Higgins and Pople [45] parameterized a model applicable to higher densities. Another route to calculate self-diffusion coefficients is given by the reduced volume theory of Assael and Dymond [12–17, 46, 47]. In this theory, a reduced volume is calculated using the so-called close-packed volume, which depends on the number of carbon atoms in the molecule. The reduced volume is subsequently combined with the transport property of a reference fluid. The approach was originally derived for n-alkanes and was expanded to other groups of substances and to mixtures. Other methods are based on the rough hard sphere theory [48], such as the effective hard sphere diameter method [49–51], or methods using simultaneous free-volume modeling [52, 53]. Of course, molecular simulations [54–57] can be used to determine transport properties such as self-diffusion.

Yaakov Rosenfeld [58, 59], in 1977, showed that transport properties such as shear viscosity, thermal conductivity and self-diffusion coefficients, if made dimensionless in a suitable way, depend only (to excellent approximation) on the residual entropy s^{res} . His considerations were limited to simple, monoatomic fluids. In subsequent work, it was seen however, that entropy scaling also holds for molecular species with complex intermolecular interactions [60–63], i.e. substances with larger molecular mass and with strongly shape non-isotropic interactions or directional polar or hydrogen-bonding interactions and for mixtures of such substances [64].

The[†] statistical mechanical backbone to entropy scaling is not yet completely

[†]The following paragraphs literally quote M. Hopp, J. Gross: Thermal Conductivity of Real Substances from Excess Entropy Scaling Using PCP-SAFT, Ind.Eng.Chem.Res.,

understood. We find it interesting to note the closeness of isomorph theory [65–67] to Rosenfeld’s entropy scaling. Some studies confirmed the mono-variable correlation of transport properties with residual entropy for transport properties determined from molecular dynamics simulations. This analysis was done for the thermal conductivity of LJ-chain-fluids [33] and other fluids with simple pair potentials [68]. Other molecular dynamics studies considered the viscosities of polymeric LJ-fluids [69] or the translational and rotational diffusivities and relaxation times of different systems [60, 61, 70]. For soft-core model fluids, several studies reported anomalous behavior in entropy scaling. For such fluids, the original Rosenfeld approach fails [71–73], but entropy scaling still holds when an appropriate reference is chosen [62, 74, 75]. Thermal conductivity is found to be less affected from anomalous behavior than viscosity or self-diffusion [71, 73]. Interestingly, entropy can be used to predict the state conditions, where anomalous behavior of different properties for soft core fluids can be expected [76].

Although Rosenfeld’s initial publication on entropy scaling appeared already in 1977 [58], it took many years for other researchers to realize the potential of entropy scaling for the description of real, molecular substances. Most recent studies concern dynamic viscosity, for which a considerable number of experimental data is available in the literature [77, 78]. For viscosity, entropy scaling is confirmed as a remarkably accurate principle for pure n-alkanes [63, 79, 80], for more complex pure substances [63, 81] and for mixtures [63, 82] over the entire fluid region. Other transport properties lag behind due to a more complex behavior, scarcity of experimental data, or both. The self-diffusion coefficient D^{self} was calculated through an entropy scaling approach only for some pure substances [69, 75, 81, 83]. The thermal conductivity of real substances has not yet been investigated thoroughly using entropy scaling.

1.2 Outline

In Chapter 2, a detailed analysis of experimental data for thermal conductivity is done. A reference thermal conductivity that is itself a simple function of the residual entropy is proposed. Entropy scaling is applied with the PCP-SAFT equation of state [84, 85]. Considering low densities, I observed the dimensionless thermal conductivity (thermal conductivity divided by a reference thermal conductivity) does not show a univariate dependence on residual entropy for obvious choices of a reference thermal conductivity. Using the proposed reference thermal conductivity, good entropy scaling behavior for the entire fluid region is obtained for water and for 147 organic substances from various chemical families: linear and branched alkanes, alkenes, aldehydes, aromatics, ethers, esters, ketones, alcohols and acids.

Chapter 3 proposes a model for self-diffusion coefficients of pure substances from entropy scaling. In accordance with the entropy scaling approach, I observe that the self-diffusion coefficient of real substances, once made dimensionless with an appropriate expression, to very good approximation only depends on residual entropy. 133 substances from more than 14 different chemical families are studied and show good correlation results. The model presents satisfying robustness for extrapolating self-diffusion coefficients to state conditions that are rather different from the conditions where experimental data is available.

The proposed model for self-diffusion coefficients is in Chapter 4 used to refine the model for thermal conductivities. The thermal conductivity of gases depends strongly on the vibrational and rotational degrees of freedom of the molecule under consideration. Entropy scaling is based on the residual entropy, which does not capture the intramolecular and rotational contributions. This Chapter proposes a model for the thermal conductivity that accounts for these degrees of freedom. The Chapman–Cowling approximation is used, where contributions of internal degrees of freedom to the thermal conductivity of an ideal gas are related to the corresponding self-diffusion coefficient. A resulting expression for the thermal conductivity, using the model for the self-diffusion coefficient, is used here as a reference in entropy scaling.

In Chapter 5, a predictive method for the thermal conductivity is derived based on entropy scaling. The model is developed as a group-contribution approach, where substances are considered to be composed of chemical (functional) groups. The excess entropy is calculated using the group-contribution PCP-SAFT equation of state. The model is applicable for gaseous phases and for liquid-phase conditions covering wide ranges of temperature and pressure. I consider pure fluids from various chemical families, and propose parameters of 29 chemical groups, by considering 231 substances with more than 50,000 experimental data points.

Finally, in Chapter 6 first results of the prediction of thermal conductivity of mixtures are presented. The model based on entropy scaling and the PCP-SAFT equation of state, previously developed throughout the thesis, is extended and applied to thermal conductivity of binary mixtures. This is the first time that thermal conductivity of mixtures is investigated using entropy scaling.

This thesis is written in the pluralis modestiae to avoid the excessive use of passive voice. Furthermore, I emphasize the research behind this thesis is done in collaboration with colleagues, supervised students and my supervisor. Contributions to this work by persons other than the author are acknowledged at the beginning of each chapter.

Bibliography

- [1] A. Mersmann, M. Kind, and J. Stichlmair, *Thermische Verfahrenstechnik - Grundlagen und Methoden*. Springer Verlag, 2005.
- [2] R. B. Bird, W. E. Stewart, and E. N. Lightfoot, *Transport Phenomena*. John Wiley & Sons: New York, 2007.
- [3] D. C. Venerus and H. C. Öttinger, *A Modern Course in Transport Phenomena*. Cambridge University Press, 2018.
- [4] S. Kjelstrup, D. Bedeaux, E. Johannessen, and J. Gross, *Non-Equilibrium Thermodynamics for Engineers*. World Scientific Publishing Co. Pte. Ltd., 2010.
- [5] R. Taylor and R. Krishna, *Multicomponent Mass Transfer*. John Wiley & Sons, Ltd., 1994.
- [6] W. Marbach, H. G. Hertz, and H. Weingärtner, “Self- and mutual diffusion coefficients of some binary liquid n-alkane mixtures - a velocity correlation study -,” *Z Phys Chem*, vol. 189, pp. 63–79, 1995.
- [7] X. Liu, A. Bardow, and T. J. H. Vlugt, “Multicomponent maxwell-stefan diffusivities at infinite dilution,” *Ind. Eng. Chem. Res.*, vol. 50, pp. 4776 – 4782, 2011.
- [8] X. Liu, T. J. H. Vlugt, and A. Bardow, “Predictive darken equation for maxwell-stefan diffusivities in multicomponent mixtures,” *Ind. Eng. Chem. Res.*, vol. 50, no. 17, pp. 10350–10358, 2011.
- [9] B. E. Poling, J. M. Prausnitz, and J. P. O’Connell, *The Properties of Gases and Liquids - fifth Edition*. McGraw-Hill, 2000.
- [10] P. M. Mathias, V. S. Parekh, and E. J. Miller, “Prediction and correlation of the thermal conductivity of pure fluids and mixtures, including the critical region,” *Ind. Eng. Chem. Res.*, vol. 41, no. 5, pp. 989–999, 2002.
- [11] M. Bugel and G. Galliero, “Thermal conductivity of the lennard-jones fluid: An empirical correlation,” *Chem. Phys.*, vol. 352, no. 1 - 3, pp. 249 – 257, 2008.
- [12] M. J. Assael, J. H. Dymond, M. Papadaki, and P. M. Patterson, “Correlation and prediction of dense fluid transport coefficients: I. n-alkanes,” *Int. J. Thermophys.*, vol. 13, no. 2, pp. 269–281, 1992.

- [13] M. J. Assael, J. H. Dymond, M. Papadaki, and P. M. Patterson, "Correlation and prediction of dense fluid transport coefficients: Ii. simple molecular fluids," *Fluid Phase Equilib*, vol. 75, no. 0, pp. 245 – 255, 1992.
- [14] M. J. Assael, J. H. Dymond, M. Papadaki, and P. M. Patterson, "Correlation and prediction of dense fluid transport coefficients: Iii. n-alkane mixtures," *Int. J. Thermophys.*, vol. 13, no. 4, pp. 659–669, 1992.
- [15] M. J. Assael, J. H. Dymond, and P. M. Patterson, "Correlation and prediction of dense fluid transport coefficients: Iv. a note on diffusion," *Int. J. Thermophys.*, vol. 13, no. 4, pp. 729–733, 1992.
- [16] M. J. Assael, J. H. Dymond, and P. M. Patterson, "Correlation and prediction of dense fluid transport coefficients: V. aromatic hydrocarbons," *Int. J. Thermophys.*, vol. 13, no. 5, pp. 895–905, 1992.
- [17] M. J. Assael, J. H. Dymond, and S. K. Polimatidou, "Correlation and prediction of dense fluid transport coefficients: Vi. n-alcohols," *Int. J. Thermophys.*, vol. 15, no. 2, pp. 189–201, 1994.
- [18] M. J. Assael, A. E. Kalyva, K. E. Kakosimos, and K. D. Antoniadis, "Correlation and prediction of dense fluid transport coefficients: Viii. mixtures of alkyl benzenes with other hydrocarbons," *Int. J. Thermophys.*, vol. 30, no. 6, pp. 1733–1747, 2009.
- [19] D. Misić and G. Thodos, "The thermal conductivity of hydrocarbon gases at normal pressures," *AIChE J.*, vol. 7, no. 2, pp. 264–267, 1961.
- [20] D. Misić and G. Thodos, "Atmospheric thermal conductivities of gases of simple molecular structure.," *J. Chem. Eng. Data*, vol. 8, no. 4, pp. 540–544, 1963.
- [21] L. I. Stiel and G. Thodos, "The thermal conductivity of nonpolar substances in the dense gaseous and liquid regions," *AIChE J.*, vol. 10, no. 1, pp. 26–30, 1964.
- [22] T. Sun and A. S. Teja, "Correlation and prediction of the viscosity and thermal conductivity of dense fluids," *J. Chem. Eng. Data*, vol. 54, no. 9, pp. 2527–2531, 2009.
- [23] E. W. Lemmon and R. T. Jacobsen, "Viscosity and thermal conductivity equations for nitrogen, oxygen, argon, and air," *Int. J. Thermophys.*, vol. 25, no. 1, pp. 21–69, 2004.
- [24] "Refprop: Reference fluid thermodynamic and transport properties, version 8.0," 2007.

- [25] R. Zwanzig, "Time-correlation functions and transport coefficients in statistical mechanics," *Annu. Rev. Phys. Chem.*, vol. 16, pp. 67–102, 1965.
- [26] J.-P. Hansen and I. R. McDonald, *Theory of simple liquids*. Elsevier, 1990.
- [27] M. P. Allen and D. Tildesley, *Molecular Simulation of Liquids*. Oxford University Press: New York, 1980.
- [28] G. A. Fernandez, J. Vrabec, and H. Hasse, "A molecular simulation study of shear and bulk viscosity and thermal conductivity of simple real fluids," *Fluid Phase Equilib.*, vol. 221, pp. 157–163, 2004.
- [29] J. Petracic, "Thermal conductivity of ethanol," *J. Chem. Phys.*, vol. 123, pp. 174503(1–7), 2005.
- [30] S. Delage-Santacreu, G. Galliero, H. Hoang, J. P. Bazile, C. Boned, and J. Fernandez, "Thermodynamic scaling of the shear viscosity of mie n-6 fluids and their binary mixtures," *J. Chem. Phys.*, vol. 142, pp. 174501(1–7), 2015.
- [31] A. E. Nasrabad, R. Laghaei, and B. C. Eu, "Molecular theory of thermal conductivity of the lennard-jones fluid," *J. Chem. Phys.*, vol. 124, pp. 084506(1–10), 2006.
- [32] R. Vogelsang, C. Hoheisel, and G. Ciccotti, "Thermal conductivity of the lennard-jones liquid by molecular dynamics calculations," *J. Chem. Phys.*, vol. 86, no. 11, pp. 6371–6375, 1987.
- [33] G. Galliero and C. Boned, "Thermal conductivity of the lennard-jones chain fluid model," *Phys. Rev. E*, vol. 80, p. 061202, 2009.
- [34] F. Müller-Plathe, "A simple nonequilibrium molecular dynamics method for calculating the thermal conductivity," *J. Chem. Phys.*, vol. 106, no. 14, pp. 6082–6085, 1997.
- [35] R. Hellmann, N. Riesco, and V. Vesovic, "Calculation of the transport properties of a dilute gas consisting of lennard-jones chains," *J. Chem. Phys.*, vol. 138, no. 8, pp. 084309(1–11), 2013.
- [36] R. Hellmann and E. Bich, "An improved kinetic theory approach for calculating the thermal conductivity of polyatomic gases," *Mol. Phys.*, vol. 113, no. 2, pp. 176–183, 2015.
- [37] J.-P. Crusius, R. Hellmann, E. Hassel, and E. Bich, "Intermolecular potential energy surface and thermophysical properties of ethylene oxide," *J. Chem. Phys.*, vol. 141, no. 16, pp. 164322(1–9), 2014.

- [38] E. A. Mason and L. Monchick, "Heat conductivity of polyatomic and polar gases," *J. Chem. Phys.*, vol. 36, no. 6, pp. 1622–1639, 1962.
- [39] H. Weingärtner, *Diffusion in Condensed Matter*. vieweg, 1998.
- [40] H. Ohno, ed., *Electrochemical Aspects of Ionic Liquids*. wiley, 2 ed., 2011.
- [41] J. M. Katzenstein, D. W. Janes, H. E. Hocker, J. K. Chandler, and C. J. Ellison, "Nanoconfined self-diffusion of poly(isobutyl methacrylate) in films with a thickness-independent glass transition," *Macromolecules*, no. 45, pp. 154–1552, 2012.
- [42] M. Rubinstein and R. Colby, *Polymer Physics*. Oxford University Press, 2003.
- [43] S. Chapman and T. G. Cowling, *The Mathematical Theory of Non-Uniform Gases*. Cambridge University Press, 3 ed., 1970.
- [44] J. O. Hirschfelder, C. F. Curtiss, and R. B. Bird, *Molecular Theory of Gases and Liquids*. New York: John Wiley & Sons, Inc., 4 ed., 1954.
- [45] H. C. Longuet-Higgins and J. A. Pople, "Transport properties of a dense fluid of hard spheres," *J. Chem. Phys.*, vol. 25, no. 5, pp. 884–887, 1956.
- [46] M. J. Assael, J. H. Dymond, and V. Tselekidou, "Correlation of high-pressure thermal conductivity, viscosity, and diffusion coefficients for n-alkanes," *Int. J. Thermophys.*, vol. 11, no. 5, pp. 863–873, 1990.
- [47] M. J. Assael, J. H. Dymond, and S. K. Polimatidou, "Correlation and prediction of dense fluid transport coefficients: Vii. refrigerants," *Int. J. Thermophys.*, vol. 16, no. 3, pp. 761–772, 1995.
- [48] D. Chandler, "Rough hard sphere theory of the self-diffusion constant for molecular liquids," *J. Chem. Phys.*, vol. 62, no. 4, pp. 1358–1363, 1974.
- [49] C. M. Silva and H. Liu, *Modelling of Transport Properties of Hard Sphere Fluids and Related Systems, and its Applications*. Springer Berlin Heidelberg, 2008.
- [50] C. M. Silva, H. Liu, and E. A. Macedo, "Comparison between different explicit expressions of the effective hard sphere diameter of lennard-jones fluid: Application to self-diffusion coefficients," *Ind. Eng. Chem. Res.*, vol. 37, pp. 221–227, 1998.
- [51] M. He, Y. Guo, Q. Zhong, and Y. Zhang, "A new correlation on predicting self- and mutual-diffusion coefficient of lennard-jones chain fluid," *Fluid Phase Equilib.*, vol. 291, no. 2, pp. 166–173, 2010.

- [52] C. Boned, A. Allal, A. Baylaucq, C. K. Zeberg-Mikkelsen, D. Bessieres, and S. E. Quinones-Cisneros, "Simultaneous free-volume modeling of the self-diffusion coefficient and dynamic viscosity at high pressure," *Phys. Rev. E*, vol. 69, 2004.
- [53] O. Suárez-Iglesias, I. Medina, C. Pizarro, and J. L. Bueno, "On predicting self-diffusion coefficients in fluids," *Fluid Phase Equilib.*, vol. 269, no. 1-2, pp. 80–92, 2008.
- [54] N. Z. Gerek and R. J. Elliott, "Self-diffusivity estimation by molecular dynamics," *Ind. Eng. Chem. Res.*, vol. 49, pp. 3411–3423, 2010.
- [55] R. Hellmann, E. Bich, E. Vogel, A. S. Dickinson, and V. Vesovic, "Calculation of the transport and relaxation properties of methane. i. shear viscosity, viscomagnetic effects, and self-diffusion," *J. Chem. Phys.*, vol. 129, no. 6, pp. 064302(1–13), 2008.
- [56] A. I. Skoulidas and D. S. Sholl, "Self-diffusion and transport diffusion of light gases in metal-organic framework materials assessed using molecular dynamics simulations," *J. Phys. Chem.*, vol. 109, pp. 15760–15768, 2005.
- [57] M. S. Zabaloy, V. R. Vasquez, and E. A. Macedo, "Description of self-diffusion coefficients of gases, liquids and fluids at high pressure based on molecular simulation data," *Fluid Phase Equilib.*, vol. 242, no. 1, pp. 43–56, 2006.
- [58] Y. Rosenfeld, "Relation between the transport coefficient and the internal entropy of simple systems," *Phys. Rev. A*, vol. 15, no. 6, pp. 2545–2549, 1977.
- [59] Y. Rosenfeld, "A quasi-universal scaling law for atomic transport in simple fluids," *J. Phys.: Condens. Matter*, vol. 11, pp. 5415–5427, 1999.
- [60] R. Chopra, T. M. Truskett, and J. R. Errington, "On the use of excess entropy scaling to describe the dynamic properties of water," *J. Phys. Chem. B*, vol. 114, no. 32, pp. 10558–10566, 2010.
- [61] R. Chopra, T. M. Truskett, and J. R. Errington, "Excess-entropy scaling of dynamics for a confined fluid of dumbbell-shaped particles," *Phys. Rev. E*, vol. 82, p. 041201, 2010.
- [62] W. P. Krekelberg, T. Kumar, J. Mittal, J. R. Errington, and T. M. Truskett, "Anomalous structure and dynamics of the gaussian-core fluid," *Phys. Rev. E*, vol. 79, p. 031203, 2009.
- [63] O. Lötgering-Lin and J. Gross, "Group contribution method for viscosities based on entropy scaling using the perturbed-chain polar statistical associating fluid theory," *Ind. Eng. Chem. Res.*, vol. 54, no. 32, pp. 7942–7952, 2015.

- [64] O. Lötgering-Lin, M. Fischer, M. Hopp, and J. Gross, “Pure substance and mixture viscosities based on entropy scaling and an analytic equation of state,” *Ind. Eng. Chem. Res.*, vol. 57, no. 11, pp. 4095–4114, 2018.
- [65] A. A. Veldhorst, J. C. Dyre, and T. B. Schrøder, “Scaling of the dynamics of flexible lennard-jones chains,” *J. Chem. Phys.*, vol. 141, no. 5, p. 054904, 2014.
- [66] N. Gnan, T. B. Schrøder, U. R. Pedersen, N. P. Bailey, and J. C. Dyre, “Pressure-energy correlations in liquids: Iv. isomorphs in liquid phase diagrams,” *J. Chem. Phys.*, vol. 131, no. 23, p. 234504, 2009.
- [67] J. C. Dyre, “Hidden scale invariance in condensed matter,” *J. Phys. Chem. B*, vol. 118, pp. 10007–10024, 2014.
- [68] R. Grover, W. G. Hoover, and B. Moran, “Corresponding states for thermal conductivities via nonequilibrium molecular dynamics,” *J. Chem. Phys.*, vol. 83, no. 3, pp. 1255–1259, 1985.
- [69] T. Goel, C. N. Patra, T. Mukherjee, and C. Chakravarty, “Excess entropy scaling of transport properties of lennard-jones chains,” *J. Chem. Phys.*, vol. 129, no. 16, pp. 164904(1–9), 2008.
- [70] R. Chopra, T. M. Truskett, and J. R. Errington, “On the use of excess entropy scaling to describe single-molecule and collective dynamic properties of hydrocarbon isomer fluids,” *J. Phys. Chem. B*, vol. 114, no. 49, pp. 16487–16493, 2010.
- [71] D. Dhabal, C. Chakravarty, V. Molinero, and H. K. Kashyap, “Comparison of liquid-state anomalies in stilling-weber models of water, silicon, and germanium,” *J. Chem. Phys.*, vol. 145, no. 21, p. 214502/16, 2016.
- [72] Y. D. Fomin, V. N. Ryzhov, and N. V. Gribova, “Breakdown of excess entropy scaling for systems with thermodynamic anomalies,” *Phys. Rev. E*, vol. 81, p. 061201, 2010.
- [73] P. Mausbach and H. O. May, “Transport anomalies in the gaussian core model fluid,” *Z. Phys. Chem.*, vol. 223, pp. 1035–1046, 2009.
- [74] M. J. Pond, W. P. Krekelberg, V. K. Shen, J. R. Errington, and T. M. Truskett, “Composition and concentration anomalies for structure and dynamics of gaussian-core mixtures,” *J. Chem. Phys.*, vol. 131, no. 16, p. 161101, 2009.
- [75] W. P. Krekelberg, M. J. Pond, G. Goel, V. Shen, J. R. Errington, and T. M. Truskett, “Generalized rosenfeld scalings for tracer diffusivities in not-so-simple fluids: Mixtures and soft particles,” *Phys. Rev.*, vol. 80, no. 6, pp. 061205(1–13), 2009.

- [76] J. R. Errington, T. M. Truskett, and J. Mittal, "Excess-entropy-based anomalies for a waterlike fluid," *J. Chem. Phys.*, vol. 125, no. 24, p. 244502, 2006.
- [77] R. L. Rowley, W. V. Wilding, J. L. Oscarson, Y. Yang, N. A. Zundel, T. E. Daubert, and R. P. Danner *DIPPR Data Compilation of Pure Chemical Properties*. Design Institute for Physical Properties, AIChE: New York, NY, 2009.
- [78] DDBST Dortmund Data Bank Software & Separation Technology GmbH, Oldenburg, Germany, 2015. <http://www.ddbst.com>.
- [79] L. T. Novak, "Fluid viscosity-residual entropy correlation," *Int. J. Chem. React. Eng.*, vol. 9, p. A107, 2011.
- [80] L. T. Novak, "Predictive corresponding-states viscosity model for the entire fluid region: n-alkanes," *Ind. Eng. Chem. Res.*, vol. 52, pp. 6841–6847, 2013.
- [81] L. T. Novak, "Self-diffusion coefficient and viscosity in fluids," *Int. J. Chem. React. Eng.*, vol. 9, no. A63, pp. 1–25, 2011.
- [82] L. T. Novak, "Predicting natural gas viscosity with a mixture viscosity model for the entire fluid region," *Ind. Eng. Chem. Res.*, vol. 52, pp. 16014–16018, 2013.
- [83] M. Dzugutov, "A universal scaling law for atomic diffusion in condensed matter," *Nature*, vol. 381, pp. 137 – 139, 1996.
- [84] J. Gross and G. Sadowski, "Perturbed-chain saft: An equation of state based on a perturbation theory for chain molecules," *Ind. Eng. Chem. Res.*, vol. 40, pp. 1244–1260, 2001.
- [85] J. Gross and J. Vrabec, "An equation-of-state contribution for polar components: Dipolar molecules," *AIChE J.*, vol. 52, pp. 1194 – 1204, 2006.

2 Thermal Conductivity of Real Substances from Excess Entropy Scaling Using PCP-SAFT

This chapter is a literal quote of:

M. Hopp, J. Gross: Thermal Conductivity of Real Substances from Excess Entropy Scaling Using PCP-SAFT, Industrial & Engineering Chemistry Research, 2017, 56, 15, 4527–4538, DOI:10.1021/acs.iecr.6b04289 .

Additions implemented in this chapter compared to the original journal publication are indicated by square brackets.

Entropy scaling is an intriguingly simple approach for correlating and predicting transport properties of real substances and mixtures. It is convincingly documented in the literature that entropy scaling is indeed a firm concept for the shear viscosity of real substances, including hydrogen bonding species and strongly non-spherical species. We investigate whether entropy scaling is applicable for thermal conductivity. It is shown that the dimensionless thermal conductivity (thermal conductivity divided by a reference thermal conductivity) does not show a single-variable dependence on residual entropy, for obvious choices of a reference thermal conductivity. We perform a detailed analysis of experimental data and propose a reference thermal conductivity that is itself a simple function of the residual entropy. We then obtain good scaling behavior for the entire fluid region for water and 147 organic substances from various chemical families: linear and branched alkanes, alkenes, aldehydes, aromatics, ethers, esters, ketones, alcohols and acids. The residual entropy is calculated from the Perturbed Chain Polar Statistical Associating Fluid Theory (PCP-SAFT) equation of state. The correlation of experimental data requires 2 parameters for pure substances with scarce experimental data and up to 5 parameters for experimentally well-characterized species. The correlation results for all substances lead to average relative deviations of 4.2% to experimental data. To further assess the approach, we analyze extrapolations to states not covered by experimental data and find very satisfying results.

2.1 Rosenfeld's Entropy Scaling

The thermal conductivity λ of a pure substance shows a rather complex dependence on temperature T and pressure p for the entire fluid region, as Fig. 2.1 illustrates. In 1977, Rosenfeld postulated and showed that dimensionless transport properties are simply mono-variable functions of residual

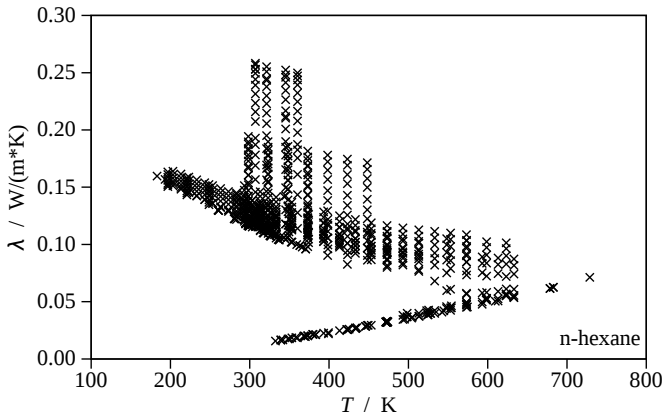


Figure 2.1: Experimental thermal conductivity λ^{exp} of hexane versus temperature for various pressures. Symbols represent data from 38 publications, all taken from ref [1].

entropy s^{res} . As transport properties, he considered dynamic viscosity, self-diffusion and thermal conductivity. Rosenfeld initially limited consideration to simple fluids and model fluids, but later extended his theory for dense fluids and dilute gases as well [2–4].

Entropy scaling, especially with focus on viscosity, has been recognized as a strong principle [5–7], applicable to a wide array of real substances including strongly hydrogen-bonding species and strongly non-spherical (wax-like) substances. For the thermal conductivity, however, there is a research need for how to best define the dimensionless thermal conductivity $\lambda^* = \lambda/\lambda^{ref}$. The first approach by Rosenfeld himself [2] was guided by a simple dimensionality analysis. He proposed $\lambda^{ref} = \rho^{2/3} k\sqrt{kT/M'}$, where k is Boltzmann’s constant, T is the temperature, ρ is the number density, and M' is the molecular mass. The so-defined dimensionless thermal conductivity λ^* leads to a monovariate dependence on s^{res} for liquid-like densities. Due to the number density ρ in the denominator of the resulting expression for λ^* , [this ansatz] diverges for the ideal gas limit.

In the following section we examine different approaches for λ^{ref} , by assessing if these approaches lead to a distinct (mono-variable) entropy scaling. We use experimental data of n-hexane as a representative example. Finally, we propose a new expression for the reference thermal conductivity λ^{ref} .

As in our preceding study on shear viscosity [7], we calculate the residual entropy needed in our work using the PCP-SAFT equation of state. The dimensionless residual entropy is defined as

$$s^* = s^{res}/(km) \quad (2.1)$$

The quantity m is a pure component parameter of the PCP-SAFT model, that represents the number of spherical segments a molecule is composed of. Dividing s^{res} by m leads to similar ranges of s^* -values for very different substances. Alternatively, one could also use the molar mass instead of m for ensuring similar ranges of s^* for different components.

2.2 Evaluation of Reference Thermal Conductivities

For defining a dimensionless thermal conductivity, $\lambda^* = \lambda/\lambda^{ref}$, we here refer to λ^{ref} as the reference thermal conductivity.

2.2.1 Chapman Enskog

The Chapman-Enskog (CE) equations are based on Boltzmann’s equation and describe transport properties of monoatomic gases, i.e. for molecules with no internal degrees of freedom, based on kinetic gas theory [8, 9]. In case of viscosity, the CE equation was seen to be a suited reference for entropy scaling [7, 10, 11]. The corresponding expression for thermal conductivity reads

$$\lambda_{CE}^{ref} = \frac{\sqrt{T/(M/m)} 83.235 \text{ kg}^{3/2} \text{ \AA}^2 \text{ m}}{\sigma^2 \Omega^{(2,2)}(T^*) 10^{3/2} \text{ K}^{3/2} \text{ mol}^{1/2} \text{ s}^3} \quad (2.2)$$

The collision integral $\Omega^{(2,2)}(T^*)$ with dimensionless temperature $T^* = kT/\epsilon$ is given in form of an empirical correlation by Neufeld et al [12]. Further, σ is a molecular diameter parameter, ϵ denotes the pair energy parameter and M is the molar weight [in kg/mol]. We take σ and ϵ from the PCP-SAFT equation of state, where they characterize spherical segments of chain-structured molecules. We introduce the segment number m to achieve a comparable behavior between different substances. That is beneficial in a later stage, where more well-behaved parameters are observed for various substances.

The entropy scaling approach can be applied to data for thermal conductivities of Lennard-Jones chain fluids from molecular simulation. We find that the data of Galliero and Boned [5] almost perfectly falls onto one line, when analyzed as $\lambda^* = \lambda/\lambda^{ref}$ using Eq. (2.2) with residual entropies calculated from PC-SAFT. The results are shown in the supporting information.

Fig. 2.2 presents the entropy scaling of n-hexane using the CE reference. We find an overall well-behaved course of $\lambda^*(s^*)$, but we observe a pronounced deviation from entropy scaling in low density limit. In this study, for brevity, we speak of ‘*entropy scaling*’ when experimental data collapses to monovari-able dependence with residual entropy. With ‘*deviation from entropy scaling*’ we refer to conditions, where experimental data does not show monovari-able dependence on residual entropy. The low-density deviations are in fact tem-perature dependent, as further analysis shows. Such deviations appear for

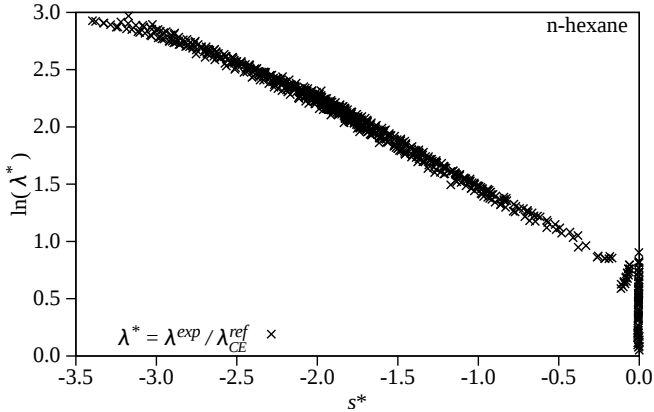


Figure 2.2: Logarithmic reduced thermal conductivity $\lambda^* = \lambda^{exp} / \lambda_{CE}^{ref}$ versus reduced residual entropy s^* . The symbols denote experimental data, reduced by $\lambda^{ref} = \lambda_{CE}^{ref}$, eq. (2.2). The reduced entropy s^* is calculated from PCP-SAFT according to given temperature and pressure, as defined in eq. (2.1).

polyatomic molecules where intra-molecular degrees of freedom exist. The deviation does not occur for monatomic molecules, e.g. noble gases.

We note that two options for modifying the CE-formula, eq. (2.2), namely by defining the dimensionless temperature as $T^* = kT / (m\epsilon)$, or by considering $m^\alpha \sigma^2$ instead of σ^2 in the denominator of equation (2.2) with varying power α , only leads to an upwards or downwards shift in the entropy-scaling diagram, Fig. 2.2. Deviations from the entropy scaling behavior in the low-density limit thereby persist.

2.2.2 Chapman Enskog with Eucken correction

The Eucken correction ψ is a simple correction term for polyatomic molecules defined through

$$\psi = \frac{4}{15} \left(\frac{c_v}{R} + \frac{3}{5} \right) \quad (2.3)$$

with isochoric heat capacity c_v . The correction is multiplied onto the CE-expression for thermal conductivity [9], according to

$$\lambda_{Eu}^{ref} = \lambda_{CE}^{ref} \psi = \lambda_{CE}^{ref} + \lambda_{Eu}^{correct} \quad (2.4)$$

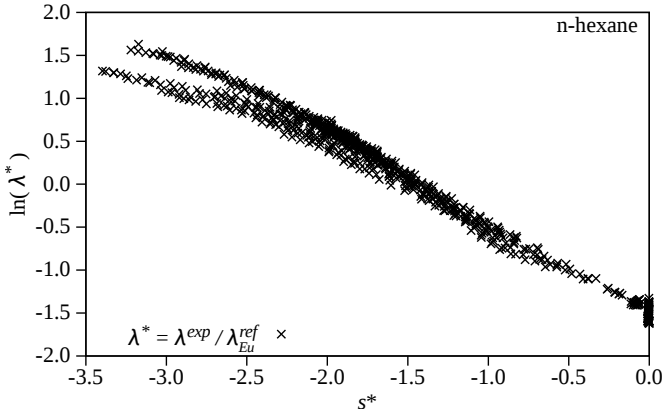


Figure 2.3: Logarithmic reduced thermal conductivity, with $\lambda^{ref} = \lambda_{Eu}^{ref}$, eq. (2.4). Detailed caption see Fig. 2.2.

With the second equality we define an additive contribution to the Chapman-Enskog term, as

$$\lambda_{Eu}^{correct} = \lambda_{CE}^{ref} (\psi - 1) \quad (2.5)$$

Writing the Eucken expression for the reference thermal conductivity into two additive contributions will be advantageous in the further course of our analysis.

The Eucken correction has a good influence on the entropy scaling in the low density limit ($s^* \rightarrow 0$) but leads to increased deviation from entropy scaling for dense, i.e. liquid states, as Fig. 2.3 illustrates. The strong deviation from entropy scaling for dense states (very negative s^* -values) results from the heat capacity c_v , as the comparison of Fig. 2.2 with Fig. 2.3 shows.

2.2.3 LTST Approach

Another prominent approach divides the thermal conductivity into a classical part and a contribution due to intra-molecular vibrational degrees of freedom, leading to

$$\lambda_{LTST}^{ref} = \lambda_{CE}^{ref} + \lambda_{LTST}^{correct} \quad (2.6)$$

An expression for the vibrational contribution of polyatomic gases to the thermal conductivity was proposed by Liang and Tsai [13] based on studies by Stiel and Thodos [14]. We refer to the approach as LTST according to the

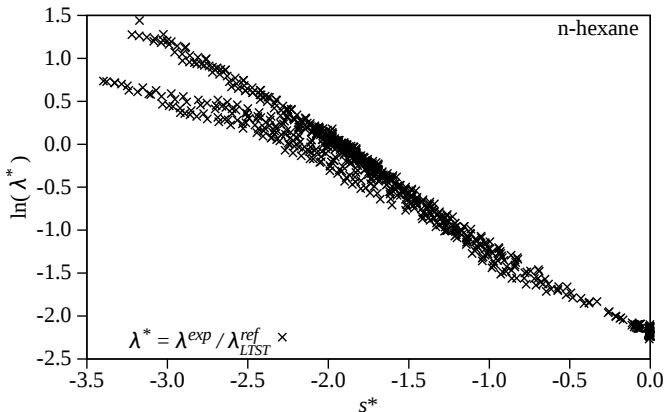


Figure 2.4: Logarithmic reduced thermal conductivity, with $\lambda^{ref} = \lambda_{LTST}^{ref}$, eq. (2.6). Detailed caption see Fig. 2.2.

authors' names. The vibrational contribution reads

$$\lambda_{LTST}^{correct} = \rho D^{self} (c_v^{ig} - 3R) \frac{\text{mol}}{\text{m s}} \quad (2.7)$$

$$\rho D^{self} = \begin{cases} 0, & \text{if } T_r < 0.3 \\ \frac{0.464}{10^5 \xi} (1.391 T_r - 0.381)^{2/3}, & \text{if } 0.3 < T_r < 1.5 \\ \frac{0.464}{10^5 \xi} T_r^{0.777}, & \text{if } T_r > 1.5 \end{cases} \quad (2.8)$$

$$\xi = \left(\frac{T_c}{\text{K}} \right)^{1/6} \left(\frac{M}{\text{g/mol}} \right)^{-1/2} \left(\frac{p_c}{\text{atm}} \right)^{-2/3}$$

with reduced temperature $T_r = T/T_c$, pressure p_c and temperature T_c at the critical point. We calculate the isochoric heat capacity in ideal gas state c_v^{ig} using correlations from the DIPPR database [15].

Fig. 2.4 evaluates how the reference thermal conductivity λ_{LTST}^{ref} performs for the entropy scaling of hexane. The result is comparable to the previously considered case (Chapman-Enskog with Eucken correction), however, with further improved entropy scaling behavior at low densities but further deteriorated entropy scaling for higher densities. In the approach given here we neglect rotational degrees of freedom, which leads to $3R$ in Eq. (2.7). We also investigated the same approach with the rotational contribution included (leading to $1.5R$), but the performance in entropy scaling was inferior to the approach presented here.

In order to understand the desired scaling behavior for ideal gases and the undesired behavior for high densities, we proceed with a detailed analysis of the low density region.

2.3 A new approach for the reference thermal conductivity

In the preceding analysis of existing expressions for the thermal conductivity of gases, we have seen the desired entropy scaling behavior for some regions of state space. The use of a CE reference term led to fine entropy scaling in the dense (i.e. liquid) states, but resulted in deviations in the low-density gas region. The observation was inverse for the Eucken corrected expression and even more so for the LTST approach: good scaling behavior at low-density conditions, but strong deviations for liquid states.

For describing the thermal conductivity of real polyatomic fluids in the complete space of fluid states, we strive at combining the benefits of the given approaches: namely the good entropy scaling behavior of CE for higher densities, and the promising Eucken correction or LTST approach for lower densities. To achieve this combination, we empirically introduce a transition function $\alpha(s^*)$ into eq. (2.6), resulting in

$$\lambda^{ref} = \lambda_{CE}^{ref} + \alpha(s^*) \lambda^{\text{correct}} \quad (2.9)$$

as a new ansatz for a reference thermal conductivity, where λ^{correct} represents a correction towards the Chapman-Enskog expression. We define the transition function $\alpha(s^*)$ as

$$\alpha(s^*) = \exp(-s^*/s_c^*) = \exp(-s^{\text{res}}/s_c^{\text{res}}) \quad (2.10)$$

to gradually add vibrational corrections at low densities, i.e. low $|s^*|$. Here $s_c^* = s^{\text{res}}(T_c, p_c)/(k m)$ is the reduced residual entropy at the critical point according to eq. (2.1). We take T_c , p_c , and $s^{\text{res}}(T_c, p_c)$ as calculated from the PCP-SAFT equation of state. This definition of $\alpha(s^*)$ leads to a comparable but substance-specific transition function. The exponential ansatz function makes a transition from the ideal gas limit, where $\alpha(s^* = 0) = 1$ gives full weight to the vibrational correction term, to the high-density liquid region, where $\alpha(s^*)$ gets small, vanishing in the limit $\alpha(s^* \rightarrow -\infty) = 0$.

The transition function $\alpha(s^*)$ can be applied to both, the Eucken correction and the LTST approach. We refer to these models as α -Eucken (with $\lambda_{\alpha, Eu}^{ref} = \lambda_{CE}^{ref} + \alpha(s^*) \lambda_{CE}^{ref}(\psi - 1)$) and as α -LTST approach (with $\lambda_{\alpha, LTST}^{ref} = \lambda_{CE}^{ref} + \alpha(s^*) \lambda_{LTST}^{\text{correct}}$), respectively. The use of $\alpha(s^*)$ drastically improves the entropy scaling behavior, as Fig. 2.5 confirms. From the previous sections, it is clear that the Eucken correction leaves some deviation from entropy scaling in the limit of ideal gases, whereas seemingly very good entropy scaling behavior is found for the LTST approach.

Nevertheless, the two given approaches ($\lambda_{\alpha, Eu}^{ref}$ and $\lambda_{\alpha, LTST}^{ref}$) are not entirely satisfying. The first deficiency of the LTST method is the non-continuous definition of ρD^{self} in eq. (2.7), which introduces a step at $T_r = 0.3$. Secondly, both approaches lead to $\ln(\lambda^*)$ -values at the ideal gas limit far from zero. That

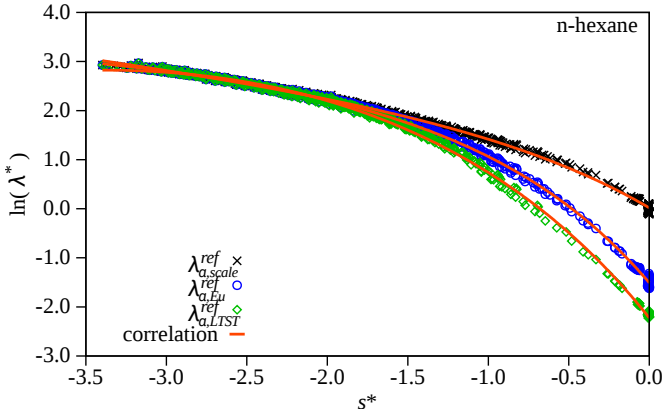


Figure 2.5: Logarithmic reduced thermal conductivity $\lambda^* = \lambda/\lambda^{ref}$ versus reduced residual entropy s^* . The symbols denote experimental data. Three reference thermal conductivities are compared, namely $\lambda_{\alpha, scale}^{ref}$, $\lambda_{\alpha, Eu}^{ref}$ and $\lambda_{\alpha, LTST}^{ref}$. The red lines represent the corresponding correlation function, eq. (2.14).

is unsatisfying from a theoretical perspective, because all reference terms are supposed to reproduce thermal conductivities of ideal gases, so that λ^* should approximately be unity for $s^* = 0$. But it is also undesired for practical application of the entropy scaling approach, because assuming $\ln(\lambda^*(s^* = 0)) = 0$ for substances lacking experimental data in the gaseous phase is then not possible. The strong deviations from $\ln(\lambda^*) = 0$ at $s^* = 0$ reveal the inability of both references to correctly describe the thermal conductivity of the ideal gas. Therefore, we continue to analyze the low density limit in the following section.

2.3.1 A new expression for Ideal Gas Limit

In this section, we propose a new expression for the ideal gas reference thermal conductivity that should overcome some of the deficiencies of the two reference expressions discussed above. The new term is based on the Chapman-Enskog theory, because of its well-behaved results of entropy scaling for dense phases. In order to obtain good agreement also for gas phases, we start by analyzing the low-density behavior. More specifically, we concentrate on the deviation between experimental data and the Chapman-Enskog theory, captured by the difference $(\lambda^{exp} - \lambda_{CE}^{ref})$. We use the condition $|s^*| < 0.1$ as a criterion for low-density states. Data points outside this criterion are not considered in our analysis.

Fig. 2.6 shows the difference $(\lambda^{exp} - \lambda_{CE}^{ref})$ over reduced temperature. The dia-

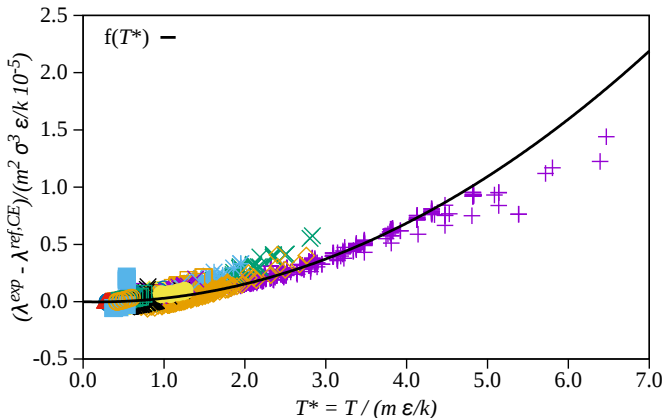


Figure 2.6: Analysis of the difference between experimental values of the thermal conductivity and values estimated from the Chapman-Enskog theory, $(\lambda^{exp} - \lambda_{CE}^{ref})$ as a function of reduced temperature T^* for 36 substances in dilute gas conditions ($|s^*| < 0.1$). Full legend given in supplementary information.

gram contains data of 36 different substances of various chemical families, e.g. alkanes (C1 to C11), branched alkanes, alkenes, aldehydes, aromatics, ethers, ketones and alcohols. We found no significant dependence of this difference on pressure. A roughly universal behavior can be achieved by dividing the difference $(\lambda^{exp} - \lambda_{CE}^{ref})$ with a measure for the intermolecular dispersive energy [16] as expressed in PCP-SAFT parameters (i.e. $m^2 \sigma^3 \epsilon / k$). We describe this temperature-dependent deviation according to

$$\frac{(\lambda^{exp} - \lambda_{CE}^{ref})}{m^2 \sigma^3 \epsilon / k} \frac{10^5 \text{ s}^3 \text{ \AA}^3 \text{ K}^2}{\text{kg}} = c_1 T^* + c_2 T^{*2} \quad (2.11)$$

with model constants $c_1 = -0.0167141$ and $c_2 = 0.0470581$ adjusted to the data displayed in Fig. 2.6. The expression contains PCP-SAFT parameters, i.e. segment number m , segment size parameter σ , energy parameter ϵ , and dimensionless temperature defined as $T^* = T / (m \epsilon / k)$. It is noteworthy that we were able to also deduce a good model for $(\lambda^{exp} - \lambda_{CE}^{ref})$ using the critical temperature and the molecular mass of each species. However, we expect more ambiguity in extending such a model to mixtures, whereas extending eq. (2.11) to mixtures is rather straightforward. The difference of thermal conductivity modeled in eq. (2.11) is in fact a model for λ^{correct} . We thus get a new equation for the reference thermal conductivity

$$\lambda_{\alpha, scale}^{ref} = \lambda_{CE}^{ref} + \alpha(s^*) \lambda_{scale}^{\text{correct}} \quad (2.12)$$

with

$$\lambda_{scale}^{correct} = (m^2 \sigma^3 \epsilon / k) (c_1 T^* + c_2 T^{*2}) \frac{\text{kg m}}{10^5 \text{ s}^3 \text{ \AA}^3 \text{ K}^2} \quad (2.13)$$

Applying this reference, a good entropy scaling behavior is found without the drawbacks observed for the other approaches, as Fig. 2.5 shows.

A further improved behavior in the gas limit can be achieved by adjusting c_1 and c_2 to individual chemical families or even individual substances. This additional adjustment is recommended if high accuracy for selected substances is targeted. We would for example expect that halogenated substances require adjustment of c_1 and c_2 . In this work, however, we value a simple but widely applicable description with low number of adjustable parameters and we therefore use eq. (2.13) with c_1 and c_2 adjusted to many species. A more detailed diagram with full legend is given in the supplementary information. Before proceeding, we mention a promising future extension of our approach. Chapman and Cowling [8] have established the relation between the internal contributions (rotational and vibrational) to the thermal conductivity, which in our notation corresponds to the correction term, as $\lambda^{correct} = \rho D^{self} c_v^{int}$, with D^{self} as the self-diffusion coefficient capturing thus the transport of internal energy. The approach is promising, because the product of ρD^{self} is yet another property that should obey Rosenfeld’s entropy scaling [4]. We have initial results for the entropy scaling of ρD^{self} , but not sufficient to further explore this approach here. [The study of the extension mentioned here, based on a self-diffusion approach, is part of this thesis as Chapter 4.]

2.3.2 Correlation Function for Thermal Conductivity

The relation between the reduced thermal conductivity λ^* and reduced residual entropy s^* is here described through the ansatz function

$$\ln(\lambda^*) = \ln(\lambda/\lambda^{ref}) = A + Bs^* + C(1.0 - \exp(s^*)) + Ds^{*2} \quad (2.14)$$

The systematically non-linear entropy scaling behavior led us to include an exponential contribution in eq. (2.14), as opposed to the simple 3rd degree polynomial for the viscosity proposed by Loetgering-Lin and Gross [7, 17]. The four parameters A - D have to be adjusted to experimental data for every pure substance. In the adjustment of parameters A - D we omit experimental points lying within a region of 10% around T_{crit} and p_{crit} , the calculated temperature and pressure at the critical point. That is done, first, because PCP-SAFT is usually not parametrized enforcing the critical point of a pure component. Second, the thermal conductivity is known to have an enhancement in the vicinity of the critical point [18–24]. This enhancement is so far not included in our description.

Fig. 2.5 compares entropy scaling using the three references, each containing

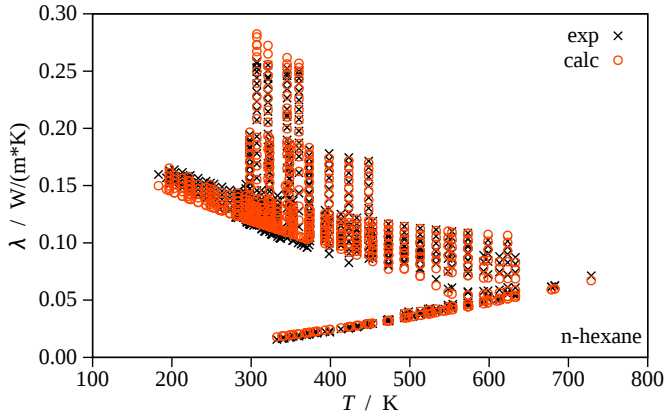
$\alpha(s^*)$. The resulting correlation functions, eq. (2.14), are also shown as red lines. All three models, namely entropy scaling using $\lambda_{\alpha, Eu}^{ref}$, $\lambda_{\alpha, LTST}^{ref}$, and $\lambda_{\alpha, scale}^{ref}$ as reference thermal conductivity, are reasonable. The main differences between the three models are the degree of curvature and the value at the ideal gas limit. The expression $\lambda_{\alpha, scale}^{ref}$ leads to a good estimate of the ideal gas limit, so that the logarithm of $(\lambda^{exp}/\lambda_{\alpha, scale}^{ref})$ approximately approaches zero for $s^* \rightarrow 0$.

We defined $D = 0$ whenever the experimental data for a substance covers only a small region of states. As a criterion, we use the experimentally covered range in residual entropy $\Delta s^* = s_{max}^* - s_{min}^*$, with $s_{min}^* = \min(s^*)$ and $s_{max}^* = \max(s^* | s^* < -0.1)$. The limitation of s_{max}^* to values lower than -0.1 decouples the D -criterion from possibly available data in gaseous phase. If $\Delta s^* < 2.0$, we set D to zero. Additionally, but only for our new reference $\lambda_{\alpha, scale}^{ref}$, we define $A = 0$ if no experimental data in gaseous phase ($\max(s^*) < -0.25$) is available. This leads to a further reduction of adjustable parameters and, more important, to a robust extrapolation for cases where experimental data is scarce. It is not possible to use $A = 0$ as an approximation for the α -Eucken or the α -LTST approaches, as Fig. 2.5 shows.

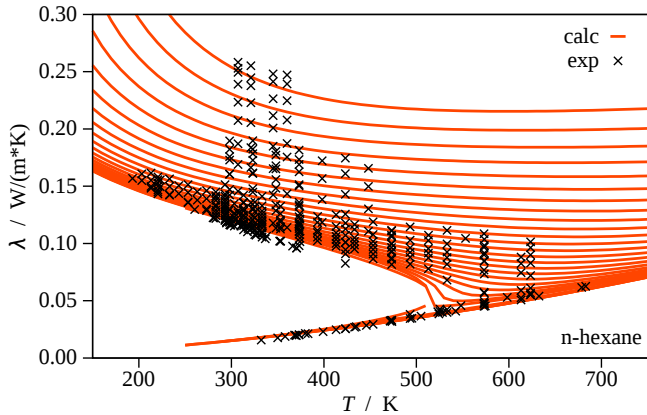
Once the parameters A - D are adjusted, it is very easy to obtain calculated thermal conductivities. Rewriting eq. (2.14) we obtain

$$\lambda^{calc} = \lambda^{ref} \cdot \lambda^* = \lambda^{ref} \cdot \exp\{A + Bs^* + C(1.0 - \exp(s^*)) + Ds^{*2}\} \quad (2.15)$$

so that the thermal conductivity can not only be calculated at temperature and pressure conditions corresponding to experimental data, but it is possible to predict the thermal conductivity for the entire fluid region (see Fig. 2.7).



(a) Calculation of experimentally given $\{T, p\}$ -points.



(b) Prediction of isobars up to 630MPa.

Figure 2.7: Thermal conductivity of n-hexane versus temperature using $\lambda_{\alpha, scale}^{ref}$. Black symbols denote experimental data. Red circles denote the corresponding calculated values. The red lines are predicted isobars.

2.4 Results and Discussion

In the preceding sections, we propose a new reference thermal conductivity for entropy scaling. The development was illustrated using n-hexane as an example, which we chose due to its good coverage of experimental data. In this section, we first show the usefulness of entropy scaling for data analysis. Next, we consider other pure substances, where experimental data of the thermal conductivity is available for both, high (liquid) densities and low (gaseous) densities. We then proceed to model the thermal conductivity for a fairly comprehensive list of substances. Experimental data for the gas-phase is thereby absent for many species. Subsequently, we assess the robustness of our model to extrapolate for substances with limited coverage of experimental data.

2.4.1 Data Analysis

Entropy scaling is powerful for identifying non-plausible experimental data, i.e. outliers. Such outliers can be detected in the entropy-scaling diagram, as for example seen for n-undecane in Fig. 2.8. In this work, we only removed outliers if a complete series of one original source was clearly in contradiction to other sources. We did not filter and remove single outlying points within an otherwise ‘good’ series of data from one source. The three points in Fig. 2.8, for example, were left in our parameterization and analysis. This is a rather conservative approach, leading to higher values for deviations compared to a procedure with more aggressive data filtering.

As another example we show isopropylbenzene, where the data of our

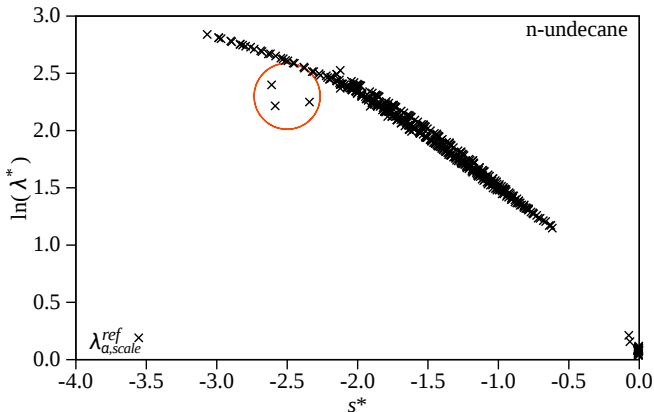
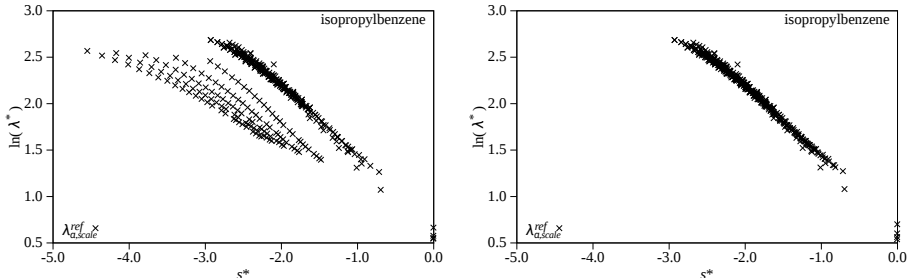


Figure 2.8: Outliers are easily detected in the entropy-scaling diagram, as here shown for n-undecane using $\lambda_{\alpha, scale}^{ref}$.

database [1] led to a strong deviation from entropy scaling. The malign scaling behavior was observed for one reference included into the commercial database with pressure values wrong by a factor of 10 (as we realized from this analysis). The error results in parallel curves in the liquid region of the entropy plot (see Fig. 2.9a). Correcting the pressure values, as correctly published in the original source [25], leads to the well-known benign entropy scaling behavior (Fig. 2.9b).



(a) Original data as contained in database [1] (b) Same data points, but now with corrected with some pressure values wrong by a factor of pressure values.

10.

Figure 2.9: Logarithmic reduced thermal conductivity λ^* of isopropyl-benzene versus reduced residual entropy s^* using $\lambda_{\alpha, scale}^{ref}$. The symbols are for experimental data.

2.4.2 Substances with experimental data of λ in gas phase

We propose entropy scaling for the thermal conductivity using a reference thermal conductivity of the form $\lambda_{\alpha, scale}^{ref} = \lambda_{CE}^{ref} + \alpha(s^*)\lambda_{scale}^{correct}$. In order to assess this ansatz, we can decompose two contributions to the model: The transition function $\alpha(s^*)$ and the proposed correlation $\lambda_{scale}^{correct}$. It is possible to single-out the suitability of the transition function $\alpha(s^*)$ for entropy scaling, by adjusting an expression for $\lambda_{scale}^{correct}$ to each substance individually.

We here consider substances with available experimental data for both, liquid-like densities and gaseous or vapor densities. For such components, it is possible to correlate the thermal conductivity by adjusting coefficients A to D of Eq. (2.15) and coefficients c_1 and c_2 of Eq. (2.12) and (2.13). In fact, once the coefficients c_1 and c_2 are treated as adjustable parameters for a substance, it is sufficient to set $A = 0$, leaving 5 adjustable parameters for this particular analysis.

We consider ethane as a non-polar substance, 1-heptanol as a mildly polar species and water as a highly polar component. The optimized parameters

are detailed in the supplementary material. The results are shown in Fig. 2.10. We find very good agreement for all three components. Table 2.1 summarizes absolute average deviations (AAD-%) for the 3 substances, as well as for other n-alkanes. We conclude the transition function $\alpha(s^*)$ leads to a convincing entropy scaling behavior of various very different substances.

Name	AAD / %	
	c_1, c_2 individually adjusted	c_1, c_2 from correlation, Eq. (2.11)
methane	5.345	6.996
ethane	3.094	6.172
propane	2.485	6.826
butane	2.221	4.947
pentane	2.368	2.645
hexane	2.765	3.175
heptane	3.287	3.680
octane	2.796	2.774
nonane	3.175	3.161
decane	2.635	2.863
undecane	2.695	2.773
1-heptane	4.139	4.260
water	4.492	6.816

Table 2.1: Deviations (expressed as absolute average deviations, AAD-%) of thermal conductivities calculated from entropy scaling using $\lambda_{\alpha, scale}^{ref}$ from experimental data. Note, the RMS-% values (not reported) for cases where c_1, c_2 were adjusted individually are always lower compared to the case where the correlation, Eq. (2.11), was used.

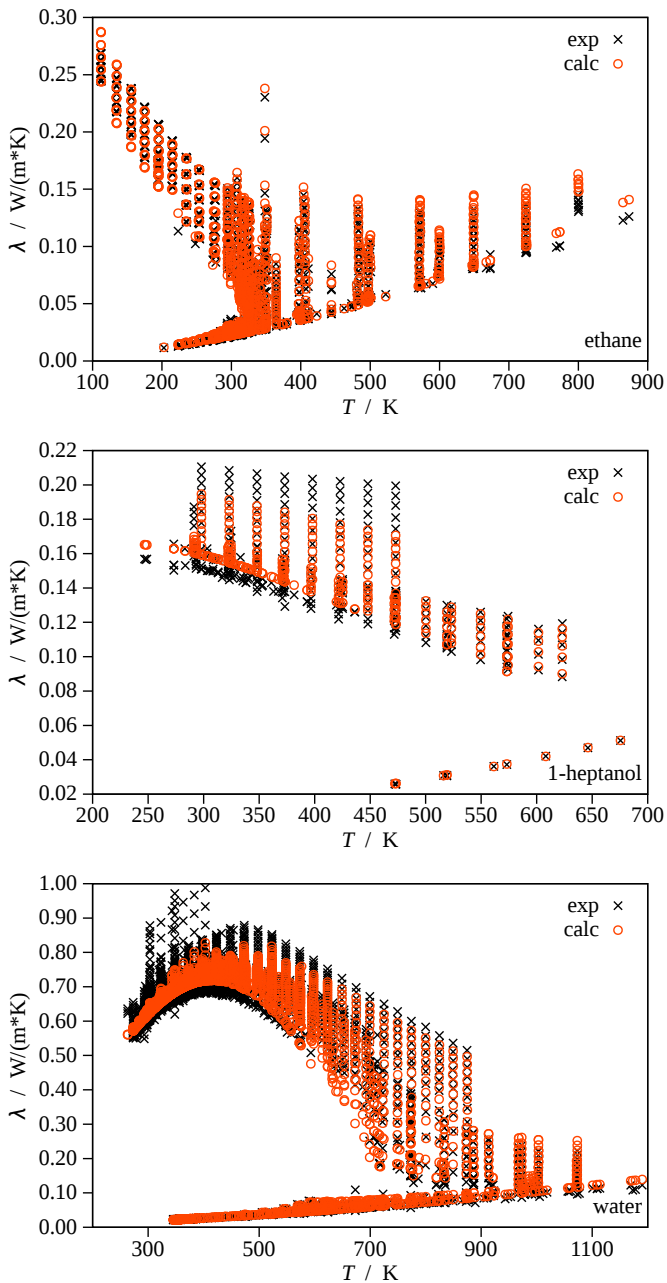


Figure 2.10: Comparison of experimental thermal conductivity data with results from entropy scaling using $\lambda_{\alpha, \text{scale}}^{\text{ref}}$. Ethane is considered as a non-polar substance, 1-heptanol as a moderately polar species, and water as a strongly polar, hydrogen bonding substance.

2.4.3 Comprehensive correlation of pure substance thermal conductivity

To comprehensively compare entropy scaling with all three approaches for the reference thermal conductivity, we calculated λ for many substances from a variety of chemical families. The average deviations of calculated thermal conductivities from experimental values for all investigated substances are summarized in Fig. 2.11 for n-alkanes, and in Fig. 2.12 for other substances grouped into chemical families. A detailed list of all individual deviations, the adjusted polynomial parameters A - D , as well as the used PCP-SAFT parameters is given in the supplementary information. Overall, we find good agreement of results from entropy scaling with experimental data for all investigated chemical families and for all three versions of λ_{α}^{ref} . The results can particularly be appreciated considering the fact that, first, the entire fluid region is covered, and second, we include a comprehensive list of experimental data without substantial data filtering. The deviations using $\lambda_{\alpha, Eu}^{ref}$ are marginally lower than the deviations from entropy scaling using $\lambda_{\alpha, scale}^{ref}$ or $\lambda_{\alpha, LTST}^{ref}$. However, we will not declare $\lambda_{\alpha, Eu}^{ref}$ as the most promising reference thermal conductivity, as the following sections will show.

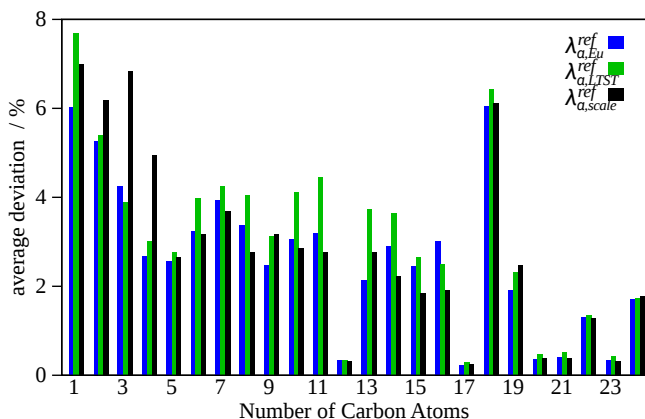


Figure 2.11: Absolute average deviations of calculated to experimental thermal conductivities for the homologous series of n-alkanes. Comparison between different reference thermal conductivities λ^{ref} .

Fig. 2.13 shows various butane derivatives. With this diagram, we consider individual substances across various chemical families. The average deviation for all butane derivatives is 4.9%. 2-Butanone is a representative example for this group of substances, because the individual deviations of correlated to experimental data is 4.7% (and thus close to average). In Fig. 2.14 we give a graphical comparison of experimental data to correlation results of 2-butanone. The diagram confirms good overall agreement, with some more

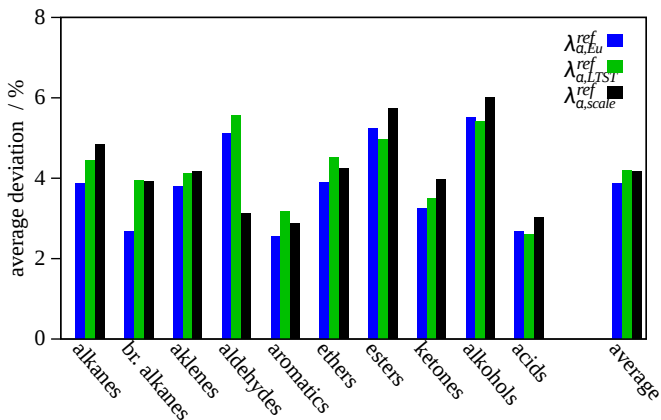


Figure 2.12: Absolute average deviations of calculated to experimental thermal conductivities for all investigated groups of substances. Comparison between different reference thermal conductivities λ^{ref} .

pronounced deviations around the critical point. One can also observe an experimental ‘outlier’ at $T = 532.9\text{K}$ that is not plausible and could have been disregarded (which would lead to lower deviations).

2.4.4 Robustness to Extrapolation

The results of the previous section show that entropy scaling using our proposed expression $\lambda_{\alpha, scale}^{ref}$ does not outperform the α -LTST model and the α -Eucken model in correlating experimental data. The rationale for developing an alternative expression for an ideal gas correction ($\lambda_{\alpha, scale}^{ref}$) was our skepticism about the robustness of the α -LTST and the α -Eucken model for extrapolations. We now explore the robustness towards extrapolations of the models.

The relevance of studying extrapolations of the models is given by the fact that, for many substances, experimental data is only available for a limited range of conditions. Data for liquid phase thermal conductivities (and often even at a rather narrow range of temperature) are significantly more prevalent than data for low densities. For these circumstances, it may not be possible to adjust meaningful parameters A - D .

Small ranges of temperature and pressure state conditions correspond to a small range of residual entropy s^* . We consider 1-heptanol and artificially limit the experimental data corresponding to a small range of s^* -values representing liquid states. In doing so, we mimic situations where for a substance only narrow conditions are covered experimentally. Practical applications

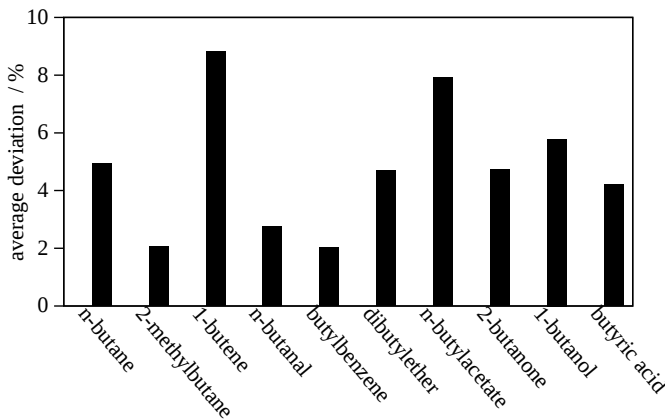


Figure 2.13: Absolute average deviations of calculated to experimental thermal conductivities for various butane derivatives, as calculated using $\lambda_{\alpha, scale}^{ref}$.

then rely on extrapolations either to low densities, or to conditions of low temperature and high pressure, meaning to high densities. For 1-heptanol, the availability of rather comprehensive experimental data allows to assess extrapolations subsequently, as Fig. 2.15 presents. The smaller the range of conditions (i.e. for a small range of s^*) considered for adjusting model parameters A to C (with definition $D = 0$), the less reliable are the extrapolation results. The α -LTST and the α -Eucken model lead to strong deviations from the experimental data for extrapolations. The proposed model in comparison, is significantly more well-behaved. For the proposed model, we set $A = 0$, whenever no data for low densities is available. Doing so increases the robustness to extrapolations significantly.

The promising extrapolation behavior shown in this section shall not mask the fact that some uncertainty about the extrapolation behavior to low temperatures and high pressures remains. For some substances, such as for toluene, we obtain decreasing thermal conductivities with decreasing temperature as well as with increasing pressures. For other species, we do not find this trend within the fluid region. The experimental data does not allow to unambiguously clarify the correct behavior for these conditions.

2.5 Conclusions

Entropy scaling relies on a suitable definition of a dimensionless thermal conductivity, where the thermal conductivity is divided by a reference thermal conductivity. Our study shows that entropy scaling does not hold (i.e. the dimensionless thermal conductivity does not show a single-variable dependence

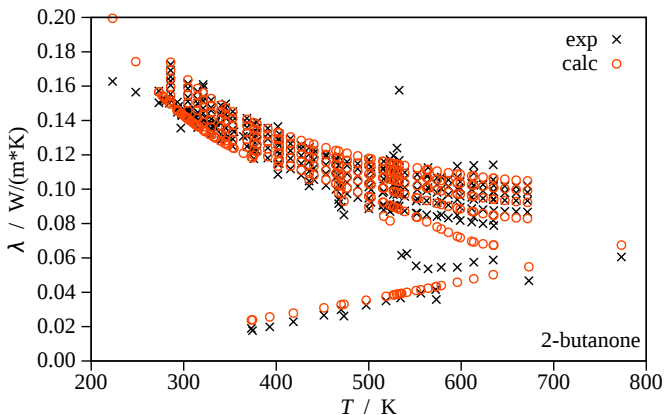


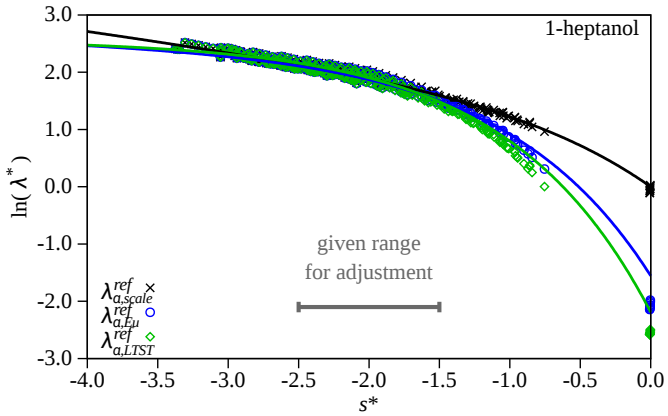
Figure 2.14: Thermal conductivities of 2-butanone. Comparison of experimental data to results from entropy scaling using $\lambda_{\alpha, scale}^{ref}$.

on residual entropy), for obvious choices of the dimensionless thermal conductivity. An exception are mono-atomic components, such as argon. This study proposes an expression for the reference thermal conductivity that is itself a function of the residual entropy. With this definition, we find good results for entropy scaling for the entire fluid region. Entropy scaling is then a powerful method to correlate and predict thermal conductivities of organic substances. We demonstrated good results for several chemical families with 2 to 4 adjustable pure component parameters per species, depending on the range of available experimental data. For 148 substances, we obtain average relative deviations of 4.2% to experimental data. Our approach shows rather robust behavior to extrapolations beyond the state conditions covered by experimental data.

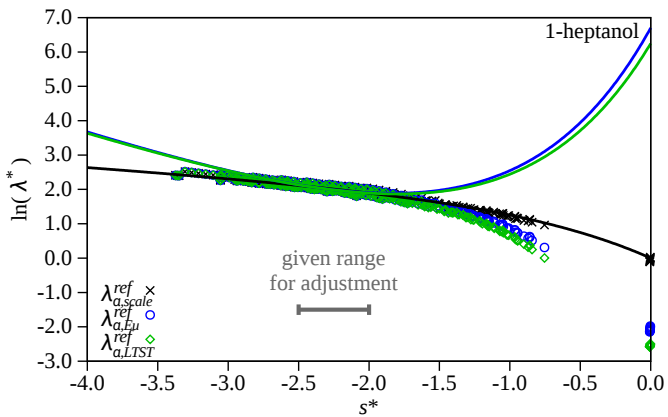
2.5.1 Supporting Information

The supporting information is given in Appendix details (1) the pure component parameters of the PCP-SAFT model for all considered substances, (2) parameters A - D for all substances and for all three references $\lambda_{\alpha, scale}^{ref}$, $\lambda_{\alpha, Eu}^{ref}$, and $\lambda_{\alpha, LTST}^{ref}$. The table (3) also details the absolute average deviations for all considered components and for all three references. Further, (4) the full legend of all 36 substances of Fig. 2.6 is given. Additionally, (5) we include a comparison between results for water using PCP-SAFT and a highly accurate equation of state, and (6) an investigation of entropy scaling for Lennard-Jones Chains as molecular model.

[The supporting information is given in Appendix A of this work.]



(a) parameters $A-C$ adjusted to data limited to $-2.5 < s^* < -1.5$



(b) parameters $A-C$ adjusted to data limited to $-2.5 < s^* < -2.0$

Figure 2.15: Assessing the robustness of extrapolating the entropy scaling approaches, by artificially limiting the range of experimental data. The symbols show all experimental data, the lines represent the correlation, eq. (2.14), obtained by adjusting $A-C$ only to the artificially limited data. Results obtained for all three choices of the reference thermal conductivities are compared (with matching line colour).

Appendix

According to the valuable proposal of an anonymous reviewer, we present an additional possibility for a reference thermal conductivity.

According to the kinetic gas theory as presented by Chapman and Cowling [8], one can decompose the thermal conductivity as $\lambda = \lambda^{\text{tr}} + \lambda^{\text{int}}$, where $\lambda^{\text{tr}} = \lambda^{CE}$ and $\lambda^{\text{int}} = \rho D^{\text{self}} c_v^{\text{int}}$. The contribution to the isochoric heat capacity from internal modes of motion c_v^{int} contains rotational and vibrational modes and can be calculated as $c_v^{\text{int}} = c_v^{ig} - c_v^{\text{tr}} = c_v^{ig} - 1.5R$, so that the reference thermal conductivity reads

$$\lambda_{CCE}^{ref} = \lambda^{CE} + \rho D^{\text{self}} (c_v^{ig} - 1.5R)$$

or, when introducing the transition function α ,

$$\lambda_{\alpha, CCE}^{ref} = \lambda^{CE} + \alpha(s^*) \rho D^{\text{self}} (c_v^{ig} - 1.5R)$$

We consider the approximation by Chapman and Enskog [8, 9], as

$$\rho D^{\text{self}} = \frac{6}{5} \frac{\Omega^{(2,2)}(T^*)}{\Omega^{(1,1)}(T^*)} \frac{\eta^{CE}}{M}$$

The collision integrals Ω with dimensionless temperature $T^* = kT/\epsilon$ are given in ref. [12]. Further, η^{CE} is the Chapman-Enskog viscosity as given in ref [8, 9]. Similar to the results obtained with other expressions for the reference thermal conductivity, the variant without transition function leads to a significant deviation from entropy scaling in the low density limit, as Fig. 2.16 shows. The collapse of data in the ideal gas limit ($s^* \rightarrow 0$) is comparable to the LTST approach, the curvature is less pronounced. The CCE approach leads to mildly lower absolute average deviations than the LTST model. The resulting deviations and correlation parameters A - D are given in the supporting information [in Appendix A of this work].

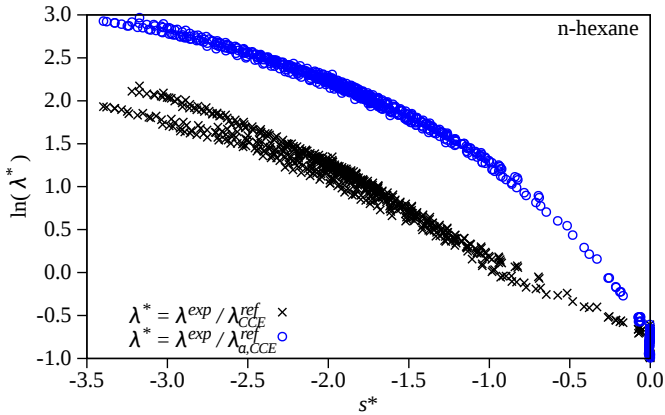


Figure 2.16: Logarithmic reduced thermal conductivity $\lambda^* = \lambda^{exp} / \lambda^{ref}$ versus reduced residual entropy s^* . The symbols denote experimental data, reduced by $\lambda^{ref} = \lambda_{CCE}^{ref}$ (black x) or by $\lambda^{ref} = \lambda_{\alpha,CCE}^{ref}$ (blue o). The reduced residual entropy s^* is calculated from PCP-SAFT according to given temperature and pressure, as defined in eq. (2.1).

Bibliography

- [1] DDBST Dortmund Data Bank Software & Separation Technology GmbH, Oldenburg, Germany, 2015. <http://www.ddbst.com>.
- [2] Y. Rosenfeld, "Relation between the transport coefficient and the internal entropy of simple systems," *Phys. Rev.*, vol. 15, no. 6, pp. 2545–2549, 1977.
- [3] Y. Rosenfeld, "Comments on the transport coefficients of dense hard core systems," *Chem. Phys. Lett.*, vol. 48, no. 3, pp. 467 – 468, 1977.
- [4] Y. Rosenfeld, "A quasi-universal scaling law for atomic transport in simple fluids," *J. Phys.: Condens.*, vol. 11, pp. 5415–5427, 1999.
- [5] G. Galliero and C. Boned, "Thermal conductivity of the lennard-jones chain fluid model," *Phys. Rev. E*, vol. 80, p. 061202, 2009.
- [6] G. Galliero, C. Boned, and J. Fernandez, "Scaling of the viscosity of the lennard-jones chain fluid model, argon, and some normal alkanes," *J. Chem. Phys.*, vol. 134, no. 6, pp. 064505(1–8), 2011.
- [7] O. Lötgering-Lin and J. Gross, "Group contribution method for viscosities based on entropy scaling using the perturbed-chain polar statistical associating fluid theory," *Ind. Eng. Chem. Res.*, vol. 54, no. 32, pp. 7942–7952, 2015.
- [8] S. Chapman and T. G. Cowling, *The Mathematical Theory of Non-Uniform Gases*. Cambridge University Press, 3 ed., 1970.
- [9] J. O. Hirschfelder, C. F. Curtiss, and B. R. B., *Molecular Theory of Gases and Liquids*. John Wiley & Sons, Inc., 1954.
- [10] L. T. Novak, "Self-diffusion coefficient and viscosity in fluids," *Int. J. Chem. React. Eng.*, vol. 9, no. A63, pp. 1–25, 2011.
- [11] L. T. Novak, "Fluid viscosity-residual entropy correlation," *Int. J. Chem. React. Eng.*, vol. 9, p. A107, 2011.
- [12] P. Neufeld, A. Janzen, and R. Aziz, "Empirical equation to calculate 16 of the transport collision integrals $\omega^{(l,s)*}$ for the lennard-jones (12-6) potential," *J. Chem. Phys.*, vol. 57, no. 3, pp. 1100 – 1102, 1972.

- [13] Z. Liang and H.-L. Tsai, "The vibrational contribution to the thermal conductivity of a polyatomic fluid," *Mol. Phys.*, vol. 108, no. 13, pp. 1707–1714, 2010.
- [14] L. I. Stiel and G. Thodos, "The self-diffusivity of dilute and dense gases," *Can. J. Chem. Eng.*, vol. 43, pp. 186–190, 1965.
- [15] R. L. Rowley, W. V. Wilding, J. L. Oscarson, Y. Yang, N. A. Zundel, T. E. Daubert, and R. P. Danner *DIPPR Data Compilation of Pure Chemical Properties*. Design Institute for Physical Properties, AIChE: New York, NY, 2009.
- [16] J. Gross and G. Sadowski, "Perturbed-chain saft: An equation of state based on a perturbation theory for chain molecules," *Ind. Eng. Chem. Res.*, vol. 40, pp. 1244–1260, 2001.
- [17] O. Lötgering-Lin, A. Guthke (geb. Schöniger), W. Nowak, and J. Gross, "Bayesian model selection helps to choose objectively between thermodynamic models: A demonstration of selecting a viscosity-model based on entropy scaling," *Ind. Eng. Chem. Res.*, vol. 55, no. 38, pp. 10191–10207, 2016.
- [18] B. L. Neindre, R. Tufeu, P. Bury, and J. V. Sengers, "Thermal conductivity of carbon dioxide and steam in the supercritical region," *Ber. Bunsen.*, vol. 77, no. 4, pp. 262–275, 1973.
- [19] B. W. Tiesinga, E. P. Sakonidou, H. R. van den Berg, J. Luettmer-Strathmann, and J. V. Sengers, "The thermal conductivity of argon in the critical region," *J. Chem. Phys.*, vol. 101, no. 8, pp. 6944–6963, 1994.
- [20] J. Luettmer-Strathmann, J. V. Sengers, and G. A. Olchowy, "Non-asymptotic critical behavior of the transport properties of fluids," *J. Chem. Phys.*, vol. 103, no. 17, pp. 7482–7500, 1995.
- [21] E. P. Sakonidou, H. R. van den Berg, C. A. ten Seldam, and J. V. Sengers, "The thermal conductivity of methane in the critical region," *J. Chem. Phys.*, vol. 105, no. 23, pp. 10535–10555, 1996.
- [22] R. A. Perkins, J. V. Sengers, I. M. Abdulagatov, and M. L. Huber, "Simplified model for the critical thermal-conductivity enhancement in molecular fluids," *Int. J. Thermophys.*, vol. 34, pp. 191–212, 2013.
- [23] F. M. Gumerov, D. G. Amirkhanov, A. G. Usmanov, and B. L. Neindre, "The thermal diffusivity of argon in the critical region," *Int. J. Thermophys.*, vol. 12, no. 1, pp. 67–83, 1991.
- [24] D. J. Searles, D. J. Evans, H. J. M. Hanley, and S. Murad, "Simulations of the thermal conductivity in the vicinity of the critical point," *Mol. Simul.*, vol. 20, pp. 385–395, 1998.

- [25] R. Mustafaev and D. Gabulov, “Experimental study of cumene thermal conductivity at high temperatures and pressures,” *Izvestiya Vysshikh Uchebnykh Zavedenii, Neft i Gaz*, vol. 19(1), p. 46, 1976. Language: Russian.

3 Self-Diffusion Coefficients from Entropy Scaling using the PCP-SAFT equation of state

This chapter is a literal quote of:

M. Hopp, J. Mele, J. Gross: Self-Diffusion Coefficients from Entropy Scaling Using the PCP-SAFT Equation of State, Industrial & Engineering Chemistry Research, 2018, 57, 38, 12942–12950, DOI:10.1021/acs.iecr.8b02406

including the correction given in

M. Hopp, J. Mele, J. Gross: Erratum to “Self-Diffusion Coefficients from Entropy Scaling Using the PCP-SAFT Equation of State”, Industrial & Engineering Chemistry Research, 2019, 58(45), 20857-20857 .

Additions implemented in this chapter compared to the original journal publication are indicated by square brackets.

Specific contributions of the authors of the original publication are as follows: Julia Mele conducted a feasibility study on the application of the Entropy Scaling approach for self-diffusion of pure substances under my supervision as part of her master thesis. She implemented and compared several models using the PCP-SAFT EOS.

I, under the supervision of Joachim Gross, defined the final model for the calculation of self-diffusion coefficients of pure substances and conducted the calculations as well as the comprehensive study of 133 substances considered in this chapter.

This study proposes a model for self-diffusion coefficients of pure substances from entropy scaling using the Perturbed-Chain Polar Statistical Associating Fluid Theory (PCP-SAFT) equation of state. In accordance with the entropy scaling approach proposed by Y. Rosenfeld [Phys. Rev. A 1977, 15, 2545-2549], we observe that the self-diffusion coefficient of real substances, once made dimensionless with an appropriate expression, only depends on residual entropy. The proposed model requires 3 parameters for each pure substance. For substances with scarce experimental data, however, a scheme is proposed to estimate one or two of these parameters. We study 133 substances from more than 14 different chemical families and find average absolute deviations of 8.2% between the proposed model and experimental data (9992 data points). The model shows satisfying robustness for extrapolating self-diffusion coefficients to conditions rather distant from state points where experimental data is available.

3.1 Entropy Scaling and Reference Self-Diffusion Coefficients

The entropy scaling principle, as proposed by Rosenfeld [1, 2], states that a dimensionless transport property, here self-diffusion coefficient D , is only a function of residual entropy s^{res} , as

$$\ln(D^*) = \ln\left(\frac{\rho D^{calc}}{\rho D^{ref}}\right) = f(s^*) \quad (3.1)$$

with number density ρ in unit m^{-3} or in \AA^{-3} .

In our preceding studies on shear viscosity [3–5] and thermal conductivity [6] we found it useful to define a reduced residual entropy as

$$s^* = s^{res}/(k_B m) \quad (3.2)$$

because the entropy scaling behavior with the so-defined residual entropy is rather similar for various substances. We use the Perturbed-Chain Polar Statistical Associating Fluid Theory (PCP-SAFT) equation of state [7, 8] to calculate the molar residual entropy s^{res} . Quantity m in eq. (3.2), is a pure component parameter of the PCP-SAFT model, representing the number of segments of a molecule. Dividing s^{res} by m leads to similar ranges of s^* -values for different substances. Alternatively, the molar mass M could be used to achieve a similar behavior. Quantity k_B is Boltzmann’s constant.

In the outset, it is unclear how to best define the dimensionless transport property $D^* = (\rho D)/(\rho D^{ref})$. A decisive decision for developing a reliable entropy scaling approach is the decision about how to define the reference value, here, the reference self-diffusion coefficient D^{ref} in eq. (3.1). We analyze six possible approaches for D^{ref} from literature, as summarized in table 3.1. Most of them were developed for the direct calculation of self-diffusion coefficients, not as reference quantities.

In his original work, Rosenfeld [1, 2] proposed using a combination of macroscopic parameters (ρ, T) from elementary kinetic theory as an expression for the reference self-diffusion coefficient D^{ref} . This combination of parameters (table 3.1) simply represents the average translational velocity and the third root of density. Dzугutov [9] chose the collision frequency according to Enskog theory [12] and the hard sphere diameter σ as scaling units of time and length, whereas Krekelberg [10] proposed a scaling approach using the second virial coefficient.

Those three approaches show a similar behavior when used as reference self-diffusion D^{ref} in an entropy scaling approach. For all three definitions of D^{ref} (i.e. D^R , D^D , D^K), a mono-variable behavior of $\ln(D^*)$ with respect to s^* is achieved, which is almost linear in the liquid phase (i.e. $|s^*|$ large), but $\ln(D^*)$ diverges in the gaseous phase ($|s^*| \rightarrow 0$). For our purpose of devising

Table 3.1: Expressions considered as candidates for the reference self-diffusion coefficient D^{ref} in the entropy scaling approach, eq. (3.1).

Author	Equation
Rosenfeld [1]	$D^R = \rho^{-1/3} \sqrt{RT/M}$
Dzugutov [9]	$D^D = 4\pi\sigma^4 g(\sigma)\rho \sqrt{RT/(\pi M)}$
Krekelberg [10]	$D^K = \frac{3}{8\sigma^2} (B + T \frac{dB}{dT}) \sqrt{RT/(\pi M)}$
Bretonnet [11]	$D^B = \frac{3}{8\sigma^2\rho} \frac{(1-\varphi)^4}{1+0.5\varphi} e^{\frac{6\varphi}{1-\varphi}} \sqrt{RT/(\pi M)}$
Chapman, Enskog [12, 13]	$D^{CE} = \frac{3}{8\sigma^2\rho} \frac{1}{\Omega^{(1,1)*}} \sqrt{RT/(\pi Mm)}$
Longuet-Higgins, Pople [14]	$D^{LH} = \frac{3}{8\sigma^2\rho} \sqrt{RT/(\pi M)}$

Reference self-diffusion coefficients D^{ref} in unit m^2/s , with: number density ρ in m^{-3} ; Gas-constant R in $\text{J}/(\text{molK})$; temperature T in K ; molecular mass M in kg/mol ; radial distribution function at contact distance $g(\sigma)$ (dimensionless); Second Virial coefficient B in m^3 ; quantity σ is usually a representative molecular diameter, but is here defined as the segment diameter-parameter σ of the PCP-SAFT equation of state in unit m ; packing fraction $\varphi = \frac{\pi}{6}\rho\sigma^3$ (dimensionless); reduced collision integral [12, 15] $\Omega^{(1,1)*} = f(T^*)$ with dimensionless temperature here defined as $T^* = k_B T/\epsilon$ with PCP-SAFT energy parameter ϵ/k_B in K .

a simple approach with few adjustable parameters suitable for the entire fluid region (and a predictive approach in future work), we much prefer a non-divergent entropy-scaling behavior at the ideal gas limit. We thus analyze other approaches in more detail.

Henceforth, for comparing expressions for the reference diffusion coefficient D^{ref} , we will speak of ‘*good entropy scaling behavior*’ when experimental data for the self-diffusion coefficient of a considered substance, once made dimensionless with D^{ref} , collapses to a single line with residual entropy s^* only. We speak of ‘*deviation from entropy scaling*’ when experimental data does not collapse to monovariabe dependence with residual entropy.

Based on Dzugutov’s scaling method, Bretonnet [11] used the packing fraction $\varphi = \frac{\pi}{6}\rho\sigma^3$ to relate the residual entropy to the radial distribution function. His approach was developed for dense fluids. When this expression is applied for D^{ref} in entropy scaling, we observed deviations from entropy scaling for the liquid phase. In contrast to Rosenfeld’s, Dzugutov’s, and Krekelberg’s approaches, however, a favorable non-divergent scaling behavior in the gaseous phase is found.

The Chapman-Enskog (CE) equation [12, 13] leads to a good entropy scaling behavior for liquid and vapor phase, without divergence in the low-density limit. The CE model was developed from kinetic gas theory and is usually suitable for low densities. The approach assumes mono-atomic, non-polar, rigid spherical molecules at dilute gas states, i.e. at moderate pressure. Novak [16] already showed the applicability of the CE equation as reference for self-diffusion in entropy scaling for some alkanes, argon and ethylene. Further, he suggested the CE equation to reduce viscosities [17–19]. In our previous work, we observed a robust behavior of the entropy-scaling approach for shear viscosities using the CE equation (but then for viscosity) [3–5]. The reduced collision integral $\Omega^{(1,1)*}$ in the CE approach, table 3.1, is calculated using an expression from Neufeld et al. [15] for the Lennard-Jones 12-6 potential. We found the CE model superior to the approach from Bretonnet when comparing the entropy scaling behavior of several substances.

The model from Longuet-Higgins and Pople [14] (LH) is based on the fundamental relation for mean square displacement $D = \lim_{t \rightarrow \infty} < r(t)^2 > / (6t)$ with $r(t)$ as the distance coordinate of a labeled molecule from an initial position at time $t = 0$, which can also be expressed as the velocity auto-correlation function. Assuming a hard sphere fluid and a local Maxwellian distribution function, this approach equals Chapman and Enskog’s first approximation. As expected, therefore, the scaling behavior obtained with both, the CE approach and with the LH expression for the reference diffusion coefficient D^{ref} is very similar, as fig. 3.1 shows. Differences between both approaches appear for example for alcohols, where a more pronounced deviation from monovariabe scaling is found for the gaseous phase for the LH expression than for the CE approach. The entropy scaling behavior in the liquid phase, however, is slightly better for the LH model as compared to the CE model. All in all, we

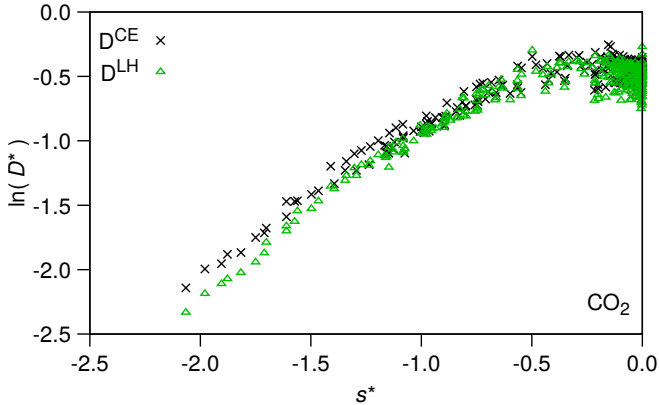


Figure 3.1: Carbon dioxide: Logarithmic reduced experimental self-diffusion $\ln(D^*) = \ln(D^{exp}/D^{ref})$ for varying reduced residual entropy s^* . The symbols represent experimental data, reduced by $D^{ref} \in \{D^{CE}, D^{LH}\}$. The reduced entropy s^* is calculated from PCP-SAFT according to given temperature and pressure, as defined in eq. (3.2). A similar diagram for other expressions for D^{ref} listed in tab. 3.1 is given in the Supporting Information.

found the Chapman-Enskog equation to provide the most suitable description for the reference diffusion coefficient ρD^{ref} as a function of temperature. We use $D^{ref} = D^{CE}$ for the remainder of this work.

Most figures in this work show data of carbon dioxide to exemplify the principles of entropy scaling for the self-diffusion coefficient, because it is one of the few substances with experimental data covering liquid and gaseous conditions. Unfortunately, experimental data for self-diffusion coefficients of pure substances is rather scarce in literature.

3.2 Ansatz Function for Correlating Self-Diffusion Coefficients

We analyzed several pure substances and found an entropy scaling behavior with a systematically non-linear relation between the logarithmic dimensionless self-diffusion coefficient $\ln(D^*)$, with a distinct plateau for s^* approaching zero and a monotonic decrease towards lower values of s^* . As a suitable Ansatz function we propose

$$\ln(D^*) = \ln\left(\frac{\rho D^{calc}}{\rho D^{ref}}\right) = a - b(1 - \exp(s^*))s^{*2} + cs^{*3} \quad (3.3)$$

to describe the relation between the reduced self-diffusion D^* and reduced residual entropy s^* . The three pure component parameters a , b and c have to be adjusted to experimental data for every pure substance. In the adjustment of parameters a - c , we omit experimental points lying within 10% around T_{crit} and p_{crit} , the calculated temperature and pressure at the critical point. That is done, because PCP-SAFT is in our work not parametrized enforcing the critical point of a pure component and higher experimental inaccuracies are expected near the critical point. It is important to note, however, that all data, including near-critical data, are considered for calculating deviations between the proposed model and experimental data in this work. Near-critical data is also included in all figures. Fig. 3.2 compares our entropy scaling model, eq. (3.3), to experimental data of self-diffusion coefficients (made dimensionless using the Chapman-Enskog expression for reference values D^{ref}).

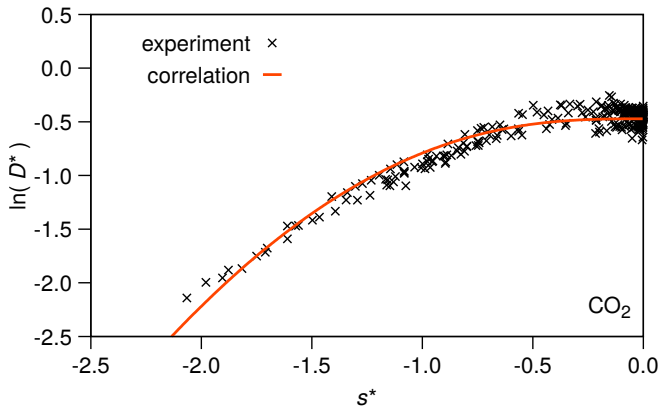


Figure 3.2: Carbon dioxide: Logarithmic reduced self-diffusion $\ln(D^*) = \ln(D/D^{CE})$ for varying reduced residual entropy s^* . The symbols denote experimental data. The red line represent the correlation function, eq. (3.3).

Once parameters a - c are adjusted to experimental data, values for the self-diffusion coefficients can easily be calculated from

$$\begin{aligned}
 D^{calc} &= D^{ref} \cdot D^* \\
 &= D^{ref} \cdot \exp\{a - b(1 - \exp(s^*))s^{*2} + cs^{*3}\}
 \end{aligned}
 \tag{3.4}$$

Through the residual entropy $s^*(T, p)$, as calculated from the PCP-SAFT model, it is thus possible to calculate the self-diffusion coefficient of the considered substance at any temperature and pressure conditions in the entire fluid, as done in Fig. 3.3.

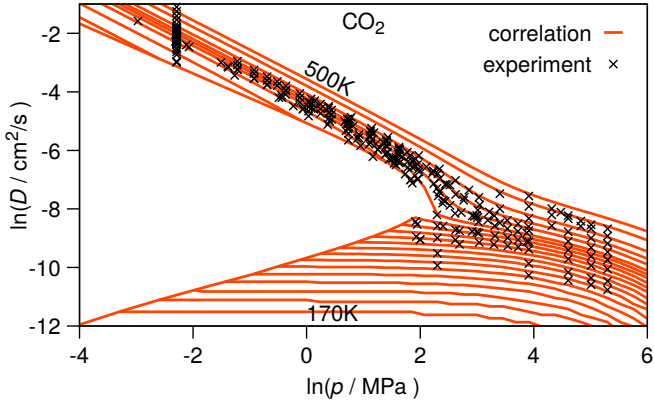


Figure 3.3: Self-diffusion coefficient of carbon dioxide. Symbols represent experimental data. Red lines are calculated isotherms, using the correlation function, eq. (3.3).

3.2.1 Robustness of Parameterizing the Entropy Scaling Model

For substances with scarce experimental data it is necessary to introduce additional rules for identifying meaningful parameters a - c . In order to describe the rules, we define two ranges in residual entropy:

The total range of residual entropy that is covered by experimental data of a considered substance is defined as $\Delta s^* = s_{max}^* - s_{min}^*$, with s_{min}^* and s_{max}^* as the minimal and the maximal value of residual entropy as calculated from the PCP-SAFT model, $s^*(T, p)$, for all experimental conditions of temperature T and pressure p . Additionally, we define the mid-value of the s^* -range covered by experimental data, as $\bar{s}^* = 0.5(s_{min}^* + s_{max}^*)$.

Because experimental data for gaseous conditions is only available for few substances, we propose a method to estimate parameter a in the absence of low density data. From an analysis of all substances with gaseous data available, we observed a dependence of a on the PCP-SAFT segment number m . We therefore propose to define parameter $a = 0.175 - 0.237m$ for all substances with $s_{max}^* < -1$ or $\Delta s^* < 0.4 \cdot \bar{s}^*$, where the last criterion concerns a too narrow s^* -range for reliably extrapolating existing data to the ideal gas limit $s^* = 0$. We limit this definition to substances with $m < 15$, since, for higher m we assume an asymptotic behavior but are missing data to verify our assumption. Substances with low critical temperatures, such as oxygen or nitrogen, with scarce experimental data for the self-diffusion coefficient in liquid phase, require particular attention in parameterization. To ensure the typical shape of the entropy scaling correlation for cases where liquid data is absent, we define an additional rule for parameter b . We propose

$b = 0.1m$ if $s_{min}^* \geq -1$. Furthermore, for components with experimental data for self-diffusion coefficients D in a narrow range of residual entropies, we define $c = 0.0$, whenever $\Delta s^* < 0.5$ or $s_{min}^* > -2$. Parameter c is then only adjusted if data for the liquid phase is available and for a sufficiently wide range of s^* . Parameters b and c are constrained to positive values. The criteria imply that parameters a and c are defined (i.e. not adjusted) for cases where experimental data only exists in a narrow range of s^* , and thus a narrow range of T and p , leaving only one adjustable parameter for those substances. In any case, at least one parameter has to be adjusted to experimental data for any given substance.

To assess the robustness of the proposed scheme for adjusting or predefining the parameters a - c of correlation function eq. (3.3), we mimic a case with experimental data available only in the liquid phase. We consider ethylene and ignore all data except for data in a liquid range, as visualized in Fig. 3.4. The situation we regard is representative for many substances where only limited experimental data in the liquid phase is available. In this case, only parameter b and c of the proposed entropy scaling model were adjusted to data in the liquid phase, whereas parameter a was defined (with $a = 0.175-0.237m$, as discussed above). Fig. 3.4 shows good agreement of the so-parameterized model to experimental data in the full range of residual entropy and thus rather robust extrapolation behavior.

A table with the resulting parameters a - c for all substances is given in the Supporting Information. Despite the encouraging test of how the proposed model extrapolates to conditions not covered by experimental data, we have some reservation about predicting self-diffusion coefficients in the gas phase, because we only have 20 substances with experimental data in the gas phase, with 4 of them missing data in the liquid phase. To clarify the behavior of the self-diffusion coefficient in gaseous phase, we consider using molecular simulations for a wide range of substances in future work.

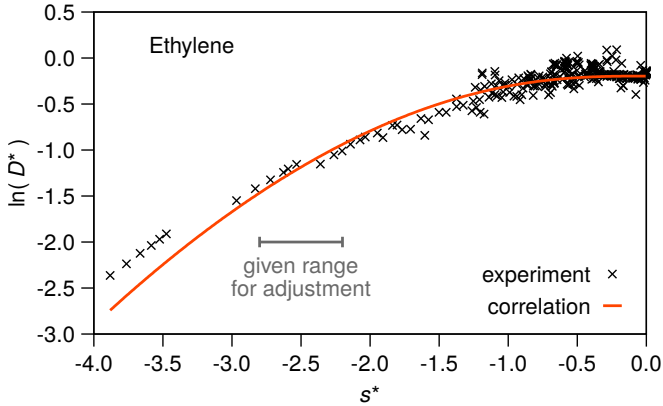


Figure 3.4: Assessment of the robustness towards extrapolation in s^* , by artificially limiting the range of experimental data. The symbols show all experimental data for ethylene. The line represents the adjusted correlation function, eq. (3.3) adjusted only to data in the indicated range of consideration ($-2.8 < s^* < -2.2$). The selected range of data for adjustment corresponds to typical experimentally given liquid phase conditions. Only parameters b and c were adjusted, parameter a was defined as discussed above.

3.2.2 Subcooled Liquids

In our study, data of subcooled liquid conditions were found for 7 substances: toluene, 1-2-diphenylbenzene, propylenecarbonate, methylformamide, methanol, 1,2,3-propantriol and water. Fig. 3.5 confirms that self-diffusion coefficients of subcooled liquids obey the entropy scaling principle, showing a monovari-able dependence $D^*(s^*)$, but with a strong increase in slope at increasingly negative s^* . For correlating the data including the subcooled conditions, an substitution to the correlation function, eq. (3.3), is proposed, as follows

$$\ln(D^*) = \ln\left(\frac{\rho D^{calc}}{\rho D^{ref}}\right) = a - b(1 - \exp(s^*))s^{*2} - c(1 - \exp(-ds^*)) \quad (3.5)$$

The substitution of cs^{*3} from eq. (3.3) by $c(1 - \exp(-ds^*))$ in eq. (3.5) allows stronger increases in slope, but needs one additional parameter. Furthermore, the parameters c and d [of eq. (3.5)] are highly sensitive to their corresponding starting values [used for adjustment] and therefore result in a less robust extrapolation capacity. Due to these reasons, we refrain from using eq. (3.5) as universal correlation function. The rules for defining or adjusting parameters a and b nevertheless remain valid.

Using the extended entropy scaling model, eq. (3.5), the entire fluid region,

including the subcooled region can be described with good agreement to experimental data, as confirmed for toluene in Fig. 3.5.

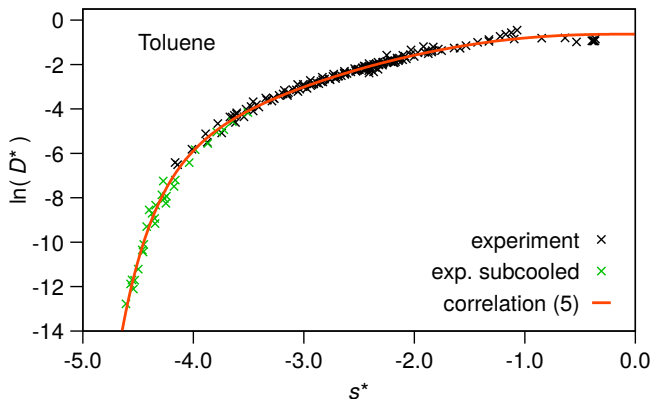


Figure 3.5: Toluene: Logarithmic reduced self-diffusion $\ln(D^*) = \ln(D/D^{CE})$ versus reduced residual entropy s^* . The green crosses denote data of subcooled states; black crosses show experimental data of stable (non-subcooled) states. The line represents the correlation function, eq. (3.5). Absolute average deviations: 13.76% (170 points) when neglecting subcooled data and using eq. (3.3); 12.76% (199 points) when using eq. (3.5) and subcooled data.

3.3 Results and Discussion

In this section, we parameterize and investigate 133 substances from more than 14 chemical families.

We generally used all experimental data we found in literature, independent of measurement technique or date of publication. Data published in older references were occasionally published without explicit mention of measurement pressure. In these cases, we assumed atmospheric pressure. We neglected experimental data for pressure conditions greater than 100MPa, because of increasing uncertainties in calculated residual entropies from the PCP-SAFT model at very high pressures. For substances with many sources, we neglected data from sources which showed obvious, pronounced inconsistencies compared to other data points. Individual outliers from otherwise seemingly reliable sources were not removed. For some substances, we found experimental data from different literature references giving contradicting entropy scaling curves, whereof none could be removed with sufficient confidence. We kept all data for these cases. In summary, although entropy scaling is rather

powerful in identifying outliers, we pursue a rather conservative approach for excluding experimental data.

A graphical representation of results from the proposed entropy scaling model for self-diffusion coefficients is given for three (of the 133 considered) substances. We exemplarily present results for xenon (Fig. 3.6(a), AAD 5.4%, 197 points) as a nonpolar substance, for 1-propanol (Fig. 3.6(b), AAD 5.1%, 147 points) as a moderately polar component, and for water (Fig. 3.6(c), AAD 12.9%, 687 points without / 17.6%, 804 points with data for subcooled liquid conditions) as a highly polar, hydrogen-bonding substance. We here use averaged absolute deviations (AAD) as a measure of error. The data for xenon does not satisfactorily collapse onto a single line, which could indicate limitations of the entropy scaling principle. From the experience with other substances, however, we suspect that the scattered data is indeed due to errors in the experimental data.

That assessment is supported by the observation that several experimental points of different authors reported for the same combination of temperature and pressure vary by 5 to 15%. 1-Propanol is a substance where self-diffusion coefficients for the gas phase are not available, to our knowledge. The entropy scaling model can be used to predict self-diffusion coefficients in the gas phase. For water, we found a very pronounced increase in slope for highly negative values of s^* even when data for subcooled liquid conditions were excluded. We thus applied correlation eq. (3.5) for water even when neglecting subcooled data. The results for all three substances show good agreement of the proposed model for the self-diffusion coefficient with an effectively monovariabile dependence of D^* on s^* .

To assess the effect of chain length, roughly every second n-alkane from C_1 to C_{36} is shown in Fig. 3.7. With increasing chain length the curvature increases and the ordinate intercept decreases. For n-alkanes, we found experimental data in gaseous phase for methane and ethane only. For those two, and for n-alkanes where experimental data covers a sufficiently large range of residual entropy (namely C_3 - C_{10} , C_{12} - C_{14} , C_{16} , C_{18} and C_{30}), the a parameter (defining the intercept) was adjusted. The criterion for predefining the a -parameter (as discussed in section *Robustness*) was activated for all other n-alkanes.

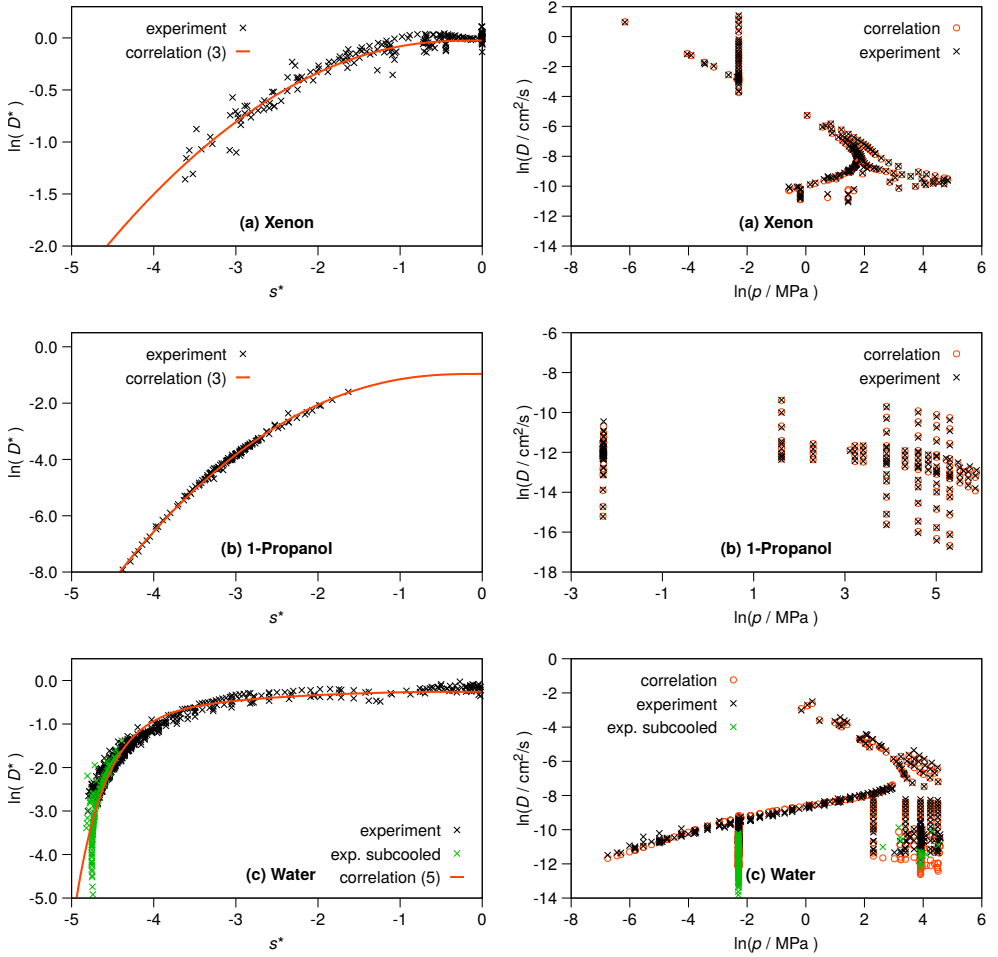


Figure 3.6: Xenon, 1-propanol, and water: Logarithmic reduced self-diffusion $\ln(D^*) = \ln(D/D^{CE})$ versus reduced residual entropy s^* as well as self-diffusion coefficients for varying pressure. Comparison of the proposed entropy scaling model (red line and red circles), eq. (3.3) to experimental data (crosses). Black and green crosses are experimental data. Red circles are the corresponding calculated values.

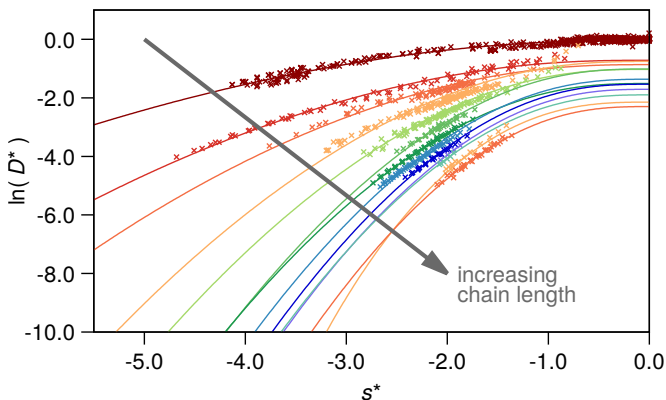


Figure 3.7: Several n-alkanes: Logarithmic reduced self-diffusion $\ln(D^*) = \ln(D/D^{CE})$ versus reduced residual entropy s^* . The symbols denote experimental data, lines represent the corresponding correlation functions, eq. (3.3).

Figure 3.8 presents deviations (as AAD%) of calculated to experimental self-diffusion coefficients. We show deviations in two different ways. The blue histogram as well as the blue circles connected with a solid blue line are the AAD% values. As a measure for the distribution of deviations, we additionally present box-and-whisker marks of the AAD%. In that representation, 50% of all data points fall within the box, and the bottom and top edge of the box correspond to the first and third quartiles (i.e., 25% and 75% of the data points), respectively. The range from the bottom of the box to the lower end of the whisker represents the AAD% range where the 25% of the data points with the lowest AAD% values lie. The upper end of the upper whisker represents the 90% value (i.e., 90% of data points have an AAD% value lower than this value). The red band inside the box gives the median (i.e., 50% of data points have an AAD% value lower than this value and vice versa).

The results of all 133 substances considered in this study grouped into 14 chemical families are summarized in Fig. 3.8(a). The group titled 'others' contains substances from chemical groups with less than 3 representatives. The overall agreement for all 133 compounds is rather satisfying with average deviations of 8.2%. A table listing absolute average deviations of all available substances individually is given in the Supporting Information.

The absolute average deviations of n-alkanes are regarded individually in Fig. 3.8(b) to investigate how the proposed model performs for increasingly non-spherical fluids, up to C36. The diagram shows no systematic increase in deviations for larger alkanes and thus confirms that the model is robust for increasingly non-spherical fluids.

In Fig. 3.8(c) we collect all substances with available data at subcooled liquid states. The average errors are somewhat higher than typically found with the proposed approach. Considering the width of state point conditions covered for these substances, however, we still consider the proposed model in satisfying agreement to the experimental data.

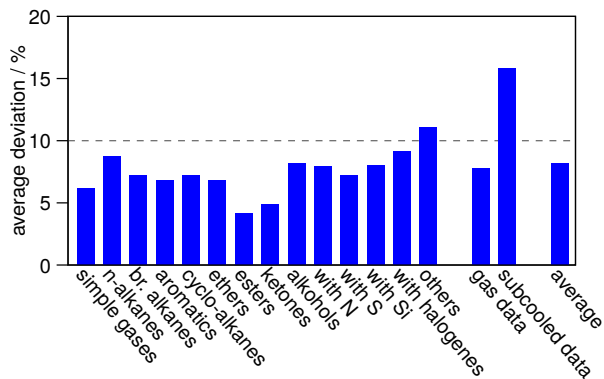
We emphasize that our work aims at a model possessing some robustness to extrapolation with a low number of adjustable parameters. We wish to provide a simple but reasonable estimation for transport properties at state points with lacking experimental data. If a higher accuracy is required, of course, the polynomial order can be increased, which leads to a higher number of parameters but a less robust extrapolation behavior outside the range given for adjustment. By applying criteria for predefining some of the model parameters (with rules detailed above), thus reducing the number of adjustable parameters, we trade high correlation quality for higher robustness to extrapolations. That is apparent for example for esters, where ignoring the rules for predefining some of the model parameters leads to an absolute average deviation of 3.51%, instead of 4.17%.

Generally, we observe a relatively high variance of the available experimental data especially across experimental data from different literature references. Although, as a theoretical study, we have to be conservative about assessing experimental data, we came to belief that much of the scatter seen in our approach is not due to severe limitations of the entropy scaling approach, but is rather caused by deviations and uncertainty in the available experimental data. Taking the skepticism about the available data into account (and the fact that contradicting experimental data exists), we consider the correlation results of the proposed model as rather satisfying.

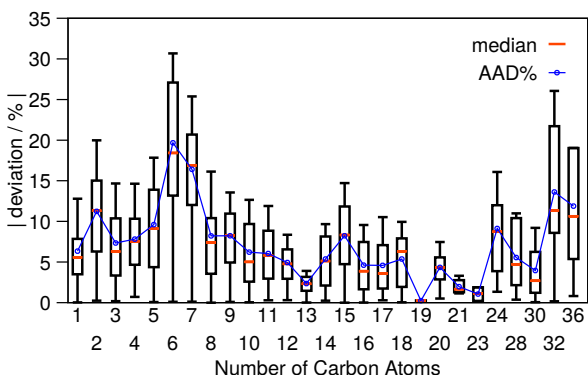
To arrive at an entirely predictive approach, we consider the development of a group contribution approach for the self-diffusion coefficient in future work.

3.4 Conclusion

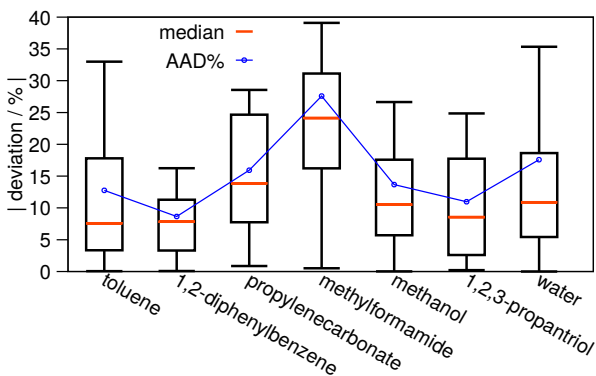
This study proposes a model for the self-diffusion coefficient of pure substances. The model is based on entropy scaling and is applicable for the entire fluid region, even including subcooled liquid conditions. We investigate 133 substances from more than 14 different chemical families and emphasize the robustness in correlating and extrapolating self-diffusion coefficients to conditions rather distant from state points where experimental data is available. The overall average deviations for all 133 compounds is 8.2%, which we assess as rather satisfying. For all considered n-alkanes (27 substances, 2082 points) we achieve an average deviation of 8.7%; for all non-polar and non-associating substances (55 components, 4604 points) 7.3%; for all polar but non-associating substances (51 species, 1381 points) 8.8%; and for all polar and associating components (27 substances, 1925 points) 9.8%.



(a) groups of substances



(b) n-alkanes



(c) substances with data for subcooled liquid conditions

Figure 3.8: Absolute average deviations of calculated to experimental self-diffusion coefficients (a) for all 133 substances averaged across chemical groups. (b) Box-and-Whisker representation of the distribution of deviations for the homologous series of n-alkanes, and (c) for substances with data for subcooled liquid conditions. Circles, connected with a solid line, are the AAD% of each substance.

Supporting Information

This material is available free of charge via the Internet at <http://pubs.acs.org>. The Supporting Information details (1) the pure component parameters of the PCP-SAFT model for all considered substances, including the origin of experimental data. (2) we summarize the parameter rules described in section *Robustness* and clarify them using a diagram. (3) the parameters *a-c* including the absolute average deviations for all considered substances are tabulated. Further, (4) the results and parameters of the enhanced model for substances with data at subcooled liquid conditions are given. Additionally, (5) we provide a similar diagram as Figure 1 for all approaches for the reference self-diffusion coefficient given in Table 1.

[The supporting information is given in Appendix B of this work.]

Bibliography

- [1] Y. Rosenfeld, "Relation between the transport coefficient and the internal entropy of simple systems," *Phys. Rev.*, vol. 15, no. 6, pp. 2545–2549, 1977.
- [2] Y. Rosenfeld, "A quasi-universal scaling law for atomic transport in simple fluids," *J. Phys.: Condens.*, vol. 11, pp. 5415–5427, 1999.
- [3] O. Lötgering-Lin and J. Gross, "Group contribution method for viscosities based on entropy scaling using the perturbed-chain polar statistical associating fluid theory," *Ind. Eng. Chem. Res.*, vol. 54, no. 32, pp. 7942–7952, 2015.
- [4] O. Lötgering-Lin, A. Guthke (geb. Schöniger), W. Nowak, and J. Gross, "Bayesian model selection helps to choose objectively between thermodynamic models: A demonstration of selecting a viscosity-model based on entropy scaling," *Ind. Eng. Chem. Res.*, vol. 55, no. 38, pp. 10191–10207, 2016.
- [5] O. Lötgering-Lin, M. Fischer, M. Hopp, and J. Gross, "Pure substance and mixture viscosities based on entropy scaling and an analytic equation of state," *Ind. Eng. Chem. Res.*, vol. 57, no. 11, pp. 4095–4114, 2018.
- [6] M. Hopp and J. Gross, "Thermal conductivity of real substances from excess entropy scaling using pcp-soft," *Ind. Eng. Chem. Res.*, vol. 56, no. 15, pp. 4527–4538, 2017.
- [7] J. Gross and G. Sadowski, "Perturbed-chain SAFT: An equation of state based on a perturbation theory for chain molecules," *Ind. Eng. Chem. Res.*, vol. 40, pp. 1244–1260, 2001.
- [8] J. Gross and J. Vrabec, "An equation-of-state contribution for polar components: Dipolar molecules," *AIChE J.*, vol. 52, pp. 1194 – 1204, 2006.
- [9] M. Dzugasov, "A universal scaling law for atomic diffusion in condensed matter," *Nature*, vol. 381, pp. 137 – 139, 1996.
- [10] W. P. Krekelberg, M. J. Pond, G. Goel, V. Shen, J. R. Errington, and T. M. Truskett, "Generalized rosenfeld scalings for tracer diffusivities in not-so-simple fluids: Mixtures and soft particles," *Phys. Rev.*, vol. 80, no. 6, pp. 061205(1–13), 2009.

- [11] J.-L. Bretonnet, "Self-diffusion coefficient of dense fluids from the pair correlation function," *Journal of chemical Physics*, vol. 117, no. 20, pp. 9370–9373, 2002.
- [12] S. Chapman and T. G. Cowling, *The Mathematical Theory of Non-Uniform Gases*. Cambridge University Press, 3 ed., 1970.
- [13] J. O. Hirschfelder, C. F. Curtiss, and R. B. Bird, *Molecular Theory of Gases and Liquids*. New York: John Wiley & Sons, Inc., 4 ed., 1954.
- [14] H. C. Longuet-Higgins and J. A. Pople, "Transport properties of a dense fluid of hard spheres," *J. Chem. Phys.*, vol. 25, no. 5, pp. 884–887, 1956.
- [15] P. D. Neufeld, A. R. Janzen, and R. A. Aziz, "Empirical equation to calculate 16 of the transport collision integrals $\omega^{(l,s)*}$ for the lennard-jones (12-6) potential," *J. Chem. Phys.*, vol. 57, no. 3, pp. 1100 – 1102, 1972.
- [16] L. T. Novak, "Self-diffusion coefficient and viscosity in fluids," *Int. J. Chem. React. Eng.*, vol. 9, no. A63, pp. 1–25, 2011.
- [17] L. T. Novak, "Fluid viscosity-residual entropy correlation," *Int. J. Chem. React. Eng.*, vol. 9, p. A107, 2011.
- [18] L. T. Novak, "Correction to: Predictive corresponding-states viscosity model for the entire fluid region: n-alkanes," *Ind. Eng. Chem. Res.*, vol. 52, no. 38, pp. 13886–13886, 2013.
- [19] L. T. Novak, "Predicting natural gas viscosity with a mixture viscosity model for the entire fluid region," *Ind. Eng. Chem. Res.*, vol. 52, pp. 16014–16018, 2013.

4 Thermal Conductivity via Entropy Scaling: An Approach that Captures the Effect of Intramolecular Degrees of Freedom

This chapter is a literal quote of:

M. Hopp, J. Mele, R. Hellmann, J. Gross: Thermal Conductivity via Entropy Scaling: An Approach That Captures the Effect of Intramolecular Degrees of Freedom, Industrial & Engineering Chemistry Research, 2019, 58, 39, 18432–18438, DOI:10.1021/acs.iecr.9b03998.

Additions implemented in this chapter compared to the original journal publication are indicated by square brackets.

Specific contributions of the authors of the original publication are as follows: Julia Mele served as a sparring partner in discussions about diffusion and the parts of this chapter which are based on her master thesis, as described in chapter 3.

Robert Hellmann made a thorough review of one of my earlier publications including some deeper questions and ideas. He kindly made himself known after final publication of that manuscript, thus encouraged us to have a further look into the topic of this chapter and helped through fruitful discussions.

I, under the supervision of Joachim Gross, defined and implemented the model and conducted the calculations using the PCP-SAFT EoS as well as the study of 109 pure substances considered in this chapter.

The thermal conductivity of gases depends strongly on the vibrational and rotational degrees of freedom of the molecule under consideration. Entropy scaling is based on the residual entropy, which does not capture the intramolecular and rotational contributions. This study proposes a model for the thermal conductivity that accounts for these degrees of freedom. We use the Chapman–Cowling approximation, where contributions of internal degrees of freedom to the thermal conductivity of an ideal gas are related to the self-diffusion coefficient. A resulting expression for the thermal conductivity is used as a reference in entropy scaling. We find experimental values for thermal conductivities in the entire fluid range to be (to good approximation) a function of residual entropy only. This study shows that entropy scaling is a strong approximation also for thermal conductivity, provided a suitable expression is chosen for the reference thermal conductivity.

4.1 Introduction

Transport properties are required for the design of process equipment [1] and for the optimization of chemical [2, 3] or energy processes [4, 5]. In previous work, we developed predictive methods for the viscosity [6, 7], self-diffusion coefficient, [8] and thermal conductivity [9] of pure substances, as well as for the viscosity of mixtures [7], based on the entropy scaling approach. [10, 11] According to Rosenfeld’s entropy scaling, there is a univariate dependence of transport properties on residual entropy if the transport property is divided by a suitable reference expression. The principle is powerful for developing models for transport properties. The dependence of the dimensionless transport property of a pure substance with residual entropy can be correlated with a surprisingly small number of adjustable parameters, say of a polynomial Ansatz function. The actual transport property can be calculated for any fluid condition of interest by combining this reference quantity with the simple correlation polynomial. An equation of state, here the *perturbed-chain polar statistical associating fluid theory* (PCP-SAFT) equation of state (EoS), [12, 13] is needed to calculate the residual entropy for any given substance at given temperature and pressure.

For thermal conductivities of gas-phase conditions, the internal degrees of freedom (vibration and rotation) have a significant contribution. That is specific to thermal conductivities and is not observed for viscosity and self diffusion coefficients. A special treatment of the reference value of the thermal conductivity is necessary to correctly account for the influence of intramolecular degrees of freedom. If this influence is not accounted for, a strong deviation from the otherwise univariate dependence of thermal conductivity on residual entropy occurs, as was shown in ref [9]. A correction covering the influence of the internal degrees of freedom on the gas-phase thermal conductivity can be described surprisingly well through a simple, quasi-universal function of temperature and molecular structure [9]. But this model fails for molecules with few or no internal degrees of freedom, such as nitrogen or rare gases.

In this work, we propose a reference thermal conductivity for entropy scaling based on an approximate theory by Chapman and Cowling [14, 15]. Using the Chapman-Cowling theory, we physically describe the underlying transport process of energy stored in the internal degrees of freedom as a diffusion process.

4.2 Entropy Scaling

The essence of entropy scaling is a univariate dependence of dimensionless transport properties on residual entropy, only. Rosenfeld [10, 11] originally investigated this dependence for dynamic viscosity η , self-diffusion D^s , and thermal conductivity λ for simple, monatomic fluids. In subsequent studies, it

was found, however, that his approach is applicable to a wide array of model fluids and real substances. [6–9, 16–48]

In this work, the residual entropy is calculated using the PCP-SAFT EoS [12, 13]. As in our preceding studies, [6–9] we define the reduced residual entropy as

$$s^* = s^{\text{res}}/(k_{\text{B}}m) \quad (4.1)$$

with Boltzmann’s constant k_{B} and segment number m of the PCP-SAFT EoS. We have good experience in adopting the segment number m , as a measure for the non-spherical shape of molecules into eq. (4.1) because that leads to similar ranges of s^* values for rather different substances. The dimensionless thermal conductivity λ^* and the dimensionless self-diffusion coefficient D^* are defined as

$$\lambda^* = \lambda/\lambda^{\text{ref}} \quad (4.2)$$

$$D^* = \rho D^{\text{s}}/\rho D^{\text{ref}} \quad (4.3)$$

A sensible choice for a reference thermal conductivity λ^{ref} and for ρD^{ref} is necessary, where D^{ref} is the reference self-diffusion coefficient and ρ is the number density. The advantage of using the product of number density and self-diffusion coefficient is that it has a finite value in the limit of zero density, just like the dynamic viscosity and the thermal conductivity [14].

Following a dimensionality analysis, Rosenfeld [10, 11] proposed $\lambda^{\text{ref}} = \rho^{2/3} k_{\text{B}} \sqrt{k_{\text{B}} T / M'}$ as reference thermal conductivity, with molecular mass M' . In our previous studies, [9] we investigated several possibilities for the reference thermal conductivity λ^{ref} and finally proposed

$$\lambda^{\text{ref},\alpha} = \lambda^{\text{CE}} + \alpha(s^*)\lambda^{\text{int}} \quad (4.4)$$

$$\lambda^{\text{CE}} = \frac{\sqrt{T/(M/m)} 83.235}{\sigma^2 \Omega^{(2,2)*}} \frac{\text{kg}^{3/2} \text{ \AA}^2 \text{ m}}{10^{3/2} \text{ K}^{3/2} \text{ mol}^{1/2} \text{ s}^3} \quad (4.5)$$

$$\lambda^{\text{int}} = (m^2 \sigma^3 \epsilon / k_{\text{B}}) (c_1 T^* + c_2 T^{*2}) \frac{\text{kg m}}{10^5 \text{ s}^3 \text{ \AA}^3 \text{ K}^2} \quad (4.6)$$

$$\alpha(s^*) = \exp(-s^*/s_c^*) = \exp(-s_c^{\text{res}}/s_c^{\text{res}}) \quad (4.7)$$

where T is the temperature and M is the molar mass. Further, m , σ and ϵ/k_{B} are the segment number, size and energy parameters of the intermolecular potential of the PCP-SAFT EoS, respectively, with Boltzmann’s constant k_{B} . Further, $\Omega^{(2,2)*}$ is a reduced collision integral for the Lennard-Jones (LJ) 12-6 fluid as given by Neufeld et al. [49], $T^* = k_{\text{B}} T / \epsilon$ is a reduced temperature, $c_1 = -0.0167141$ and $c_2 = 0.0470581$ are model constants [9], and $s_c^* = s_c^{\text{res}}/(k_{\text{B}}m) = s_c^{\text{res}}(T_c, p_c)/(k_{\text{B}}m)$ is the reduced residual entropy at the critical point calculated from PCP-SAFT. The reference thermal conductivity

ity is divided into the classical contribution $\lambda^{\text{tr}} = \lambda^{\text{CE}}$ covering translational degrees of freedom and a contribution λ^{int} that accounts for internal degrees of freedom, i.e. vibration and rotation. Both contributions are connected by the transition function α .

Using eq. (4.4) for the reference term in eq. (4.2) leads to a benign, nearly univariate dependence of the thermal conductivity λ^* on reduced residual entropy s^* [9]. To correlate this dependence of λ^* on reduced residual entropy s^* we earlier proposed the correlation function [9]

$$\ln(\lambda^*) = A + Bs^* + C[1 - \exp(s^*)] + Ds^{*2} \quad (4.8)$$

with correlation parameters A to D adjusted to experimental data. Correlation parameters for many substances can be found in our previous work [9]. Parameters for all substances not considered in our previous work are given in the Supporting Information. Equation (4.8) can be used to predict thermal conductivities of pure substances outside the range of temperature and pressure used for correlating the parameters A to D . Using the proposed scaling approach $\lambda^{\text{ref},\alpha}$ as given in eq. (4.4) leads to a good description of pure organic fluids from various chemical families [9].

Limitations of the Previous Model $\lambda^{\text{ref},\alpha}$

The term λ^{int} in the reference thermal conductivity, eq. (4.6), accounts for contributions from intramolecular degrees of freedom to the thermal conductivity in low-density fluids. In developing an expression for λ^{int} , we had focused on substances with sufficiently many internal degrees of freedom (bond vibrations and rotational contributions). In our previous work, we applied the term λ^{int} to all substances (through eqs. (4.4) to (4.7)), regardless of the number of intramolecular degrees of freedom a given molecule has. For substances with few internal degrees of freedom, the contribution λ^{int} is not suitable. For rare gases, for example, the contribution should be zero altogether. As a result, for simple substances, such as xenon or nitrogen, the reference $\lambda^{\text{ref},\alpha}$ as suggested earlier [9], is limited to fluid conditions in the liquid phase, where the contribution from λ^{int} becomes negligible. In this work, molecules with a reduced number of internal degrees of freedom (e.g., N_2 , O_2 , and the rare gases) will be referred to as *simple molecules*. Applying $\lambda^{\text{ref},\alpha}$ to simple fluids, as done in Figure 4.1 for xenon and nitrogen, clearly shows the inappropriateness of the model. The Figure reveals strong deviations of the reduced thermal conductivity λ^* from a univariate dependence on the reduced residual entropy s^* for the dilute gas limit ($s^* \rightarrow 0$). If, in contrast, only the classical contribution $\lambda^{\text{ref}} = \lambda^{\text{CE}}$ (eq. (4.5)) is used as reference thermal conductivity, corresponding to $\lambda^{\text{int}} = 0$, one finds very good results for monatomic molecules (rare gases, Figure 4.1 a) and only small deviations for diatomic molecules (e.g., N_2 ; Figure 4.1 b). These results show that monatomic fluids or fluids with

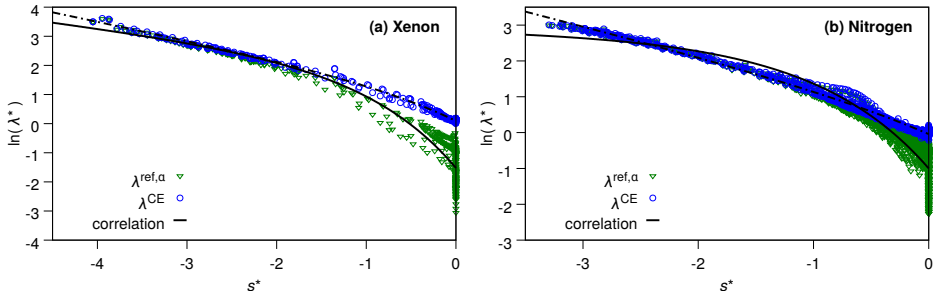


Figure 4.1: Thermal conductivities of xenon and nitrogen, comparing two reference thermal conductivities, namely $\lambda^{\text{ref},\alpha}$ (eq. (4.4)) and λ^{CE} (eq. (4.5)). Logarithmic reduced thermal conductivity $\lambda^* = \lambda/\lambda^{\text{ref}}$ versus reduced residual entropy s^* . The symbols denote results obtained using experimental data for λ . The black lines represent the corresponding correlation function, eq. (4.8).

low number of internal degrees of freedom are not correctly described with the reference thermal conductivity $\lambda^{\text{ref},\alpha}$, according to eq. (4.4).

4.3 Improved Reference Thermal Conductivity

To overcome the limitations of the previously published model for thermal conductivities discussed above, we apply the approximate Chapman and Cowling (CC) theory [14, 15]. The approach assumes that no energy is exchanged between the translational and intramolecular degrees of freedom during collision events between molecules. As a consequence, the energy stored by each molecule in its internal degrees of freedom is effectively conserved and is transported solely by the self-diffusion of the molecule. As in the CE theory, a spherically-symmetric intermolecular potential is assumed in the CC approach. The resulting CC expression for the thermal conductivity reads

$$\lambda^{\text{CC}} = \lambda^{\text{CE}} + \rho D^{\text{CE}} (c_v^{\text{ig}} - 1.5k_B) \quad (4.9)$$

with ideal-gas heat capacity at constant volume c_v^{ig} . The second term subtracts $3/2 \cdot k_B$ from c_v^{ig} to eliminate the contribution due to translational motion of molecules because translational degrees of freedom are already covered by the CE term. Fouad and Vega [29] approximated ρD^{CE} via the CE viscosity as proposed in the CE theory [14, 15], achieving good results for the calculation of saturated and liquid thermal conductivities of hydrofluorocarbon and hydrofluoroolefin refrigerants. Calculations for the gas phase, where the relative influence of the intramolecular degrees of freedom on the thermal

conductivity is the highest, were not shown. To improve the CC approach, we propose, first, to use the full density-dependent self-diffusion coefficients $\rho D^s = \rho D^{\text{ref}} D^*$ instead of the ideal gas contribution ρD^{CE} and, second, use the heat capacities c_v of the substances at the considered state point rather than c_v^{ig} in eq. (4.9), yielding

$$\begin{aligned}\lambda^{\text{ref},\rho D} &= \lambda^{\text{CE}} + \rho D^s (c_v - 1.5k_B) \\ &= \lambda^{\text{CE}} + \rho D^{\text{ref}} (c_v - 1.5k_B) D^*\end{aligned}\quad (4.10)$$

This equation replaces the earlier model, eq. (4.4), in the entropy scaling approach. More specifically, the empirical contribution $\alpha\lambda^{\text{int}}$ of eq. (4.4) is not needed any more; it is replaced by the second term on the right-hand side of eq. (4.10). With this approach we investigate the hypothesis that a self-diffusion mechanism captures the thermal conductivity contribution for gas phases due to internal degrees of freedom (rotation and vibrations) reasonably well to yield an improvement by using $\lambda^{\text{ref},\rho D}$ instead of $\lambda^{\text{ref},\alpha}$ as the reference thermal conductivity.

In a recent study, we showed that self-diffusion coefficients of pure substances can be correlated accurately employing entropy scaling [8]. In contrast to the thermal conductivity, we did not find a pronounced influence of the number of intramolecular degrees of freedom on the quality of the model for the self-diffusion coefficient. This could be due to the fact that the transport of mass, i.e. diffusion, is not significantly influenced by the presence of internal degrees of freedom. Within the above-mentioned assumptions that lead to the CC approximation for the thermal conductivity, the internal degrees of freedom indeed have no influence at all on the self-diffusion coefficient.

Introducing the correlation function $D^*(s^*)$ into eq. (4.10) using the entropy-scaling approach given in ref [8] leads to the new reference thermal conductivity

$$\lambda^{\text{ref},\rho D} = \lambda^{\text{CE}} + \rho D^{\text{ref}} (c_v - 1.5k_B) \exp\{a + b[1 - \exp(s^*)]s^{*2} + cs^{*3}\} \quad (4.11)$$

The self-diffusion correlation parameters a to c were adjusted to experimental data points for an array of real substances and can be found in ref [8]. We calculate $c_v = c_v^{\text{ig}} + c_v^{\text{res}}$ using correlations from the DIPPR database [50] for the ideal gas heat capacity c_v^{ig} and PCP-SAFT for the residual contribution c_v^{res} . For the new approach using $\lambda^{\text{ref}} = \lambda^{\text{ref},\rho D}$ according to eq. (4.11) as the reference thermal conductivity in eq. (4.2), no empirical transition function $\alpha(s^*)$ is needed to combine the classical and non-classical contribution to the reference thermal conductivity.

4.4 Results

In this section, we show results for the calculation of the thermal conductivity of pure substances. We compare results of the new model $\lambda^{\text{ref},\beta D}$ (eq. (4.11)) with calculations using the old model $\lambda^{\text{ref},\alpha}$ (eq. (4.4)) for substances with many internal degrees of freedom. For the group of simple molecules, we compare the new model $\lambda^{\text{ref},\beta D}$ with the pure CE reference λ^{CE} (eq. (4.5)). In total, we investigated 109 substances representing 15 chemical families. The group of simple molecules contains 9 substances. As in our previous studies, we generally used all experimental data we found in literature, independent of measurement technique or date of publication. Data published in older references were occasionally published without explicit mention of measurement pressure. In these cases, we assumed atmospheric pressure. We neglected experimental data for pressure conditions greater than 100 MPa because of increasing uncertainties in calculated residual entropies from the PCP-SAFT model at very high pressures. For substances with many literature sources, we neglected data from sources which showed obvious, pronounced deviations compared to other data points. Individual outliers from otherwise seemingly reliable sources were not removed. For some substances, we found experimental data from different literature references giving contradicting entropy scaling curves, of which none could be removed with sufficient confidence. We kept all data in these cases. In summary, although entropy scaling is rather powerful in identifying outliers [9], our approach for excluding experimental data is rather conservative.

4.4.1 Fluids with a Low Number of Intramolecular Degrees of Freedom: Simple Fluids

We investigate the group of simple molecules first because our previously published model [9], using $\lambda^{\text{ref},\alpha}$ according to eq. (4.4), showed serious deficiencies for this group. In Figure 4.1 we already showed the inappropriateness of the earlier model for simple fluids. Rather than comparing the new approach, eq. (4.11,) for the reference thermal conductivity to the earlier model, we select a different, better approach for comparison. Figure 4.1 suggests that the simple Chapman–Enskog equation is a suitable expression for the reference thermal conductivity λ^{ref} of simple molecules. For simple fluids, we therefore compare results using the new expression for the reference thermal conductivity to the calculations using the simple Chapman–Enskog equation. For xenon as a monatomic fluid and for N_2 as a diatomic molecule, Figure 4.2 shows a drastic improvement of the approach proposed in this work compared to our earlier approach (Figure 4.1). For xenon, the result of the proposed approach is almost indistinguishable from the result obtained using the simple Chapman–Enskog equation for the reference thermal conductivity. For xenon, the heat capacity c_v in the range of temperatures covered by the experimental

data is sufficiently close to $3/2k_{\text{B}}$, so that the second term of eq. (4.11) has no substantial contribution. For nitrogen, however, as a substance, where the rotational energy and bond-vibrational energy contributes to c_v , leading to values of $c_v > 3/2k_{\text{B}}$ in eq. (4.11), the proposed entropy scaling approach shows better agreement to experimental data than does the model where the simple Chapman–Enskog equation is used for the reference thermal conductivity.

In Figure 4.3, we compare averaged absolute deviations (AADs) for all 9 substances investigated in the group of simple molecules. For $\lambda^{\text{ref},\rho^{\text{D}}}$ as reference thermal conductivity, we achieve similar AADs (on average 5.5%) as for λ^{CE} (on average 5.7%). We note also that these average deviations are much lower than for our original model, ref [9].

4.4.2 Fluids with Higher Number of Intramolecular Degrees of Freedom

Thermal conductivities for molecules with many internal degrees of freedom are shown in Figure 4.4. Results obtained using the reference thermal conductivity $\lambda^{\text{ref},\alpha}$ (eq. (4.4)) and the new CC-based model $\lambda^{\text{ref},\rho^{\text{D}}}$ (eq. (4.11)) are compared. For both models, the reduced thermal conductivity λ^* shows an approximately univariate dependence on reduced residual entropy s^* . Towards the ideal gas limit ($s^* \rightarrow 0$), the new model to a lesser degree collapses onto a single line. The reason may lie in the CC assumptions or in the approximate description of gas-phase self-diffusion with the entropy-scaling approach [8]. Generally, both models lead to a differently shaped function $\lambda^*(s^*)$. Nonetheless, we use the same functional form for the correlation polynomial (eq. (4.8)) for both models.

We analysed a database of 100 organic substances, where experimental data for thermal conductivities was available to us and where self diffusion D^s was parameterized from entropy scaling [8]. The average correlation results for all substances of the database obtained for both models are similar: the AADs are 7.7% for the model using $\lambda^{\text{ref},\rho^{\text{D}}}$ and 6.4% for the model previously proposed using the empirical $\lambda^{\text{ref},\alpha}$ expression. Average deviations from both models for various chemical families are summarized in Figure 4.5. It might be possible to improve the results for the new model by using a better ansatz function for $\lambda^*(s^*)$, noting that eq. (4.8) was proposed specifically for the previous model, but we were not successful in finding a more suitable function with an equally small number of parameters. However, we expect that another, more suitable ansatz function, would only lead to mildly improved results for organic substances with many degrees of freedom.

The results indicate that the influence of the internal degrees of freedom on the gas-phase thermal conductivity is captured reasonably well by the self-diffusion mechanism underlying the CC equation. Our study suggests that substances with varying number of internal degrees of freedom can now be described consistently using only one reference thermal conductivity, namely

$\lambda^{\text{ref},\rho^{\text{D}}}$ (eq. (4.11)), in the entropy-scaling approach. A full list of investigated substances, averaged absolute deviations, and polynomial parameters is given in the Supporting Information.

4.5 Conclusion

In this work, we proposed a new reference thermal conductivity for entropy scaling based on a kinetic-theory approach by Chapman and Cowling that describes the influence of intramolecular degrees of freedom on the thermal conductivity by a self-diffusion mechanism.

This study shows that an entropy-scaling model proposed in our previous work, using an empirically modified Chapman–Enskog expression $\lambda^{\text{ref},\alpha}$, leads to pronounced deviations for molecules with a low number of internal degrees of freedom, such as rare gases and diatomic molecules. The new reference thermal conductivity $\lambda^{\text{ref},\rho^{\text{D}}}$ overcomes these shortcomings, at the same time eliminating the need for an empirical expression. We investigated 9 monatomic or diatomic substances, which are described with average deviations of 5.5% (AAD) using the new model. For the 100 investigated substances with many internal degrees of freedom from more than 14 chemical families, the new model gives an average deviation of 7.7% (AAD), which is comparable to 6.4% for the former model $\lambda^{\text{ref},\alpha}$. The advantage of the new model for the thermal conductivity is its applicability to substances ranging from simple monatomic to complex molecules with many internal degrees of freedom.

4.5.1 Supporting Information

The Supporting Information details (1) the AADs for the investigated approaches, the quality of the underlying approach for D^{s} , as well as the number of available data for all investigated substances. Further, (2) parameters A - D for the group of simple molecules using λ^{CE} are given, and (3) parameters A - D for all considered substances using the new model $\lambda^{\text{ref},\rho^{\text{D}}}$ are listed, and (4) parameters A - D using the formerly published model $\lambda^{\text{ref},\alpha}$ are provided for all substances not considered in the Supporting Information of ref [9]. [The supporting information is given in Appendix C of this work.]

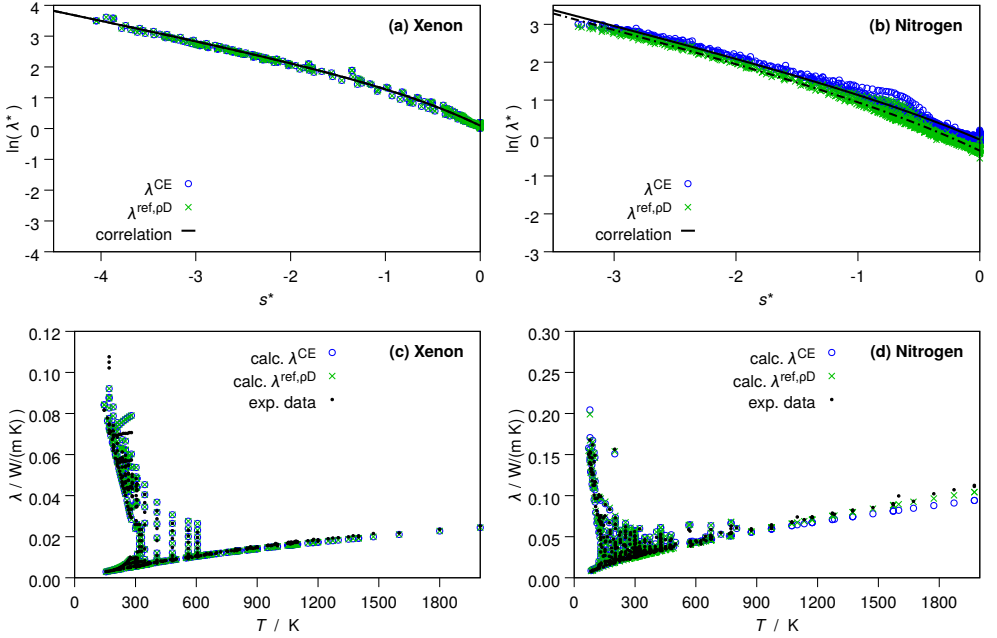


Figure 4.2: Thermal conductivities of xenon and nitrogen. Comparing results from entropy scaling using two different reference thermal conductivities, namely $\lambda^{\text{ref},\rho D}$ (eq. (4.11), green x) and λ^{CE} (eq. (4.5), blue circles). Experimental data for xenon covers the range $145 \text{ K} < T < 2000 \text{ K}$ and $0.01 \text{ MPa} < p < 107 \text{ MPa}$, for nitrogen it covers $68 \text{ K} < T < 2470 \text{ K}$ and $0.01 \text{ MPa} < p < 260 \text{ MPa}$. **a and b:** Logarithmic reduced thermal conductivity $\lambda^* = \lambda/\lambda^{\text{ref}}$ versus reduced residual entropy s^* . The symbols denote results obtained using experimental data for λ . The black lines represent the corresponding correlation function, eq. (4.8). All residual entropies are calculated from the PCP-SAFT model. **c and d:** Experimental (black dots) and calculated (colored crosses and circles) thermal conductivities versus temperature.

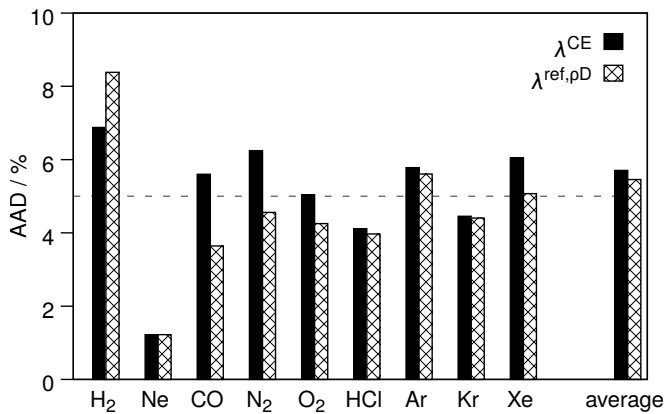


Figure 4.3: Averaged absolute deviations of calculated thermal conductivities from experimental values. All investigated simple substances are shown, sorted by molar mass. The entropy scaling model using the reference thermal conductivity λ^{CE} is presented as full black bars, the model using $\lambda^{ref,\rho D}$ is shown in patterned bars. The dashed line represents an AAD of 5% and serves as a guide to the eye.

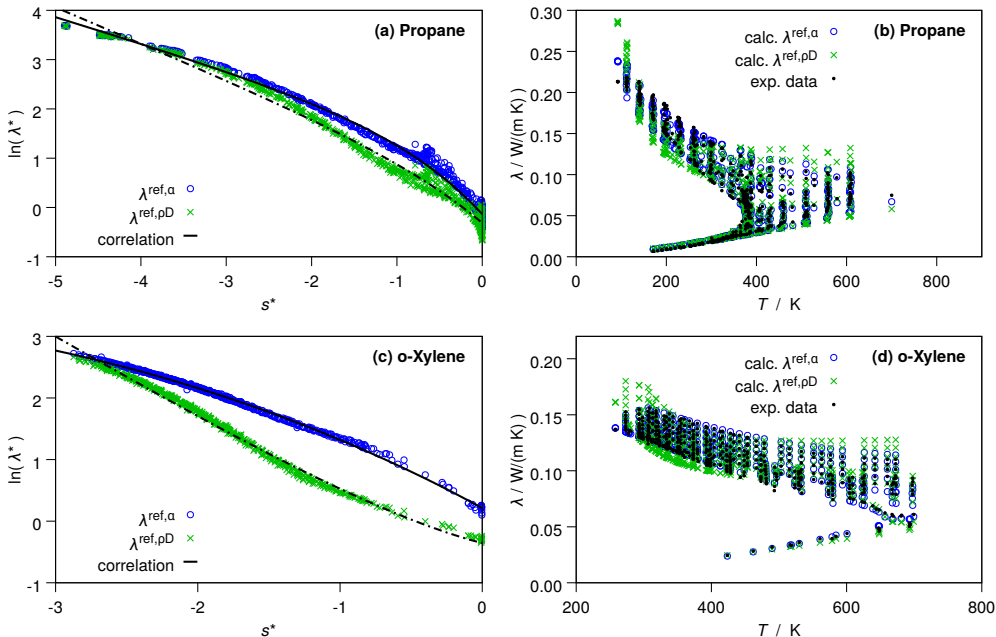


Figure 4.4: Thermal conductivities of propane and *o*-xylene. Comparing results from entropy scaling using two reference thermal conductivities, namely $\lambda^{\text{ref},\alpha}$ (eq. (4.4), blue circles) and $\lambda^{\text{ref},\rho D}$ (eq. (4.11), green x). Experimental data for propane covers the range $90 \text{ K} < T < 810 \text{ K}$ and $0.5 \text{ Pa} < p < 80 \text{ MPa}$, for *o*-Xylene it covers $257 \text{ K} < T < 700 \text{ K}$ and $0.1 \text{ MPa} < p < 100 \text{ MPa}$. **a and c:** Logarithmic reduced thermal conductivity $\lambda^* = \lambda/\lambda^{\text{ref}}$ versus reduced residual entropy s^* . The symbols denote experimental data. The black lines represent the corresponding correlation function, eq. (4.8). All residual entropies are calculated from the PCP-SAFT model. **b and d:** Experimental (black dots) and calculated (colored crosses and circles) thermal conductivities versus temperature.

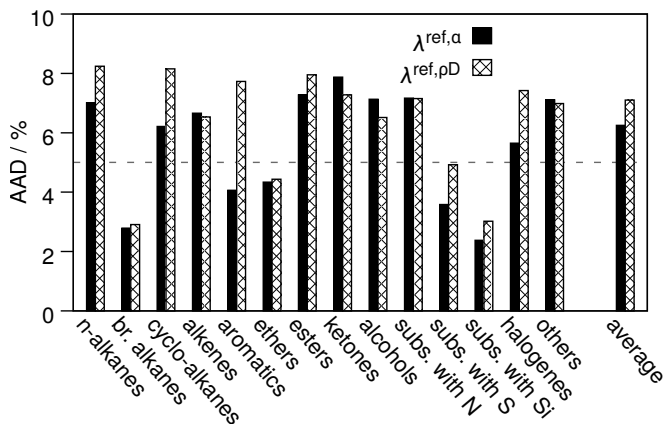


Figure 4.5: Averaged absolute deviations of calculated from experimental thermal conductivities for groups of substances with many internal degrees of freedom for the reference thermal conductivities $\lambda^{\text{ref},\alpha}$ (eq. (4.4)) and $\lambda^{\text{ref},\rho D}$ (eq. (4.11)). The dashed line represents an AAD of 5% and serves as a guide to the eye.

Bibliography

- [1] C. J. Geankoplis, *Transport processes and separation process principles (includes unit operations)*. Prentice Hall Professional Technical Reference, 2003.
- [2] A. Bardow, K. Steur, and J. Gross, “Continuous-molecular targeting for integrated solvent and process design,” *Ind. Eng. Chem. Res.*, vol. 49, no. 6, pp. 2834–2840, 2010.
- [3] M. Stavrou, M. Lampe, A. Bardow, and J. Gross, “Continuous molecular targeting computer-aided molecular design (comt camd) for simultaneous process and solvent design for CO₂ capture,” *Ind. Eng. Chem. Res.*, vol. 53, no. 46, pp. 18029–18041, 2014.
- [4] J. Schilling, M. Lampe, J. Gross, and A. Bardow, “1-stage CoMT-CAMD: An approach for integrated design of ORC process and working fluid using PC-SAFT,” *Chem. Eng. Sci.*, vol. 159, pp. 217–230, 2017.
- [5] J. Schilling, D. Tillmanns, M. Lampe, M. Hopp, J. Gross, and A. Bardow, “From molecules to dollars: integrating molecular design into thermo-economic process design using consistent thermodynamic modeling,” *Mol. Syst. Des. Eng.*, vol. 2, no. 3, pp. 301–320, 2017.
- [6] O. Lötgering-Lin and J. Gross, “Group contribution method for viscosities based on entropy scaling using the perturbed-chain polar statistical associating fluid theory,” *Ind. Eng. Chem. Res.*, vol. 54, no. 32, pp. 7942–7952, 2015.
- [7] O. Lötgering-Lin, M. Fischer, M. Hopp, and J. Gross, “Pure substance and mixture viscosities based on entropy scaling and an analytic equation of state,” *Ind. Eng. Chem. Res.*, vol. 57, no. 11, pp. 4095–4114, 2018.
- [8] M. Hopp, J. Mele, and J. Gross, “Self-diffusion coefficients from entropy scaling using the pcp-saft equation of state,” *Ind. Eng. Chem. Res.*, vol. 57, pp. 12942–12950, 2018.
- [9] M. Hopp and J. Gross, “Thermal conductivity of real substances from excess entropy scaling using pcp-saft,” *Ind. Eng. Chem. Res.*, vol. 56, no. 15, pp. 4527–4538, 2017.
- [10] Y. Rosenfeld, “Relation between the transport coefficient and the internal entropy of simple systems,” *Phys. Rev. A*, vol. 15, no. 6, pp. 2545–2549, 1977.

- [11] Y. Rosenfeld, "A quasi-universal scaling law for atomic transport in simple fluids," *J. Phys.: Condens. Matter*, vol. 11, pp. 5415–5427, 1999.
- [12] J. Gross and G. Sadowski, "Perturbed-chain saft: An equation of state based on a perturbation theory for chain molecules," *Ind. Eng. Chem. Res.*, vol. 40, pp. 1244–1260, 2001.
- [13] J. Gross and J. Vrabec, "An equation-of-state contribution for polar components: Dipolar molecules," *AIChE J.*, vol. 52, pp. 1194 – 1204, 2006.
- [14] S. Chapman and T. G. Cowling, *The Mathematical Theory of Non-Uniform Gases*. Cambridge University Press, 3 ed., 1970.
- [15] J. O. Hirschfelder, C. F. Curtiss, and R. B. Bird, *Molecular Theory of Gases and Liquids*. New York: John Wiley & Sons, Inc., 4 ed., 1954.
- [16] M. Hopp, J. Mele, R. Hellmann, and J. Gross, "Thermal conductivity via entropy scaling: An approach that captures the effect of intramolecular degrees of freedom," *Ind. Eng. Chem. Res.*, vol. 58, no. 39, pp. 18432–18438, 2019.
- [17] M. Hopp and J. Gross, "Thermal conductivity from entropy scaling: A group-contribution method," *Ind. Eng. Chem. Res.*, vol. 58, no. 44, pp. 20441–20449, 2019.
- [18] M. Agarwal, M. Singh, B. Shadrack Jabes, and C. Chakravarty, "Excess entropy scaling of transport properties in network-forming ionic melts (SiO_2 and BeF_2)," *J. Chem. Phys.*, vol. 134, no. 1, p. 014502, 2011.
- [19] I. H. Bell, "Probing the link between residual entropy and viscosity of molecular fluids and model potentials," *Proceedings of the National Academy of Sciences*, vol. 116, no. 10, pp. 4070–4079, 2019.
- [20] J.-L. Bretonnet, "Excess entropy scaling for the diffusion coefficient in expanded liquid metals," *J. Chem. Phys.*, vol. 120, no. 23, pp. 11100–11106, 2004.
- [21] Q.-L. Cao, D.-H. Huang, J.-S. Yang, M.-J. Wan, and F.-H. Wang, "Transport properties and the entropy-scaling law for liquid tantalum and molybdenum under high pressure," *Chinese Physics Letters*, vol. 31, no. 6, p. 066202, 2014.
- [22] Q.-L. Cao, P.-P. Wang, D.-H. Huang, J.-S. Yang, M.-J. Wan, and F.-H. Wang, "Transport coefficients and entropy-scaling law in liquid iron up to earth-core pressures," *J. Chem. Phys.*, vol. 140, no. 11, p. 114505, 2014.

- [23] Q.-L. Cao, J.-X. Shao, P.-P. Wang, and F.-H. Wang, “Entropy-scaling laws for diffusion coefficients in liquid metals under high pressures,” *J. Appl. Phys.*, vol. 117, no. 13, p. 135903, 2015.
- [24] R. Chopra, T. M. Truskett, and J. R. Errington, “On the use of excess entropy scaling to describe the dynamic properties of water,” *J. Phys. Chem. B*, vol. 114, no. 32, pp. 10558–10566, 2010.
- [25] R. Chopra, T. M. Truskett, and J. R. Errington, “Excess-entropy scaling of dynamics for a confined fluid of dumbbell-shaped particles,” *Phys. Rev. E*, vol. 82, p. 041201, 2010.
- [26] R. Chopra, T. M. Truskett, and J. R. Errington, “On the use of excess entropy scaling to describe single-molecule and collective dynamic properties of hydrocarbon isomer fluids,” *J. Phys. Chem. B*, vol. 114, no. 49, pp. 16487–16493, 2010.
- [27] J. C. Dyre, “Perspective: Excess-entropy scaling,” *J. Chem. Phys.*, vol. 149, no. 21, p. 210901, 2018.
- [28] M. Dzugasov, “A universal scaling law for atomic diffusion in condensed matter,” *Nature*, vol. 381, pp. 137 – 139, 1996.
- [29] W. A. Fouad and L. F. Vega, “Transport properties of HFC and HFO based refrigerants using an excess entropy scaling approach,” *J. Supercrit. Fluids*, vol. 131, pp. 106–116, 2018.
- [30] T. Goel, C. N. Patra, T. Mukherjee, and C. Chakravarty, “Excess entropy scaling of transport properties of lennard-jones chains,” *J. Chem. Phys.*, vol. 129, no. 16, pp. 164904(1–9), 2008.
- [31] P. He, H. Li, and X. Hou, “Excess-entropy scaling of dynamics for methane in various nanoporous materials,” *Chem. Phys. Lett.*, vol. 593, pp. 83–88, 2014.
- [32] J. J. Hoyt, M. Asta, and B. Sadigh, “Test of the universal scaling law for the diffusion coefficient in liquid metals,” *Phys. Rev. Lett.*, vol. 85, no. 3, pp. 594–597, 2000.
- [33] N. Jakse and A. Pasturel, “Excess entropy scaling law for diffusivity in liquid metals,” *Scientific Reports*, vol. 6, no. 1, 2016.
- [34] W. P. Krekelberg, M. J. Pond, G. Goel, V. Shen, J. R. Errington, and T. M. Truskett, “Generalized rosenfeld scalings for tracer diffusivities in not-so-simple fluids: Mixtures and soft particles,” *Phys. Rev.*, vol. 80, no. 6, pp. 061205(1–13), 2009.

- [35] G. X. Li, C. S. Liu, and Z. G. Zhu, “Excess entropy scaling for transport coefficients: diffusion and viscosity in liquid metals,” *J. Non-Cryst. Solids*, vol. 351, no. 10-11, pp. 946–950, 2005.
- [36] G. X. Li, C. S. Liu, and Z. G. Zhu, “Scaling law for diffusion coefficients in simple melts,” *Phys. Rev. B*, vol. 71, no. 9, 2005.
- [37] Y. Liu, J. Fu, and J. Wu, “Excess-entropy scaling for gas diffusivity in nanoporous materials,” *Langmuir*, vol. 29, no. 42, pp. 12997–13002, 2013.
- [38] M. Malvaldi and C. Chiappe, “Excess entropy scaling of diffusion in room-temperature ionic liquids,” *J. Chem. Phys.*, vol. 132, no. 24, p. 244502, 2010.
- [39] J. Mittal, J. R. Errington, and T. M. Truskett, “Relationships between self-diffusivity, packing fraction, and excess entropy in simple bulk and confined fluids,” *J. Phys. Chem. B*, vol. 111, no. 34, pp. 10054–10063, 2007.
- [40] L. T. Novak, “Fluid viscosity-residual entropy correlation,” *Int. J. Chem. React. Eng.*, vol. 9, p. A107, 2011.
- [41] L. T. Novak, “Self-diffusion coefficient and viscosity in fluids,” *Int. J. Chem. React. Eng.*, vol. 9, no. A63, pp. 1–25, 2011.
- [42] L. T. Novak, “Predictive corresponding-states viscosity model for the entire fluid region: *n*-alkanes,” *Ind. Eng. Chem. Res.*, vol. 52, pp. 6841–6847, 2013.
- [43] L. T. Novak, “Correction to: Predictive corresponding-states viscosity model for the entire fluid region: *n*-alkanes,” *Ind. Eng. Chem. Res.*, vol. 52, no. 38, pp. 13886–13886, 2013.
- [44] L. T. Novak, “Predicting natural gas viscosity with a mixture viscosity model for the entire fluid region,” *Ind. Eng. Chem. Res.*, vol. 52, pp. 16014–16018, 2013.
- [45] S. Pieprzyk, D. M. Heyes, and A. C. Brańka, “Thermodynamic properties and entropy scaling law for diffusivity in soft spheres,” *Phys. Rev. E*, vol. 90, no. 1, 2014.
- [46] M. J. Pond, J. R. Errington, and T. M. Truskett, “Communication: Generalizing rosenfeld’s excess-entropy scaling to predict long-time-diffusivity in dense fluids of brownian particles: From hard to ultrasoft interactions,” *J. Chem. Phys.*, vol. 134, no. 081101, pp. 081101/1–4, 2011.
- [47] A. Samanta, S. M. Ali, and S. K. Ghosh, “Universal scaling laws of diffusion: Application to liquid metals,” *J. Chem. Phys.*, vol. 123, no. 8, p. 084505, 2005.

- [48] K. Seki and B. Bagchi, "Relationship between entropy and diffusion: A statistical mechanical derivation of rosenfeld expression for a rugged energy landscape," *J. Chem. Phys.*, vol. 143, no. 19, 2015.
- [49] P. D. Neufeld, A. R. Janzen, and R. A. Aziz, "Empirical equation to calculate 16 of the transport collision integrals $\omega^{(l,s)*}$ for the lennard-jones (12-6) potential," *J. Chem. Phys.*, vol. 57, no. 3, pp. 1100 – 1102, 1972.
- [50] R. L. Rowley, W. V. Wilding, J. L. Oscarson, Y. Yang, N. A. Zundel, T. E. Daubert, and R. P. Danner *DIPPR Data Compilation of Pure Chemical Properties*. Design Institute for Physical Properties, AIChE: New York, NY, 2009.

5 Thermal Conductivity from Entropy Scaling: A Group-Contribution Method

*This chapter, except for Appendix section 5.B, is a literal quote of:
M. Hopp, J. Gross: Thermal Conductivity from Entropy Scaling: A Group-
Contribution Method, Industrial & Engineering Chemistry Research, 2019,
58, 44, 20441–20449,*

DOI:10.1021/acs.iecr.9b04289.

*Additions implemented in this chapter compared to the original journal publi-
cation are indicated by square brackets.*

Entropy scaling has proven to be a powerful method for calculating transport properties. The applicability of the entropy scaling approach to predict the viscosity, thermal conductivity and self-diffusion coefficients of pure substances based on substance-specific parameters was over last years convincingly demonstrated in literature. In this work, we derive a predictive method for the thermal conductivity based on entropy scaling. The model is developed as a group-contribution approach, where substances are considered to be composed of chemical (functional) groups. The excess entropy is calculated using the group-contribution PCP-SAFT equation of state. The model is applicable for gaseous phases and for liquid-phase conditions covering wide ranges of temperature and pressure. We consider pure fluids from various chemical families, namely alkanes, branched alkanes, cyclic alkanes, alkenes, aldehydes, aromatics, esters, ethers, ketones and alcohols, and some individual substances, such as water, carbon dioxide and alike. We propose parameters of 29 chemical groups, by considering 231 substances with more than 50,000 experimental data points. The group-contribution method for the thermal conductivity proposed in this work is shown to be in convincing agreement with experimental data, with 6.17% average absolute deviation for all considered data points.

5.1 Introduction

Group-contribution (GC) methods allow for the description of macroscopic properties of interest based on the chemical groups the considered substance or mixture is composed of. Defining functional groups and describing molecules as a combination of functional groups leads to a drastically reduced number of adjustable parameters, compared to substance-specific modelling of properties. At the same time, and most importantly, the approach allows for

predicting the properties of substances where experimental data is absent or scarce. An overview on GC methods for thermophysical properties was recently given by Su et al. [1]. While static properties, as density, vapor pressure or heat capacity, can be described through a variety of approaches, correlative or predictive approaches for transport properties are rare.

Our engagement for developing group-contribution methods was triggered by the objective to simultaneously optimize products and processes [2–5], which can only be accomplished satisfyingly when transport properties can be predicted with sufficient accuracy. In these optimization problems, the considered process, say an absorption-desorption process, or an organic Rankine cycle, and the solvent or working fluid (mixture) are optimized simultaneously. When transport properties can be predicted directly using an equation of state, it is possible to minimize an economic objective functions in product and process design problems. In such a way, extended CAMD approaches were for example proposed in [6, 7] for organic Rankine cycles or summarized in [1] for thermodynamic cycles. Group contribution methods are powerful for enabling simultaneous product and process design approaches.

Our previous studies showed that entropy scaling can be used to develop models for transport properties. These models allowed to correlate, and subsequently to predict, experimental viscosities of pure substances [8] and of mixtures [9]. Further, models for thermal conductivities [10] and for self-diffusion coefficients [11] of pure substances were proposed. These studies showed that, based on limited number of experimental data used for correlating the parameters, transport properties could be predicted well outside the correlated range of temperature and pressure, i.e. within the whole fluid region.

Over the last decades, group contribution methods describing the liquid phase viscosity as a function of temperature were developed for a variety of substances [12–17]. Previous work from our group led to a group-contribution model for viscosities in the whole fluid region based on residual entropy [8, 9], which was surprisingly accurate given the richness of experimental database and the low number of adjustable parameters.

For thermal conductivities, also group contribution approaches were developed as functions of temperature, but these are limited to a description of either the vapor phase [18, 19] or the liquid phase [18, 20–25]. Very recently, a group-contribution method for thermal conductivity of hydrocarbon mixtures described as pseudo-components based on entropy-scaling and our early studies was developed by Rokni et al. [26].

In this study we develop a group-contribution method for thermal conductivities for substances of various chemical families on the basis of entropy scaling, combined with the group-contribution *perturbed-chain polar statistical associating fluid theory* (PCP-SAFT) equation of state (EoS) [27, 28] to calculate the residual entropy.

5.2 Theoretical Background

We briefly review the group-contribution (GC) PCP-SAFT equation of state. Then, we give a short introduction to Rosenfeld’s entropy scaling [29, 30]. Finally, we describe the proposed GC model for thermal conductivities and the approach for identifying the model parameters.

5.2.1 Group-Contribution EoS

Within the PCP-SAFT equation of state, molecules are considered to be chains of tangentially-bonded identical segments [27, 28]. Molecules are described by the following pure component parameters: segment number m_i , segment size parameter σ_{ii} , and van der Waals (dispersive) energy parameter ϵ_{ii} . Polar substances are further characterized by a dipole moment μ_i and a quadrupole moment Q_i , while hydrogen-bonding (associating) species have an energy parameter ϵ_{AB} and a range-parameter κ_{AB} determining the short-range attractive potential between site A and site B . For association parameters, we use the index AB as short-hand notation, rather than $AiBi$. In a group-contribution approach, similar parameters are assigned, but now to each individual functional group α , namely: m_α , $\sigma_{\alpha\alpha}$, $\epsilon_{\alpha\alpha}$, μ_α , ϵ_{AB} , and κ_{AB} . functional groups are for example $\alpha \in \{-\text{CH}_3, -\text{CH}_2-, -\text{OH}, \dots\}$.

For the PCP-SAFT model, we can distinguish two GC approaches. In a *homosegmented* group-contribution method, one uses mixing rules to calculate molecular parameters by averaging group-parameters of the considered substance. Such mixing rules were proposed by Vijande et al. [31], Tamouza et al. [32] and Tihic et al. [33].

Heterosegmented GC approaches, in contrast, do not require mixing rules because they consider molecular chains composed of different segment types. Two important representatives of the heterosegmented approach are the SAFT- γ method by Lympieriadis et al. [34] and the GC-SAFT-VR method by Peng et al. [35]. Heterosegmented GC approaches based on the PC-SAFT EoS were presented by Gross et al. [36] (although only copolymers were considered in their study), by Padászyński and Domańska [37], by Peters et al. [38], and by Sauer et al [39].

The study of Sauer et al. showed the heterosegmented approach to be superior to the homosegmented model for phase equilibria [39]. While liquid densities are described about equally well with both approaches, vapor pressures are represented more accurately by the heterosegmented approach. For predicting transport properties (namely viscosity), however, the heterosegmented GC approach did not lead to significant improvements, as Lötgering-Lin and Gross showed [8].

Therefore, in this work, we use the homosegmented group-contribution method based on the PCP-SAFT EoS using mixing rules by Vijande et al. [31] as de-

scribed and parameterized by Sauer et al. [39]. For n -alkanes, where only m_i , σ_{ii} and ϵ_{ii} of a component i are needed, the mixing rules are

$$\begin{aligned}
 m_i &= \sum_{\alpha} n_{i,\alpha} m_{\alpha} \\
 m_i \sigma_{ii}^3 &= \sum_{\alpha} n_{i,\alpha} m_{\alpha} \sigma_{\alpha\alpha}^3 \\
 m_i \epsilon_{ii} &= \sum_{\alpha} n_{i,\alpha} m_{\alpha} \epsilon_{\alpha\alpha}
 \end{aligned}
 \tag{5.1}$$

where $n_{i,\alpha}$ denotes the number of functional groups of type α in substance i . Group parameters have been adjusted to vapor pressure and saturated liquid density data by Sauer et al. [39] and we use these parameters in this work without any readjustment.

We note that the study of Sauer et al. [39] compared two concepts for developing a group-contribution equation of state, the homosegmented and the heterosegmented approach. The study used a comparably low number of adjustable parameters in order to clearly discriminate between the two modelling concepts. The resulting group-contribution PCP-SAFT equation in the current parameterization [39] (with low number of adjustable parameters) therefore leads to higher deviations in liquid density (4.3% average) and vapor pressure (9.7% average) than one would otherwise expect. The study of Lötgering-Lin and Gross [8] showed that such deficiencies didn't propagate into the entropy scaling model for viscosity in an overly pronounced way, when the entropy scaling model is parameterized to the group-contribution PCP-SAFT model.

5.2.2 Transport Properties from Entropy Scaling

The central statement of entropy scaling as proposed by Rosenfeld [29, 30] is, that transport properties, such as shear viscosity η , thermal conductivity λ , and self diffusion coefficients D^s can be regarded as only dependent on residual entropy, provided the transport property is written in an appropriate dimensionless form. The dimensionless thermal conductivity λ^* is

$$\lambda^* = \lambda / \lambda^{\text{ref}}
 \tag{5.2}$$

In this subchapter, we omit index i for a considered substance. A suitable expression for the reference thermal conductivity λ^{ref} is not known a priori. Rosenfeld, in his original publication suggested simple expressions for λ^{ref} (as well as expressions for reference viscosity and for reference self diffusion coefficients). These expressions lead to good results only for simple, spherically symmetric fluids and lead to divergences in λ^* towards the ideal gas (i.e. towards zero residual entropy). In previous work, we proposed expressions for

the reference thermal conductivity [10] λ^{ref} and also expressions for η^{ref} and D_s^{ref} for viscosity and self diffusion coefficients [8, 9, 11], respectively.

In agreement to preceding studies [8–11], we define the reduced residual entropy as

$$s^* = s^{\text{res}}/(k m) \quad (5.3)$$

with Boltzmann’s constant k and segment number m of the PCP-SAFT equation of state. We emphasize that the residual entropy $s^{\text{res}}(T, v) = s - s^{\text{ig}}(T, v)$ is defined with respect to an ideal gas system at same temperature and molar volume v . [27] Introducing the segment number into Eq. 5.3 leads to a comparable range of s^* -values for different substances. In our previous work [10], we investigated several possibilities for the reference thermal conductivity λ^{ref} and proposed a new expression. This expression is slightly redefined here, as

$$\lambda^{\text{ref}} = \lambda^{\text{CE}} + \phi(s^*)\lambda^{\text{int}} \quad (5.4)$$

$$\lambda^{\text{CE}} = \frac{\sqrt{T/(M/m)} 83.235}{\sigma^2 \Omega^{(2,2)*}} \frac{10^{-20} \text{ kg}^{3/2} \text{ m}^3}{10^{3/2} \text{ K}^{3/2} \text{ mol}^{1/2} \text{ s}^3}$$

$$\lambda^{\text{int}} = (m^2 \sigma^3 \epsilon/k) (c_1 T^* + c_2 T^{*2}) \frac{10^{25} \text{ kg}}{\text{s}^3 \text{ m}^2 \text{ K}^2}$$

$$\phi(s^*) = \exp(-s^*/(-0.5))$$

with model constants $c_1 = -0.0167141$ and $c_2 = 0.0470581$ and thermal conductivity λ in $\text{W}/(\text{m K})$. The size parameter σ is in these equations used in unit m. Further, $\Omega^{(2,2)*}$ represents the collision integral, which is calculated according to Neufeld et al. [40]. The dimensionless temperature is defined as $T^* = kT/(m\epsilon)$. The reference thermal conductivity λ^{ref} consists of a classical contribution λ^{CE} , coming from translational contributions, and a contribution λ^{int} that accounts for internal degrees of freedom (vibration and rotation). Contribution λ^{int} is relevant for low densities and is activated by the transition function ϕ . The difference of Eq. 5.4 to our previous work is in the definition of the transition function ϕ . In our previous study [10] we defined the transition function as $\phi = \exp(-s^*/s_c^*)$ using the reduced residual entropy at critical temperature and pressure s_c^* [see eq. (2.10) in Chapter 2 of this work]. As a step towards the description of mixtures, we simply approximate s_c^* by -0.5 , the average value of reduced residual entropy for the calculated critical points of all considered substances.

The form of the internal contribution λ^{int} in Eq. 5.4 resulted from an analysis of experimental data for 26 substances at low-density conditions. In the meantime, we expanded our database and can now validate the proposed gas-phase correction λ^{int} for 128 substances from various chemical families. Figure 5.1 analyses the difference between experimental data at low densities and values as calculated from the Chapman-Enskog term. This difference ($\lambda^{\text{exp}} - \lambda^{\text{CE}}$)

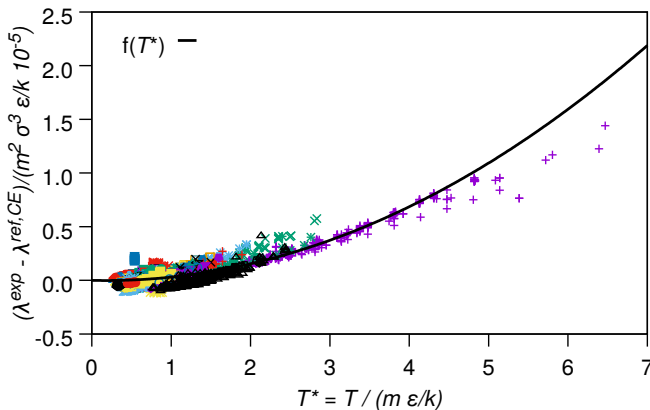


Figure 5.1: Analysis of the difference between experimental values of the thermal conductivity and values estimated from the Chapman-Enskog theory ($\lambda^{\text{exp}} - \lambda^{\text{CE}}$) as a function of reduced temperature T^* for 128 substances in dilute gas conditions ($|s^*| < 0.1$). Full legend given in the Supporting Information.

corresponds to the gas-phase correction λ^{int} , as Eq. 5.4 clarifies (noting that $\phi(s^*)$ approaches unity for low densities, because s^* approaches zero). Figure 5.1 confirms a rather good representation of the low-density limit of all substances.

We shall now consider the functional dependence of dimensionless thermal conductivity λ^* on reduced residual entropy s^* . We proposed the function [10]

$$\ln(\lambda^*) = A + Bs^* + C(1 - \exp(s^*)) + Ds^{*2} \quad (5.5)$$

with correlation parameters A - D specific to each substance. The parameters A - D were adjusted to experimental data. The functional form of Eq. 5.5 was proposed because it led to rather well-behaved correlations for cases where experimental data is scarce. We proposed criteria for defining some of the parameters independently, depending on how comprehensive the available experimental data is. For substances with scarce data, only two parameters are adjusted [10]. We refer to the resulting entropy scaling model based on PCP-SAFT equation of state as the *individual* approach (where parameters A - D are individually adjusted for each substance).

With an extended database of experimental data, we here revise the correlation, Eq. 5.5. In contrast to our earlier work, we realized that parameter D has a small influence on the quality of the correlation and that parameter D can deteriorate the robustness of extrapolations, especially towards high pressures (highly negative s^*). We set $D = 0$ for all substances which were

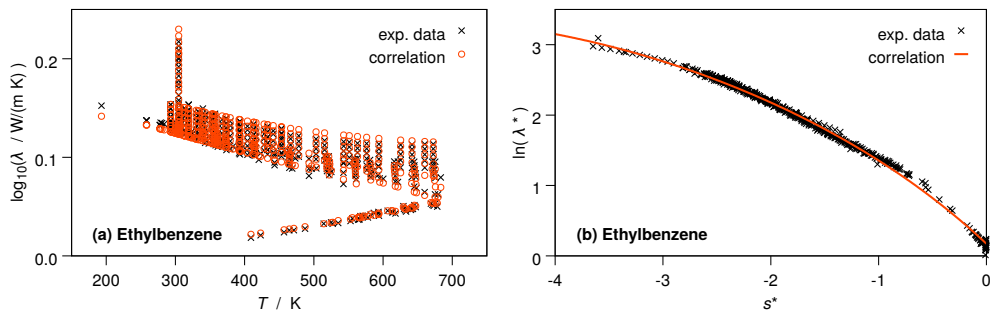


Figure 5.2: Correlation results of the individual entropy scaling approach using PCP-SAFT. a) Experimental and calculated thermal conductivity for various temperatures and for varying pressures. b) The same data is shown as logarithmic reduced thermal conductivity versus reduced residual entropy.

not part of our earlier work and for which parameters were newly adjusted in this study using the individual approach. The resulting A - D parameters are detailed in the Supporting Information.

Once the model parameters A - D are defined in the individual approach, the thermal conductivity can be calculated for any given temperature T and pressure p in the fluid range of a pure substance through three simple steps. First, the EoS is used to calculate the residual entropy $s^{\text{res}}(T, v)$ for given $\{T, p\}$. Second, calculate s^* using Eq. (5.3) and evaluate Eq. (5.5) to receive dimensionless λ^* . Based on Eq. (5.4) and (5.2), finally calculate λ . The strength of the approach lies in the few adjustable model parameters needed and in the surprising robustness to extrapolations. Results for ethylbenzene are shown in figure 5.2 as an example with rather comprehensive experimental data covering a wide range of conditions, from vapor to liquid and at elevated pressures.

5.2.3 Group-Contribution Model for Thermal Conductivity

With the objective of devising a predictive approach for thermal conductivity, we apply the GC-PCP-SAFT model for the residual entropy and for delivering suitable parameters for Eq. (5.3) and (5.4). The group-contribution concept is also used for the model parameters A - D , by defining parameters A_α - D_α from eq. (5.5) based on functional groups (index α). The number of adjustable parameters for the group-contribution approach is rather limited. All n -alkanes, for example, only require six parameters ($A_{\text{-CH}_3}$ to $C_{\text{-CH}_3}$ and $A_{\text{-CH}_2-}$ to $C_{\text{-CH}_2-}$). For thermal conductivity, we propose the following

group-contribution scheme

$$\begin{aligned}
 A_i &= \sum_{\alpha} n_{i,\alpha} A_{\alpha} & B_i &= \sum_{\alpha} n_{i,\alpha} B_{\alpha} \\
 C_i &= \sum_{\alpha} n_{i,\alpha} C_{\alpha} & D_i &= \sum_{\alpha} \begin{cases} n^t D_{\alpha} & \text{for } \alpha = -\text{OH} \\ 0 & \text{otherwise} \end{cases}
 \end{aligned}
 \tag{5.6}$$

with $n_{i,\alpha}$ as the number of functional groups of type α in substance i and with $n^t = \sum_{\alpha} n_{i,\alpha}$ as the total number of functional groups. We set D_{α} to zero for all functional groups α , except for the alcohol (hydroxyl) functional group ($-\text{OH}$).

The development of these correlation summation rules is empirical. The procedure for finding these rules is described in the appendix.

Procedure for Adjusting Model Parameters

The group-specific model parameters A_{α} - C_{α} (and $D_{-\text{OH}}$) have to be adjusted to experimental data for the thermal conductivity of pure substances. This is done in a consecutive scheme for different chemical families. First, the parameters for the segments $-\text{CH}_3$ and $-\text{CH}_2-$ are adjusted using data from the homologous series of n -alkanes only. Once adjusted, these chemical-group parameters are fixed for all other chemical families. As the second step, the junction segments $-\text{CH}<$ and $>\text{C}<$ are adjusted to branched alkanes and afterward kept fixed. In this fashion, all chemical-group parameters are adjusted subsequently to different groups of substances, while already adjusted chemical-group parameters are kept fixed. We have also performed simultaneous optimization calculations, where the parameters reported below were used as starting values and all parameters were simultaneously adjusted to the entire data base. However, we have the impression that the model then loses some robustness towards extrapolations, which is why we report parameters that were consecutively adjusted to homologous series of chemical families.

Parameters A_{α} - C_{α} are adjusted according to the following procedure. After reading all experimental data of a chemical family, the substance-specific PCP-SAFT parameters are determined from Eqs. (5.1) for every substance. For every experimental condition $\{T, p\}$ of the database, the reduced residual entropy s^* (in variables T, v) is calculated. That requires first, a density iteration ($\rho = 1/v$) for a considered condition $\{T, p\}$ and with that density or molar volume, the reduced residual entropy s^* (in variables T, v) is calculated. The group-contribution parameters A_{α} - C_{α} are optimized using a Levenberg-Marquardt algorithm [41] by minimizing the squared relative deviations of calculated values of logarithmic reduced thermal conductivity $\ln(\lambda^{\text{calc}}/\lambda^{\text{ref}})$ from values containing experimental data, $\ln(\lambda^{\text{exp}}/\lambda^{\text{ref}})$.

Experimental data for thermal conductivity was taken from the Dortmund Database [42]. As in our previous studies [10, 11, 43], we generally used all

experimental data we found in literature, independent of measurement technique or date of publication. For references that do not specify experimental pressures, we assumed atmospheric pressure. We neglected experimental data for pressures greater than 100 MPa because the PCP-SAFT equation of state shows increasing uncertainties in calculated residual entropies at very high pressures. For substances with experimental data from many literature references, we neglected data from sources that showed pronounced and obvious deviations compared to other data sets. Individual outliers from otherwise seemingly reliable sources were not removed. Some substances have experimental data from different literature sources with contradicting entropy scaling curves, where none could be removed with sufficient confidence. In these cases we kept all data. In summary, although entropy scaling is rather powerful in identifying outliers [10], our approach for excluding experimental data is rather conservative [43].

Data points in a temperature-range and (at the same time) a pressure-range of 10% around the critical point were neglected in the parameter regression. First, thermal conductivity is known to undergo a critical enhancement [44–50], and second analytical equations of state without a renormalization theory [51–53] are known to overestimate the critical point. We emphasize, however, that all results presented graphically or as deviations or as average deviations, contain all available experimental data, including points in the vicinity of the critical point. And further, we only report deviations based on the thermal conductivity λ , not on the logarithmic thermal conductivity, $\ln(\lambda)$.

Because the underlying GC PCP-SAFT model was not parameterized for substances with multiple polar or hydrogen-bonding functional groups [39], such substances were omitted in adjusting of parameters $A_\alpha - C_\alpha$. The resulting parameters $A_\alpha - C_\alpha$ are given in Table S1 of the Supporting Information.

5.3 Results and Discussion

We assess the proposed group-contribution model through comparison to experimental thermal conductivities of pure substances. A variety of substances from different chemical families are thereby considered. Deviations of the model to experimental data is given as averaged absolute deviations (AAD). The definition of AAD is given in the Supporting Information. We further investigate the robustness of extrapolation towards substances not considered in the training set, including substances with multiple functional groups, and we compare results of the group-contribution model to results of the individual approach [10] (i.e. the model for thermal conductivity where each substance is individually parameterized).

5.3.1 Model assessment

To assess the correlating capability of the GC method, we first compare experimental thermal conductivities with results from the proposed group-contribution model using entropy scaling and the GC PCP-SAFT equation of state. Fig. 5.3 regards a non-polar substance, an associating (hydrogen bonding) species and water. The average deviations of the model to experimental data are AAD=6.2% for propane (2888 points), AAD=7.7% for 1-propanol (402 points), and AAD=5.7% for water (2923 points). The deviations for propane and 1-propanol are approximately representative for the entire group of *n*-alkanes and 1-alcohols, respectively. One observes an overall good agreement of the calculated thermal conductivity compared with the experimental data for a wide range in temperature and pressure. Figures showing the deviation over the range of reduced residual entropy for these three substances are given in the Supporting Information.

The proposed group-contribution model is based on two separable group-contribution models: First, the GC PCP-SAFT equation of state for calculating residual entropies s^* and reference thermal conductivities λ^{ref} . And secondly, the group-contribution model for the thermal conductivity (eq. (5.5) and (5.6)). We proceed by first assessing the first group-contribution model, namely GC PCP-SAFT, in comparison to the PCP-SAFT model. In PCP-SAFT, parameters m_i , σ_{ii} and ϵ_{ii} are adjusted individually to each substance, which implies lower deviations to experimental data for properties used for parameter regression (vapor pressure and liquid densities) as compared to the GC PCP-SAFT equation of state. In order to single out how the choice of the underlying equation of state acts on calculated thermal conductivities, we use GC PCP-SAFT and adjust the correlation parameters *A-D* for each substance individually. In doing so, we get the best possible result for GC PCP-SAFT and can compare the results to results obtained using the PCP-SAFT model (with also individually adjusted *A-D* parameters).

In the comparison, we also include the proposed full group-contribution model, which uses GC PCP-SAFT but also applies the group-contribution equations for the thermal conductivity, eq. (5.6). The comparison of the full group-contribution model to the GC PCP-SAFT approach with substance-specific parameters *A-D* allows to assess to what extent the results deteriorate by using the group-contribution approach for the thermal conductivity, eq. (5.6). For the comparison of all three models, we determined deviations of the models to experimental values (expressed as AAD-values) using the same substances as in our previous work [10], namely the homologous series of *n*-alkanes, the set of butane-based substances from every chemical family, and the averaged results from all considered chemical families. The comparison is presented in Fig. 5.4. A detailed list of all individual deviations, the resulting polynomial parameters *A-D*, as well as the used GC PCP-SAFT parameters, is given in the Supplementary Information.

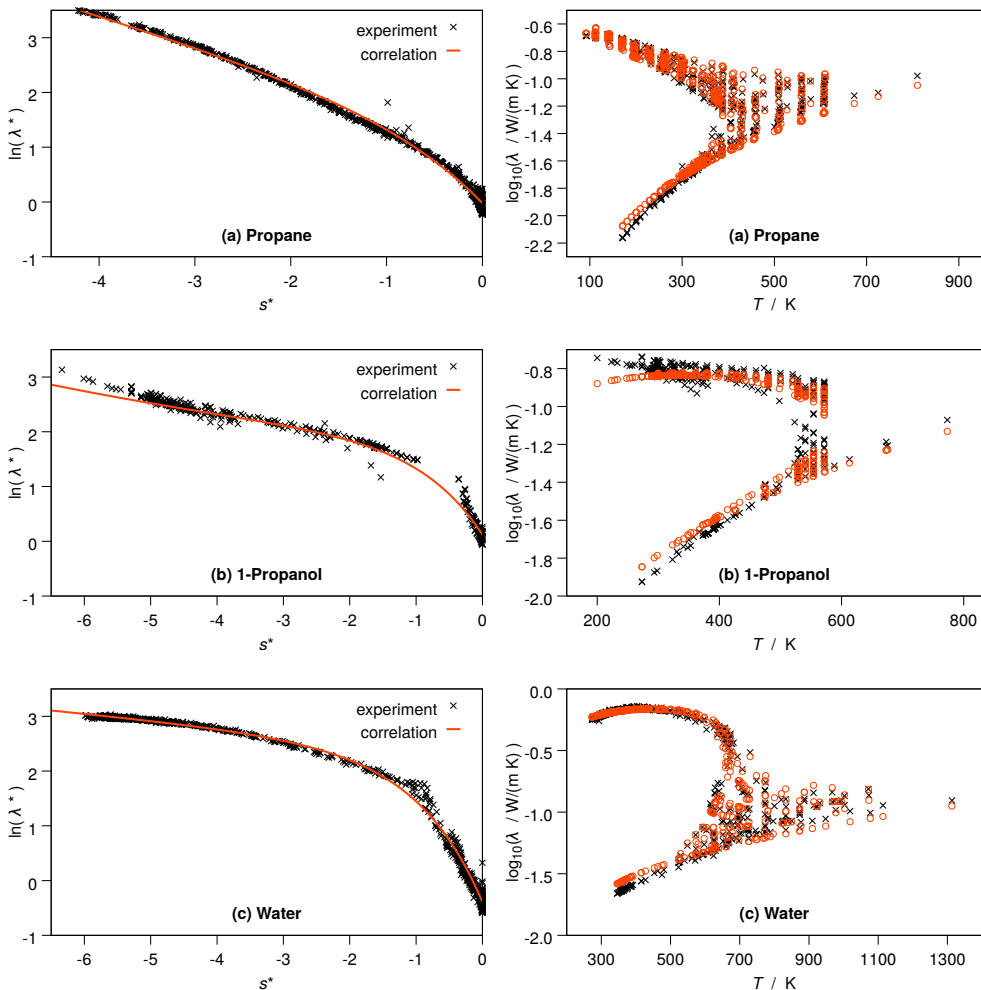
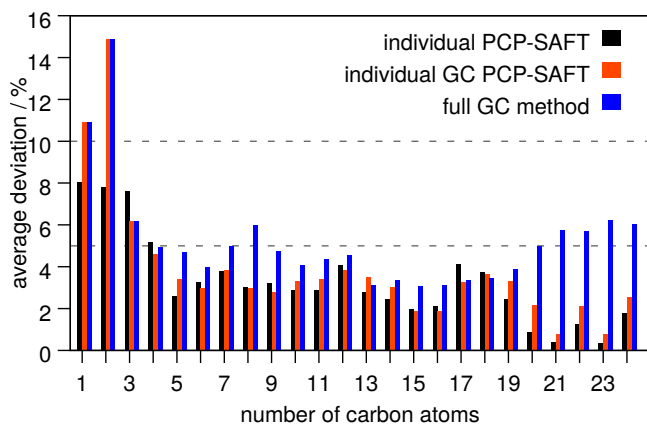
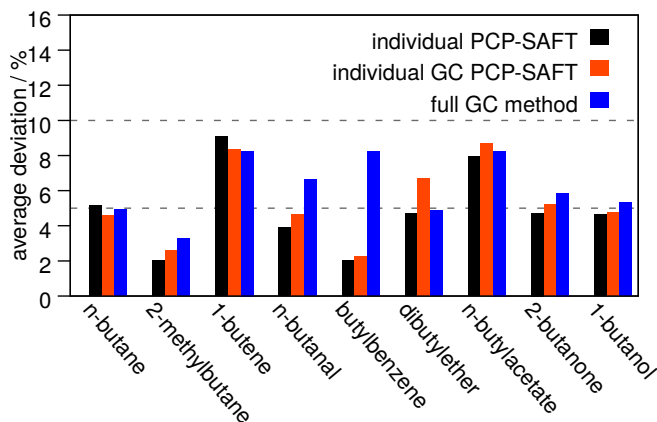


Figure 5.3: Thermal conductivity of n-propane, 1-propanol and water. Left diagrams show the logarithmic reduced thermal conductivity $\ln(\lambda_*)$ versus reduced residual entropy s^* . Right diagrams give thermal conductivities for varying temperature. Comparison of the proposed group-contribution entropy scaling model (red line and red circles) to experimental data (black crosses).



(a) homologous series of n -alkanes



(b) butane-based substances from every considered chemical family

Figure 5.4: Comparison of averaged absolute deviations of three models to experimental data: PCP-SAFT with A - D parameters individually adjusted for every substance, GC-PCP-SAFT with A - D parameters individually adjusted for every substance, and the full group-contribution model using GC-PCP-SAFT and A - D from eq. (5.6) (with parameters listed in Table S1 of the Supporting Information).

We find only slightly changed average deviations using individual GC PCP-SAFT as compared to the PCP-SAFT model. We can conclude that the GC PCP-SAFT does not lead to marked deterioration of results compared to the individually parameterized PCP-SAFT model. Fig. 5.4 further shows the full group-contribution model with somewhat higher deviations than for the other two models where parameters A to D are obtained individually for each substance. Considering the substantially reduced number of adjustable parameters for the full group-contribution model, however, the results of this model are convincing, with average deviations of 6.17% for the full group-contribution model compared to 5.38% for the individually adjusted PCP-SAFT approach. We find it a remarkable result to achieve a comparable quality of correlation for the thermal conductivity of such a variety of chemical families and such a broad range of temperature and pressure using our GC approach, with only a fraction of the number of adjustable parameters compared to the individually parametrized model.

5.3.2 Transferability of group-contribution parameters

The main advantage of a group-contribution method is the possibility to predict the properties of substances with scarce or completely missing experimental data, using information from chemically comparable substances. To assess how well parameter of a functional group are transferable to substances not considered in the training set, we divided our total database in a training set and test set.

First, we regard the homologous series of n -alkanes and artificially limit the experimental data used for the parameterization of A_α - C_α to 4 or 5 substances, as illustrated in Fig. 5.5. When predicting the thermal conductivity of the missing substances, we observe a benign transferability to substances in the test set. It is not surprising that a narrow training set (covering a narrow range of alkane chain lengths) leads to higher deviations the further one ‘extrapolates’ in alkane chain length.

Predicting properties of chemically comparable substances, as shown above for a homologous series, is the main strength of a GC approach. The proposed model indeed shows the capability of predicting within homologous series. In a second step of analyzing the transferability of model parameters, we now regard substances with multiple functional groups. With ‘multiple functional groups’ we refer to substances containing more than one chemical groups other than simple or branched alkane-groups. In general, group-contribution methods are known for their limitations in predicting properties of substances with multiple functional groups, especially when multiple polar or associating functional groups are involved. That is evident because group contribution methods cannot natively capture details such as intramolecular hydrogen bonds or shielding effects of polar groups through other groups. Nevertheless, we want to assess how the proposed GC approach performs when applied to

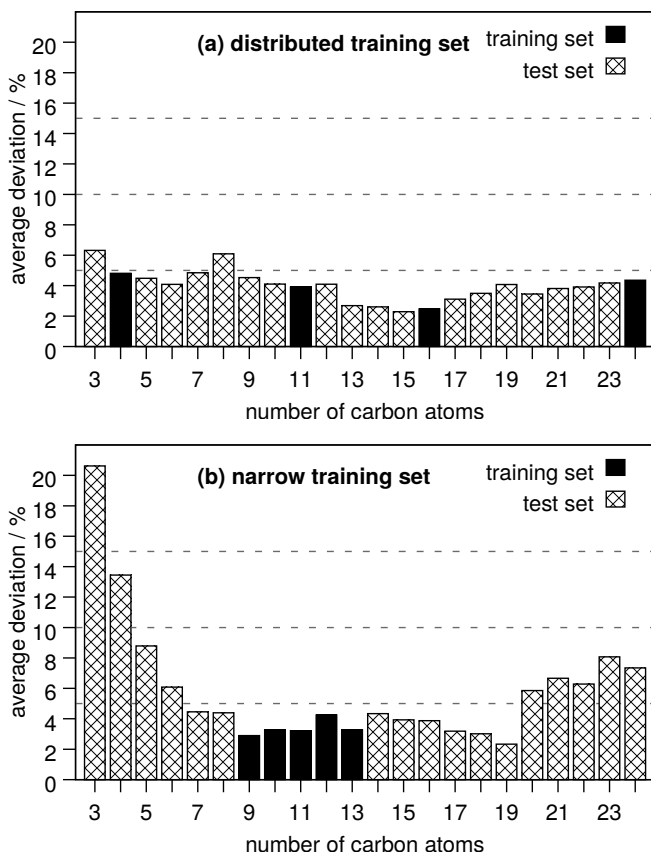


Figure 5.5: Assessing the transferability of group-contribution parameters of the proposed model for thermal conductivity. The homologous series of *n*-alkanes is divided into a training set and a test set. The diagrams report averaged absolute deviations for all *n*-alkanes contained in our database.

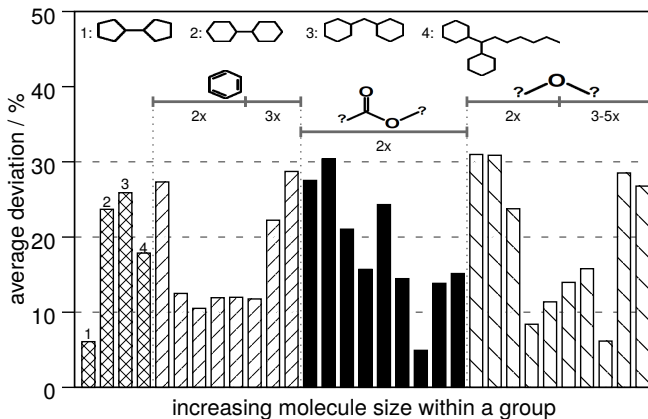


Figure 5.6: Averaged absolute deviations for substances consisting of multiple functional groups of same type. Grouped by functional-group type, and within a group sorted by increasing chain length.

substances with multiple functional groups. We note also that the underlying GC PCP-SAFT equation of state was not primarily intended for such substances, because GC PCP-SAFT was also parameterized only using substances containing one polar functional group [39]. For these reasons, we regard substances with multiple functional groups as a tough and interesting test case for a group contribution model and, of course, we do expect higher deviations for predictions on substances containing more than one functional group.

When using the proposed group contribution model to predict thermal conductivities of substances with multiple functional groups of the same type we have two observations: (1) substances with multiple $-\text{OH}$ -groups are predicted in poor agreement to experimental data, and (2) for all other substances one finds rather satisfying results (see Fig. 5.6). Figure 5.7 shows the entropy-scaling behavior of substances with single and multiple groups of the same type for esters and for alcohols. Data for the various esters are all grouped in a rather well-behaved way. This is true for all chemical families for which we found experimental data, except for alcohols. For the multi-functional alcohols (primary alcohol, diol to triol) we see a retracting (yo-yo) behavior with increasing number of hydroxyl-groups in Fig. 5.7. We consider an n -alkane (with no hydroxyl-group) of comparable chain length as a reference. A lowering of thermal conductivity is seen when a hydroxyl is added to an alkyl-chain. Upon adding a second hydroxyl-group (diol), however, the thermal conductivity increases and for a triol it proceeds to increase. The yo-yo behavior would also have to persist in parameter A_α - D_α (mainly B_α). The linear structure of the mixing rules, eq. (5.6), does not allow for such a yo-yo

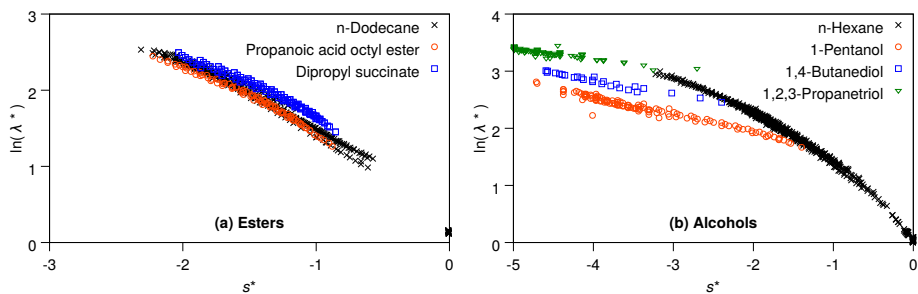


Figure 5.7: Logarithmic reduced experimental thermal conductivity versus reduced residual entropy for several substances of comparable chain-length. Black crosses: *n*-Alkane of corresponding chain-length. Colored open symbols: Substances with one (red circles), two (blue boxes), or three (green triangles) functional groups of same type.

behaviour without additional, specific parameterization.

Results for substances that contain two or more different functional groups are presented in the Supplementary Material in more detail. [A short study concerning multi-functional alcohols is summarized in section 5.B within the appendix of this chapter.]

5.3.3 Overall correlation results

The overall correlation result of the group contribution model is summarized in Fig. 5.8. We regard 12 chemical groups with 231 substances and overall more than 50,000 experimental data points. The group referred to as ‘others’ contains water, carbon dioxide, and ethyne. Average deviations of predicted thermal conductivities from experimental values are 6.17% for the proposed GC-model. The deviations are rather low, considering that the model with individual, substance-specific parameters leads to comparable average deviations of 5.38%.

5.4 Conclusion

This work proposes a group-contribution method for the thermal conductivity of pure organic substances covering wide ranges in temperature and pressure for both vapor phases and liquid-phase conditions. Based on the entropy scaling approach and the group-contribution PCP-SAFT equation of state, we develop a parameterization for 29 chemical (functional) groups. This enabled us to investigate 231 substances of 12 chemical families (containing only one functional group) and 123 substances containing multiple functional groups,

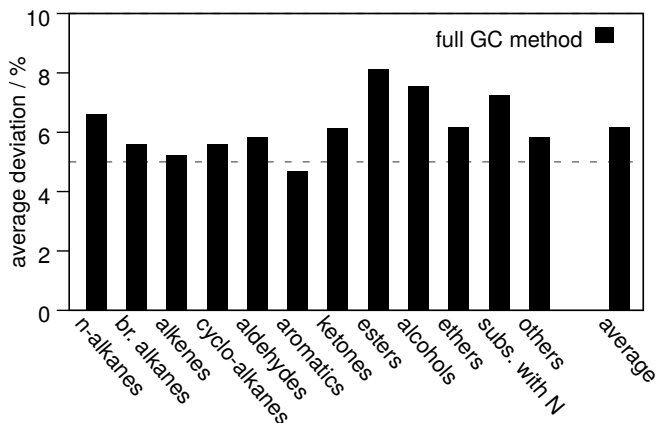


Figure 5.8: Averaged absolute deviations in thermal conductivities as predicted from the group-contribution model towards experimental data for all considered chemical families. The group-contribution model uses GC-PCP-SAFT and A - D from eq. (5.6) (with parameters listed in Table S1 of the Supporting Information).

for which experimental data was available to us. For all substances defined by one functional group, we obtained averaged absolute deviations of only 6.17% for the group-contribution model from experimental values for thermal conductivities. More than 50,000 experimental data points for gaseous or liquid states was thereby considered.

Supporting Information

This material is available free of charge via the Internet at <http://pubs.acs.org>. The Supporting Information details:

- the definition of AAD.
- the resulting parameters $A_\alpha - C_\alpha$.
- the full legend of Fig. 1 of the manuscript.
- diagrams supplementing Fig. 3 of the manuscript.
- the list of components shown in Fig. 6 of the manuscript.
- results of the full GC method for substances containing two or more functional groups.
- the AADs for the individual approach using PCP-SAFT and the full GC method using GC PCP-SAFT, as well as the number of available data for all investigated substances.

- the individual correlation parameters A - D for PCP-SAFT for all investigated components, for which no parameters were published yet,
- as well as the according individual PCP-SAFT parameters.
- group decomposition of all considered substances.

[The supporting information is given in Appendix D of this work.]

Appendices

5.A Mixing rules

The mixing rules given in eq. (5.6) are empirical equations. We here share our rational in developing these rules.

For each of the correlation parameters A - C a mixing rule is needed. We considered the number of functional groups as well as the PCP-SAFT-parameters m_α , σ_α and ϵ_α as descriptors (i.e. weights) in a group-contribution framework. We assumed any parameter $P_i \in \{A_i, B_i, C_i\}$ of substance i consisting of groups $\alpha \in \{\text{CH}_3, \text{CH}_2, \text{OH}, \dots\}$ can be expressed as a ratio of descriptors (each to some power), so that parameter P_i is obtained from a mixing rule as

$$P_i = \frac{\sum_\alpha m_\alpha^{\gamma_1} \sigma_\alpha^{\gamma_2} \epsilon_\alpha^{\gamma_3} n_{i,\alpha}^{\gamma_4} P_\alpha}{\sum_\alpha m_\alpha^{\delta_1} \sigma_\alpha^{\delta_2} \epsilon_\alpha^{\delta_3} n_{i,\alpha}^{\delta_4}} \quad (5.7)$$

where γ_k and δ_k are a priori unknown adjustable parameters. We reduced the number of adjustable parameters γ_k and δ_k through some intuitive decisions. First, we set $\gamma_k = \delta_k$ to enforce balanced units. Second, we assumed the energy parameter ϵ to be of no influence and set $\gamma_3 = \delta_3 = 0$. To describe the size of a functional group, often the ‘volume’ of the functional group is used. In terms of the PCP-SAFT EoS, the parameter combination $m_\alpha \sigma_\alpha^3$ can be viewed as a representative repulsive ‘volume’, so we defined $\gamma_1 = \gamma_2/3$. Applying these intuitive decisions to Eq.(5.7) leads to

$$P_i = \frac{\sum_\alpha (m_\alpha \sigma_\alpha^3)^{\gamma_1} n_{i,\alpha}^{\gamma_2} P_\alpha}{\left(\sum_\alpha (m_\alpha \sigma_\alpha^3)^{\gamma_1} n_{i,\alpha}^{\gamma_2}\right)^{\gamma_3}} \quad (5.8)$$

Additionally, we allow only 1 or 0 as values for all γ . Considering 3 parameters (A - C), with 3 exponents each (γ_1 - γ_3), with 2 possibilities each (0 or 1), leads to $2^{3 \cdot 3} = 2^9 = 512$ possible combinations for the mixing rules. We tested all of these combinations for a test-set consisting of substances from all considered chemical families. We thereby followed the (consecutive) scheme for adjusting model parameters as described in the main text above. From the

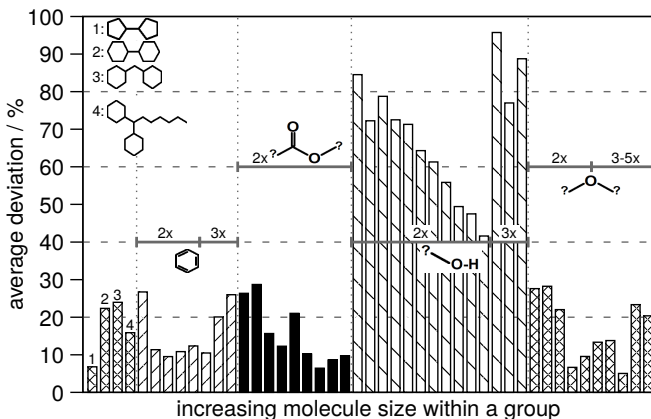


Figure 5.9: Figure 5.6 from the main part of this chapter, but with multi-functional alcohols included. Averaged absolute deviations for substances consisting of multiple functional groups of same type. Grouped by functional-group type, and within a group sorted by increasing chain length.

512 combinations, only 370 converged, partly with very high average deviations. All converged combinations show a clear preference to $\gamma_2 = 1$ for all P_i . We therefore neglected all combinations with $\gamma_2 = 0$. Sorting the remaining combinations by their performance (in terms of AADs), we selected the best 3 combining rules for further investigation. For these 3 candidate mixing rules we adjusted parameters A_α , B_α , C_α to all available data and compared the performances of the group contribution models in predicting substances with multiple functional groups. The most robust mixing rule was selected, which is Eq. (5.6).

5.B Multi-functional alcohols

This section is not a part of the original publication but was added to this work for further explanation.

In section 5.3.2 of this chapter, we explicitly excluded multi-functional alcohols from our study. If these substances are added to Fig. 5.6, which was given above, the explained limitation becomes visible (see Fig. 5.9).

As a possible step to overcome this limitation, we adjusted the correlation parameters A – C individually for all substances containing any number of $-\text{OH}$ -groups, but no other functional groups (D kept constant at given value). Afterwards, we calculated the portion of the parameters which is already covered by the combination of the basic functional groups A_{basic} – C_{basic} . The

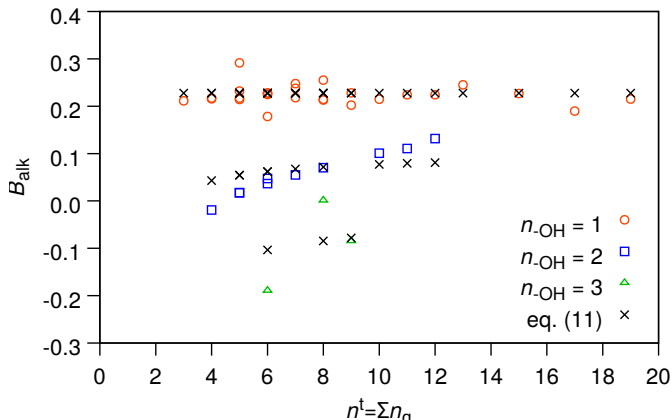


Figure 5.10: Colored empty symbols: Expected values of the alcohol-portion B_{alk} of correlation parameter B , for simple alcohols (red circles), substances with two $-\text{OH}$ -groups (blue boxes), and substances with three $-\text{OH}$ -groups (green triangles). Black crosses: Calculated values of B_{alk} using eq. 5.9 and $B_{-\text{OH}}$ from Table D.2 given in the supporting Information.

difference of the individually adjusted A - C to the corresponding portion of the basic functional groups $A_{\text{basic}}-C_{\text{basic}}$ gives us the expected values for the alcohol-portion of the parameters, $A_{\text{alk}}-C_{\text{alk}}$. We found that the expected values A_{alk} and C_{alk} can be described using the quasi-mixing rules given in eq. 5.6. Only for the expected alcohol-portion of parameter B , $B_{\text{alk}} = B - B_{\text{basic}}$, a different description is needed. In Figure 5.10 we show the dependency of B_{alk} on the number of $-\text{OH}$ -groups $n_{-\text{OH}}$ and on the size of the molecule n^t . For each $n_{-\text{OH}}$, a linear dependency of B_{alk} on n^t can be seen, but with different slope and intercept. To describe this array of curves we propose the alcohol-specific extension of the quasi-mixing rule of parameter B as follows

$$B = \sum_{\alpha} \begin{cases} B_{\alpha} + (1 - n_{\alpha}) \left[\frac{(n^t + 1)}{n^t} B_{\alpha} - 0.1 \right] & \text{for } \alpha = -\text{OH} \\ n_{\alpha} B_{\alpha} & \text{otherwise} \end{cases} \quad (5.9)$$

For $n_{-\text{OH}} = 1$ this extension equals the original quasi-mixing rule, so the original $B_{-\text{OH}}$ as given in Table D.2 can still be used. Therefore, substances with multiple $-\text{OH}$ -groups can now be described using parameters which were adjusted to simple alcohols only.

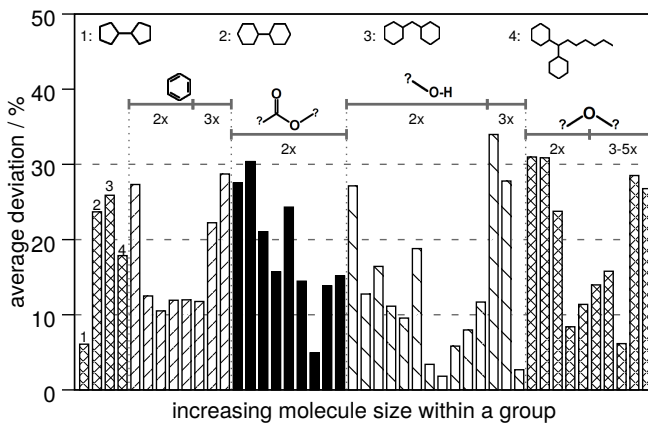


Figure 5.11: Figure 5.6 from the main part of this chapter again, but with multi-functional alcohols included and eq. (5.9) applied. Averaged absolute deviations for substances consisting of multiple functional groups of same type. Grouped by functional-group type, and within a group sorted by increasing chain length.

Bibliography

- [1] W. Su, L. Zhao, and S. Deng, “Group contribution methods in thermodynamic cycles: Physical properties estimation of pure working fluids,” *Renew. Sust. Energ. Rev.*, vol. 79, pp. 984–1001, 2017.
- [2] A. Bardow, K. Steur, and J. Gross, “Continuous-molecular targeting for integrated solvent and process design,” *Ind. Eng. Chem. Res.*, vol. 49, no. 6, pp. 2834–2840, 2010.
- [3] M. Stavrou, M. Lampe, A. Bardow, and J. Gross, “Continuous molecular targeting–computer-aided molecular design (comt–camd) for simultaneous process and solvent design for co2 capture,” *Ind. Eng. Chem. Res.*, vol. 53, no. 46, pp. 18029–18041, 2014.
- [4] M. Lampe, M. Stavrou, H. Buckner, J. Gross, and A. Bardow, “Simultaneous optimization of working fluid and process for organic rankine cycles using pc-saft,” *Ind. Eng. Chem. Res.*, vol. 53, no. 21, pp. 8821–8830, 2014.
- [5] J. Schilling, M. Lampe, J. Gross, and A. Bardow, “1-stage comt-camd: An approach for integrated design of orc process and working fluid using pc-saft,” *Chem. Eng. Sci.*, vol. 159, pp. 217–230, 2017.
- [6] J. Schilling, M. Lampe, J. Gross, and A. Bardow, “1-stage CoMT-CAMD: An approach for integrated design of ORC process and working fluid using PC-SAFT,” *Chem. Eng. Sci.*, vol. 159, pp. 217–230, 2017.
- [7] J. Schilling, D. Tillmanns, M. Lampe, M. Hopp, J. Gross, and A. Bardow, “From molecules to dollars: integrating molecular design into thermoeconomic process design using consistent thermodynamic modeling,” *Mol. Syst. Des. Eng.*, vol. 2, no. 3, pp. 301–320, 2017.
- [8] O. Lötgering-Lin and J. Gross, “Group contribution method for viscosities based on entropy scaling using the perturbed-chain polar statistical associating fluid theory,” *Ind. Eng. Chem. Res.*, vol. 54, no. 32, pp. 7942–7952, 2015.
- [9] O. Lötgering-Lin, M. Fischer, M. Hopp, and J. Gross, “Pure substance and mixture viscosities based on entropy scaling and an analytic equation of state,” *Ind. Eng. Chem. Res.*, vol. 57, no. 11, pp. 4095–4114, 2018.

- [10] M. Hopp and J. Gross, “Thermal conductivity of real substances from excess entropy scaling using pcp-saft,” *Ind. Eng. Chem. Res.*, vol. 56, no. 15, pp. 4527–4538, 2017.
- [11] M. Hopp, J. Mele, and J. Gross, “Self-diffusion coefficients from entropy scaling using the pcp-saft equation of state,” *Ind. Eng. Chem. Res.*, vol. 57, pp. 12942–12950, 2018.
- [12] B. E. Poling, J. M. Prausnitz, and J. P. O’Connell, *The Properties of Gases and Liquids - fifth Edition*. McGraw-Hill, 2000.
- [13] S. Sastri and K. Rao, “A new group contribution method for predicting viscosity of organic liquids,” *Chem Eng. J.*, vol. 50, no. 1, pp. 9–25, 1992.
- [14] S. Sastri and K. Rao, “A new method for predicting saturated liquid viscosity at temperatures above the normal boiling point,” *Fluid Phase Equilib.*, vol. 175, no. 1, pp. 311 – 323, 2000.
- [15] Y. Liang, P. Ma, and P. Li, “Estimation of liquid viscosity of pure compounds at different temperatures by a corresponding-states group-contribution method,” *Fluid Phase Equilib.*, vol. 198, no. 1, pp. 123 – 130, 2002.
- [16] R. Ceriani, C. B. Gonçalves, J. Rabelo, M. Caruso, A. C. C. Cunha, F. W. Cavaleri, E. A. C. Batista, and A. J. A. Meirelles, “Group contribution model for predicting viscosity of fatty compounds,” *J. Chem. Eng. Data*, vol. 52, no. 3, pp. 965–972, 2007.
- [17] R. L. Gardas and J. A. Coutinho, “Group contribution methods for the prediction of thermophysical and transport properties of ionic liquids,” *AIChE J*, vol. 55, no. 5, pp. 1274–90, 2009.
- [18] K. Müller and W. Arlt, “An estimation method for thermal conductivity in the fluid phase,” *J. Chem. Eng. Data*, vol. 59, no. 4, pp. 946–953, 2014.
- [19] D. Roy and G. Thodos, “Thermal conductivity of gases. organic compounds at atmospheric pressure,” *Ind. Eng. Chem. Fund.*, vol. 9, no. 1, pp. 71–79, 1970.
- [20] M. Nagvekar and T. E. Daubert, “A group contribution method for liquid thermal conductivity,” *Ind. & Eng. Chem. Res.*, vol. 26, no. 7, pp. 1362–1365, 1987.
- [21] S. Sastri and K. Rao, “Quick estimating for thermal conductivity,” *Chem. Engin.*, vol. 100, no. 8, p. 106, 1993.

- [22] S. Sastri and K. Rao, "A new temperature–thermal conductivity relationship for predicting saturated liquid thermal conductivity," *Chem. Eng. J.*, vol. 74, no. 3, pp. 161–169, 1999.
- [23] C. M. Rodenbush, D. S. Viswanath, and F.-H. Hsieh, "A group contribution method for the prediction of thermal conductivity of liquids and its application to the prandtl number for vegetable oils," *Ind. & Eng. Chem. Res.*, vol. 38, no. 11, pp. 4513–4519, 1999.
- [24] K.-J. Wu, C.-X. Zhao, and C.-H. He, "Development of a group contribution method for determination of thermal conductivity of ionic liquids," *Fluid Phase Equilib.*, vol. 339, pp. 10 – 14, 2013.
- [25] F. Gharagheizi, P. Ilani-Kashkouli, M. Sattari, A. H. Mohammadi, and D. Ramjugernath, "A group contribution method for determination of thermal conductivity of liquid chemicals at atmospheric pressure," *J. Mol. Liq.*, vol. 190, pp. 223 – 230, 2014.
- [26] H. B. Rokni, J. D. Moore, A. Gupta, M. A. MHugh, R. R. Mallepally, and M. Gavaises, "General method for prediction of thermal conductivity for well-characterized hydrocarbon mixtures and fuels up to extreme conditions using entropy scaling," *Fuel*, vol. 245, pp. 594 – 604, 2019.
- [27] J. Gross and G. Sadowski, "Perturbed-chain saft: An equation of state based on a perturbation theory for chain molecules," *Ind. Eng. Chem. Res.*, vol. 40, pp. 1244–1260, 2001.
- [28] J. Gross and J. Vrabec, "An equation-of-state contribution for polar components: Dipolar molecules," *AIChE J.*, vol. 52, pp. 1194 – 1204, 2006.
- [29] Y. Rosenfeld, "Relation between the transport coefficient and the internal entropy of simple systems," *Phys. Rev. A*, vol. 15, no. 6, pp. 2545–2549, 1977.
- [30] Y. Rosenfeld, "A quasi-universal scaling law for atomic transport in simple fluids," *J. Phys.: Condens. Matter*, vol. 11, pp. 5415–5427, 1999.
- [31] J. Vijande, M. M. Pineiro, D. Bessieres, H. Saint-Guirons, and J. L. Legido, "Description of pvt behaviour of hydrofluoroethers using the pc-saft eos," *Phys. Chem. Chem. Phys.*, vol. 6, pp. 766–770, 2004.
- [32] S. Tamouza, J. P. Passarello, P. Tobaly, and J.-C. de Hemptinne, "Group contribution method with SAFT EOS applied to vapor liquid equilibria of various hydrocarbon series," *Fluid Phase Equilib.*, vol. 222, pp. 67–76, 2004.

- [33] A. Tihic, G. Kontogeorgis, N. von Solms, M. L. Michelsen, and L. Constantinou, "A predictive group-contribution simplified pc-saft equation of state: Application to polymer systems," *Ind. Eng. Chem. Res.*, vol. 47, no. 15, pp. 5092–5101, 2008.
- [34] A. Lymperiadis, C. S. Adjiman, A. Galindo, and G. Jackson, "A group contribution method for associating chain molecules based on the statistical associating fluid theory (saft- γ)," *J. Chem. Phys.*, vol. 127, p. 234903, 2007.
- [35] Y. Peng, K. D. Goff, M. dos Ramos, and C. McCabe, "Developing a predictive group-contribution-based saft-vr equation of state," *Fluid Phase Equilib.*, vol. 277, no. 2, pp. 131–144, 2009.
- [36] J. Gross, O. Spuhl, F. Tumakaka, and G. Sadowski, "Modeling copolymer systems using the perturbed-chain SAFT equation of state," *Ind. Eng. Chem. Res.*, vol. 42, no. 6, pp. 1266–1274, 2003.
- [37] K. Paduszyński and U. Domańska, "Heterosegmented perturbed-chain statistical associating fluid theory as a robust and accurate tool for modeling of various alkanes. 1. pure fluids," *Ind. Eng. Chem. Res.*, vol. 51, no. 39, pp. 12967–12983, 2012.
- [38] F. T. Peters, F. S. Laube, and G. Sadowski, "Development of a group contribution method for polymers within the pc-saft model," *Fluid Phase Equilib.*, vol. 324, no. 0, pp. 70 – 79, 2012.
- [39] E. Sauer, M. Stavrou, and J. Gross, "Comparison between a homo- and a heterosegmented group contribution approach based on the perturbed-chain polar statistical associating fluid theory equation of state," *Ind. Eng. Chem. Res.*, vol. 53, no. 38, pp. 14854–14864, 2014.
- [40] P. D. Neufeld, A. R. Janzen, and R. A. Aziz, "Empirical equation to calculate 16 of the transport collision integrals $\omega^{(l,s)*}$ for the lennard-jones (12-6) potential," *J. Chem. Phys.*, vol. 57, no. 3, pp. 1100 – 1102, 1972.
- [41] D. W. Marquardt, "An algorithm for least-squares estimation of non-linear parameters," *SIAM J. Appl. Math.*, vol. 11, no. 2, pp. 431–441, 1963.
- [42] DDBST Dortmund Data Bank Software & Separation Technology GmbH, Oldenburg, Germany, 2015. <http://www.ddbst.com>.
- [43] M. Hopp, J. Mele, R. Hellmann, and J. Gross, "Thermal conductivity via entropy scaling: An approach that captures the effect of intramolecular degrees of freedom," *Ind. Eng. Chem. Res.*, 2019.

- [44] B. Le Neindre, R. Tufeu, P. Bury, and J. V. Sengers, "Thermal conductivity of carbon dioxide and steam in the supercritical region," *Ber. Bunsen.*, vol. 77, no. 4, pp. 262–275, 1973.
- [45] B. W. Tiesinga, E. P. Sakonidou, H. R. van den Berg, J. Luettmer-Strathmann, and J. V. Sengers, "The thermal conductivity of argon in the critical region," *J. Chem. Phys.*, vol. 101, no. 8, pp. 6944–6963, 1994.
- [46] J. Luettmer-Strathmann, J. V. Sengers, and G. A. Olchowy, "Non-asymptotic critical behavior of the transport properties of fluids," *J. Chem. Phys.*, vol. 103, no. 17, pp. 7482–7500, 1995.
- [47] E. P. Sakonidou, H. R. van den Berg, C. A. ten Seldam, and J. V. Sengers, "The thermal conductivity of methane in the critical region," *J. Chem. Phys.*, vol. 105, no. 23, pp. 10535–10555, 1996.
- [48] R. A. Perkins, J. V. Sengers, I. M. Abdulagatov, and M. L. Huber, "Simplified model for the critical thermal-conductivity enhancement in molecular fluids," *Int. J. Thermophys.*, vol. 34, pp. 191–212, 2013.
- [49] F. M. Gumerov, D. G. Amirkhanov, A. G. Usmanov, and B. Le Neindre, "The thermal diffusivity of argon in the critical region," *Int. J. Thermophys.*, vol. 12, no. 1, pp. 67–83, 1991.
- [50] D. J. Searles, D. J. Evans, H. J. M. Hanley, and S. Murad, "Simulations of the thermal conductivity in the vicinity of the critical point," *Mol. Simul.*, vol. 20, pp. 385–395, 1998.
- [51] K. G. Wilson, "Renormalization group and critical phenomena. ii. phase-space cell analysis of critical behavior," *Phys. Rev. B*, vol. 4, no. 9, p. 3184, 1971.
- [52] J. A. White, "Contribution of fluctuations to thermal properties of fluids with attractive forces of limited range: theory compared with p^t and cv data for argon," *Fluid Phase Equilib.*, vol. 75, pp. 53–64, 1992.
- [53] X. Tang and J. Gross, "Renormalization-group corrections to the perturbed-chain statistical associating fluid theory for binary mixtures," *Ind. Eng. Chem. Res.*, vol. 49, no. 19, pp. 9436–9444, 2010.

6 Thermal Conductivity from Entropy Scaling: Mixtures

In this chapter, I present a first approach for predicting thermal conductivity of mixtures from entropy scaling.

6.1 Introduction

The previous chapters proposed models based on entropy scaling for predicting thermal conductivity and self-diffusion coefficients for pure substances. Transport coefficients of pure substances are usually used as building block for most of the available models for transport coefficients of mixtures. As was shown by Schilling et al. [1, 2], an economic optimization of thermodynamic processes is possible if a model for the thermal conductivity of mixtures is available. In this chapter, I prove the applicability of the entropy scaling approach for the thermal conductivity of mixtures based on the entropy scaling approach for pure substances (Chapter 2). The model is thereby defined without binary mixture parameter, so that thermal conductivities of mixtures are described predictively.

Whereas entropy scaling is investigated in a significant number of studies for the description of pure fluids, the number of literature on mixtures is rather limited. The first literature on thermal conductivity of gas mixtures is based on kinetic gas theory [3] and is further developed in the 50s [4, 5] using the work of Chapman-Cowling [6]. Based on these works, mixing rules, e.g. mixing rule of Wilke [7], were developed. Alternative models are based on experimentally fitted constitutive equations [8]. The previously mentioned models are limited to gas mixtures or simple fluid mixtures. Extrapolation to more complex fluid mixtures is not possible. In the last decades, molecular dynamics simulations are used to predict thermal conductivity [9]. Molecular simulations are still costly and limited due to the complexity of the molecules. For diffusion coefficients, there already exist some approaches to calculate binary diffusion coefficients which take the self-diffusion coefficients of the involved pure substances as input parameter [10–14]. A comparable simple predictive approach, preferably without any further adjustable parameters, is still lacking for thermal conductivity of mixtures.

In the context of entropy scaling, the first approach to predict transport coefficients using entropy scaling was recently presented by O. Lötgering-Lin, who investigated viscosity of mixtures using PCP-SAFT [15]. There is no

literature on entropy scaling of thermal conductivity of mixtures.

6.2 Theoretical Background

The basic principle of entropy scaling can be summarized in one simple correlation

$$\lambda^{*\text{exp}} = \lambda^{\text{exp}} / \lambda^{\text{ref}} \approx \lambda^*(s^*, \Theta) \quad (6.1)$$

The reduced thermal conductivity $\lambda^{*\text{exp}}$, which is defined by dividing the thermal conductivity by an appropriate reference value λ^{ref} , can be approximated well using an ansatz function $\lambda^*(s^*, \Theta)$ as a univariate function of residual entropy s^* only, through a set of model parameters Θ . In previous chapters, we proposed suitable ansatz functions and we determined the vector of model parameters $\Theta = [A, B, C, D]$ of many pure substances. Now, entropy scaling for thermal conductivity of mixtures is investigated using the same structure of equations. The quality of the results for thermal conductivity of mixtures is analyzed. As a model for the mixture thermal conductivity, entropy scaling can be used for correlating or predicting mixtures by rearranging eq. 6.1, as

$$\lambda = \lambda^{\text{ref}} \cdot \lambda^*(s^*, \Theta) \quad \text{with } \Theta = [A, B, C, D] \quad (6.2)$$

where $\lambda^{\text{ref}}(T, x, \Theta^{\text{PC-SAFT}})$ is the reference thermal conductivity and $\Theta^{\text{PC-SAFT}}$ is the vector of pure component parameters of the PC-SAFT equation of state (and it is the same vector that enters in the calculation of $s^*(T, \rho, x, \Theta^{\text{PC-SAFT}})$). In this chapter, λ refers to a calculated thermal conductivity, whereas experimental values are indicated as λ^{exp} . The reduced residual entropy s^* is calculated using PCP-SAFT.

Up to this point, the equations of this chapter can be read for both mixtures and pure substances. In the remainder of this chapter, properties of pure substances are identified by superscript pure . An identifying superscript mix for mixture quantities is omitted, to enhance readability. Furthermore, I will use N as the number of components within a mixture.

One may consider several approaches for extending a model for thermal conductivity of a pure substance to mixtures. In the simplest approach (approach **A**), we calculate the thermal conductivity λ_i^{pure} at given temperature and pressure using every pure substance correlation $\lambda_i^{*\text{pure}}$ individually. In a second step, these λ_i^{pure} are then combined via mixing rules to the mixture value λ , using different weighting factors ω .

$$\lambda = \sum \omega \lambda_i^{\text{pure}} \quad \text{with } \lambda_i^{\text{pure}} = \lambda_i^{\text{ref, pure}} \cdot \lambda_i^{*\text{pure}}(s_i^{*\text{pure}}, \Theta_i^{\text{pure}}) \quad (6.3)$$

with $s_i^{*\text{pure}}(T, \rho_i^{\text{pure}}(T, p))$ as the residual entropy of pure substance i .

In contrast, approach **B** defines a mixture reference λ^{ref} , by either combining $\lambda_i^{\text{ref,pure}}$ using mixing-rules or by direct approaches from literature. Once λ^{ref} is defined, we still have two choices. Either the pure substances' polynomials λ_i^{pure} are evaluated and combined using mixing-rules (approach **B.1**).

$$\lambda = \lambda^{\text{ref}} \cdot \sum \omega \lambda_i^{\text{pure}}(s_i^*, \Theta_i^{\text{pure}}) \quad (6.4)$$

where $s_i^*(T, \rho(T, p, \bar{x}), \bar{x})$ is the partial molar quantity to s^* of species i in the mixture, and ω is a weighting factor.

Second, a polynomial can be directly defined for mixtures by combining Θ_i^{pure} to mixture parameters Θ and using the mixture's residual entropy s^* for entropy scaling (approach **B.2**).

$$\lambda = \lambda^{\text{ref}} \cdot \lambda^* \quad \text{with } \lambda^*(s^*, \Theta) \quad (6.5)$$

with $s^*(T, \rho(T, p, \bar{x}), \bar{x})$ as residual entropy of the mixture.

The possible advantages and drawbacks of the three approaches summarized in equations (6.3), (6.4) and (6.5) are further described in the following subsections.

6.2.1 Approach A - Trivial Mixing Rules

The first approach (Approach **A**) is based on weighted arithmetic means (mixing rules), using the thermal conductivity of the pure substance. First, the thermal conductivity $\lambda_i^{\text{pure}} = \lambda_i^{\text{ref,pure}} \cdot \lambda_i^{\text{pure}}(s_i^{\text{pure}}, \Theta_i^{\text{pure}})$ is calculated for each component i of the mixture. Afterwards, all λ_i^{pure} are combined to a mixture thermal conductivity λ using simple mixing rules. Four different mixing rules are tested. They differ in the weighing of λ_i , although all versions contain the molar fraction x_i (see Table 6.1). It is investigated if considering attributes of chain length (\mathcal{N}^{e} A.2), shadow area (\mathcal{N}^{e} A.3) or volume (\mathcal{N}^{e} A.4) have a distinct influence on the quality of the predictions.

Table 6.1: Equations for mixture thermal conductivity λ of approach A.

\mathcal{N}^{e}	symbol	equation
A1	λ^{A1}	$= \sum_{i=1}^N x_i \lambda_i^{\text{pure}}$
A2	λ^{A2}	$= \sum_{i=1}^N \frac{x_i m_i}{m_{\text{mix}}} \lambda_i^{\text{pure}}$
A3	λ^{A3}	$= \sum_{i=1}^N \frac{x_i m_i \sigma_i^2}{(m \sigma^2)_{\text{mix}}} \lambda_i^{\text{pure}}$
A4	λ^{A4}	$= \sum_{i=1}^N \frac{x_i m_i \sigma_i^3}{(m \sigma^3)_{\text{mix}}} \lambda_i^{\text{pure}}$

Here and in the remainder of this chapter, abbreviations for differently com-

binned PCP-SAFT parameters are used as follows

$$m_{mix} = \sum_{i=1}^N x_i m_i \quad (m\sigma^2)_{mix} = \sum_{i=1}^N x_i m_i \sigma_i^2 \quad (m\sigma^3)_{mix} = \sum_{i=1}^N x_i m_i \sigma_i^3$$

We note that, in many applications, not all components i of a mixture may be stable (at given temperature and pressure) in the desired phase. Thus, using the residual entropy of a pure substance $s_i^{*pure}(T, \rho_i^{pure}(T, p))$ at these conditions to calculate λ_i^{pure} and subsequently λ can only be a rough estimation for mixtures consisting of fairly similar substances, e.g. only linear alkanes with nearly same chain length. Nevertheless, the approaches A1 to A4 (Table 6.1) are investigated in a first step to show how far off such simple approaches can be, to raise awareness against the usage of these easy ansatz functions in the design of thermodynamic processes. A different choice could have been geometric weighting, using $\lambda = \prod(\lambda_i^{pure})^{\omega x_i}$, with different weighting factors ω . Due to the limitation named above, these approaches were directly neglected.

6.2.2 Approach B - Mixture Reference

Instead of calculating pure substance thermal conductivities and subsequently combining them, the definition of a dedicated reference thermal conductivity for mixtures seems appropriate. To define such a mixture reference thermal conductivity, several approaches can be thought of. The most trivial approach would be to combine the PCP-SAFT parameters using the Lorentz-Berthelot rules and introduce these into the pure-substance reference equation (№ R1 in table 6.2). Second, a combination of the individual references $\lambda_i^{ref,pure}$ using the molar fraction, maybe weighted by shape or volume indicators could be a sensible choice (№ R2 to R5). Additionally, some dedicated approaches from literature designed to describe the thermal conductivity of mixtures in restricted phase areas, e.g. only for diluted gases, can be tested (№ R6 to R9).

For mixture viscosities [15], the mixing rule according to Wilke [10, 16] was found to be most reliable. We will evaluate how well this approach works for thermal conductivities as well, since first calculations by other groups [1] are using this ansatz. The approach by Wilke, when directly substituting λ for η , is defined as

$$\lambda^{Wilke} = \sum_{i=1}^N \frac{x_i \lambda_i^{ref,pure}}{\sum_{k=1}^N x_k \Phi_{ik}} \quad \text{with} \quad \Phi_{ik} = \frac{\left[1 + \left(\lambda_i^{ref,pure} / \lambda_k^{ref,pure} \right)^{1/2} (M_k / M_i)^{1/4} \right]^2}{[8 (1 + M_i / M_k)]^{1/2}}$$

In *Molecular Theory of Gases and Liquids* Hirschfelder, Curtiss and Bird [6] analyse in detail the theory from Chapman and Cowling [17]. Apart from

the basic Chapman–Enskog equations for pure substances as an ideal gas, approaches for binary mixtures are described there as well. The ansatz for the thermal conductivity of a binary mixture consisting of two species as an ideal gas reads as follows:

$$\begin{aligned}\lambda^{\text{HCB}} &= \frac{1 + Z_\lambda}{X_\lambda + Y_\lambda} \\ X_\lambda &= \frac{x_1^2}{\lambda_1^{\text{ref,pure}}} + \frac{2x_1x_2}{\lambda_{12}} + \frac{x_2^2}{\lambda_2^{\text{ref,pure}}} \\ Y_\lambda &= \frac{x_1^2}{\lambda_1^{\text{ref,pure}}} U_1 + \frac{2x_1x_2}{\lambda_{12}} U_Y + \frac{x_2^2}{\lambda_2^{\text{ref,pure}}} U_2 \\ Z_\lambda &= x_1^2 U_1 + 2x_1x_2 U_Z + x_2^2 U_2 \\ \lambda_{12} &= \frac{1989.1}{10^3} \frac{\sqrt{T(M_1 + M_2)/(2M_1M_2)}}{\sigma_{12}^2 \Omega_{12}^{2,2}} \\ U_1 &= \frac{4}{15} - \frac{1}{12} \left(\frac{12}{5} + 1 \right) \frac{M_1}{M_2} + \frac{(M_1 - M_2)^2}{M_1 M_2} \\ U_2 &= \frac{4}{15} - \frac{1}{12} \left(\frac{12}{5} + 1 \right) \frac{M_2}{M_1} + \frac{(M_2 - M_1)^2}{M_1 M_2} \\ U_Y &= \frac{4}{15} \left(\frac{(M_1 + M_2)^2}{4M_1 M_2} \right) \frac{\lambda_{12}^2}{\lambda_1^{\text{ref,pure}} \lambda_2^{\text{ref,pure}}} - \frac{1}{12} \left(\frac{12}{5} + 1 \right) - \frac{5}{32} \left(\frac{12}{5} - 5 \right) \frac{(M_1 - M_2)^2}{M_1 M_2} \\ U_Z &= \frac{4}{15} \left(\left(\frac{(M_1 + M_2)^2}{4M_1 M_2} \right) \left(\frac{\lambda_{12}}{\lambda_1^{\text{ref,pure}}} + \frac{\lambda_{12}}{\lambda_2^{\text{ref,pure}}} \right) - 1 \right) - \frac{1}{12} \left(\frac{12}{5} + 1 \right)\end{aligned}$$

In *The Properties of Gases and Liquids* Poling, Prausnitz and O’Connel [10] list two approaches describing low pressure gas mixtures, three for high pressure gas mixtures and three for liquid mixtures are listed. Most of them suggest to use pure substance descriptions and provide mixing rules for all occurring parameters. These mixing-rules either need additional parameters, e.g. the accentric factor, or propose separate mixing rules for varying densities or different chemical families. One exception is the approach by Wassiljewa combined with the modification by Mason and Saxena ([10] p.10.30ff), which we will call the WMS approach based on the abbreviated names of the original authors.

$$\lambda^{\text{WMS}} = \frac{\sum_{i=1}^N x_i \lambda_i^{\text{ref,pure}}}{\sum_{k=1}^N x_k A_{ik}} \quad (6.6)$$

with

$$\begin{aligned}A_{ik} &= \frac{\left[1 + (\lambda_{tr,i}/\lambda_{tr,k})^{1/2} (M_i/M_k)^{1/4} \right]^2}{\left[8(1 + M_i/M_k) \right]^{1/2}} \\ (CE) &\rightarrow \lambda_{tr,i} = \lambda_i^{\text{ref,pure,CE}} \\ (\alpha) &\rightarrow \lambda_{tr,i} = \lambda_i^{\text{ref,pure,\alpha}}\end{aligned}$$

where M_i is the molecular mass (in g/mol) and λ_{tr} is referred to as monatomic value of the thermal conductivity. Here, we evaluate two possibilities to define this value: using the Chapman-Enskog thermal conductivity $\lambda_{tr,i} = \lambda_i^{CE}$ and using our own pure-component description $\lambda_{tr,i} = \lambda_i^{ref,\alpha}$ as detailed in (4.4) or (5.4). According to [10], the Wassiljewa equation (6.6) can represent low-pressure mixtures which show either monotonic variation of λ_{mix} with composition, or show one extremum. For monatomic gases, A_{ik} can be converted to Wilke's Φ_{ik} , when substituting $\frac{\lambda_i}{\lambda_k} = \frac{\eta_i M_k}{\eta_k M_i}$.

An overview of all described approaches including the definition of a reference thermal conductivity for mixtures is given in table 6.2. For the approaches R1 to R5 I

Table 6.2: Equations for reference thermal conductivity for mixtures λ_{mix}^{ref} of approach B.

N ^o	symbol	equation
R1	$\lambda^{ref,R1}$	$= \lambda^{ref}(M_{mix}, m_{ij}, \sigma_{ij}, \epsilon_{ij})$
R2	$\lambda^{ref,R2}$	$= \sum_{i=1}^N x_i \lambda_i^{ref,pure}$
R3	$\lambda^{ref,R3}$	$= \sum_{i=1}^N \frac{x_i m_i}{m_{mix}} \lambda_i^{ref,pure}$
R4	$\lambda^{ref,R4}$	$= \sum_{i=1}^N \frac{x_i m_i \sigma_i^2}{(m \sigma^2)_{mix}} \lambda_i^{ref,pure}$
R5	$\lambda^{ref,R5}$	$= \sum_{i=1}^N \frac{x_i m_i \sigma_i^3}{(m \sigma^3)_{mix}} \lambda_i^{ref,pure}$
R6	$\lambda^{ref,R6}$	$= \lambda^{Wilke}$
R7	$\lambda^{ref,R7}$	$= \lambda^{HCB}$
R8	$\lambda^{ref,R8}$	$= \lambda^{WMS}(CE)$
R9	$\lambda^{ref,R9}$	$= \lambda^{WMS}(\alpha)$

expect reasonable results only for mixtures containing similar substances. A better performance is expected from the approaches λ^{HCB} (R7) and $\lambda^{WMS}(CE)$ (R8). The approaches from Wilke λ^{Wilke} (R6) and Wassiljewa, Mason and Saxena $\lambda^{WMS}(\alpha)$ (R9) are expected to yield the best results. Main reasons for these expectations are the results of entropy scaling of mixture viscosity described by O. Lötgering-Lin [15], who investigated partially similar approaches.

After defining a reference thermal conductivity for mixtures, a polynomial λ^* for mixtures is needed as well. Again, two principles can be followed: First, using mixing rules after calculating $\lambda_i^{*pure}(s_i^*, \Theta_i^{pure})$ as given in eq. (6.4) with Θ_i^{pure} as pure substance parameters of the entropy scaling model (approach B.1). Second, evaluating the polynomial using mixture parameters Θ that enter $\lambda^*(s^*, \Theta)$ (approach B.2, see eq. (6.5)).

6.2.3 Approach B.1 - Mixing Rules for Pure Polynomials

The polynomial $\lambda_i^{*\text{pure}}(s_i^*, \Theta_i^{\text{pure}})$ is evaluated using entropy scaling parameters $\Theta_i^{\text{pure}} = [A_i, B_i, C_i, D_i]$ of every component i of the mixture first. Afterwards, variants of the arithmetic mean are used for combining all $\lambda_i^{*\text{pure}}(s_i^*, \Theta_i^{\text{pure}})$ to a mixture value λ^* . All models defined in this way are listed in table 6.3. The partial molar residual entropy

Table 6.3: Equations of approach B.1.

N^{q}	symbol	equation
B1.1	$\lambda^{*\text{B1.1}}$	$= \sum_{i=1}^N x_i \lambda_i^{*\text{pure}}(s_i^*, \Theta_i^{\text{pure}})$
B1.2	$\lambda^{*\text{B1.2}}$	$= \sum_{i=1}^N \frac{x_i m_i}{m_{\text{mix}}} \lambda_i^{*\text{pure}}(s_i^*, \Theta_i^{\text{pure}})$
B1.3	$\lambda^{*\text{B1.3}}$	$= \sum_{i=1}^N \frac{x_i m_i \sigma_i^2}{(m\sigma^2)_{\text{mix}}} \lambda_i^{*\text{pure}}(s_i^*, \Theta_i^{\text{pure}})$
B1.4	$\lambda^{*\text{B1.4}}$	$= \sum_{i=1}^N \frac{x_i m_i \sigma_i^3}{(m\sigma^3)_{\text{mix}}} \lambda_i^{*\text{pure}}(s_i^*, \Theta_i^{\text{pure}})$

$s_i^*(T, \rho, \bar{x})$ can, for sufficiently non-ideal mixtures, take on values that are outside the s^* -range, where pure substance i is in fluid (liquid or vapor) state. In fact, s^* -values can also be positive. Due to this, our expectations on the quality of results is the same as in subsection 6.2.1: Acceptable for simple mixtures (e.g. alkane-alkane of similar length) but not applicable to complex mixtures because of the structure of the mixing rule which does not account well for complex interactions between, e.g., polar substances.

6.2.4 Approach B.2 - Mix the Parameters

Instead of calculating $\lambda_i^{*\text{pure}}(s_i^*, \Theta_i^{\text{pure}})$ and combining these to λ^* , the parameters Θ_i^{pure} themselves can be combined to mixture-parameters Θ . These mixture parameters can then be used to evaluate the correlation polynomial (see e.g. eq. (5.5))

$$\ln(\lambda^{*,5}(s^*, \Theta)) = A + Bs^* + C(1 - \exp(s^*)) + Ds^{*2} \quad (6.7)$$

The parts of the given polynomial represent different areas of influence to the thermal conductivity. E.g. is the behavior in the ideal gas limit exclusively described through the parameter A . By the application of mixing rules for the individual polynomial parameters, those areas can be weighted according to their main influencing property, making this approach much more robust than the other approaches described so far.

The vector of entropy scaling parameters Θ comprises several model parameters ($\theta \in \{A, B, C, D\}$) that all require mixing rules. In table 6.4, I define candidate mixing rules for all parameters. The combinations lead to $4^4 = 256$ different approaches for $\lambda^{*,5}(s^*, \Theta)$ when considering four parameters A to D . Since we base our investigations on the GC approach described in chapter 5, where D is set to zero except for alcohols, we limit our investigations to the parameters A to C and apply simple molar weighing (ansatz B2.1, table 6.4) for parameter D where necessary. Thus, $4^3 = 64$ combinations for parameters A to C remain.

Table 6.4: Approaches for the mixture polynomial parameters Θ .

N°	symbol	equation
B2.1	θ_1	$= \sum_{i=1}^N x_i \theta_i$
B2.2	θ_2	$= \sum_{i=1}^N \frac{x_i m_i}{m_{mix}} \theta_i$
B2.3	θ_3	$= \sum_{i=1}^N \frac{x_i m_i \sigma_i^2}{(m\sigma^2)_{mix}} \theta_i$
B2.4	θ_4	$= \sum_{i=1}^N \frac{x_i m_i \sigma_i^3}{(m\sigma^3)_{mix}} \theta_i$

6.2.5 Combinational Possibilities

Combining all variants for λ_{mix}^* from subsections 6.2.3 and 6.2.4 with all choices for mixture reference thermal conductivity given in subsection 6.2.2, leads to the matrix of possibilities given in table 6.5. The four trivial approaches A1 to A4 from subsection 6.2.1 are summarized separately at the end of the table. Doing the math, that's $9 \lambda_{mix}^{ref} \cdot (4 + 4^3) \lambda_{mix}^* + 4 = 616$ candidate models.

Table 6.5: Combinational possibilities to calculate the thermal conductivity of mixtures λ based on

$\lambda^?$		λ^{ref}								
		R1	R2	R3	R4	R5	R6	R7	R8	R9
* λ	B1_1									
	B1_2									
	B1_3				★					
	B1_4									
	B2_111									
	...									
	B2_444									
direct	A1									
	A2									
	A3									
	A4									

In the remainder of this work, the ? in the symbol $\lambda^?$ will be replaced by a short but unique identifier referring to this table. The unique identifier ? states first the approach used to calculate the mixture reference thermal conductivity λ^{ref} . Second, it defines which method is used for λ^* . Both parts are separated with a point, leading to the general structure ? = < reference > . < polynomial > for the unique identifier. For example, the symbol $\lambda^{R4.B1.3}$ (marked with ★ in the table 6.5), where the ? was replaced by "R4.B1.3", denotes that in this case λ was calculated using λ^{refR4} (thus the "R4") and $\lambda^{*B1.3}$ (thus the ".B1.3"). The approach for mixture

viscosities as proposed by Lötgering et al. [15] is written here as $\lambda^{R6.B2.122}$, since it uses the Wilke approach as reference term (R6 in Tab. 6.2) combined with a mixture polynomial, in which A is weighted linearly with composition only (θ_1 in Table 6.4), and the parameters B and C are weighted by segment number and composition (θ_2 in Table 6.4).

6.3 Results and Discussion

All calculations in this chapter are based on the group-contribution approach for thermal conductivity presented in chapter 5.

In the DDB [18] we found thermal conductivity data for 223 binary (11001 data sets), 20 ternary (888 data sets), 6 quaternary (26 data sets) and one quintary mixture (30 data sets). Most data is available in liquid phase, often with a limited range of temperature or composition, and with constant pressure near 1 bar. A pressure value is missing for all quaternary data and for 3957 sets of the binary data, belonging to 98 binary mixtures. When including this data and assuming 1 bar for all this data, correlation results deteriorate only slightly, so we assume that most of these experiments were done at ambient pressure.

6.3.1 Definition of Datasets

The available data was divided in several groups. For this grouping, three molecular properties were used: polarity, association (i.e. hydrogen bonding) and the number of intramolecular degrees of freedom. All substances with experimental data on thermal conductivity can be clearly marked as being polar (P) or non-polar (nP), being associating (A) or non-associating (nA), and having a full or reduced number of internal degrees of freedom (e.g., N₂, O₂, and the rare gases). Molecules with a reduced number of internal degrees of freedom were already defined in chapter 4 as *simple molecules*.

Using these properties, we defined 10 groups of mixtures summarized in table 6.6. Here, a single qualifier as "nPnA" means, that all components of a mixture are

Table 6.6: Groups of mixtures investigated in this work.

group	polar and/or associating	simple molecules	binary		ternary		n=4 / *n=5	
			mixtures	data sets	mix.	data	mix.	data
(I)	nPnA	only	20	855	10	105	4	24
(II)	nPnA	mixed	25	972	-	-	-	-
(III)	nPnA-PnA	mixed	9	24	1	2	-	-
(IV)	nPnA-PA	mixed	13	176	1	202	1*	30*
(V)	nPnA	no	25	1648	-	-	-	-
(VI)	nPnA-PnA	no	23	833	-	-	-	-
(VII)	nPnA-PA	no	13	168	-	-	-	-
(VIII)	PnA	no	13	51	-	-	-	-
(IX)	PnA-PA	no	46	343	3	320	1	1
(X)	PA	no	25	2011	5	259	1	1

non-polar and non-associating substances. A double qualifier as "PnA-PA" states, that some components of the mixture are polar but non-associating, and some components are polar and associating.

6.3.2 First Elimination-round for Candidate Models

As stated in section 6.2.5, we defined 616 candidate models for the calculation of mixture thermal conductivities. That are too many approaches to analyze each in detail. So, this *first elimination-round* is meant to reduce the number of candidate models, based on roughly assembled averaged absolute deviations. All possible approaches summarized in table 6.5 were applied to all available binary data sets, with one exception. Only the symmetric variants from λ^{*B2} were analyzed, meaning that all parameters θ_i^{pure} were combined to mixture parameters θ using the same rule. Thus, an initial assessment of all approaches can be done based on 76 models. For all calculations done within this first analysis, we dismissed data without given pressure.

For the calculation of mixture properties using PCP-SAFT, the binary interaction parameter k_{ij} is needed, especially for mixtures containing polar or associating components. Here, we did every calculation twice: one time with $k_{ij} = 0$ for all mixtures and a second time using the QSPR method from Stavrou et al. [19] to calculate k_{ij} for the considered mixtures. No adjustment of k_{ij} to individual mixtures was done, to achieve a mixture-calculation without further adjustable parameters. Overall, using the QSPR method for the binary interaction parameter showed a slight improvement in the results compared to the use of $k_{ij} = 0$. Accordingly, only results using the QSPR method for k_{ij} will be shown in the remainder of this chapter.

For each binary mixture, the averaged absolute deviation (AAD) of calculated to experimental thermal conductivities was evaluated for each of the 76 candidate models. These averaged absolute deviations of all binary mixtures belonging to one of the groups defined in table 6.6 were averaged to only one deviation value per group. Those summarized AADs per group, using the QSPR method for k_{ij} , are given in tables 6.7 and 6.8. The tables are color-coded to highlight the lowest deviation per table in green, the highest deviations per table in red, and all other values in according transition colors.

Comparing the magnitude of the numerical values in the two tables, or the distribution of the color gradients without going into detail, clear differences can be seen. In table 6.7, which shows the results for mixtures containing *simple* components, the averaged absolute deviations are generally much larger. The best models seem to be based on the reference thermal conductivity $\lambda^{\text{ref},R7}$, but still show AADs of 15% or more. In contrast, for groups (V), (VI), and (VIII) in table 6.8 it is precisely these R7-based approaches that perform the worst, but still show comparable averaged absolute deviations between 20% and 30%. Thus, the description of mixtures containing components with full and components with reduced number of internal degrees of freedom seems to be more challenging.

Building the average of the four groups shown in table 6.7 and averaging the 6 groups listed in table 6.7 we create an even more condensed overview of the first results. The averaged AADs for groups (I) to (IV), which include mixtures with one or more *simple molecule*, and for groups (V) to (X) are given in table 6.9 and provide a rough overview of which of the candidate models are promising approaches.

Table 6.7: Assembled averaged absolute deviations for all considered models according to Table 6.5, for groups (I) to (IV) according to Table 6.6.

group (I) nPnA, only small molecules									
AAD/%	R1	R2	R3	R4	R5	R6	R7	R8	R9
B1_1	83.1	119.8	109.1	105.2	103.8	84.6	42.1	91.0	82.4
B1_2	76.8	111.8	101.7	97.8	96.4	78.2	37.6	85.2	73.3
B1_3	77.2	111.6	101.5	97.6	96.3	78.7	37.9	85.6	78.2
B1_4	77.4	112.1	101.9	98.1	96.7	78.8	38.1	77.0	75.7
B2_111	79.0	114.7	104.4	100.5	99.1	80.4	39.2	87.0	79.4
B2_222	73.5	107.7	97.9	94.0	92.6	74.9	35.4	69.5	68.2
B2_333	73.8	107.6	97.8	93.9	92.5	75.2	35.7	71.2	71.7
B2_444	73.9	107.6	97.8	93.9	92.6	75.4	35.9	73.4	80.2
A1:	134.6								
A2:	115.8								
A3:	111.7								
A4:	110.2								

group (III) nPnA-PnA, partly small molecules									
AAD/%	R1	R2	R3	R4	R5	R6	R7	R8	R9
B1_1	35.2	40.5	38.8	39.9	39.8	39.7	21.7	38.4	43.6
B1_2	29.0	33.9	32.4	33.4	33.3	37.1	21.2	36.4	35.4
B1_3	33.0	38.2	36.6	37.6	37.5	37.4	21.3	36.3	40.8
B1_4	34.5	39.7	38.1	39.1	39.1	38.9	21.5	38.7	36.3
B2_111	31.4	36.5	34.8	35.9	35.8	35.6	21.1	34.0	36.2
B2_222	25.6	30.1	28.6	29.6	29.5	29.4	21.9	27.5	29.2
B2_333	30.3	35.3	33.7	34.7	34.6	34.5	21.0	34.1	37.7
B2_444	32.4	37.6	35.9	37.0	36.9	36.7	21.1	36.9	37.1
A1:	42.5								
A2:	34.3								
A3:	39.6								
A4:	41.7								

group (II) nPnA, partly small molecules									
AAD/%	R1	R2	R3	R4	R5	R6	R7	R8	R9
B1_1	34.6	53.7	51.2	44.4	41.0	43.8	19.5	45.4	45.7
B1_2	26.4	41.4	40.8	33.5	30.4	34.4	15.8	37.6	37.8
B1_3	30.5	45.8	44.8	37.6	34.3	38.9	16.6	38.6	35.7
B1_4	31.6	48.3	47.1	39.8	36.4	40.1	17.1	37.0	41.4
B2_111	29.8	46.4	44.9	37.6	34.4	38.3	16.4	40.7	34.8
B2_222	24.5	37.3	37.2	30.1	27.2	31.2	16.9	31.0	29.4
B2_333	27.5	41.2	41.1	34.0	31.0	35.4	15.8	36.5	34.5
B2_444	29.3	43.4	43.1	36.0	33.0	37.2	15.9	42.4	41.1
A1:	57.2								
A2:	42.0								
A3:	39.8								
A4:	39.0								

group (IV) nPnA-PA, partly small molecules									
AAD/%	R1	R2	R3	R4	R5	R6	R7	R8	R9
B1_1	52.2	59.8	58.6	59.4	59.6	59.6	48.0	60.8	61.7
B1_2	49.5	56.6	55.6	56.3	56.5	56.5	45.5	59.3	52.4
B1_3	51.2	58.6	57.5	58.3	58.4	58.4	46.7	56.9	62.8
B1_4	51.8	59.3	58.2	59.0	59.2	59.1	47.2	62.8	59.4
B2_111	50.9	58.1	57.0	57.8	57.9	57.9	46.9	62.5	55.9
B2_222	48.0	54.6	53.7	54.3	54.5	54.5	44.1	57.6	50.7
B2_333	49.6	56.6	55.6	56.3	56.5	56.5	45.3	54.1	58.6
B2_444	50.4	57.5	56.5	57.2	57.4	57.4	45.9	65.7	60.8
A1:	61.3								
A2:	57.2								
A3:	59.9								
A4:	61.0								

In the following, detailed AADs are omitted and replaced by symbols indicating if the AAD of the approach is below or above the median. A summary of the applicability of all mentioned approaches is given in table 6.10 for all datasets of mixtures containing simple molecules and in table 6.11 for all others. For brevity for this first analysis, I defined *applicability* as resulting in an averaged AADs in the better half of all considered approaches. This better half of models is marked with ✓ and the worse half using ✗.

The results of tables 6.10 and 6.11 can be combined to show the applicability of the different approaches to both, mixtures with and mixtures without simple molecules. If an approach is marked with ✓ in both tables, it will be considered in further studies. If in one of the tables an approach was marked with ✗, it will not be considered any longer. As a result of this combination of tables 6.11 and 6.10, some rows or columns are filled completely with ✗, indicating that this ansatz for λ^* or λ^{ref} performs below average. Such columns are removed from subsequent tables. This analysis leads to the exclusion of the following models:

- the simple approaches from section 6.2.1, (A1 to A4)
- the mixture reference candidates $\lambda^{\text{ref},R2}$, $\lambda^{\text{ref},R3}$ and $\lambda^{\text{ref},R7} = \lambda^{\text{HCB}}$
- as well as the λ^* candidates N^o B2_1, B2_4 and B2_4444.

These results lead to a more compact list of promising approaches towards the calculation of mixture thermal conductivities and are summarized in table 6.12. Surprisingly, $\lambda^{\text{ref},R1} = \lambda^{\text{ref}}(M_{\text{mix}}, m_{\text{mix}}, \sigma_{\text{mix}}, \epsilon_{\text{mix}})$ does not show higher deviations in terms of AADs compared to the other remaining approaches for λ^{ref} . The same holds for $\lambda^{\text{ref},R1.2}$ and $\lambda^{\text{ref},R1.3}$.

Table 6.8: Assembled averaged absolute deviations for all considered models according to Table 6.5, for groups (V) to (X) according to Table 6.6.

group (V) nPnA, no small molecules									
AAD/%	R1	R2	R3	R4	R5	R6	R7	R8	R9
B1_1	9.2	11.2	12.2	11.3	10.5	12.1	21.4	12.9	11.6
B1_2	6.1	5.2	5.5	5.1	5.2	5.3	25.7	5.3	5.0
B1_3	5.5	7.2	8.2	7.3	6.6	8.0	23.8	8.8	7.3
B1_4	6.4	8.4	9.5	8.6	7.8	9.3	22.9	9.6	8.8
B2_111	4.8	5.6	6.2	5.4	4.9	6.0	25.3	6.0	6.2
B2_222	7.2	6.1	5.1	5.6	6.1	5.2	27.0	4.9	5.7
B2_333	4.8	5.4	6.1	5.3	4.8	6.0	25.1	6.6	5.5
B2_444	4.8	6.6	7.4	6.6	5.8	7.3	24.2	7.1	7.6
A1:	10.1								
A2:	5.1								
A3:	6.2								
A4:	7.0								

group (VIII) PnA, no small molecules									
AAD/%	R1	R2	R3	R4	R5	R6	R7	R8	R9
B1_1	3.6	4.4	4.5	4.3	4.2	3.4	15.2	3.6	3.3
B1_2	4.2	4.8	4.6	4.6	4.6	3.9	16.2	4.3	3.6
B1_3	4.1	4.7	4.5	4.5	4.5	3.8	16.0	4.2	3.7
B1_4	4.1	4.7	4.5	4.5	4.5	3.8	15.9	3.7	3.7
B2_111	4.8	5.3	5.1	5.1	5.2	4.5	16.8	4.3	4.8
B2_222	4.8	5.4	5.2	5.1	5.2	4.5	16.7	4.7	4.5
B2_333	5.1	5.7	5.5	5.5	5.5	4.8	16.8	4.8	4.5
B2_444	5.2	5.8	5.6	5.6	5.7	5.0	16.8	5.0	4.9
A1:	4.4								
A2:	4.5								
A3:	4.3								
A4:	4.3								

group (VI) nPnA-PnA, no small molecules									
AAD/%	R1	R2	R3	R4	R5	R6	R7	R8	R9
B1_1	7.8	8.1	7.9	7.8	7.8	7.7	18.3	7.4	8.4
B1_2	7.7	8.0	7.8	7.6	7.7	7.6	18.5	7.2	7.8
B1_3	7.6	7.9	7.7	7.6	7.6	7.6	18.6	8.1	7.1
B1_4	7.7	8.0	7.8	7.7	7.7	7.6	18.5	7.9	7.6
B2_111	7.6	7.9	7.7	7.6	7.6	7.5	18.7	7.4	7.2
B2_222	7.6	7.9	7.7	7.6	7.6	7.5	18.7	8.5	7.4
B2_333	7.8	8.1	7.9	7.8	7.8	7.8	18.4	7.7	7.0
B2_444	8.0	8.3	8.1	8.0	8.0	7.9	18.2	7.6	7.2
A1:	8.3								
A2:	7.9								
A3:	7.8								
A4:	7.8								

group (IX) PnA-PA, no small molecules									
AAD/%	R1	R2	R3	R4	R5	R6	R7	R8	R9
B1_1	15.8	20.9	19.2	17.1	16.8	14.4	8.9	15.3	15.3
B1_2	11.6	16.3	14.7	12.8	12.5	10.4	8.1	9.6	10.7
B1_3	12.5	17.3	15.8	13.9	13.6	11.1	7.6	10.5	10.5
B1_4	13.7	18.5	17.1	15.1	14.7	12.2	7.5	13.5	12.9
B2_111	8.5	12.7	10.8	9.1	8.9	7.8	11.7	8.2	7.6
B2_222	10.1	13.8	11.6	10.0	10.1	9.7	11.4	10.0	9.8
B2_333	14.1	18.4	15.8	14.0	14.1	13.6	12.9	13.8	14.3
B2_444	16.9	21.7	18.9	17.0	17.0	16.2	14.4	17.6	17.2
A1:	17.3								
A2:	11.4								
A3:	10.4								
A4:	10.5								

group (VII) nPnA-PA, no small molecules									
AAD/%	R1	R2	R3	R4	R5	R6	R7	R8	R9
B1_1	15.6	19.9	19.5	16.3	15.7	14.5	10.8	15.5	14.1
B1_2	15.3	19.3	18.6	15.4	14.8	13.5	11.4	14.2	14.5
B1_3	19.5	24.1	23.4	20.0	19.4	17.8	10.7	18.1	16.5
B1_4	23.0	28.0	27.3	23.6	23.0	21.3	11.1	23.6	21.1
B2_111	9.9	13.6	13.1	10.2	9.8	9.0	13.7	10.0	8.4
B2_222	12.4	16.0	15.0	12.0	11.6	10.8	14.2	10.2	11.3
B2_333	19.7	24.1	23.0	19.5	19.1	17.7	15.9	19.8	18.7
B2_444	25.8	30.8	29.6	25.8	25.4	23.8	18.5	25.7	23.0
A1:	12.6								
A2:	11.4								
A3:	12.4								
A4:	14.0								

group (X) PA, no small molecules									
AAD/%	R1	R2	R3	R4	R5	R6	R7	R8	R9
B1_1	24.3	26.5	24.2	23.6	24.2	23.9	13.2	29.0	28.5
B1_2	11.8	13.4	12.6	12.1	12.4	12.9	16.1	12.5	12.2
B1_3	10.8	11.9	11.7	11.3	11.4	11.5	16.1	10.7	10.8
B1_4	10.8	11.8	11.7	11.3	11.4	11.5	16.1	10.9	10.5
B2_111	11.5	12.8	12.7	12.3	12.6	12.1	18.5	12.4	12.0
B2_222	10.8	11.9	10.9	10.5	10.7	11.4	17.3	11.1	10.7
B2_333	11.4	12.6	11.2	10.9	11.1	11.9	16.9	11.5	11.4
B2_444	12.0	13.3	11.8	11.4	11.7	12.5	16.8	12.2	12.9
A1:	29.0								
A2:	14.4								
A3:	12.2								
A4:	11.9								

Table 6.9: Summarized AADs for all considered models, averaged for several groups. *Left:* Groups (I) to (IV) from tab. 6.7; *Right:* Groups (V) to (X) from tab. 6.8.

groups (I) to (IV)									
AAD/%	R1	R2	R3	R4	R5	R6	R7	R8	R9
B1_1	21.5	31.4	30.1	26.9	25.3	26.7	13.8	27.5	27.7
B1_2	17.3	25.2	24.7	21.4	19.9	21.8	11.8	23.7	23.2
B1_3	19.5	27.5	26.9	23.5	22.0	24.2	12.3	23.9	23.1
B1_4	20.1	28.8	28.1	24.7	23.1	24.8	12.6	23.7	25.5
B2_111	19.1	27.7	26.9	23.5	22.0	23.8	12.2	25.4	22.0
B2_222	16.2	23.0	22.8	19.5	18.1	20.1	12.2	20.3	19.0
B2_333	17.8	25.1	24.9	21.6	20.2	22.3	11.8	22.7	22.1
B2_444	18.8	26.3	26.0	22.7	21.2	23.3	11.9	26.5	25.5
A1:	33.3								
A2:	25.5								
A3:	24.7								
A4:	24.5								

groups (V) to (X)									
AAD/%	R1	R2	R3	R4	R5	R6	R7	R8	R9
B1_1	15.6	17.7	16.9	16.1	16.1	17.0	16.3	18.6	18.1
B1_2	9.3	10.1	9.7	9.2	9.3	9.3	19.0	9.1	9.0
B1_3	8.9	10.4	10.5	9.8	9.5	9.8	18.3	9.8	9.2
B1_4	9.4	11.0	11.2	10.4	10.1	10.4	18.0	10.5	9.9
B2_111	8.4	9.6	9.6	8.9	8.8	8.9	20.1	9.0	8.8
B2_222	9.0	9.5	8.6	8.4	8.6	8.5	20.2	8.5	8.4
B2_333	9.0	10.2	9.6	9.0	8.9	9.5	19.5	9.6	9.1
B2_444	9.7	11.4	10.8	10.1	9.9	10.6	19.4	10.5	10.8
A1:	17.8								
A2:	9.9								
A3:	9.3								
A4:	9.5								

Table 6.10: Applicability of available approaches to mixtures containing simple molecules, i.e. groups (I) to (IV). Abstract representation of the results in tab. 6.9 left.

$\lambda^?$		λ^{ref}								
		R1	R2	R3	R4	R5	R6	R7	R8	R9
λ^*	B1_1	✓	✗	✗	✗	✗	✗	✓	✗	✗
	B1_2	✓	✗	✗	✓	✓	✓	✓	✓	✓
	B1_3	✓	✗	✗	✓	✓	✓	✓	✓	✓
	B1_4	✓	✗	✗	✗	✗	✓	✓	✓	✓
	B2_111	✓	✗	✗	✓	✓	✓	✓	✓	✓
	B2_222	✓	✗	✗	✓	✓	✓	✓	✓	✓
	B2_333	✓	✗	✗	✓	✓	✓	✓	✓	✓
	B2_444	✓	✗	✗	✗	✗	✓	✓	✗	✗
direct	A1	✗								
	A2	✗								
	A3	✗								
	A4	✗								

Table 6.11: Applicability of available approaches to mixtures without simple molecules, i.e. groups (V) to (X). Abstract representation of the results in tab. 6.9 right.

$\lambda^?$		λ^{ref}								
		R1	R2	R3	R4	R5	R6	R7	R8	R9
λ^*	B1_1	✗	✗	✗	✗	✗	✗	✗	✗	✗
	B1_2	✓	✗	✗	✓	✓	✓	✗	✓	✓
	B1_3	✓	✗	✗	✓	✓	✓	✗	✓	✓
	B1_4	✗	✗	✗	✗	✗	✗	✗	✗	✗
	B2_111	✓	✓	✓	✓	✓	✓	✗	✓	✓
	B2_222	✓	✓	✓	✓	✓	✓	✗	✓	✓
	B2_333	✗	✗	✗	✓	✓	✓	✗	✓	✓
	B2_444	✗	✗	✗	✗	✗	✗	✗	✗	✗
direct	A1	✗								
	A2	✗								
	A3	✗								
	A4	✗								

Table 6.12: Promising model-candidates after combining tables 6.10 and 6.11. If in both tables an approach was marked with \checkmark , it is marked with \checkmark here as well, otherwise it gets a \times . If in the result a complete row or column is filled with \times , it is eliminated.

$\lambda_i^?$		λ^{ref}					
		R1	R4	R5	R6	R8	R9
\prec	B1_2	\checkmark	\checkmark	\checkmark	\checkmark	\checkmark	\checkmark
	B1_3	\checkmark	\checkmark	\checkmark	\checkmark	\checkmark	\checkmark
	B2_111	\checkmark	\checkmark	\checkmark	\checkmark	\checkmark	\checkmark
	B2_222	\checkmark	\checkmark	\checkmark	\checkmark	\checkmark	\checkmark
	B2_333	\times	\checkmark	\checkmark	\checkmark	\checkmark	\checkmark

In the remaining candidates of promising models given in tab. 6.12, the approach $\lambda^{\text{R6.B2-122}}$ which was proposed for the calculation of mixture viscosity is still included. Hence, this approach $\lambda^{\text{R6.B2-122}}$ belongs to the more promising approaches and thus can be used with care until the decision for a dedicated approach for thermal conductivity is made.

6.3.3 Further investigation of Approach B.2

In the first analysis of all possible approaches to calculate thermal conductivities of mixtures, only the four symmetric representatives of the approaches given in section 6.2.4 were included. Now, I continue to investigate the influence of the combining rules given in table 6.4 for the polynomial parameters. Thus, for this analysis, we applied 64 possible parameter combining rules for each of the remaining candidates for λ^{ref} to the test dataset. For this study, we limited the data to a representative set of binary mixtures from each of the 10 groups of mixtures defined in table 6.6. These representative mixtures were chosen based on availability of data for gas and liquid phase and are listed in table 6.13. The average absolute deviations of these 21 mixtures are combined to one value per model-candidate, and are shown in table 6.14. The results of each reference ("column") are grouped by mixing rule for parameter A (B2_1**, B2_2**, ...), sorted by increasing index number (B2_111, B2_112, B2_113, ...). The introduced color-scale visualizes the distribution of deviations for each reference ("within each column"). We find the AAD values to be roughly sorted and to be increasing from top to bottom within the shown sub-tables, independent from the chosen mixture reference. For that reason, only the first four model-candidates of each sub-table in table 6.14 will be taken into account for further analysis. This is equivalent to setting mixing rule B2_1 as given in table 6.4 for parameter B .

Summarizing the remaining model-candidates in one table, and applying a color-scale per reference and per mixing rule for A to help identifying patterns, another similarity becomes visible (see tab. 6.15). Within the first, third and fourth cluster, the model-candidates using θ_2 for parameter C (B2_**2) show the highest deviations. This leads to the elimination of model-candidates using θ_2 for parameter C , except

Table 6.13: Representative 21 binary mixtures forming the test data-set for the investigation fo approach B.2.

group	components		data sets
(I)	Krypton	Argon	21
(I)	Nitrogen	Neon	54
(II)	Neon	Methane	72
(II)	Ethylene	Hydrogen	69
(III)	n-Hexane	n-Heptane	294
(III)	Methane	Carbon dioxide	290
(IV)	Nitrogen	Dinitrogenmonoxid	24
(V)	Benzene	Toluene	132
(V)	ChlorBenzene	Benzene	151
(V)	Acetone	n-Heptane	21
(VI)	Argon	1-Propanol	20
(VI)	Water	Neon	9
(VII)	Ethanol	n-Hexane	29
(VII)	Methanol	Benzene	7
(VIII)	Butylacetate	Toluene	10
(VIII)	Acetone	Ethylacetate	21
(IX)	Methanol	Cyclohexanone	7
(IX)	Toluene	Ethanol	12
(IX)	Dimethylsulfoxid	Water	63
(X)	12-Propandiol	Water	25
(X)	1-Propanol	Water	254

Table 6.14: Averaged absolute deviations of model-candidates based on approach B.2 (see section 6.2.4) for six approaches for λ^{ref} . Grouped by mixing rule for parameter A , sorted by increasing index number. Color scale per reference and per table, with green color for best and red for weakest results of each individual reference ("column").


AAD/%	R1	R4	R5	R6	R8	R9
B2_111	16,0	17,3	17,5	19,3	19,7	19,5
B2_112	17,5	19,3	17,8	20,7	20,0	19,9
B2_113	17,0	18,3	17,7	19,8	19,3	19,0
B2_114	16,9	18,0	17,6	19,4	19,0	18,7
B2_121	16,9	18,1	18,5	20,2	20,7	20,4
B2_122	17,7	19,3	18,2	20,9	20,6	20,4
B2_123	17,3	18,5	18,1	20,0	19,9	19,6
B2_124	17,3	18,2	18,1	19,7	19,6	19,3
B2_131	17,9	18,9	19,6	21,2	21,8	21,6
B2_132	18,3	19,9	18,9	21,4	21,3	21,1
B2_133	18,0	19,0	18,8	20,6	20,5	20,2
B2_134	17,9	18,8	18,8	20,3	20,3	20,0
B2_141	18,6	19,5	20,3	21,8	22,5	22,3
B2_142	18,7	20,3	19,3	21,8	21,7	21,5
B2_143	18,4	19,4	19,2	21,0	21,0	20,7
B2_144	18,3	19,2	19,3	20,7	20,8	20,5



AAD increasing

AAD/%	R1	R4	R5	R6	R8	R9
B2_311	15,7	16,6	16,6	18,9	18,6	18,5
B2_312	16,9	18,1	16,6	20,0	18,8	18,7
B2_313	16,4	17,3	16,5	19,1	18,0	17,9
B2_314	16,3	17,0	16,5	18,8	17,8	17,6
B2_321	16,7	17,5	17,6	19,9	19,7	19,6
B2_322	17,4	18,5	17,4	20,6	19,6	19,6
B2_323	17,0	17,7	17,3	19,7	18,9	18,7
B2_324	17,0	17,4	17,3	19,4	18,6	18,5
B2_331	17,7	18,3	18,8	20,9	20,8	20,7
B2_332	18,1	19,2	18,1	21,2	20,3	20,3
B2_333	17,7	18,3	18,0	20,3	19,6	19,4
B2_334	17,7	18,1	18,0	20,0	19,4	19,2
B2_341	18,4	19,0	19,6	21,6	21,6	21,5
B2_342	18,5	19,6	18,5	21,6	20,8	20,8
B2_343	18,2	18,8	18,5	20,8	20,1	19,9
B2_344	18,1	18,5	18,5	20,5	19,9	19,7

AAD/%	R1	R4	R5	R6	R8	R9
B2_211	18,0	16,4	19,3	17,7	20,1	19,0
B2_212	18,6	17,3	19,0	17,9	19,4	18,4
B2_213	18,7	17,3	19,0	17,9	19,4	18,4
B2_214	18,6	17,3	18,9	17,9	19,4	18,4
B2_221	19,0	17,4	20,3	18,7	21,2	20,2
B2_222	19,2	17,8	19,7	18,5	20,3	19,3
B2_223	19,2	17,8	19,7	18,5	20,3	19,3
B2_224	19,2	17,8	19,7	18,5	20,3	19,3
B2_231	20,1	18,4	21,5	19,8	22,4	21,4
B2_232	19,9	18,5	20,4	19,2	21,0	20,0
B2_233	19,9	18,5	20,4	19,2	21,1	20,1
B2_234	19,9	18,5	20,4	19,2	21,1	20,1
B2_241	20,8	19,0	22,3	20,5	23,2	22,2
B2_242	20,4	18,9	20,9	19,6	21,5	20,5
B2_243	20,4	18,9	20,9	19,6	21,6	20,5
B2_244	20,4	18,9	20,9	19,6	21,6	20,6



AAD increasing

AAD/%	R1	R4	R5	R6	R8	R9
B2_411	16,5	18,3	16,2	20,7	19,9	20,0
B2_412	17,8	19,8	16,8	21,9	20,4	20,4
B2_413	17,0	19,0	16,2	21,0	19,5	19,5
B2_414	16,7	18,6	16,0	20,6	19,2	19,2
B2_421	17,4	19,2	17,3	21,6	21,0	21,1
B2_422	18,4	20,3	17,5	22,5	21,2	21,3
B2_423	17,6	19,4	16,9	21,6	20,3	20,4
B2_424	17,4	19,1	16,7	21,2	20,1	20,1
B2_431	18,3	20,0	18,4	22,7	22,2	22,2
B2_432	19,0	20,9	18,2	23,1	21,9	22,0
B2_433	18,3	20,1	17,6	22,2	21,0	21,1
B2_434	18,0	19,8	17,4	21,9	20,8	20,8
B2_441	19,0	20,6	19,1	23,4	23,0	23,0
B2_442	19,5	21,4	18,7	23,5	22,4	22,5
B2_443	18,7	20,5	18,1	22,6	21,6	21,6
B2_444	18,5	20,2	17,9	22,4	21,3	21,4

Table 6.15: Averaged absolute deviations of model-candidates based on approach B.2 (see section 6.2.4) for six different approaches for λ^{ref} . Grouped by mixing rule for parameter A . Color scale per reference approach and per mixing rule for A .

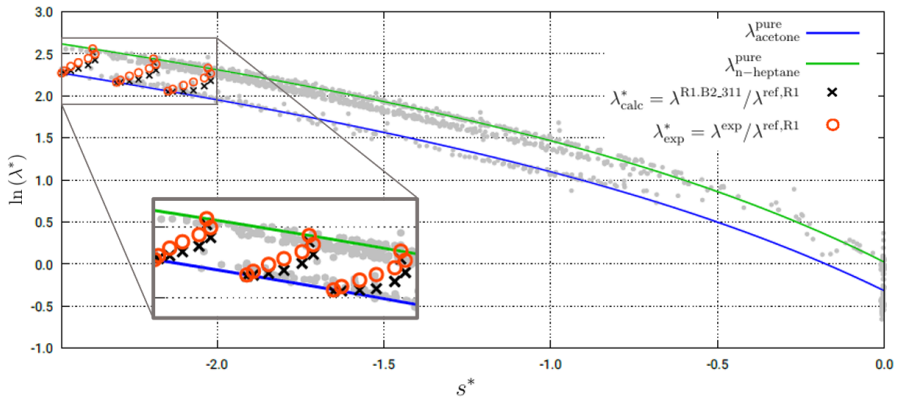
AAD/%	R1	R4	R5	R6	R8	R9
B2_111	16,0	17,3	16,0	19,3	19,7	19,5
B2_112	17,5	19,3	17,5	20,7	20,0	19,9
B2_113	17,0	18,3	17,0	19,8	19,3	19,0
B2_114	16,9	18,0	16,9	19,4	19,0	18,7
B2_211	18,0	16,0	19,3	17,7	20,1	19,0
B2_212	18,6	17,5	19,0	17,9	19,4	18,4
B2_213	18,7	17,0	19,0	17,9	19,4	18,4
B2_214	18,6	16,9	18,9	17,9	19,4	18,4
B2_311	15,7	16,0	16,6	18,9	18,6	18,5
B2_312	16,9	17,5	16,6	20,0	18,8	18,7
B2_313	16,4	17,0	16,5	19,1	18,0	17,9
B2_314	16,3	16,9	16,5	18,8	17,8	17,6
B2_411	16,5	16,0	16,2	20,7	19,9	20,0
B2_412	17,8	17,5	16,8	21,9	20,4	20,4
B2_413	17,0	17,0	16,2	21,0	19,5	19,5
B2_414	16,7	16,9	16,0	20,6	19,2	19,2

when using θ_2 for parameter A as well (the second cluster). These findings reduce the original 65 model-candidates based on approach B.2 to 13 promising ones.

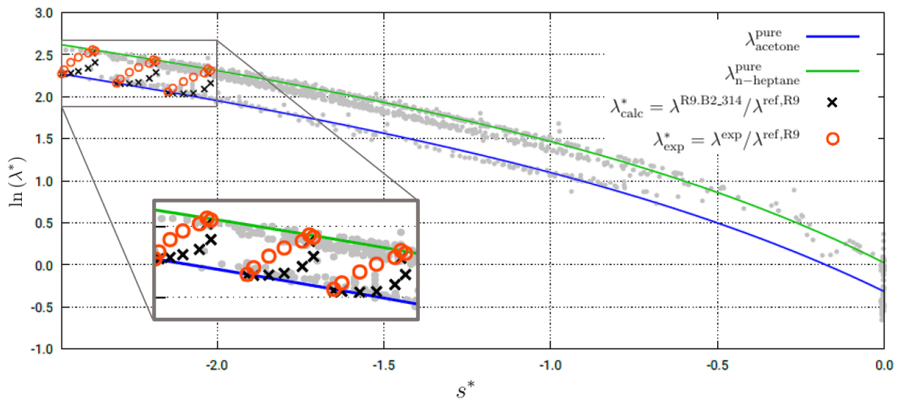
Comparing the AAD values of $\lambda^{\text{ref},R8}$ to those of $\lambda^{\text{ref},R9}$ (the two variants of $\lambda^{\text{ref},WMS}$), the majority shows higher deviations for $\lambda^{\text{ref},R8}$ than those of $\lambda^{\text{ref},R9}$. This supports our initial expectation, that it will be more appropriate to use $\lambda_i^{\text{ref},\text{pure},\alpha}$ instead of $\lambda_i^{\text{ref},\text{pure},\text{CE}}$ within the Wassiljewa approach (see section 6.2.2). Therefore, we eliminate approaches based on $\lambda^{\text{ref},R8}$ as model-candidates as well.

At this stage, no further general statements valid for either all λ^{ref} or all λ^{B2} can be made. For each λ^{ref} , different combination rules for the polynomial parameters are beneficial, as is summarized in table 6.16. The five approaches marked with a \star in table 6.16 result in averaged absolute deviations from 15.7% to 17.7% for the test data-set defined in table 6.13. Despite similar averaged deviation values, the approaches show different results for different binary mixtures. I will illustrate this by considering two exemplary binary mixtures, namely acetone with n-heptane and 1,2-propanediol with water.

The logarithmic reduced thermal conductivity $\ln(\lambda^*)$ versus reduced residual entropy s^* of the binary mixture acetone with n-heptane is shown in figure 6.1. Experimental data of the pure components is denoted by gray dots, the entropy scaling approach for pure substances as described in chapter 2 is shown using solid colored lines. Black crosses represent experimental values for the thermal conductivity of the binary mixture, red circles the according calculated values. In the two figures, structurally different behavior can be seen. The calculated thermal conductivities of mixtures follow the curvature of the experimental values for the approaches $\lambda^{\text{R1.B2.311}}$ (AAD= 5.7%), $\lambda^{\text{R4.B2.211}}$ (AAD= 3.6%) and $\lambda^{\text{R6.B2.211}}$ (AAD= 3.4%). The results of $\lambda^{\text{R1.B2.311}}$ as representative for these three approaches are given in fig-



(a) approach $\lambda^{\text{R1.B2.311}}$, AAD = 5.7% (similar to $\lambda^{\text{R4.B2.211}}$ and $\lambda^{\text{R6.B2.211}}$)



(b) approach $\lambda^{\text{R9.B2.314}}$, AAD = 11.9% (similar to $\lambda^{\text{R5.B2.414}}$)

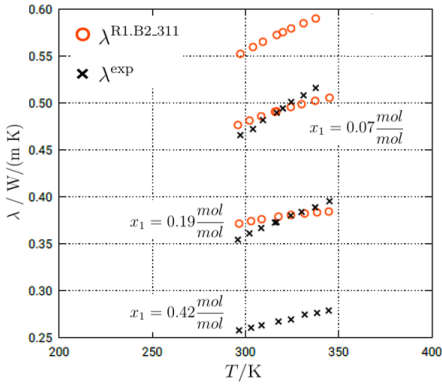
Figure 6.1: Thermal conductivity of binary mixture acetone with n-heptane for three temperatures (273.15K, 253.15K, 293.15K) and varying composition [20]. Logarithmic reduced thermal conductivity $\ln(\lambda^*)$ versus reduced residual entropy s^* . Comparison of entropy scaling model (red circles) to experimental data (black crosses).

Table 6.16: Remaining promising approaches for λ^* defined in subsection 6.2.4 after analysis of patterns in AAD values. For each λ^{ref} (each column) the lowest AAD value is marked with \star , AAD values below the median are marked with \checkmark and values above the median with \times .

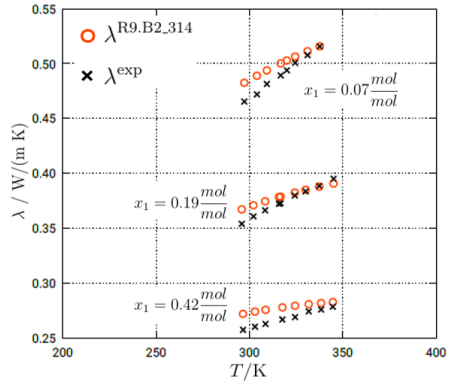
$\lambda^?$	λ^{ref}				
	R1	R4	R5	R6	R9
B2.111	\checkmark	\checkmark	\checkmark	\times	\times
B2.113	\times	\times	\times	\times	\times
B2.114	\checkmark	\times	\times	\times	\checkmark
B2.211	\times	\star	\times	\star	\times
B2.212	\times	\checkmark	\times	\checkmark	\checkmark
B2.213	\times	\times	\times	\checkmark	\checkmark
B2.214	\times	\checkmark	\times	\checkmark	\checkmark
B2.311	\star	\checkmark	\checkmark	\checkmark	\checkmark
B2.313	\checkmark	\checkmark	\checkmark	\checkmark	\checkmark
B2.314	\checkmark	\checkmark	\checkmark	\checkmark	\star
B2.411	\checkmark	\times	\checkmark	\times	\times
B2.413	\times	\times	\checkmark	\times	\times
B2.414	\checkmark	\times	\star	\times	\times

ure 6.1 (a). For other mixture schemes (e.g. $\lambda^{\text{R9.B2.314}}$ and $\lambda^{\text{R5.B2.414}}$), in contrast, the curvature of calculated thermal conductivity of mixtures deviates significantly from experimental values, as figure 6.1 (b) shows. Here, the results of $\lambda^{\text{R9.B2.314}}$ (AAD= 11.5%) are shown, which are similar as approach $\lambda^{\text{R5.B2.414}}$ (AAD= 11.1%). Considering the second example-mixture, the observed behavior is reversed. In figure 6.2, the thermal conductivity of the binary mixture 1,2-propanediol with water is shown. Black crosses represent experimental values for three different compositions ($x_1 \in \{0.07, 0.19, 0.42\} \frac{\text{mol}}{\text{mol}}$) [21]; red circles the calculated values. The approaches $\lambda^{\text{R9.B2.314}}$ (AAD = 2.4%) and $\lambda^{\text{R5.B2.414}}$ (AAD = 2.7%), which showed systematic deviations in the previous mixture, show significantly smaller deviations here. The three other \star approaches $\lambda^{\text{R1.B2.311}}$ (AAD= 29.7%), $\lambda^{\text{R4.B2.211}}$ (AAD= 25.0%) and $\lambda^{\text{R6.B2.211}}$ (AAD= 29.7%) show a clear offset in this second binary mixture, see fig. 6.2 (a).

The binary mixture of 1-propanol with water is presented in figure 6.3. The approach $\lambda^{\text{R1.B2.311}}$ leads to mean absolute deviations of AAD = 4.1%. Increasing deviation towards the critical region of water can be seen, but apart from that a reasonable prediction of the mixture thermal conductivity is obtained. This example shows, that different binary mixtures can be described successfully by a predictive entropy scaling approach.

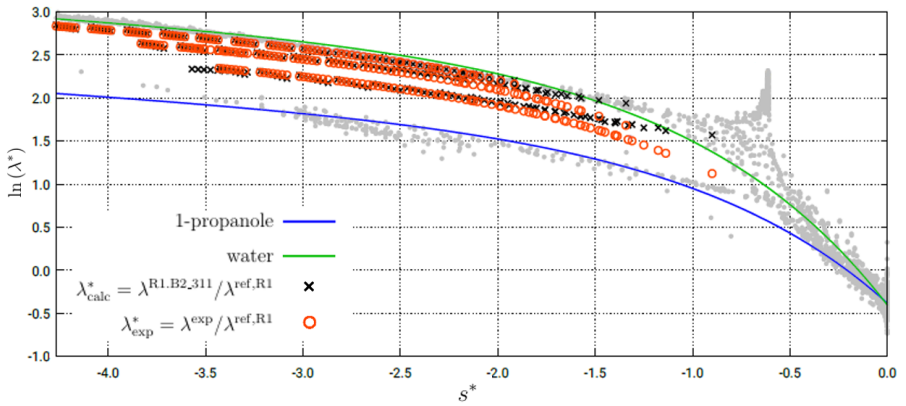


(a) approach $\lambda^{\text{R1.B2.311}}$, AAD = 29.7%
(similar to $\lambda^{\text{R4.B2.211}}$ and $\lambda^{\text{R6.B2.211}}$)

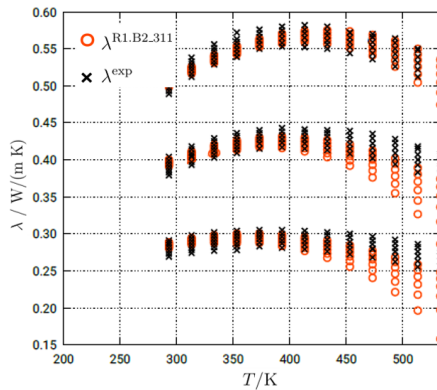


(b) approach $\lambda^{\text{R9.B2.314}}$, AAD = 2.4%
(similar to $\lambda^{\text{R5.B2.414}}$)

Figure 6.2: Thermal conductivity of binary mixture 1,2-propanediol with water. Thermal conductivity over temperature for three compositions. Comparison of entropy scaling model (circles) to experimental data (crosses).



(a) Logarithmic reduced thermal conductivity $\ln(\lambda^*)$ versus reduced residual entropy s^*



(b) Thermal conductivity versus temperature

Figure 6.3: Thermal conductivity of binary mixture 1-propanol with water. Comparison of entropy scaling model $\lambda^{\text{R1.B2.311}}$ (red circles) to experimental data (black crosses).

6.4 Conclusion

Based on the analyses described above, the original 616 model-candidates could be reduced to 47 promising approaches. But, a final decision regarding the best approach to describe the thermal conductivity of mixtures can not yet be made. To enable a sound decision, a detailed analysis of the strengths and weaknesses of the remaining approaches regarding the different groups of mixtures defined in section 6.3.1 is necessary. As illustrated with the two binary mixtures of acetone with n-heptane and 1,2-propanediol with water in the last section, the approach with the smallest overall averaged deviation is not necessarily the most reasonable one. Accordingly, the first basic filtering of all possible approaches based on deviations described in this chapter must be followed in further studies by a detailed investigation of the most promising approaches in terms of robustness. Overall, the applicability of the entropy scaling method to thermal conductivity of mixtures can be confirmed.

Bibliography

- [1] J. Schilling, M. Entrup, M. Hopp, J. Gross, and A. Bardow, "Towards optimal mixtures of working fluids: Integrated design of process and mixtures for organic rankine cycles," *Renewable & Sustainable Energy Research*, vol. 135, p. 110179, 2021.
- [2] J. Gross and A. Bardow, "Germany's next top molecule: Prädiktive Thermodynamik als Schlüssel der simultanen Optimierung von Prozess und Lösungsmittel," *Chemie Ingenieur Technik*, vol. 90, pp. 1304–1304, 2018.
- [3] A. Wassiljewa, "Wärmeleitung in Gasgemischen," *Physikalische Zeitschrift*, vol. 5, no. 737, 1904.
- [4] A. L. Lindsay and L. A. Bromley, "Thermal conductivity of gas mixtures," *Ind. Eng. Chem.*, vol. 42, no. 8, 1950.
- [5] E. A. Mason and S. C. Saxena, "Approximate formula of the thermal conductivity of gas mixtures," *Physics of Fluids*, vol. 1, no. 5, 1958.
- [6] J. O. Hirschfelder, C. F. Curtiss, and R. B. Bird, *Molecular Theory of Gases and Liquids*. New York: John Wiley & Sons, Inc., 4 ed., 1954.
- [7] H. Cheung, L. A. Bromley, and C. R. Wilke, "Thermal conductivity of gas mixtures," *A.I.Ch.E. Journal*, vol. 8, no. 2, 1962.
- [8] U. N. Gaitonde, D. D. Deshpande, and S. P. Sukhatme, "The thermal conductivity of liquid mixtures," *Ind. Eng. Chem. Fundamen.*, vol. 17, no. 4, 1978.
- [9] M. Pourali and A. Maghari, "Non-equilibrium molecular dynamics simulation of thermal conductivity and thermal diffusion of binary mixtures confined in a nanochannel," *Chem. Phys.*, vol. 444, pp. 30–38, 2014.
- [10] B. E. Poling, J. M. Prausnitz, and J. P. O'Connell, *The Properties of Gases and Liquids - fifth Edition*. McGraw-Hill, 2000.
- [11] W. Marbach, H. G. Hertz, and H. Weingärtner, "Self- and mutual diffusion coefficients of some binary liquid n-alkane mixtures - a velocity correlation study -," *Z Phys Chem*, vol. 189, pp. 63–79, 1995.
- [12] X. Liu, A. Bardow, and T. J. H. Vlucht, "Multicomponent maxwell-stefan diffusivities at infinite dilution," *Ind. Eng. Chem. Res.*, vol. 50, pp. 4776 – 4782, 2011.
- [13] X. Liu, T. J. H. Vlucht, and A. Bardow, "Predictive darken equation for maxwell-stefan diffusivities in multicomponent mixtures," *Ind. Eng. Chem. Res.*, vol. 50, no. 17, pp. 10350–10358, 2011.
- [14] H. Weingärtner, *Diffusion in Condensed Matter*. vieweg, 1998.
- [15] O. Lötgering-Lin, M. Fischer, M. Hopp, and J. Gross, "Pure substance and mixture viscosities based on entropy scaling and an analytic equation of state," *Ind. Eng. Chem. Res.*, vol. 57, no. 11, pp. 4095–4114, 2018.

- [16] C. R. A. Wilke, "Viscosity equation for gas mixtures," *J. Chem. Phys.*, vol. 18, pp. 517–519, 1950.
- [17] S. Chapman and T. G. Cowling, *The Mathematical Theory of Non-Uniform Gases*. Cambridge University Press, 3 ed., 1970.
- [18] DDBST Dortmund Data Bank Software & Separation Technology GmbH, Oldenburg, Germany, 2015. <http://www.ddbst.com>.
- [19] M. Stavrou, A. Bardow, and J. Gross, "Estimation of the binary interaction parameter k_{ij} of the pc-saft equation of state based on pure component parameters using a qspr method," *Fluid Phase Equilib.*, vol. 416, pp. 138 – 149, 2016. Special Issue: {SAFT} 2015.
- [20] Q.-F. Lei, R.-S. Lin, D.-Y. Ni, and Y.-C. Hou, "Thermal conductivities of some organic solvents and their binary mixtures," *J. Chem. Eng. Data*, vol. 42, no. 5, pp. 971–974, 1997.
- [21] M. Assael, E. Charitidou, S. Avgoustiniatos, and W. Wakeham, "Absolute measurements of the thermal conductivity of mixtures of alkene-glycols with water," *Int.J.Thermophys.*, vol. 10, no. 6, pp. 1127–1140, 1989.

7 Conclusions

In this thesis, prediction of thermal conductivity and self-diffusion of pure substances, and thermal conductivity of mixtures are studied using entropy scaling. PC-SAFT is used as an equation of state to calculate residual entropy. A suitable choice of a reference thermal conductivity and self-diffusion coefficient, respectively, enables a projection on a master curve. Several approaches of reference thermal conductivity and self-diffusion coefficient are investigated to determine dimensionless thermal conductivity and self-diffusion. The prediction of transport coefficients are validated against experimental data.

In the chapters 2 and 3 of this thesis, it is shown that entropy scaling holds when a suitable dimensionless thermal conductivity or self-diffusion coefficient, respectively, is used. The dimensionless transport coefficient of each individual substance is verified to fall on a master curve with single-variable dependence on residual entropy. It is shown for thermal conductivity and self-diffusion coefficient that entropy scaling holds for the entire fluid region and therefore is a powerful method to correlate and predict thermal conductivity and self-diffusion of organic substances. Good results are obtained for several chemical families with only 2 to 4 adjustable pure component parameters per species, depending on the range of available experimental data. More than hundred substances are investigated with overall good results. Even extrapolation shows reasonable accuracy of the prediction of the transport coefficients.

Based on the foundations laid in the first chapters, a new reference thermal conductivity for entropy scaling based on a kinetic-theory approach by Chapman and Cowling is proposed. Chapter 4 summarizes the investigations to improve the empirically modified Chapman–Enskog expression. The influence of intramolecular degrees of freedom on the thermal conductivity is described by a self-diffusion mechanism. The new reference thermal conductivity overcomes the previous shortcomings and eliminates the need for an empirical expression. The performance of the new reference thermal conductivity is demonstrated for over hundred substances from several chemical families and showed overall good results. One of the major advantages of the new approach is its applicability to substances ranging from simple mono-atomic to complex molecules with many internal degrees of freedom. This enables the model to be successfully applied to other chemical families.

Next, a group-contribution method for the thermal conductivity of pure organic substances is introduced. It covers wide ranges in temperature and pressure for both vapor phases and liquid-phase conditions. The group-contribution method is based on the GC PCP-SAFT equation of state. A parametrization of the model parameters of the entropy scaling approach for different functional groups was developed. A study of the performance of entropy scaling of hundreds of substances from several chemical families, containing one or more functional groups, shows good results compared to experimental data. The accuracy is comparable to the previous approaches but offers a more fundamental basis with outlook to better extrapolation to substances with scarce or absent experimental data.

This thesis is finalized investigations towards a predictive entropy scaling approach for the thermal conductivity of mixtures. Several references for thermal conductivity, i.e. combinations of pure component parameters, are studied as well as a variety of ways to combine the substance specific polynomials. Promising combinations of mixture reference thermal conductivity and composition based quasi mixing rules for polynomial parameters are found. Each showing advantages at varying mixture properties. Thus, the applicability of the entropy scaling method to thermal conductivity of mixtures can be affirmed.

Appendices

A Supporting Information for Chapter 2: Thermal Conductivity of real Substances from Excess Entropy Scaling using PCP-SAFT

This supporting Information details (1) the pure component parameters of the PCP-SAFT model for all considered substances, (2) parameters A - D for all substances and for all three references $\lambda_{\alpha, scale}^{ref}$, $\lambda_{\alpha, Eu}^{ref}$, $\lambda_{\alpha, LTST}^{ref}$ and the reference given in the appendix $\lambda_{\alpha, CCE}^{ref}$. These tables (3) also give the absolute average deviations for all considered components and for all three references. Further, (4) the full legend of all 36 substances of Fig. 2.6 is given. Additionally, (5) we include a comparison between results for water using PCP-SAFT and a highly accurate equation of state, and (6) an investigation of entropy scaling for Lennard-Jones Chains as molecular model.

A.1 PCP-SAFT Parameters

Name	Molar Mass g/mol	m -	σ \AA	ϵ/k K	κ^{AB} -	ϵ^{AB} K	DM Debye
Alkanes							
Methane	16.04250	1.00569	3.69663	149.59768	0.00000	0.00000	0.00000
Ethane	30.06900	1.61391	3.51957	190.87107	0.00000	0.00000	0.00000
Propane	44.09560	1.98977	3.62466	208.90124	0.00000	0.00000	0.00000
nButane	58.12220	2.30042	3.72380	224.66558	0.00000	0.00000	0.00000
nPentane	72.14880	2.70158	3.75385	230.86699	0.00000	0.00000	0.00000
nHexane	86.17540	3.08624	3.77945	235.78273	0.00000	0.00000	0.00000
nHeptane	100.20200	3.45473	3.80746	239.65357	0.00000	0.00000	0.00000
nOctane	114.22900	3.82709	3.83154	242.48818	0.00000	0.00000	0.00000
nNonane	128.25500	4.26110	3.82377	242.88293	0.00000	0.00000	0.00000
nDecane	142.28200	4.64969	3.83872	244.30975	0.00000	0.00000	0.00000
nUndecane	156.30800	5.01775	3.85254	245.99302	0.00000	0.00000	0.00000
nDodecane	170.33500	5.44152	3.85128	246.12545	0.00000	0.00000	0.00000
nTridecane	184.36100	5.84545	3.85736	246.62215	0.00000	0.00000	0.00000
nTetradecane	198.38800	6.17017	3.87319	248.63938	0.00000	0.00000	0.00000
nPentadecane	212.41500	6.49637	3.89134	250.17744	0.00000	0.00000	0.00000
nHexadecane	226.44100	6.88869	3.89365	250.44335	0.00000	0.00000	0.00000
nHeptadecane	240.46800	7.21576	3.91086	251.84360	0.00000	0.00000	0.00000
nOctadecane	254.49400	7.60850	3.91096	251.75916	0.00000	0.00000	0.00000
nNonadecane	268.52100	7.95055	3.92106	252.50169	0.00000	0.00000	0.00000
nEicosane	282.54700	8.32605	3.92466	252.93385	0.00000	0.00000	0.00000
nHeneicosane	296.57400	8.74950	3.91924	252.38775	0.00000	0.00000	0.00000
nDocosane	310.60100	8.98864	3.94656	253.95140	0.00000	0.00000	0.00000
Tricosane	324.62700	9.38515	3.94158	254.14393	0.00000	0.00000	0.00000

Continued on next page

Table – continued from previous page

Name	Molar Mass g/mol	m -	σ Å	ϵ/k K	κ^{AB} -	ϵ^{AB} K	DM Debye
Tetracosane	338.65400	9.79587	3.93844	253.55057	0.00000	0.00000	0.00000
Branched Alkanes							
2-Methylpropane	58.12220	2.20442	3.79086	219.51844	0.00000	0.00000	0.13191
2-Methylbutane	72.14880	2.53203	3.83312	232.59426	0.00000	0.00000	0.13011
2-Methylpentane	86.17540	2.93508	3.84299	235.63648	0.00000	0.00000	0.00000
3-Methylpentane	86.17540	2.85652	3.86312	241.99664	0.00000	0.00000	0.00000
3-Ethylpentane	100.20200	3.18862	3.88703	247.05554	0.00000	0.00000	0.00000
2-Methylhexane	100.20200	3.30243	3.86572	239.38199	0.00000	0.00000	0.00000
3-Methylhexane	100.20200	3.24565	3.86254	243.42861	0.00000	0.00000	0.00000
2-Methylheptane	114.22900	3.66257	3.88474	242.68695	0.00000	0.00000	0.00000
3-Methylheptane	114.22900	3.61235	3.88548	245.70129	0.00000	0.00000	0.00000
2,2-Dimethylpropan	72.14880	2.35532	3.95145	225.71568	0.00000	0.00000	0.00000
2,2-Dimethylbutane	86.17540	2.66193	3.97267	240.25776	0.00000	0.00000	0.00000
2,3-Dimethylbutane	86.17540	2.70133	3.93866	245.27055	0.00000	0.00000	0.00000
2,2-Dimethylpentane	100.20200	3.00066	3.98954	244.05288	0.00000	0.00000	0.00000
3,3-Dimethylpentane	100.20200	2.85375	4.05393	256.32368	0.00000	0.00000	0.00000
2,3-Dimethylpentane	100.20200	3.02557	3.94517	251.62877	0.00000	0.00000	0.00000
2,4-Dimethylpentane	100.20200	3.12346	3.93459	239.70053	0.00000	0.00000	0.00000
2,2,3-Trimethylbutane	100.20200	2.73493	4.09192	258.78612	0.00000	0.00000	0.00000
2,2,4-Trimethylpentane	114.22900	3.13521	4.09180	250.00587	0.00000	0.00000	0.00000
2,3,4-Trimethylpentane	114.22900	3.19800	4.02504	258.59586	0.00000	0.00000	0.00000
Alkenes							
Ethylene	28.05320	1.56738	3.42823	178.75466	0.00000	0.00000	0.00000
1-Propene	42.07970	1.98506	3.51787	205.86876	0.00000	0.00000	0.36574
1-Butene	56.10630	2.36634	3.60306	217.77625	0.00000	0.00000	0.33876
1-Pentene	70.13290	2.60890	3.72989	231.67011	0.00000	0.00000	0.50964

Continued on next page

Table – continued from previous page

Name	Molar Mass g/mol	m	σ Å	ϵ/k	κ^{AB}	ϵ^{AB}	DM Debye
1-Hexene	84.15950	3.08593	3.71527	233.10023	0.00000	0.00000	0.44969
1-Heptene	98.18610	3.28633	3.81384	243.75593	0.00000	0.00000	0.62956
1-Octene	112.21300	3.95033	3.73304	236.37226	0.00000	0.00000	0.41971
1-Nonene	126.23900	4.06167	3.84521	247.07088	0.00000	0.00000	0.59958
1-Decene	140.26600	4.45030	3.85438	248.22912	0.00000	0.00000	0.41971
1-Undecene	154.29200	4.78609	3.87627	250.45665	0.00000	0.00000	0.53962
1-Dodecene	168.31900	5.21507	3.87155	250.09753	0.00000	0.00000	0.51864
1-Tridecene	182.34600	5.67530	3.86080	249.02093	0.00000	0.00000	0.50964
1-Tetradecene	196.37200	5.83150	3.91895	254.49724	0.00000	0.00000	0.50964
1-Pentadecene	210.39900	6.18757	3.92894	255.21496	0.00000	0.00000	0.41971
1-Hexadecene	224.42500	6.51907	3.94060	256.27883	0.00000	0.00000	0.30878
cis-2-Butene	56.10630	2.38241	3.56154	226.30778	0.00000	0.00000	0.29979
trans-2-Butene	56.10630	2.32821	3.61672	226.14304	0.00000	0.00000	0.00000
Aldehydes							
Decanal	156.26500	5.28847	3.66341	251.96549	0.00000	0.00000	2.57819
Butanal	72.10570	2.83388	3.46296	248.90304	0.00000	0.00000	2.71910
n-Pentanal	86.13230	3.25179	3.51340	252.90963	0.00000	0.00000	2.56920
Heptanal	114.18500	3.85273	3.65996	260.69837	0.00000	0.00000	2.57819
n-Dodecanal	184.31800	5.82868	3.75381	256.50170	0.00000	0.00000	2.57819
3-Methyl-butylaldehyde	86.13230	3.00042	3.61882	255.20468	0.00000	0.00000	2.60817
Acetaldehyde	44.05260	2.11875	3.24603	229.85048	0.00000	0.00000	2.68912
2-Methyl-propanal	72.10570	2.61571	3.56986	251.50721	0.00000	0.00000	2.69811
Benzaldehyde	106.12200	3.03726	3.61458	316.39666	0.00000	0.00000	3.20775
Aromatics							
Benzene	78.11180	2.46021	3.64300	287.81738	0.00000	0.00000	0.00000
Ethylbenzene	106.16500	3.06198	3.79545	288.46503	0.00000	0.00000	0.59958

Continued on next page

Table – continued from previous page

Name	Molar Mass g/mol	m	σ Å	ϵ/k	κ^{AB}	ϵ^{AB}	DM Debye
Propylbenzene	120.19200	3.34934	3.85392	287.70439	0.00000	0.00000	0.36874
Butylbenzene	134.21800	3.73961	3.86330	284.51919	0.00000	0.00000	0.36874
sec-Butylbenzene	134.21800	3.70232	3.86817	279.12854	0.00000	0.00000	0.38973
tert-Butylbenzene	134.21800	3.58389	3.89860	281.45932	0.00000	0.00000	0.69851
Toluene	92.13840	2.75791	3.73658	289.36321	0.00000	0.00000	0.35975
1,2-Dimethyl-benzene	106.16500	3.10049	3.76557	293.08147	0.00000	0.00000	0.62956
1,3-Dimethyl-benzene	106.16500	3.16545	3.75653	285.21713	0.00000	0.00000	0.29979
1,4-Dimethyl-benzene	106.16500	3.12058	3.78634	286.67702	0.00000	0.00000	0.00000
Isopropylbenzene	120.19200	3.37794	3.83764	281.53239	0.00000	0.00000	0.38973
1,2,4-Trimethylbenzene	120.19200	3.50995	3.77672	288.07267	0.00000	0.00000	0.29979
1,3,5-Trimethylbenzene	120.19200	3.48356	3.76126	294.54957	0.00000	0.00000	0.56061
1,3,5-Triisopropylbenzene	204.35100	5.55147	3.90485	254.88566	0.00000	0.00000	0.23444
Ethers							
Di-nPropyl-ether	102.17500	3.48815	3.69613	234.04436	0.00000	0.00000	1.21115
Dimethyl-ether	46.06840	2.23415	3.28359	211.92289	0.00000	0.00000	1.30109
Diphenylether	170.20700	3.61320	3.99040	340.35433	0.00000	0.00000	1.16019
Di-nButyl-ether	130.22800	4.41263	3.69965	233.98374	0.00000	0.00000	1.16918
Methylpropylether	74.12160	2.98101	3.48745	222.68749	0.00000	0.00000	1.24113
Methylbutylether	88.14820	3.12449	3.64425	237.09241	0.00000	0.00000	1.25012
Ethylpropylether	88.14820	3.22678	3.61257	227.93354	0.00000	0.00000	1.15999
Ethylbutylether	102.17500	3.69459	3.61591	228.16193	0.00000	0.00000	1.22015
Methyl-tertButyl-ether	88.14820	2.92856	3.71099	233.95727	0.00000	0.00000	1.36105
Di-nPentyl-ether	158.28100	4.81969	3.83907	246.50822	0.00000	0.00000	1.19916
Diisopropyl-ether	102.17500	3.54663	3.67373	216.85084	0.00000	0.00000	1.13021
Esters							
Methylacetate	74.07850	3.14055	3.18917	233.39113	0.00000	0.00000	1.67882

Continued on next page

Table – continued from previous page

Name	Molar Mass g/mol	m -	σ Å	ϵ/k K	κ^{AB} -	ϵ^{AB} K	DM Debye
nButyl-acetate	116.15800	4.12456	3.48092	237.53469	0.00000	0.00000	1.84071
IsobutylAcetate	116.15800	4.17134	3.46531	229.82064	0.00000	0.00000	1.87069
IsopropylAcetate	102.13200	3.63113	3.46005	230.92848	0.00000	0.00000	1.75077
nPentyl-acetate	130.18500	4.10662	3.64603	249.35813	0.00000	0.00000	1.72079
nHexylAcetate	144.21100	4.77283	3.59680	243.11682	0.00000	0.00000	1.85870
nHeptyl-acetate	158.23800	5.34135	3.58180	240.13706	0.00000	0.00000	1.87069
Ethynyl-acetate	86.08920	3.39455	3.26916	232.22340	0.00000	0.00000	1.78975
2-EthylhexylAcetate	172.26500	4.99438	3.77684	250.11702	0.00000	0.00000	1.88268
Ketones							
Acetone	58.07910	2.70616	3.27780	234.42441	0.00000	0.00000	2.88098
2-Butanone	72.10570	2.87682	3.43174	249.99059	0.00000	0.00000	2.76107
2-Pentanone	86.13230	3.26850	3.50755	249.75675	0.00000	0.00000	2.77006
3-Pentanone	86.13230	3.27707	3.49369	248.67312	0.00000	0.00000	2.82102
2-Hexanone	100.15900	3.59507	3.58136	254.40173	0.00000	0.00000	2.68012
3-Hexanone	100.15900	3.59232	3.57373	250.57975	0.00000	0.00000	2.86899
2-Heptanone	114.18500	3.96870	3.62333	255.47704	0.00000	0.00000	2.61117
3-Heptanone	114.18500	4.40771	3.48137	239.27624	0.00000	0.00000	2.80903
4-Heptanone	114.18500	3.73471	3.69584	259.19723	0.00000	0.00000	2.50025
2-Octanone	128.21200	4.46696	3.62221	252.43533	0.00000	0.00000	2.46128
5-Nonanone	142.23900	4.62579	3.70784	254.83863	0.00000	0.00000	2.74008
6-Undecanone	170.29200	5.81717	3.64639	246.06343	0.00000	0.00000	2.67113
Methyl-Isobutyl-ketone	100.15900	3.47301	3.62962	250.53002	0.00000	0.00000	2.68912
Acetophenone	120.14900	3.49475	3.61623	310.80391	0.00000	0.00000	3.02788
Cyclopentanone	84.11640	2.69230	3.57528	295.71514	0.00000	0.00000	3.23773
Cyclohexanone	98.14300	2.76986	3.74259	313.98506	0.00000	0.00000	3.08784
Alkoholes							

Continued on next page

Table – continued from previous page

Name	Molar Mass g/mol	m	σ Å	ϵ/k	κ^{AB}	ϵ^{AB}	K	DM Debye
Methanol	32.04190	1.50733	3.32485	211.59747	0.03000	2519.71165	1.69981	1.69981
Ethanol	46.06840	2.37226	3.19636	203.82447	0.03000	2514.06086	1.69082	1.69082
1-Butanol	74.12160	4.27684	3.06589	217.70817	0.03000	1846.20289	1.66983	1.66983
1-Propanol	60.09500	3.46042	3.07418	217.37453	0.03000	2044.52977	1.67882	1.67882
1-Pentanol	88.14820	4.30502	3.24211	228.62144	0.03000	1835.03147	1.69999	1.69999
1-Hexanol	102.17500	4.39742	3.38972	235.53091	0.03000	1930.62315	1.64885	1.64885
1-Heptanol	116.20100	4.72476	3.46096	237.60687	0.03000	1956.84236	1.73878	1.73878
1-Octanol	130.22800	5.72042	3.35617	228.85155	0.03000	1869.84462	1.64885	1.64885
1-Nonanol	144.25500	4.74902	3.72901	253.62910	0.03000	2073.35551	1.60987	1.60987
1-Decanol	158.28100	5.73281	3.59600	243.70889	0.03000	1967.83118	1.61887	1.61887
1-Undecanol	172.30800	7.35947	3.37999	225.13814	0.03000	1888.86814	1.66983	1.66983
1-Dodecanol	186.33400	6.23535	3.69988	249.09519	0.03000	2002.96131	1.69082	1.69082
1-Tetradecanol	214.38700	5.91031	3.98316	266.33539	0.03000	2238.18376	1.54999	1.54999
1-Hexadecanol	242.44100	7.09165	3.88449	259.40444	0.03000	2140.25449	1.66983	1.66983
1-Octadecanol	270.49400	7.33426	3.99623	266.51427	0.03000	2150.74824	1.66084	1.66084
Acids								
Formic acid	46.02570	0.69207	4.50084	534.61162	0.03000	1192.58403	1.41501	1.41501
Butyric acid	88.10510	2.35525	3.77403	227.97227	0.03000	3392.93577	1.64885	1.64885
Pentanoic acid	102.13200	3.25117	3.64027	267.44169	0.03000	2624.77706	1.60987	1.60987
Nonanoic acid	158.23800	5.00870	3.67887	257.91640	0.03000	2817.56748	1.67882	1.67882
Decanoic acid	172.26500	5.31756	3.72193	253.09181	0.03000	3039.39001	1.67882	1.67882
Dodecanoic acid	200.31800	6.34523	3.70262	253.77161	0.03000	2868.75109	1.63985	1.63985
Tetradecanoic acid	228.37100	7.61811	3.64194	253.87261	0.03000	2451.86614	1.67882	1.67882
Caprylic acid	144.21100	4.46653	3.70527	256.31753	0.03000	2934.20568	1.69981	1.69981
Hexanoic acid	116.15800	3.88404	3.57964	252.59380	0.03000	2852.07860	1.57090	1.57090
Acetic acid	60.05200	0.99068	4.49483	316.35748	0.03000	2575.48216	1.73878	1.73878

Continued on next page

Table – continued from previous page

Name	Molar Mass g/mol	m -	σ Å	ϵ/k K	κ^{AB} -	ϵ^{AB} K	DM Debye
Propionic acid	74.07850	1.76523	3.87425	223.40348	0.03000	3336.82497	1.75077
Hexadecanoic acid	256.42400	8.31733	3.68361	254.07309	0.03000	2492.36511	1.73878
Octadecanoic acid	284.47700	9.09147	3.70445	253.25527	0.03000	2546.03369	1.66983
Oleic acid	282.46100	10.77334	3.46786	237.71647	0.03000	1867.03634	1.43899

A.2 Parameters ($A-D$) and Absolute Average Deviations

The three following tables list the polynomial parameters $A-D$, the number of experimental data points, and the resulting absolute average relative deviations AAD-% for all considered substances. One table is given for each of the three investigated reference thermal conductivities $\lambda_{\alpha, scale}^{ref}$, $\lambda_{\alpha, Eu}^{ref}$, and $\lambda_{\alpha, LTST}^{ref}$.

Name	points	AAD / %	A	B	C	D
Alkanes						
Methane	3251	6.996	-0.01569	-0.74420	0.71889	-0.01337
Ethane	1450	6.172	-0.21439	-0.44594	1.52545	0.02553
Propane	3040	6.826	-0.15348	-0.63880	1.21342	-0.01664
nButane	2959	4.946	-0.08781	-0.40731	1.52225	0.02280
nPentane	614	2.645	-0.01966	-1.12894	0.37636	-0.10154
nHexane	767	3.175	0.01894	-0.52471	1.39729	-0.01169
nHeptane	1447	3.680	0.02368	-0.66392	1.21106	-0.03414
nOctane	581	2.774	0.02886	-0.35368	1.79912	0.00264
nNonane	618	3.161	0.06736	-1.03103	0.70518	-0.11122
nDecane	779	2.863	0.08278	-0.76076	1.07724	-0.05448
nUndecane	476	2.773	0.10924	-0.76431	1.11718	-0.06918
nTridecane	651	2.763	0.19977	-0.77374	1.03743	-0.07272
nTetradecane	474	2.451	0.26694	-0.50944	1.25355	0.00000
nPentadecane	368	1.965	0.30086	-0.50916	1.24386	0.00000
nHexadecane	466	2.117	0.36701	-0.52738	1.15300	0.00000
nHeptadecane	17	0.241	0.00000	-0.35564	2.06301	0.00000
nOctadecane	384	6.103	0.00000	-0.40156	1.98005	0.00000
nNonadecane	327	2.466	0.00000	-0.22979	2.34268	0.0000
nEicosane	48	0.374	0.00000	-0.45282	1.84027	0.00000
nHeneicosane	48	0.390	0.00000	-0.44269	1.87784	0.00000
nDocosane	54	1.276	0.00000	-0.41253	1.98725	0.00000
Tricosane	42	0.321	0.00000	-0.41797	1.98074	0.00000
Tetracosane	55	1.769	0.00000	-0.37195	2.10371	0.00000
Branched Alkanes						

Continued on next page

Table – continued from previous page

Name	points	AAD / %	A	B	C	D
2-Methylpropane	1982	4.798	-0.08288	-0.75546	0.93788	-0.03688
2-Methylbutane	68	2.173	-0.01653	-0.48454	1.41339	0.00000
2-Methylpentane	17	0.776	0.00000	-0.64118	1.02566	0.00000
3-Methylpentane	20	1.629	0.00000	-0.63021	1.06261	0.00000
3-Ethylpentane	16	0.227	0.00000	-0.61548	1.14823	0.00000
2-Methylhexane	16	0.308	0.00000	-0.61652	1.12979	0.00000
3-Methylhexane	26	0.256	0.00000	-0.62400	1.10491	0.00000
2-Methylheptane	16	0.256	0.00000	-0.57059	1.27096	0.00000
3-Methylheptane	16	0.385	0.00000	-0.57308	1.26861	0.00000
2,2-Dimethylpropan	5	0.348	-0.20351	9367.48000	9430.62000	0.00000
2,2-Dimethylbutane	17	0.771	0.02909	-0.63255	0.99674	0.00000
2,3-Dimethylbutane	81	1.947	0.00000	-0.42594	1.54389	0.00000
2,2-Dimethylpentane	15	0.285	0.00000	-0.63008	1.06922	0.00000
3,3-Dimethylpentane	16	0.315	0.00000	-0.61584	1.12692	0.00000
2,3-Dimethylpentane	27	0.423	0.00000	-0.61575	1.11879	0.00000
2,4-Dimethylpentane	17	0.486	0.06635	-0.63416	0.99964	0.00000
2,2,3-Trimethylbutane	16	0.630	0.00000	-0.59586	1.15637	0.00000
2,2,4-Trimethylpentane	524	2.802	0.03591	-1.34302	0.12382	-0.15103
2,3,4-Trimethylpentane	15	0.216	0.00000	-0.55699	1.27961	0.00000
Alkenes						
Ethylene	530	6.185	-0.30156	-0.07335	2.08619	0.12408
1-Propene	422	12.427	-0.08738	-0.99466	0.75856	-0.11268
1-Butene	31	9.085	-0.19357	-0.64490	1.22663	0.00000
1-Pentene	32	1.983	-0.16210	-0.64003	1.22451	0.00000
1-Hexene	320	3.483	-0.05849	-0.39465	1.57660	0.01888
1-Heptene	423	3.071	-0.01510	-0.46245	1.50562	0.00784
1-Octene	493	3.276	-0.05251	-0.85665	0.96794	-0.06895

Continued on next page

Table – continued from previous page

Name	points	AAD / %	A	B	C	D
1-Nonene	343	3.483	0.02508	-0.45101	1.42485	0.01748
1-Decene	312	2.432	0.04268	-0.59144	1.27993	-0.01622
1-Undecene	257	2.255	0.10697	-0.47802	1.42320	0.00000
1-Dodecene	313	2.444	0.00000	0.51894	2.84152	0.23012
1-Tridecene	246	2.290	0.00000	-0.33547	1.89009	0.00000
1-Tetradecene	279	2.408	0.00000	0.23635	2.68848	0.12618
1-Pentadecene	249	2.468	0.00000	-0.29934	2.05952	0.00000
1-Hexadecene	249	2.600	0.00000	-0.28374	2.12309	0.00000
cis-2-Butene	19	6.574	-0.22671	-0.69161	1.14543	0.00000
trans-2-Butene	23	5.838	-0.20289	-0.70339	1.11963	0.00000
Aldehydes						
Decanal	21	1.250	0.00000	-0.43324	1.61213	0.00000
Butanal	79	3.154	0.18677	-0.78450	0.33826	0.00000
n-Pentanal	8	0.192	0.00000	-0.54546	1.14329	0.00000
Heptanal	12	0.421	0.00000	-0.51936	1.33542	0.00000
n-Dodecanal	16	1.515	0.00000	-0.40675	1.84634	0.00000
3-Methyl-butylaldehyde	54	2.292	0.25725	-0.75726	0.37709	0.00000
Acetaldehyde	96	5.223	-0.66246	-1.25671	0.10486	0.00000
2-Methyl-propanal	67	4.107	0.14101	-1.17889	-0.00230	-0.10038
Benzaldehyde	9	0.753	0.00000	-0.68390	0.75499	0.00000
Aromatics						
Benzene	1061	3.186	0.01047	-0.86681	0.81098	-0.06524
Ethylbenzene	654	2.766	0.17248	-0.97157	0.46862	-0.08552
Propylbenzene	94	1.973	0.45849	-0.59145	0.68572	0.00000
Butylbenzene	152	2.023	0.00000	-0.43124	1.54514	0.00000
sec-Butylbenzene	11	0.544	0.00000	-0.54957	1.31500	0.00000
tert-Butylbenzene	140	1.648	0.00000	-0.36646	1.71091	0.00000

Continued on next page

Table – continued from previous page

Name	points	AAD / %	A	B	C	D
Toluene	3760	3.315	-1.28000	-0.71100	2.59000	-0.06230
1,2-Dimethyl-benzene	649	2.029	0.21294	-1.11824	0.14618	-0.10415
1,3-Dimethyl-benzene	600	2.900	0.13761	-0.94221	0.53258	-0.07949
1,4-Dimethyl-benzene	553	1.990	0.45165	-0.87773	0.13529	-0.03916
Isopropylbenzene	413	2.166	0.51308	-0.57468	0.67839	-0.06761
1,2,4-Trimethylbenzene	171	1.575	0.00000	-0.45935	1.44014	0.00000
1,3,5-Trimethylbenzene	18	0.259	0.00000	-0.42988	1.51728	0.00000
1,3,5-Triisopropylbenzene	4	0.105	0.00000	0.45826	3.69910	0.00000
Ethers						
Di-nPropyl-ether	142	2.412	-0.00950	-0.54095	1.41948	0.00000
Dimethyl-ether	355	4.209	-0.29339	-0.10355	1.96062	0.10196
Diphenylether	37	2.020	0.00000	-0.39790	1.87147	0.00000
Di-nButyl-ether	263	4.695	0.10056	0.37022	2.52690	0.17115
Methylpropylether	146	5.834	-0.12273	-0.92020	0.58839	0.00000
Methylbutylether	8	0.644	0.62317	-18429.10000	-18588.40000	0.00000
Ethylpropylether	6	0.433	-0.15458	4669.95000	4697.39000	0.00000
Ethylbutylether	9	2.459	-0.06616	-1.37107	-0.44201	0.00000
Methyl-tertButyl-ether	7	0.074	0.00000	-0.47015	1.34986	0.00000
Di-nPentyl-ether	241	6.852	0.21939	-0.63850	1.16954	-0.03388
Diisopropyl-ether	143	1.347	-0.10270	-0.64079	1.12749	0.00000
Esters						
Methylacetate	308	8.136	-0.17527	-0.14041	1.72639	0.11550
nButyl-acetate	200	7.914	-0.06702	1.79368	4.16724	0.53278
IsobutylAcetate	126	4.740	0.03140	3.58544	5.91169	1.02983
IsopropylAcetate	21	1.232	0.00000	-0.59056	1.13094	0.00000
nPentyl-acetate	166	10.143	0.12284	-1.31579	-0.22664	-0.11486

Continued on next page

Table – continued from previous page

Name	points	AAD / %	A	B	C	D
nHexylAcetate	272	3.847	0.00000	-0.52820	1.40863	0.00000
nHeptyl-acetate	273	3.770	0.00000	-0.55305	1.31511	0.00000
Etheryl-acetate	5	1.026	0.00000	-0.68141	0.87751	0.00000
2-EthylhexylAcetate	125	0.907	0.00000	-0.43337	1.65683	0.00000
Ketones						
Acetone	407	6.691	-0.44152	-0.54655	1.60334	-0.01533
2-Butanone	347	4.718	-0.01624	0.27836	2.04038	0.20099
2-Pentanone	174	2.415	0.00000	-0.55448	1.09366	0.00000
3-Pentanone	22	1.515	0.00000	-0.51819	1.22417	0.00000
2-Hexanone	111	6.090	0.19579	-0.47675	1.18900	0.00000
3-Hexanone	163	1.994	0.00000	-0.55650	1.15718	0.00000
2-Heptanone	11	0.488	0.00000	-0.53055	1.27619	0.00000
3-Heptanone	175	1.765	0.00000	-0.67049	0.81844	0.00000
4-Heptanone	97	7.505	0.13481	0.61975	2.64019	0.26801
2-Octanone	30	1.012	0.00000	-0.49312	1.36351	0.00000
5-Nonanone	168	1.326	0.00000	-0.54889	1.29829	0.00000
6-Undecanone	184	1.084	0.00000	-0.57677	1.25024	0.00000
Methyl-Isobutyl-ketone	9	0.119	0.00000	-0.38393	1.52213	0.00000
Acetophenone	15	18.951	0.00000	-0.18683	2.40623	0.00000
Cyclopentanone	20	3.394	-0.23406	-0.43589	1.69280	0.00000
Cyclohexanone	7	5.152	0.00000	-0.32931	1.76426	0.00000
Alkoholes						
Methanol	1206	8.165	-0.43692	0.24243	2.35442	0.07029
Ethanol	964	7.182	-0.46397	0.88610	3.32311	0.18246
1-Butanol	325	5.783	-0.43680	0.81942	3.31821	0.18374
1-Propanol	419	8.214	-0.33688	1.11329	3.55571	0.23074
1-Pentanol	132	2.686	0.00000	0.15027	1.92441	0.07464

Continued on next page

Table – continued from previous page

Name	points	AAD / %		A	B	C	D
1-Hexanol	269	2.599	-0.10144	-0.05987	1.84934	0.04167	
1-Heptanol	307	4.260	-0.06162	-0.33780	1.47921	-0.00360	
1-Octanol	211	3.295	-0.14167	0.51309	2.80912	0.15357	
1-Nonanol	182	2.161	0.08242	-0.30061	1.57121	0.00871	
1-Decanol	286	3.990	0.04992	-0.93608	0.66046	-0.10728	
1-Undecanol	92	2.069	0.00000	-0.42469	1.31581	0.00000	
1-Dodecanol	94	2.081	0.00000	-0.47277	1.39141	0.00000	
1-Tetradecanol	14	1.098	0.00000	-0.19242	2.34391	0.00000	
1-Hexadecanol	4	1.073	0.00000	-0.06665	2.74811	0.00000	
1-Octadecanol	13	1.188	0.00000	-0.22835	2.40049	0.00000	
Acids							
Formic acid	86	0.839	0.00000	-0.57907	1.14536	-0.02238	
Butyric acid	27	4.220	-0.16459	3.44250	8.24177	0.52180	
Pentanoic acid	17	0.859	0.00000	-0.36341	1.07419	0.00000	
Nonanoic acid	8	0.291	0.00000	-0.40621	1.21198	0.00000	
Decanoic acid	10	0.400	0.00000	-0.42570	1.21001	0.00000	
Dodecanoic acid	7	8.135	0.00000	-0.50535	1.21875	0.00000	
Tetradecanoic acid	6	0.316	0.00000	-0.33821	1.65013	0.00000	
Caprylic acid	16	0.535	0.09518	-0.42231	1.00195	0.00000	
Hexanoic acid	7	4.660	0.04930	-0.12531	1.78753	0.00000	
Acetic acid	309	30.027	0.63173	1.79027	6.61451	0.18106	
Propionic acid	116	27.044	0.14591	4.19240	10.56320	0.53308	
Hexadecanoic acid	18	6.503	0.00000	-0.56686	1.14622	0.00000	
Octadecanoic acid	16	10.232	0.00000	-0.47082	1.43176	0.00000	
Oleic acid	6	15.543	0.00000	-0.57667	1.17205	0.00000	

Proposed scaling approach with individually adjusted c_1 and c_2 coefficients

In subsection 2.4.2(*Substances with experimental data of λ in gas phase*), we adjust coefficients c_1 and c_2 for the ideal gas reference (Eq. (2.12) and (2.13)) individually for each substance. Because the coefficients c_1 and c_2 are treated as adjustable, it is sufficient to set $A = 0$. The resulting coefficients are:

Name	AAD / %	c1	c2	B	C	D
methane	5.345	0.00810	0.03826	-0.94513	0.33840	-0.04088
ethane	3.094	-0.06876	0.07712	-1.07173	0.29741	-0.07140
propane	2.485	-0.05455	0.08158	-1.10766	0.24258	-0.08287
butane	2.221	-0.04061	0.07845	-0.95826	0.56764	-0.06613
pentane	2.368	-0.03305	0.07173	-1.18945	0.26402	-0.11202
hexane	2.765	-0.02708	0.06452	-0.68573	1.18944	-0.04189
heptane	3.287	-0.02132	0.05673	-0.80122	1.04822	-0.06109
octane	2.796	-0.01849	0.05213	-0.44554	1.70144	-0.01483
nonane	3.175	-0.01606	0.04899	-0.94596	0.91609	-0.09751
decane	2.635	-0.01532	0.04798	-0.81783	1.11755	-0.07083
undecane	2.695	-0.01564	0.04957	-0.60039	1.48794	-0.04101
1-heptanol	4.131	-0.02929	0.06958	-0.41825	1.28098	-0.01637
water	4.750	-0.24983	0.10982	-0.65521	1.32381	-0.062415

A.2.2 α -Eucken approach $\lambda_{\alpha, Eu}^{ref}$

Name	points	AAD / %	A	B	C	D
Alkanes						
Methane	3251	6.012	0.01608	-0.69621	0.75614	-0.00609
Ethane	1450	5.255	-0.67142	-0.54677	1.90156	0.00495
Propane	3040	4.245	-0.92502	-0.68695	2.01999	-0.02952
nButane	2959	2.666	-1.13744	-0.54389	2.55540	-0.01223
nPentane	614	2.562	-1.33087	-0.72909	2.57511	-0.05514
nHexane	767	3.246	-1.50871	-0.47938	3.36737	-0.03641
nHeptane	1447	3.930	-1.68425	-0.59787	3.48167	-0.06719
nOctane	581	3.367	-1.83853	-0.00019	4.68038	0.02104
nNonane	618	2.462	-1.97049	-0.56842	3.99613	-0.08247
nDecane	779	3.062	-2.11367	-0.54079	4.35285	-0.10287
nUndecane	476	3.183	-2.21686	0.04103	5.32874	0.00730
nTridecane	651	2.128	-2.44939	0.49984	6.40013	0.07025
nTetradecane	474	2.899	-2.48895	0.23567	6.16265	0.00000
nPentadecane	368	2.455	-2.59788	0.31727	6.50478	0.00000
nHexadecane	466	3.003	-2.67228	0.38136	6.76121	0.00000
nHeptadecane	17	0.232	-1.59129	0.02349	4.77515	0.00000
nOctadecane	384	6.047	-1.81696	-0.08661	4.82497	0.00000
nNonadecane	327	1.921	-2.47521	0.40409	6.68263	0.00000
nEicosane	48	0.359	-1.67063	-0.01822	4.77018	0.00000
nHeneicosane	48	0.407	-1.53040	-0.04648	4.55776	0.00000
nDocosane	54	1.291	-1.13717	-0.15448	3.89545	0.00000
Tricosane	42	0.339	-1.49129	-0.01171	4.63494	0.00000
Tetracosane	55	1.697	-0.45022	-0.36023	2.65684	0.00000
Branched Alkanes						

Continued on next page

Table -- continued from previous page

Name	points	AAD / %	A	B	C	D
2-Methylpropane	182	2.898	-1.06542	-0.79075	2.02608	-0.05144
2-Methylbutane	68	1.967	-1.25855	-0.35876	3.10256	0.00000
2-Methylpentane	17	0.779	-2.10322	-0.26543	4.30583	0.00000
3-Methylpentane	20	1.587	-3.22055	-0.04215	6.12728	0.00000
3-Ethylpentane	16	0.038	-1.63339	-0.37563	3.56607	0.00000
2-Methylhexane	16	0.093	-1.72575	-0.33159	3.76412	0.00000
3-Methylhexane	26	0.092	-1.69142	-0.35303	3.66575	0.00000
2-Methylheptane	16	0.043	-1.80133	-0.27875	4.00961	0.00000
3-Methylheptane	16	0.177	-2.17886	-0.21166	4.60528	0.00000
2,2-Dimethylpropan	5	0.395	-1.32029	6708.96000	6757.60000	0.00000
2,2-Dimethylbutane	17	0.807	-1.35234	-0.44782	2.98886	0.00000
2,3-Dimethylbutane	81	0.799	-2.65611	-0.13389	5.24751	0.00000
2,2-Dimethylpentane	15	0.080	-1.82578	-0.35297	3.79362	0.00000
3,3-Dimethylpentane	16	0.075	-1.95528	-0.35180	3.96278	0.00000
2,3-Dimethylpentane	27	0.322	-2.09199	-0.29459	4.25370	0.00000
2,4-Dimethylpentane	17	0.375	-1.60278	-0.37930	3.49307	0.00000
2,2,3-Trimethylbutane	16	0.625	-2.68735	-0.21358	5.10855	0.00000
2,2,4-Trimethylpentane	524	3.296	-1.61998	-1.34381	2.11610	-0.17740
2,3,4-Trimethylpentane	15	0.068	-1.74877	-0.33054	3.79136	0.00000
Alkenes						
Ethylene	530	5.001	-0.62484	-0.27656	2.22678	0.07248
1-Propene	422	11.937	-0.80335	-2.23652	0.12798	-0.42643
1-Butene	31	7.125	-1.15392	-0.49756	2.65967	0.00000
1-Pentene	32	1.472	-1.34798	-0.46315	2.98084	0.00000
1-Hexene	320	3.876	-1.52167	-0.35337	3.44890	-0.00104
1-Heptene	423	3.374	-1.62733	-0.26503	3.81577	0.00714
1-Octene	493	3.234	-1.92139	-0.11856	4.43196	0.01686

Continued on next page

Table – continued from previous page

Name	points	AAD / %	A	B	C	D
1-Nonene	343	3.275	-1.98479	-0.10246	4.52346	0.02626
1-Decene	312	3.675	-2.15477	0.00404	4.99853	0.02872
1-Undecene	257	2.065	-2.17498	-0.04774	5.07031	0.00000
1-Dodecene	313	1.894	-2.70969	1.65598	8.12613	0.33429
1-Tridecene	246	1.181	-2.46238	0.23589	6.06914	0.00000
1-Tetradecene	279	1.403	-2.81955	1.70112	8.55417	0.29786
1-Pentadecene	249	1.408	-2.40635	0.22657	6.07252	0.00000
1-Hexadecene	249	1.445	-2.35204	0.22018	6.02485	0.00000
cis-2-Butene	19	4.189	-1.17362	-0.54604	2.56211	0.00000
trans-2-Bute	23	4.709	-1.17728	-0.56635	2.54350	0.00000
Aldehydes						
Decanal	21	1.262	-1.26172	-0.22243	3.55351	0.00000
Butanal	79	3.929	-1.14053	-0.62103	2.22894	0.00000
n-Pentanal	8	0.156	-1.10433	-0.38109	2.78162	0.00000
Heptanal	12	0.097	-1.55706	-0.24800	3.75244	0.00000
n-Dodecanal	16	1.475	-2.43839	0.29784	6.27479	0.00000
3-Methyl-butylaldehyde	54	2.592	-1.20005	-0.54888	2.52199	0.00000
Acetaldehyde	96	10.969	-1.29308	465.40000	463.30700	0.00000
2-Methyl-propanal	67	4.228	-1.07615	-2.00353	0.46793	-0.31392
Benzaldehyde	9	0.774	-1.15678	-0.58449	2.27987	0.00000
Aromatics						
Benzene	1061	2.778	-1.14782	-1.23287	1.74176	-0.16454
Ethylbenzene	654	2.301	-1.39302	-0.72024	2.75485	-0.06961
Propylbenzene	94	2.011	-1.27317	-0.35702	3.20904	0.00000
Butylbenzene	152	1.993	-1.71830	-0.20306	4.03783	0.00000
sec-Butylbenzene	11	0.124	-1.74578	-0.27000	3.96784	0.00000
tert-Butylbenzene	140	1.710	-1.36929	-0.20429	3.64147	0.00000

Continued on next page

Table -- continued from previous page

Name	points	AAD / %	A	B	C	D
Toluene	3777	3.146	-1.28000	-0.71100	2.59000	-0.06230
1,2-Dimethyl-benzene	649	1.377	-1.38104	-0.99616	2.30817	-0.11750
1,3-Dimethyl-benzene	600	2.025	-1.44482	-0.71938	2.82010	-0.07232
1,4-Dimethyl-benzene	553	1.448	-1.24408	-0.82146	2.39939	-0.08049
Isopropylbenzene	413	2.135	-1.17011	-1.16292	1.89674	-0.15577
1,2,4-Trimethylbenzene	171	1.557	-1.49637	-0.27047	3.58338	0.00000
1,3,5-Trimethylbenzene	18	0.054	-1.63097	-0.26730	3.73469	0.00000
1,3,5-Triisopropylbenzene	4	0.115	-1.54212	0.78325	6.22147	0.00000
Ethers						
Di-nPropyl-ether	142	2.305	-1.65805	-0.36397	3.74361	0.00000
Dimethyl-ether	355	2.904	-1.08893	-0.43561	2.56382	0.00248
Diphenylether	37	1.963	-1.92593	-0.15650	4.62891	0.00000
Di-nButyl-ether	263	4.240	-1.90962	0.65175	5.58999	0.15344
Methylpropylether	146	6.332	-1.49764	-0.81548	2.43773	0.00000
Methylbutylether	8	0.644	-0.88180	-19723.40000	-19884.10000	0.00000
Ethylpropylether	6	0.433	-1.70549	5297.41000	5337.23000	0.00000
Ethylbutylether	9	2.382	-1.78044	-0.96464	2.45610	0.00000
Methyl-tertButyl-ether	7	0.055	0.81706	-0.85524	-0.50645	0.00000
Di-nPentyl-ether	241	6.835	-1.96109	-1.10700	3.54217	-0.23177
Diisopropyl-ether	143	0.966	-1.74993	-0.32237	3.76053	0.00000
Esters						
Methylacetate	308	7.743	-1.38333	-0.67197	2.75326	-0.07403
nButyl-acetate	200	6.978	-1.87046	1.71178	6.55996	0.42591
IsobutylAcetate	126	3.852	-1.78355	2.38209	7.02069	0.63432
IsopropylAcetate	21	1.256	0.61614	-0.88804	-0.28499	0.00000
nPentyl-acetate	166	10.196	-1.80756	-0.99808	2.79984	-0.12811
nHexylAcetate	272	3.308	-2.61237	0.20456	6.11970	0.00000

Continued on next page

Table -- continued from previous page

Name	points	AAD / %	A	B	C	D
nHeptyl-acetate	273	3.327	-2.59098	0.19970	6.04733	0.00000
Etheryl-acetate	5	0.482	6.38900	-2.73169	-11.23820	0.00000
2-EthylhexylAcetate	125	0.207	-1.74154	-0.16438	4.28797	0.00000
Ketones						
Acetone	407	5.321	-1.45145	-0.29836	3.21142	0.00978
2-Butanone	347	4.204	-1.32513	0.05101	3.43610	0.11043
2-Pentanone	174	1.500	-1.35730	-0.44026	2.92384	0.00000
3-Pentanone	22	1.513	-0.76866	-0.43548	2.28183	0.00000
2-Hexanone	111	5.642	-1.48921	-0.21574	3.73319	0.00000
3-Hexanone	163	1.111	-1.61245	-0.34710	3.50473	0.00000
2-Heptanone	11	0.228	-1.52339	-0.25601	3.66308	0.00000
3-Heptanone	175	1.435	-1.92831	-0.23756	4.04930	0.00000
4-Heptanone	97	6.959	-1.66775	0.11458	4.38732	0.08832
2-Octanone	30	0.706	-1.58706	-0.22477	3.81323	0.00000
5-Nonanone	168	0.688	-2.21592	-0.05143	5.00795	0.00000
6-Undecanone	184	0.747	-2.49772	0.14380	5.79793	0.00000
Methyl-Isobutyl-ketone	9	0.088	0.02240	-0.48297	1.24497	0.00000
Acetophenone	15	18.922	-16.17640	1.98340	25.97640	0.00000
Cyclopentanone	20	1.710	-1.47778	-0.31391	3.37582	0.00000
Cyclohexanone	7	5.294	0.61446	-0.45720	0.72937	0.00000
Alkoholes						
Methanol	1206	7.780	-0.81872	0.09314	2.35615	0.05518
Ethanol	964	6.021	-1.33215	0.51884	3.50749	0.13298
1-Butanol	325	5.547	-1.97953	1.64199	6.48040	0.29462
1-Propanol	419	6.434	-1.63036	1.23156	5.27189	0.23275
1-Pentanol	132	2.821	-1.58307	0.85076	4.94592	0.16409
1-Hexanol	269	2.625	-2.01411	0.80182	5.52469	0.15270

Continued on next page

Table – continued from previous page

Name	points	AAD / %	A	B	C	D
1-Heptanol	307	4.318	-2.11581	0.69495	5.59049	0.13427
1-Octanol	211	3.217	-2.42680	2.22114	8.24920	0.40286
1-Nonanol	182	2.343	-2.16845	0.62449	5.75267	0.12527
1-Decanol	286	4.151	-2.43833	0.82226	6.41679	0.14821
1-Undecanol	92	2.790	-1.85291	0.01540	4.49523	0.00000
1-Dodecanol	94	2.681	-2.16045	-0.03277	4.92260	0.00000
1-Tetradecanol	14	1.183	-1.20460	-0.05739	4.02828	0.00000
1-Hexadecanol	4	0.416	-4.82229	0.73504	10.16820	0.00000
1-Octadecanol	13	0.920	0.63394	-0.40133	1.24822	0.00000
Acids						
Formic acid	86	0.890	16.18740	-0.67083	-15.38980	-0.02853
Butyric acid	27	3.914	-1.17645	2.23559	6.74850	0.37220
Pentanoic acid	17	0.665	0.92887	-0.44794	-0.19086	0.00000
Nonanoic acid	8	0.117	-0.08459	-0.42230	1.24771	0.00000
Decanoic acid	10	0.255	-0.19271	-0.44339	1.35733	0.00000
Dodecanoic acid	7	6.111	-20.03980	2.13508	30.28380	0.00000
Tetradecanoic acid	6	0.286	-0.61432	-0.25075	2.55548	0.00000
Caprylic acid	16	0.816	-1.97997	-0.27362	3.65593	0.00000
Hexanoic acid	7	3.952	-1.73810	-0.05561	3.87970	0.00000
Acetic acid	309	27.025	0.77130	1.59109	5.88455	0.16440
Propionic acid	116	26.187	-0.55037	3.93329	10.50130	0.51025
Hexadecanoic acid	18	5.990	5.88580	-1.84243	-8.65283	0.00000
Octadecanoic acid	16	10.022	9.18811	-2.73771	-14.51650	0.00000
Oleic acid	6	7.678	-11.94240	2.36962	21.97000	0.00000

A.2.3 α -LTST approach $\lambda_{\alpha,LTST}^{ref}$

Name	points	AAD / %	A	B	C	D
Alkanes						
Methane	2101	8,926147	0,153939	-0,852925	0,350744	-0,0282769
Ethane	837	5,415081	-0,822771	-1,32346	0,860141	-0,119464
Propane	1521	3,083953	-1,28403	-0,935065	1,99522	-0,0670006
nButane	2032	2,627257	-1,65787	-1,19721	2,10807	-0,120559
nPentane	575	2,801012	-1,96264	-1,11886	2,71389	-0,129282
nHexane	696	3,710086	-2,19615	-1,4994	2,66873	-0,228189
nHeptane	1402	4,171081	-2,37587	-2,10426	2,14087	-0,359557
nOctane	539	3,074172	-2,54465	-0,566693	4,68852	-0,0917373
nNonane	618	3,099032	-2,66542	-2,05837	2,70755	-0,374599
nDecane	715	3,514653	-2,8005	-2,19334	2,94375	-0,4521
nUndecane	446	4,245814	-2,89854	-1,56972	3,90054	-0,314411
nDodecane	17	0,335931	-2,75668	-2859,98	-2897,71	0,00000
nTridecane	651	3,726171	-3,11877	-1,33692	4,75192	-0,31837
nTetradecane	474	3,613761	-3,15343	0,101169	6,64138	0,00000
nPentadecane	368	2,633131	-3,29967	0,239701	7,15474	0,00000
nHexadecane	466	2,479205	-3,33706	0,311805	7,38799	0,00000
nHeptadecane	17	0,291345	-2,57634	0,251083	6,43926	0,00000
nOctadecane	384	6,427807	-3,39771	0,346248	7,65478	0,00000
nNonadecane	327	2,308052	-4,01424	0,835844	9,46084	0,00000
nEicosane	48	0,472637	-2,48186	0,175126	6,15393	0,00000
nHeneicosane	48	0,50776	-2,2554	0,129234	5,80137	0,00000
nDocosane	54	1,346828	-1,8323	0,012246	5,08394	0,00000
nTricosane	42	0,414695	-2,19167	0,170003	5,86261	0,00000
nTetracosane	55	1,735187	-1,10442	-0,18502	3,81617	0,00000

Continued on next page

Table – continued from previous page

Name	points	AAD / %	A	B	C	D
Branched Alkanes						
2-Methylpropane	1556	4,894927	-1,63484	-1,45556	1,55973	-0,154278
2-Methylbutane	66	1,143824	-1,94129	-0,319681	3,93984	0,00000
2-Methylpentane	17	0,79069	-3,40767	-0,0947858	6,18158	0,00000
3-Methylpentane	20	1,598758	-4,57144	0,121258	8,03492	0,00000
3-Ethylpentane	16	0,043985	-2,89566	-0,228747	5,33418	0,00000
2-Methylhexane	16	0,106268	-2,96403	-0,169422	5,54688	0,00000
3-Methylhexane	26	0,106132	-3,0308	-0,180097	5,5876	0,00000
2-Methylheptane	16	0,041756	-2,8439	-0,147386	5,49778	0,00000
3-Methylheptane	16	0,17034	-3,27647	-0,0762203	6,16457	0,00000
2,2-Dimethylpropane	5	0,857299	-1,95629	-1289,97	-1289,6	0,00000
2,2-Dimethylbutane	17	0,774611	-2,14314	-0,448936	3,85047	0,00000
2,3-Dimethylbutane	81	0,872508	-3,57794	-0,075639	6,39698	0,00000
2,2-Dimethylpentane	15	0,081356	-3,58768	-0,141344	6,27836	0,00000
3,3-Dimethylpentane	16	0,075891	-3,81302	-0,162176	6,492	0,00000
2,3-Dimethylpentane	27	0,327554	-3,70302	-0,110011	6,5029	0,00000
2,4-Dimethylpentane	17	0,568778	-2,36723	-0,362988	4,37546	0,00000
2,2,3-Trimethylbutane	16	0,621609	-4,76495	-0,011009	7,90982	0,00000
2,2,4-Trimethylpentane	498	5,360162	-2,61242	-2,9502	0,759514	-0,458031
2,3,4-Trimethylpentane	15	0,057518	-3,40561	-0,159923	6,05267	0,00000
Alkenes						
Ethylene	391	5,781548	-0,660045	-0,370781	2,1659	0,0495483
Propylene	297	2,903648	-1,25128	-3,42202	-0,793015	-0,70859
1-Butene	31	2,841344	-1,60289	-0,49083	3,17666	0,00000
1-Pentene	32	0,451604	-1,90654	-0,425949	3,68903	0,00000
1-Hexene	296	4,605793	-2,15644	-1,47293	2,49689	-0,198812
1-Heptene	405	3,423764	-2,33563	-1,59906	2,68294	-0,24156

Continued on next page

Table – continued from previous page

Name	points	AAD / %	A	B	C	D
1-Octene	468	3,365965	-2,5207	-1,17975	3,63163	-0,191302
1-Nonene	343	4,051421	-2,65184	-1,99135	2,61707	-0,335533
1-Decene	312	5,067198	-2,80705	-1,97894	2,97561	-0,358415
1-Undecene	257	5,855781	-2,95888	-0,361645	5,29884	0,00000
1-Dodecene	313	1,872657	-4,11302	1,18576	9,36646	0,182505
1-Tridecene	246	1,099066	-4,03127	0,556781	8,62778	0,00000
1-Tetradecene	279	1,270866	-4,62703	2,39525	11,9295	0,367735
1-Pentadecene	249	1,202905	-4,16869	0,624018	9,03047	0,00000
1-Hexadecene	249	1,347147	-4,12959	0,63935	9,0512	0,00000
cis-2-Butene	19	2,708272	-1,61797	-0,521866	3,11556	0,00000
trans-2-Butene	23	2,416233	-1,64723	-0,56121	3,07479	0,00000
Aldehydes						
n-Decanal	21	1,403884	-2,0587	-0,0979914	4,75821	0,00000
n-Butanal	75	6,208932	-1,71332	-0,740494	2,58543	0,00000
n-Pentanal	8	0,156551	-1,70936	-0,310217	3,63043	0,00000
n-Heptanal	12	0,13352	-2,57415	-0,102216	5,25167	0,00000
n-Dodecanal	16	1,436196	-3,68083	0,588835	8,37859	0,00000
3-Methylbutyraldehyde	54	4,408634	-1,86228	-0,681445	2,94905	0,00000
Acetaldehyde	96	8,97931	-1,36841	4735,01	4756,6	0,00000
2-Methylpropanal	61	5,134029	-1,69923	-3,95426	-1,46695	-0,71914
Benzaldehyde	9	0,772122	-1,72454	-0,548004	2,9911	0,00000
Aromatics						
Benzene	956	2,961318	-1,93277	-2,9641	0,173148	-0,502599
Ethylbenzene	623	3,339474	-2,27847	-1,94589	1,89327	-0,288613
Propylbenzene	94	5,156702	-2,22024	-0,472555	3,94401	0,00000
Butylbenzene	152	2,145627	-2,95768	-0,082965	5,71182	0,00000
sec-Butylbenzene	11	0,248319	-3,37743	-0,0621762	6,30579	0,00000

Continued on next page

Table – continued from previous page

Name	points	AAD / %	A	B	C	D
tert-Butylbenzene	140	1,930722	-2,87573	-0,0601499	5,6703	0,00000
Toluene	3214	2,857086	-2,20059	-1,1435	2,9571	-0,139659
1,2-Dimethyl-benzene	639	2,219686	-2,28717	-2,58285	1,03054	-0,417543
1,3-Dimethyl-benzene	556	2,525308	-2,31152	-2,06114	1,82232	-0,32062
1,4-Dimethyl-benzene	547	1,671309	-2,22348	-2,92659	0,610883	-0,507207
Isopropylbenzene	413	3,014731	-2,0808	-3,1639	0,0861318	-0,544375
1,2,4-Trimethylbenzene	171	1,682212	-2,62375	-0,164517	5,09642	0,00000
1,3,5-Trimethylbenzene	18	0,059363	-2,19395	-0,227149	4,45251	0,00000
1,3,5- Triisopropylbenzene	4	0,122372	-2,76284	1,01342	8,15587	0,00000
Ethers						
Di-n-propylether	142	4,434104	-2,36873	-0,695985	3,82682	0,00000
Dimethylether	191	2,029429	-1,31327	-0,477516	2,74208	0,00000
Diphenylether	37	2,008145	-4,19259	0,0591147	7,67911	0,00000
Dibutylether	237	3,462403	-2,63547	-1,15525	4,00951	-0,223767
Methylpropylether	146	9,622926	-2,08848	-1,08552	2,54083	0,00000
Methylbutylether	8	0,643989	-1,65722	-18692,7	-18826,8	0,00000
Ethylpropylether	6	0,432527	-2,44765	6808,1	6877,5	0,00000
Ethylbutylether	9	2,120236	-2,34971	-0,936397	3,17259	0,00000
Methyl-tert-butylether	7	0,054725	-0,619573	-0,637804	1,62997	0,00000
Dipentylether	194	7,556651	-2,74173	-3,79831	0,898453	-0,806804
Diisopropylether	140	1,25963	-2,36695	-0,284992	4,54121	0,00000
Esters						
Methylacetate	256	7,547739	-1,7661	-2,4142	0,97025	-0,46491
nButylacetate	189	5,23598	-2,43452	-0,283793	4,58005	0,00000
IsobutylAcetate	99	2,709234	-2,36537	-0,852336	3,67831	-0,12202
IsopropylAcetate	21	1,253074	-0,245152	-0,739641	1,0447	0,00000
nPentylAcetate	166	10,245762	-2,51815	-3,26635	0,59097	-0,605501

Continued on next page

Table – continued from previous page

Name	points	AAD / %	A	B	C	D
nHexylAcetate	272	2,995517	-4,08074	0,506269	8,51177	0,00000
nHeptylAcetate	273	3,07374	-3,92274	0,497606	8,27555	0,00000
Vinylacetate	5	0,484949	5,85053	-2,63607	-10,4008	0,00000
2-EthylhexylAcetate	125	0,252022	-2,42548	-0,0849244	5,24978	0,00000
Ketones						
Acetone	386	3,587488	-1,67495	-0,751022	2,79819	-0,0717666
2-Butanone	336	4,159609	-1,83143	-1,29401	2,21608	-0,172058
2-Pentanone	174	2,702514	-2,34457	-0,347493	4,27053	0,00000
3-Pentanone	22	1,503194	-1,35453	-0,370392	3,09476	0,00000
2-Hexanone	101	8,32653	-2,15809	-0,36779	4,13383	0,00000
3-Hexanone	163	2,254177	-2,78605	-0,210696	5,16836	0,00000
2-Heptanone	11	0,218763	-2,36124	-0,139687	4,88835	0,00000
3-Heptanone	175	2,036581	-2,94788	-0,0370157	5,69165	0,00000
4-Heptanone	79	3,259306	-2,49196	-3,75188	0,311435	-0,751399
2-Octanone	30	0,783612	-2,24776	-0,137365	4,76995	0,00000
5-Nonanone	168	1,202058	-3,78784	0,251573	7,5212	0,00000
6-Undecanone	184	1,262748	-3,83836	0,486792	8,14046	0,00000
4-Methyl-2-pentanone	9	0,086192	-0,866212	-0,358584	2,54349	0,00000
Acetophenone	15	18,913367	-16,8235	2,04295	26,8408	0,00000
Cyclopentanone	20	1,539574	-2,00087	-0,289529	4,00429	0,00000
Cyclohexanone	7	5,30837	-0,521732	-0,380356	2,16506	0,00000
Alkoholes						
Methanol	1055	7,882668	-0,840989	-0,178455	1,77514	0,0249201
Ethanol	864	5,681866	-1,48335	0,189142	3,03979	0,0886236
1-Butanol	321	5,367502	-2,07472	1,61801	6,55948	0,288836
1-Propanol	367	6,17116	-1,771	0,99168	5,05605	0,191651
1-Pentanol	132	2,859236	-2,17978	1,12025	6,09565	0,198504

Continued on next page

Table – continued from previous page

Name	points	AAD / %	A	B	C	D
1-Hexanol	241	3,14528	-2,44173	0,472153	5,54794	0,0873419
1-Heptanol	293	4,664308	-2,57791	0,318886	5,58118	0,0606781
1-Octanol	194	3,340884	-2,73679	1,82307	8,09856	0,31612
1-Nonanol	169	3,287457	-2,87249	-0,143104	5,42538	-0,0179855
1-Decanol	268	4,63893	-2,9576	0,208157	6,18116	0,0219253
1-Undecanol	92	3,118447	-2,36356	0,148884	5,4004	0,00000
1-Dodecanol	94	3,108774	-3,37782	0,192065	6,85422	0,00000
1-Tetradecanol	14	1,110215	-1,81314	-0,0042963	4,83484	0,00000
1-Hexadecanol	4	0,405081	-5,15437	0,774692	10,6372	0,00000
1-Octadecanol	13	0,916595	0,0808476	-0,327414	2,0506	0,00000
Acids						
Formic acid	50	0,864493	-90,0026	-0,279913	92,1268	0,00000
Butyric acid	27	4,336098	-2,08582	2,36821	7,57434	0,408773
Pentanoic acid	17	0,688129	-0,325772	-0,407953	1,24455	0,00000
Nonanoic acid	8	0,116813	-0,747624	-0,379973	2,07907	0,00000
Capric acid	10	0,277584	-1,00713	-0,387217	2,3908	0,00000
Lauric acid	7	6,105886	-20,3995	2,16712	30,7613	0,00000
Myristic acid	6	0,268846	-0,945675	-0,201188	3,05052	0,00000
Caprylic acid	16	0,759622	-2,72548	-0,244073	4,53076	0,00000
Hexanoic acid	7	4,602517	-2,43938	-0,0264711	4,70533	0,00000
Acetic acid	309	33,059547	-0,721787	1,63011	6,89069	0,179506
Propionic acid	116	28,932851	-1,38147	3,52826	9,94585	0,483767
Palmitic acid	18	5,987593	5,64058	-1,80523	-8,28553	0,00000
Stearic acid	16	10,026876	8,90781	-2,68827	-14,0792	0,00000
cis-9-Octadecenoic acid	6	7,672842	-11,9777	2,37687	22,028	0,00000

A.2.4 α -CCE approach $\lambda_{\alpha,CCE}^{ref}$

Name	points	AAD / %	A	B	C	D
Alkanes						
Methane	2101	4,78152	-0,0802344	-0,824656	0,622559	-0,0234474
Ethane	837	4,527951	-0,531356	-0,788529	1,35909	-0,0319312
Propane	1521	3,337749	-0,727126	-0,840871	1,53911	-0,0507458
nButane	2032	2,993773	-0,780742	-0,523316	2,18568	-0,0065776
nPentane	575	2,708762	-0,788158	-0,760514	1,87875	-0,0523538
nHexane	696	3,604322	-0,821694	-0,171339	2,97681	0,0320417
nHeptane	1402	4,088588	-0,898877	-0,16168	3,1239	0,0329615
nOctane	539	3,44725	-0,937362	0,268692	3,94237	0,0909037
nNonane	618	3,700402	-0,969798	-0,0931725	3,40536	0,0321617
nDecane	715	2,839633	-1,01856	0,297301	4,03158	0,110204
nUndecane	446	3,492101	-1,04655	0,554317	4,51381	0,142403
nDodecane	17	0,339312	-0,678123	-10675,6	-10747,3	-2962,66
nTridecane	651	3,171254	-1,10203	1,10914	5,4153	0,245389
nTetradecane	474	2,751515	-1,1223	2,77611	7,51567	0,635277
nPentadecane	368	2,07168	-1,19294	2,86309	7,79902	0,640778
nHexadecane	466	2,191614	-1,20672	3,40808	8,54803	0,761709
nHeptadecane	17	0,202473	-0,472633	-0,250286	2,87507	-0,0049224
nOctadecane	384	5,147062	-1,5307	6,08452	12,4728	1,35865
nNonadecane	327	1,113512	-0,0569311	-0,456472	2,00667	-0,0224754
nEicosane	48	0,302208	-0,0109715	-1,52105	0,448718	-0,231231
nHeneicosane	48	0,348708	-0,111278	-1,1277	1,13547	-0,15478
nDocosane	54	1,255507	1,04992	-2,87763	-2,80927	-0,458126
nTricosane	42	0,295952	0,204236	-1,73253	-0,0406515	-0,272658
nTetracosane	55	1,676596	1,32527	-2,3105	-2,44241	-0,315885

Continued on next page

Table – continued from previous page

Name	points	AAD / %	A	B	C	D
Branched Alkanes						
2-Methylpropane	1556	3,747837	-0,736089	-0,628371	1,91404	-0,0243685
2-Methylbutane	66	2,435031	-0,772544	-1,03361	1,51773	-0,113417
2-Methylpentane	17	0,701166	-10,9283	12,0344	33,4062	2,06851
3-Methylpentane	20	1,523806	-12,7503	12,1015	35,9823	2,00423
3-Ethylpentane	16	0,036128	-0,247774	-1,31549	0,455855	-0,140444
2-Methylhexane	16	0,093087	-0,243258	-1,45599	0,260309	-0,172208
3-Methylhexane	26	0,090886	-0,613981	-0,942634	1,45703	-0,0833514
2-Methylheptane	16	0,040313	-0,085273	-1,62222	-0,115495	-0,205995
3-Methylheptane	16	0,174028	-0,329595	-1,67761	0,131311	-0,225042
2,2-Dimethylpropane	5	0,307066	-0,938606	6986,11	7052,55	-1344,31
2,2-Dimethylbutane	17	0,795981	-0,81856	-0,387414	2,42388	0,0227499
2,3-Dimethylbutane	81	0,73217	-3,66729	0,860312	8,06032	0,146817
2,2-Dimethylpentane	15	0,077097	-0,0321626	-1,74467	-0,491079	-0,214123
3,3-Dimethylpentane	16	0,075304	-0,465684	-1,27547	0,750579	-0,135398
2,3-Dimethylpentane	27	0,324429	-1,93132	0,185859	4,78462	0,0892744
2,4-Dimethylpentane	17	0,371078	-0,918739	-0,958581	1,84524	-0,100085
2,2,3-Trimethylbutane	16	0,621036	0,782287	-3,04816	-3,43136	-0,434102
2,2,4-Trimethylpentane	498	3,013706	-0,876135	-0,956527	1,82515	-0,100742
2,3,4-Trimethylpentane	15	0,060114	0,544954	-1,99135	-1,5295	-0,249305
Alkenes						
Ethylene	391	5,898373	-0,532566	-0,0376979	2,41204	0,126745
Propylene	297	5,369118	-0,628921	-0,36154	2,28944	0,00960051
1-Butene	31	8,887986	-0,777655	0,536231	3,53606	0,232225
1-Pentene	32	2,037119	-0,873714	-3,74215	-2,13234	-0,648098
1-Hexene	296	4,191417	-0,862928	0,0333001	3,22235	0,0761662
1-Heptene	405	4,151195	-0,902686	0,0704566	3,41197	0,0820047

Continued on next page

Table – continued from previous page

Name	points	AAD / %	A	B	C	D
1-Octene	468	3,449763	-1,05224	-0,0642023	3,41076	0,0484726
1-Nonene	343	4,894297	-1,07105	0,620422	4,39365	0,18356
1-Decene	312	3,85751	-1,15149	0,755665	4,77204	0,198886
1-Undecene	257	2,121381	-1,04329	1,82711	5,99905	0,452805
1-Dodecene	313	2,155554	-0,502914	-0,116187	2,69904	0,0709694
1-Tridecene	246	1,086348	-0,532951	0,350231	3,42993	0,148074
1-Tetradecene	279	1,670286	-0,227617	-0,780682	1,61338	-0,0891995
1-Pentadecene	249	1,141304	-0,273392	-0,125957	2,54439	0,0542114
1-Hexadecene	249	1,022257	-0,239892	0,079929	2,79712	0,100098
cis-2-Butene	19	5,692193	-0,789969	-2,03445	0,111606	-0,302297
trans-2-Butene	23	5,767335	-0,801542	-2,46636	-0,426181	-0,391484
Aldehydes						
n-Decanal	21	1,090574	-1,33542	0,99386	5,42009	0,224814
n-Butanal	75	2,695264	-0,539869	-1,22298	0,778774	-0,132714
n-Pentanal	8	0,15981	3,09645	-4,59231	-8,70966	-0,669666
n-Heptanal	12	0,098571	-0,329788	-1,08406	0,986162	-0,124202
n-Dodecanal	16	1,423982	2,17469	-7,71055	-10,8834	-1,44733
3-Methylbutyraldehyde	54	2,037687	-0,565492	-0,98582	1,22179	-0,0919355
Acetaldehyde	96	3,95652	-1,05588	-20,5062	-26,5926	-3,76113
2-Methylpropanal	61	3,988775	-0,564885	-0,99254	1,15004	-0,0831459
Benzaldehyde	9	0,583342	150,507	-83,6958	-311,134	-11,482
Aromatics						
Benzene	956	2,93666	-0,701005	-0,630587	2,0437	-0,0385874
Ethylbenzene	623	2,738866	-0,67186	-0,541087	2,15922	-0,0271015
Propylbenzene	94	2,109914	-0,50268	-0,0046537	2,76455	0,0826803
Butylbenzene	152	1,855753	1,71074	-3,03815	-4,49043	-0,428763
sec-Butylbenzene	11	0,106713	-0,723665	-0,705409	2,05186	-0,055843

Continued on next page

Table – continued from previous page

Name	points	AAD / %	A	B	C	D
tert-Butylbenzene	140	1,616727	1,49132	-2,46654	-3,30951	-0,340469
Toluene	3214	2,656616	-0,738146	-0,769837	1,86684	-0,065199
1,2-Dimethylbenzene	639	1,836258	-0,64195	-0,693499	1,84227	-0,0469383
1,3-Dimethylbenzene	556	2,795157	-0,706038	-0,506705	2,23192	-0,0202331
1,4-Dimethylbenzene	547	1,860059	-0,393631	-0,443147	1,84195	0,0186148
Isopropylbenzene	413	2,22687	-0,38468	-0,719718	1,55334	-0,053608
1,2,4-Trimethylbenzene	171	1,386136	2,06733	-3,19993	-5,258	-0,442135
1,3,5-Trimethylbenzene	18	0,052308	-1,44861	-0,232891	3,58262	0,00738578
1,3,5-Triisopropylbenzene	4	0	-22,8515	36,1874	83,888	6,24265
Ethers						
Di-n-propylether	142	3,161768	-0,872137	0,907573	4,41172	0,295048
Dimethylether	191	4,358231	-0,796699	-1,68579	0,533039	-0,249262
Diphenylether	37	1,855396	4,71823	-6,00084	-12,446	-0,890466
Dibutylether	237	2,941281	-0,947339	1,07267	4,93203	0,265088
Methylpropylether	146	5,614139	-0,87628	0,147109	2,92523	0,219844
Methylbutylether	8	0,644001	-0,150668	-6872,58	-7049,13	6819,17
Ethylpropylether	6	0,432477	-0,941315	9257,56	9277,23	2673
Ethylbutylether	9	2,3469	-0,968899	-9,76586	-9,9589	-1,93259
Methyl-tert-butylether	7	0,054082	21,9233	-33,1436	-73,5119	-5,63741
Dipentylether	194	6,615461	-0,846825	-0,205185	3,28621	-0,0062709
Diisopropylether	140	0,924653	-0,990116	-0,92539	1,97323	-0,101712
Esters						
Methylacetate	256	7,91012	-0,815954	-0,0645645	2,72307	0,0970352
nButylacetate	189	7,466611	-1,01368	2,10166	5,95659	0,537205
IsobutylAcetate	99	3,775334	-0,888846	3,1373	6,81024	0,834459
IsopropylAcetate	21	1,262688	0,211373	0,67701	2,45744	0,292671
nPentylAcetate	166	10,484154	-0,882458	-0,194752	2,66998	0,0693706

Continued on next page

Table – continued from previous page

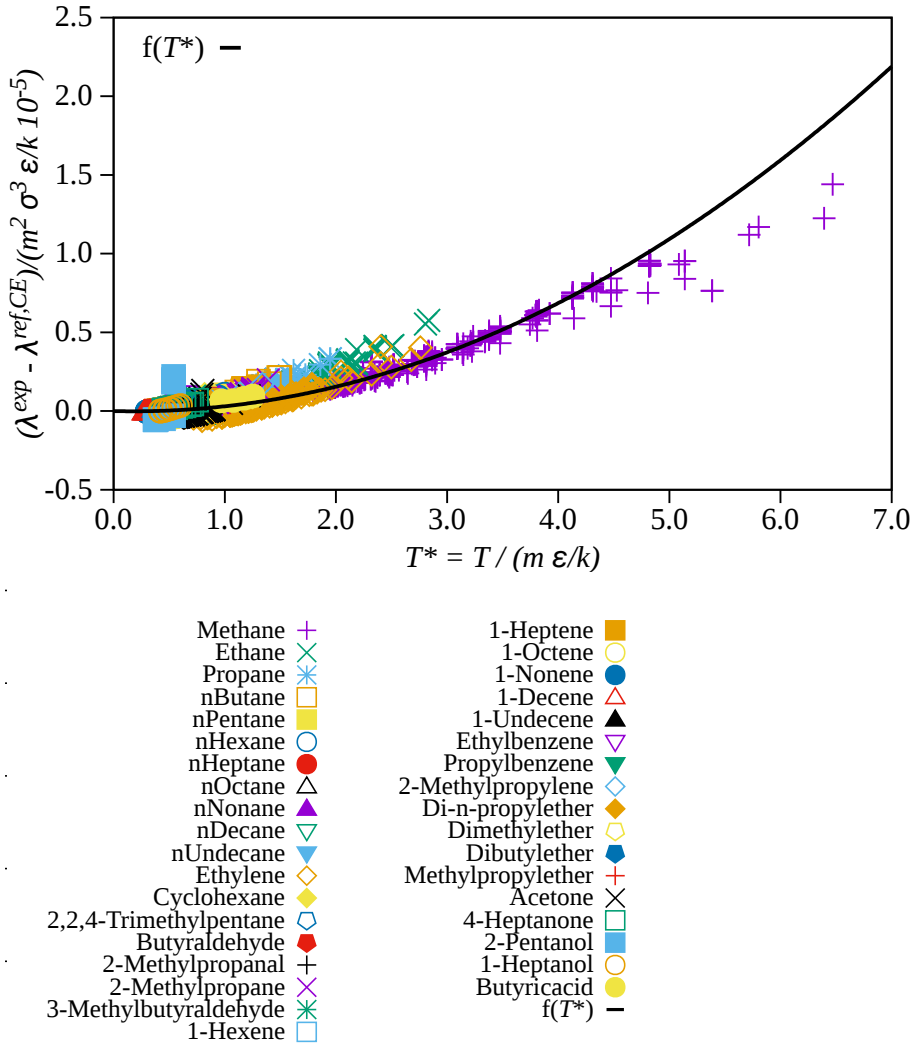
Name	points	AAD / %	A	B	C	D
nHexylAcetate	272	3,327991	-2,02323	2,19617	7,99354	0,442113
nHeptylAcetate	273	3,309171	-1,8322	1,98704	7,3838	0,413675
Vinylacetate	5	0,030084	-61,8744	114,33	242,122	20,8357
2-EthylhexylAcetate	125	0,208822	-0,677845	-0,815437	1,99359	-0,0933665
Ketones						
Acetone	386	5,3801	-1,01843	-0,44755	2,47577	-0,010663
2-Butanone	336	4,624502	-0,750465	0,627675	3,49325	0,243425
2-Pentanone	174	0,937374	-0,243684	-1,34822	0,259772	-0,154159
3-Pentanone	22	1,61672	-7,16396	6,56852	20,789	1,10618
2-Hexanone	101	6,336427	-0,671002	0,766989	3,98152	0,231947
3-Hexanone	163	0,592255	-0,235025	-1,55955	0,0591502	-0,203514
2-Heptanone	11	0,21918	7,56927	-11,7722	-24,6631	-1,90661
3-Heptanone	175	1,057049	-0,343524	-1,38474	0,323044	-0,162692
4-Heptanone	79	2,778277	-0,894551	0,0657888	3,42666	0,0829559
2-Octanone	30	0,6752	-2,28815	1,27192	6,92325	0,254146
5-Nonanone	168	0,661756	-0,223009	-1,75208	-0,0153925	-0,260639
6-Undecanone	184	0,606064	-0,331721	-1,55419	0,459035	-0,234835
4-Methyl-2-pentanone	9	0,089479	0,0120335	0,198592	2,25804	0,127204
Acetophenone	15	17,781956	114,996	-102,036	-294,296	-15,548
Cyclopentanone	20	2,442718	-1,01	0,972497	4,75921	0,23505
Cyclohexanone	7	4,896292	-114,459	74,9709	258,741	10,7028
Alkoholes						
Methanol	1055	8,1679	-0,738803	-0,18702	1,7158	0,0211516
Ethanol	864	6,449777	-0,999071	0,641222	3,43508	0,147307
1-Butanol	321	5,774754	-1,16559	1,34894	5,03817	0,259096
1-Propanol	367	7,573796	-1,01631	1,2982	4,67638	0,24933
1-Pentanol	132	2,7278	-0,466861	0,351244	2,80625	0,100135

Continued on next page

Table – continued from previous page

Name	points	AAD / %	A	B	C	D
1-Hexanol	241	2,724684	-1,04526	0,707355	4,1991	0,153966
1-Heptanol	293	4,420385	-1,06907	0,525975	4,04955	0,124984
1-Octanol	194	3,320251	-1,2159	2,05699	6,43443	0,409714
1-Nonanol	169	2,189287	-1,04962	0,63015	4,39253	0,14703
1-Decanol	268	4,040808	-1,17082	0,478214	4,29316	0,119215
1-Undecanol	92	1,654231	-0,641455	1,03077	4,11745	0,279751
1-Dodecanol	94	2,100506	-1,11533	0,773369	4,64931	0,197549
1-Tetradecanol	14	0,740907	5,7617	-4,99019	-12,1414	-0,711844
1-Hexadecanol	4	0	17,4463	-20,0295	-48,6921	-3,22504
1-Octadecanol	13	0,963521	-4,16826	5,46292	15,9721	0,952896
Acids						
Formic acid	50	0,98342	55,1187	-1,18101	-56,3495	-0,0611487
Butyric acid	27	3,865811	-0,708711	2,32735	6,55027	0,379278
Pentanoic acid	17	0,591232	-4,86967	1,79778	10,3561	0,279927
Nonanoic acid	8	0,13532	6,88067	-4,38557	-13,4013	-0,54712
Capric acid	10	0,232632	-0,0255297	-0,187351	1,59207	0,0421126
Lauric acid	7	5,66204	27,2105	-32,2018	-80,3934	-5,03832
Myristic acid	6	0,238707	2,52138	-3,61991	-6,35077	-0,541865
Caprylic acid	16	0,342266	-0,951886	0,270487	3,34892	0,0989842
Hexanoic acid	7	3,659805	-0,862848	0,864783	4,55919	0,138479
Acetic acid	309	27,415722	0,568026	1,56086	5,94881	0,162807
Propionic acid	116	25,892028	-0,340442	4,03593	10,59	0,519256
Palmitic acid	18	6,414539	109,079	-126,97	-322,464	-20,5303
Stearic acid	16	10,09478	42,5666	-49,1874	-124,218	-7,85118
cis-9-Octadecenoic acid	6	7,540171	19,5458	-44,8479	-86,3603	-8,04892

A.3 Full Legend of Fig.2.6



Analysis of the difference between experimental values of the thermal conductivity and values estimated from the Chapman-Enskog theory, $(\lambda^{exp} - \lambda_{CE}^{ref})$ as a function of reduced temperature T^* for 36 substances in dilute gas conditions ($|s^*| < 0.1$).

A.4 Entropy Scaling of Water

Entropy scaling is not limited to a certain equation of state model used for calculating the residual entropy. Water is a demanding substance for all equations of state based on a molecular model, such as PCP-SAFT. Therefore, we additionally apply

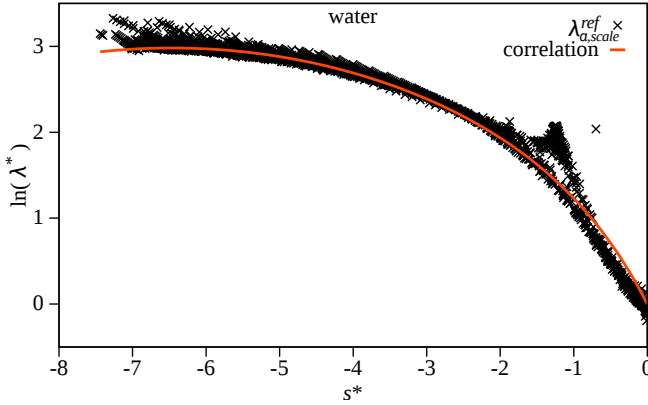


Figure A.1: Logarithmic reduced thermal conductivity $\lambda^* = \lambda/\lambda_{\alpha, scale}^{ref}$ of water. The reduced entropy s^* is calculated from the IAPWS model for given conditions of temperature and pressure. The symbols denote experimental data. The red line represents the correlation function Eq. (2.14) in the manuscript.

entropy scaling to water using the highly accurate Span-Wagner equation of state (IAPWS) [1] as implemented in CoolProp [2, 3].

Fig. A.1 gives the resulting entropy scaling diagram. It gets clear that water does not obey entropy scaling particularly well, using our proposed expression for the reference thermal conductivity. Deviations are pronounced for conditions around the critical point (at around $s^* = -1.2$). Also the low temperature and high pressure data (most negative values of s^*) does not show monovariate dependence on s^* for this choice of the reference thermal conductivity. Those deviations for very high pressures at low temperatures can also be seen in Fig. A.2. Lastly, we realize that the correlation function, Eq. (2.14), is not sufficiently flexible for water, as the diagram also shows. However, Fig. A.1 suggests that the general principle of entropy scaling is valid even for water, and with future refinements on the expression for the reference thermal conductivity, one can hope to further develop the approach.

We find it interesting to note that the thermal conductivity of water decreases for decreasing temperature in liquid phase, for temperatures above the density anomaly from water (at 277.15 K).

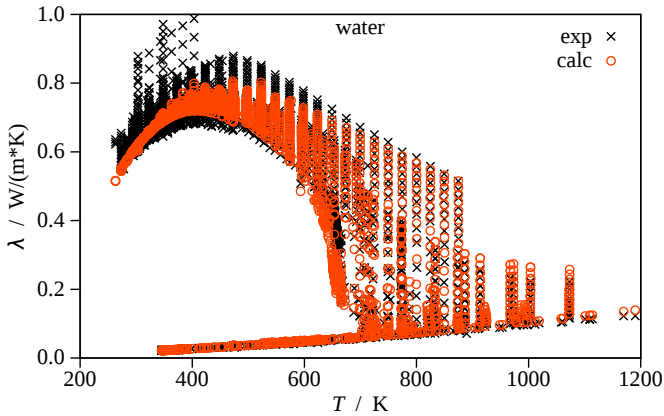


Figure A.2: Thermal conductivity of water versus temperature using $\lambda_{\alpha, scale}^{ref}$ and IAPWS. Black symbols denote experimental data, red circles the corresponding calculated values.

A.5 Entropy Scaling of Lennard-Jones Chains

We investigate entropy scaling of model fluids using the data for thermal conductivities of Lennard-Jones chains from molecular simulations presented by Galliero and Boned 2009 [4]. We find that the data convincingly follows the principle of entropy-scaling (Fig.A.3). We used PCP-SAFT to calculate the residual entropy for the given values of temperature and pressure. Figure A.3 shows results for the LJ-fluid ($m = 1$), for the LJ-dimer ($m = 2$), where the two LJ interaction sites are a distance of σ apart. Further, data of 4-mer and 8-mer chains are shown, where the LJ interaction sites of a chain are not constrained with angle- or torsional potentials [4, 5].

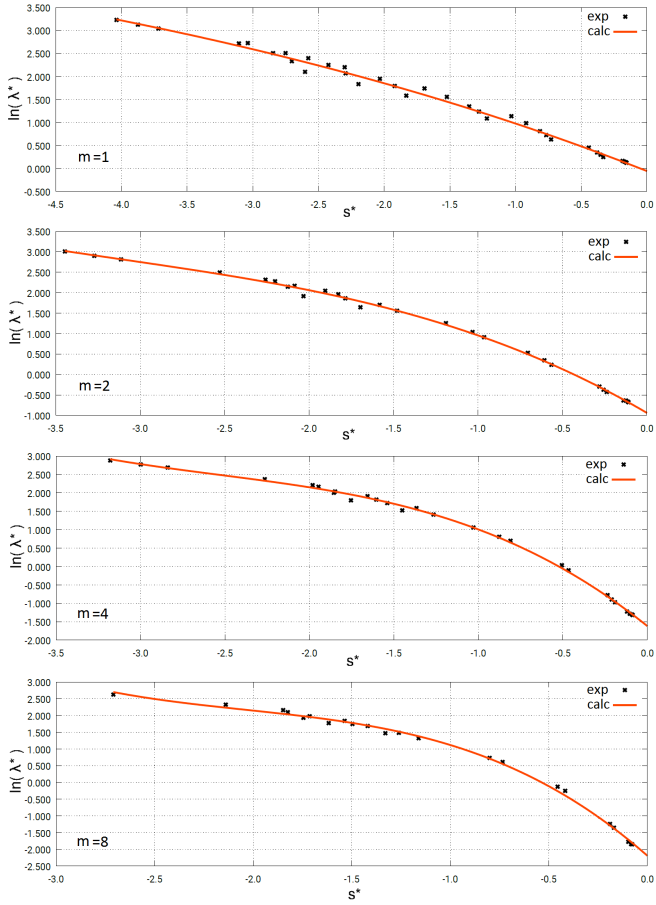


Figure A.3: Logarithmic reduced thermal conductivity λ^* of Lennard-Jones chains versus reduced residual entropy s^* . The symbols denote data from molecular simulations, reduced by λ_{CE}^{ref} , eq.(2.2).

Bibliography

- [1] W. Wagner, J. Cooper, A. Dittmann, J. Kijima, H.-J. Kretzschmar, A. Kruse, R. Mares, K. Oguchi, H. Sato, I. Stöcker, o. Sifner, Y. Takaishi, I. Tanishita, J. Trübenbach, and T. Willkommen, “The iapws industrial formulation 1997 for the thermodynamic properties of water and steam,” *Journal of Engineering for Gas Turbines and Power*, vol. 122, pp. 150–182, 2000.
- [2] I. H. Bell, J. Wronski, S. Quoilin, and V. Lemort, “Pure and pseudo-pure fluid thermophysical property evaluation and the open-source thermophysical property library coolprop,” *Industrial & Engineering Chemistry Research*, vol. 53, no. 6, pp. 2498–2508, 2014.
- [3] “Coolprop: Open-source thermophysical property library.”
- [4] G. Galliero and C. Boned, “Thermal conductivity of the lennard-jones chain fluid model,” *Phys. Rev. E*, vol. 80, p. 061202, 2009.
- [5] G. Galliero, “Equilibrium, interfacial and transport properties of n-alkanes: Towards the simplest coarse grained molecular model,” *Chem. Eng. Res. Des.*, vol. 92, no. 12, pp. 3031 – 3037, 2014. *Advances in Thermodynamics for Chemical Process and Product Design.*

B Supporting Information for Chapter 3: Self-Diffusion Coefficients from Entropy Scaling using the PCP-SAFT equation of state

This Supporting Information details (1) the pure component parameters of the PCP-SAFT model for all considered substances, including the origin of experimental data. Further, (2), we summarize the parameter rules described in section *Robustness* in the manuscript and clarify them using a diagram. Moreover, (3), the parameters *a-c* including the absolute average deviations for all considered substances are tabulated. Additionally, (4), the results and parameters of the enhanced model for substances with data at subcooled liquid conditions are given. Lastly, (5) we provide a similar diagram as Figure 3.1 in the manuscript for all approaches for the reference self-diffusion coefficient given in Table 3.1 in the manuscript.

B.1 PCP-SAFT Parameters

Pure substance PCP-SAFT parameters for all considered substances.

Name	Molar Mass g/mol	m -	σ \AA	ϵ/k K	κ^{AB} -	ϵ^{AB} K	DM Debye
simple gases							
neon	20.1797	0.6046322	3.47891954	40.8184424	0	0	0
argon	39.9480	0.9285	3.4784	122.2300	0	0	0
krypton	83.8000	0.96233642	3.65982007	167.135844	0	0	0
xenon	131.2900	0.91747631	4.06133891	237.839158	0	0	0
nitrogen	28.0134	1.24514088	3.29289628	89.0882561	0	0	0
carbondioxide	44.0095	2.54380536	2.5712611	153.006693	0	0	0
hydrogen	2.0160	1.0000	2.9280	37.0000	0	0	0
carbonmonoxide	28.0100	1.3097	3.2507	92.1500	0	0	0
oxygen	31.9988	1.15891096	3.16562139	112.903179	0	0	0
N-alkane							
methane	16.0425	1.00568694	3.69662664	149.597675	0	0	0
ethane	30.0690	1.61391445	3.51956732	190.871071	0	0	0
propane	44.0956	1.98977217	3.62465904	208.901242	0	0	0
butane	58.1222	2.3004177	3.72379587	224.665583	0	0	0
pentane	72.1488	2.70157783	3.75384978	230.866989	0	0	0
hexane	86.1754	3.08624271	3.77945124	235.782728	0	0	0
heptane	100.2020	3.45472812	3.80745646	239.65357	0	0	0
octane	114.2290	3.82709107	3.83154195	242.488182	0	0	0
nonane	128.2550	4.26110251	3.8237706	242.882928	0	0	0
decane	142.2820	4.64969323	3.83871523	244.309751	0	0	0
undecane	156.3080	5.01774748	3.85253692	245.993023	0	0	0
dodecane	170.3350	5.44151985	3.85128442	246.125452	0	0	0
tridecane	184.3610	5.8454503	3.85735664	246.622153	0	0	0

Continued on next page

Table – continued from previous page

Name	Molar Mass g/mol	m	σ	ϵ/k	κ^{AB}	ϵ^{AB}	DM Debye
		-	\AA	K	-	K	
tetradecane	198.3880	6.17017174	3.87319243	248.639375	0	0	0
pentadecane	212.4150	6.49636601	3.89133993	250.177445	0	0	0
hexadecane	226.4410	6.88869397	3.89365214	250.443346	0	0	0
heptadecane	240.4680	7.21575894	3.91085574	251.843595	0	0	0
octadecane	254.4940	7.60850462	3.91095954	251.759155	0	0	0
nonadecane	268.5210	7.95055198	3.92105763	252.501694	0	0	0
eicosane	282.5470	8.3260504	3.92466029	252.933847	0	0	0
heneicosane	296.5740	8.74949572	3.91924101	252.387747	0	0	0
tricosane	324.6270	9.38514776	3.941579	254.14393	0	0	0
tetracosane	338.6540	9.79587001	3.93844475	253.55057	0	0	0
octacosane	394.7600	11.4145377	3.93183152	252.364312	0	0	0
triacontane	422.8130	11.4887631	4.01422619	258.303052	0	0	0
dotriacontane	450.8660	12.1111774	4.0303379	258.464863	0	0	0
hexatriacontane	506.9730	13.0293997	4.09058437	261.299767	0	0	0
branches alkanes							
2-methylpentane	86.1754	2.9350835	3.84298603	235.636478	0	0	0
3-methylpentane	86.1754	2.85651534	3.86312065	241.996643	0	0	0
2,3-dimethylbutane	86.1754	2.70133084	3.93866088	245.270553	0	0	0
2,2-dimethylbutane	86.1754	2.6619263	3.97266866	240.257757	0	0	0
2,2,3-trimethylbutane	100.2020	2.73492683	4.09191592	258.786124	0	0	0
squalane	422.8130	9.73404698	4.25249259	263.766387	0	0	0
cycloalkane							
cyclopentane	70.1329	2.28814097	3.75012305	271.072817	0	0	0
methylcyclopentane	84.1595	2.62099475	3.81669188	264.395444	0	0	0
cyclohexane	84.1595	2.48702377	3.8574019	281.191912	0	0	0
methylcyclohexane	98.1861	2.64310095	4.00629184	283.411549	0	0	0

Continued on next page

Table – continued from previous page

Name	Molar Mass g/mol	m	σ	\dot{A}	ϵ/k	κ^{AB}	ϵ^{AB}	DM
		-	\dot{A}		K	-	K	Debye
cycloheptane	98.1861	2.68955735	3.93603496		296.55482	0	0	0
cyclooctane	112.2130	2.92363977	3.98308216		304.863579	0	0	0
cyclopropane	42.0797	1.80352769	3.51717602		236.344484	0	0	0
aromatics								
benzene	78.1118	2.46020689	3.64300499		287.817381	0	0	0
toluene	92.1384	2.75790579	3.73658296		289.363208	0	0	0.359748
1,3-Dimethylbenzen	106.1650	3.16544872	3.75653095		285.217128	0	0	0.29979
1,4-Dimethylbenzen	106.1650	3.12057619	3.7863385		286.677017	0	0	0
1,2-Dimethylbenzen	106.1650	3.10049409	3.76556936		293.081466	0	0	0.629559
1,3,5-triisopropylbenzene	204.3510	5.55146863	3.90484991		254.885656	0	0	0.234443578
1,2-Diphenylbenzen	230.3040	5.64759027	3.78293646		307.252552	0	0	0.10312776
1,3,5-Trimethylbenzene	120.1920	3.67095955	3.72844091		277.657581	0	0	0
ether								
dimethylether	46.0684	2.2341486	3.28358739		211.922895	0	0	1.3010886
diethylether	74.1216	2.98289106	3.5008022		219.351377	0	0	1.1511936
1,2-dimethoxyethane	90.1210	3.57109481	3.35635917		232.349939	0	0	1.70998417
esters								
methylacetate	74.0785	3.1405457	3.18916665		233.391128	0	0	1.678824
ethylacetate	88.1051	3.51820033	3.30171255		230.038559	0	0	1.7807526
butylacetate	116.1580	4.12455674	3.48092256		237.534688	0	0	1.8407106
hexylacetate	144.2110	4.77282517	3.59680122		243.116818	0	0	1.858698
octylacetate	172.2650	5.51430678	3.65814406		245.08285	0	0	1.8407106
decylacetate	200.3180	6.78167906	3.59649025		236.454987	0	0	1.9006686
ketones								
acetone	58.0791	2.70615582	3.27779526		234.424415	0	0	2.8809819
2-pentanone	86.1323	3.26849668	3.50754685		249.756751	0	0	2.7700596

Continued on next page

Table – continued from previous page

Name	Molar Mass g/mol	m	σ	\hat{A}	ϵ/k	κ^{AB}	ϵ^{AB}	D_M
		-	\hat{A}		K	-	K	Debye
2-hexanone	100.1590	3.59507111	3.58136314	254.401725	0	0	0	2.6801226
2-heptanone	114.1850	3.96870457	3.62333228	255.477037	0	0	0	2.6111709
2-octanone	128.2120	4.46695727	3.62220668	252.435333	0	0	0	2.4612759
alcohols								
methanol	32.0419	1.50732955	3.32484846	211.59747	0.03	0.03	2519.71165	1.6998093
ethanol	46.0684	2.37225708	3.19636159	203.824465	0.03	0.03	2514.06086	1.6908156
1-propanol	60.0950	3.46041511	3.07418332	217.37453	0.03	0.03	2044.52977	1.678824
2-propanol	60.0950	4.02493369	2.91798235	198.595301	0.03	0.03	1871.87883	1.6608366
1-butanol	74.1216	4.27683532	3.06588957	217.708168	0.03	0.03	1846.20289	1.6698303
1,3-propanediol	76.0944	2.52712784	3.42373216	247.561011	0.03	0.03	3834.69356	2.5512129
1,2-propanediol	76.0944	3.27969084	3.19308703	260.186521	0.03	0.03	2482.19331	3.627459
2-pentanol	88.1482	5.28389603	3.00756173	200.079314	0.03	0.03	1713.24289	1.6668324
3-pentanol	88.1482	4.79825411	3.09473894	203.965794	0.03	0.03	1806.00113	1.6398513
1-pentanol	88.1482	4.30501902	3.24211238	228.621444	0.03	0.03	1835.03147	1.69998618
1,4-butanediol	90.1210	4.14379766	3.08455457	199.008965	0.03	0.03	4078.17363	3.927249
1,3-butanediol	90.1210	3.57039081	3.30568004	276.969494	0.03	0.03	2674.47752	2.5212339
1-hexanol	102.1750	4.3974231	3.38971666	235.53091	0.03	0.03	1930.62315	1.648845
1-octanol	130.2280	5.72041573	3.35617499	228.851547	0.03	0.03	1869.84462	1.648845
1,2-Ethandiol	62.0678	2.61243968	3.15363551	310.113954	0.03	0.03	2711.65908	2.4103116
2-methylpropan-2-ol	74.1216	4.46605971	3.00938939	191.217897	0.03	0.03	1741.56707	1.6698303
1,2,3-Propantriol	92.0938	3.68222234	3.09407582	344.814982	0.03	0.03	2711.56809	2.6801226
acids								
aceticacid	60.0520	0.99068484	4.49483279	316.357479	0.03	0.03	2575.48216	1.738782
nonanoicacid	158.2380	5.00869983	3.67886844	257.916396	0.03	0.03	2817.56748	1.678824
stearicacid	284.4770	9.09147043	3.70444607	253.25527	0.03	0.03	2546.03369	1.6698303
substances containing nitrogen								

Continued on next page

Table – continued from previous page

Name	Molar Mass g/mol	m	σ	\dot{A}	ϵ/k	κ^{AB}	ϵ^{AB}	DM	
		-	\dot{A}	K	-	K	K	Debye	
acetoneitrile	41.0519	2.35779801	3.1543888	206.848301	0	0	0	3.927249	
trimethylamine	59.1103	2.44683921	3.56389602	221.445213	0	0	0	0.6115716	
nitromethane	61.0400	2.60076035	3.06668947	252.927733	0	0	0	3.447585	
pyridine	79.0999	2.63342054	3.47797032	302.724075	0	0	0	2.1914649	
triethylamine	101.1900	3.32577422	3.77670161	238.938727	0	0	0	0.659538	
methylamine	31.0571	1.619138	3.33697718	246.379674	0.03	1103.60877	1.3100823		
methanamid	45.0406	1.86243253	3.24201016	345.152627	0.03	1980.23207	3.717396		
aniline	93.1265	1.66559525	4.36223372	379.872027	0.03	2332.62439	1.528929		
ammonia	17.0305	1.32746048	3.02021831	237.610438	0.03	866.469835	1.468971		
nitrogenoxide	30.0061	5.78423487	1.64236476	65.1423557	0	0	0	0.1528929	
dinitrogenmonoxide	44.0128	2.15532647	2.75349807	167.829707	0	0	0	0.16698303	
methylformamide	59.0672	1.50358583	3.94475832	309.243496	0.03	2586.31354	3.837312		
others									
water #	18.0153	1.27084414	2.81979214	281.943549	0.0043539	952.657528	1.855		
tetrahydrofuran	72.1057	2.47517154	3.51186698	274.134389	0	0	0	1.6308576	
propylenecarbonate	102.0890	3.33855866	3.35063257	312.749636	0	0	0	4.976514	
ethylene	28.0532	1.56738048	3.42823448	178.754661	0	0	0	0	
cyclopentene	68.1170	2.27693354	3.6757828	269.015013	0	0	0	0.19995993	
substances containing sulfur									
hydrogensulfide	34.0809	1.64739561	3.05278793	225.91708	0	0	0	0.9683217	
carbondsulfide	76.1407	1.60418982	3.6812249	346.560404	0	0	0	0	
dimethylsulfoxide	78.1334	3.04708846	3.23338616	308.685765	0	0	0	3.957228	
thiophene	84.1396	2.40261067	3.53451111	298.995654	0	0	0	0.539622	
substances containing silicium									
decamethylcyclopentasiloxane	370.7700	6.46541856	4.29080146	215.159476	0	0	0	1.349055	
decamethyltetrasiloxane	310.6850	6.44092772	4.1972062	208.73109	0	0	0	1.2201453	

Continued on next page

Table – continued from previous page

Name	Molar Mass g/mol	m	σ Å	ϵ/k	κ^{AB}	ϵ^{AB}	D_M Debye
dodecamethylpentasiloxane	384.8390	7.238186	4.31727963	211.369267	0	0	0.9503343
hexamethyldisiloxane	162.3780	4.11570379	4.02422687	212.729679	0	0	0.659538
octamethylcyclotetrasiloxane	296.6160	5.88770183	4.08236175	211.56347	0	0	0.659538
octamethyltrisiloxane	236.5310	5.33191491	4.11812732	209.558534	0	0	1.079244
substances containing halogenes							
dichloromethane	84.9326	2.59491365	3.16108941	248.748202	0	0	1.6008786
tert-butylchloride	92.5673	2.20193387	4.00421765	268.034768	0	0	2.128509
fluorobenzene	96.1023	2.6539802	3.60716357	276.46325	0	0	1.59998523
1,2-dichloroethane	98.9592	2.60220014	3.4323684	283.188196	0	0	1.438992
chlorobenzene	112.5570	2.64666926	3.75831712	313.813999	0	0	1.6908156
chloroform	119.3780	2.60869651	3.41850581	264.55356	0	0	1.0102923
hexafluorobenzene	186.0550	3.77671386	3.3949167	221.783146	0	0	0.32999684
hydrogenchloride	36.4609	1.52244988	2.9855652	203.868393	0	0	1.079244
fluorine	37.9968	1.33800735	2.9042083	98.3499975	0	0	0
trimethylchlorosilane	108.6420	2.84635826	3.830241	235.94657	0	0	2.0805426
trifluoroaceticacid	114.0230	1.77617834	3.92289539	281.343264	0.03	1516.37215	2.2799809
bromobenzene	157.0080	2.6895595	3.79567177	329.79891	0	0	1.69998618
1,2-dibromoethane	187.8610	2.0794796	3.87308202	369.274195	0	0	1.0102923
iodobenzene	204.0080	2.70356591	3.88868589	354.098652	0	0	1.6998093
1,2-dibromotetrafluoroethane	259.8230	2.69564233	3.81375865	239.315236	0	0	0.0299979

water has one additional parameter, the quadrupole moment $Q=3.43534786736533$

B.1.1 Criteria for predefining parameters

In the main text to this publication we argue it is useful to independently determine some pure component parameters whenever there is severely limited experimental data available for the component at hand. We here describe the criteria that determine whether a certain pure component parameter (a to c of Eq. (3.3)) is considered an adjustable parameters or is otherwise defined through an approximate relation. We use criteria based on the reduced residual entropy as calculated from the PCP-SAFT model, $s^*(T, p)$, for experimental conditions of temperature T and pressure p . We define s_{min}^* and s_{max}^* as the minimal and the maximal value of residual entropy given by experimental data of a considered substance. Using these values, the total range of residual entropy that is covered by experimental data of a considered substance is defined as $\Delta s^* = s_{max}^* - s_{min}^*$. Additionally, we define the mid-value of Δs^* as $\bar{s}^* = 0.5(s_{min}^* + s_{max}^*)$. The parameter rules are explained in the manuscript,

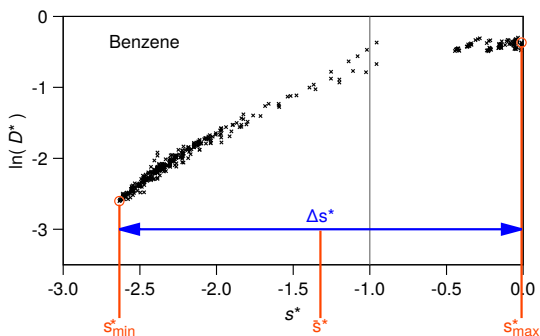


Figure B.1: Logarithmic reduced self-diffusion via residual entropy. Example to clarify the defined ranges in s^* .

so we will only summarize them here.

$$\begin{aligned}
 a &= 0.175 - 0.237m && \text{if } s_{max}^* < -1 \text{ or } \Delta s^* < 0.4 \cdot \bar{s}^* \\
 b &= 0.1m && \text{if } s_{min}^* \geq -1 \\
 c &= 0.0 && \text{if } \Delta s^* < 0.5 \text{ or } s_{min}^* > -2
 \end{aligned}$$

B.2 Correlation Parameters (a - c) and Absolute Average Deviations

Resulting parameters a - c for all considered substances, using $D^{ref} = D^{CE}$ and correlation Eq. (3.3). Further, the literature sources of the experimental data is detailed for every substance. If data at subcooled liquid conditions is available for a given substance, it was ignored here for parameter adjustment and average calculations. Further below we give a table for substances with subcooled data.

Name	points	AAD / %	a	b	c	Literature
simple gases						
neon	79	3.22571	0.221854	0.056496	0	[1, 2]
argon	214	7.86227	-0.022454	0.105345	0	[1-13]
krypton	208	8.02107	-0.015216	0.102235	0	[2, 14]
xenon	197	5.40039	-0.025539	0.083192	0.002669	[1, 2, 15, 16]
nitrogen	57	1.3888	-0.079515	0.124514*	0*	[2, 17, 18]
carbondioxide	305	6.93725	-0.471826	0.504955	0	[2, 11, 19, 20]
hydrogen	81	6.32052	-0.140289	0.134984	0	[2]
carbonmonoxide	60	2.37101	-0.046786	0.130567	0	[2, 17]
oxygen	32	2.0051	-0.030615	0.115892*	0*	[2, 17]
n-alkanes						
methane	624	6.33889	-0.036578	0.09581	0	[2, 11, 17, 21-30]
ethane	145	11.23427	-0.336378	0.132181	0	[2, 17, 22, 26, 31]
propane	70	7.34136	-0.717482	0.158285	0	[2, 26]
butane	25	7.81325	-0.851991	0.170628	0	[2]
pentane	73	9.61118	-0.865589	0.210235	0	[2, 32-35]
hexane	197	19.67001	-0.547402	0.327182	0	[2, 31, 32, 35-39]
heptane	134	16.41395	-0.756795	0.333134	0	[2, 32-35, 37, 40]
octane	115	8.21625	-0.918687	0.371196	0	[2, 31, 32, 35, 40, 41]
nonane	104	8.22832	-1.0276	0.398778	0	[2, 32, 35, 40, 41]
decane	113	6.21995	-1.15352	0.439113	0	[2, 35, 40-45]
undecane	36	6.05477	-1.01421*	0.518675	0	[2, 41]
dodecane	61	4.94493	-1.36914	0.47466	0	[2, 41, 46]
tridecane	56	2.34874	-1.51086	0.488631	0	[2, 41]
tetradecane	48	5.37381	-1.54706	0.516765	0	[2, 41, 46]
pentadecane	56	8.23799	-1.36464*	0.577484	0	[2, 41]
hexadecane	66	4.62016	-1.54932	0.596089	0	[2, 41]
heptadecane	27	4.58966	-1.53513*	0.621416	0	[2]

Continued on next page

Table – continued from previous page

Name	points	AAD / %	a	b	c	Literature
octadecane	22	5.36979	-1.71421	0.630106	0.000004	[2]
nonadecane	4	0.24395	-1.70928*	0.648603	0*	[2]
eicosane	17	4.3477	-1.79827*	0.599675	0.021516	[2]
heneicosane	6	1.96868	-1.89863*	0.625782	0*	[2]
tricosane	4	1.05637	-2.04928*	0.623165	0*	[2]
tetracosane	18	9.12718	-2.14662*	0.439844	0.10818	[2]
octacosane	6	5.55766	-2.53025*	0.635008	0*	[2]
triacontane	33	3.94974	-2.29894	0.71283	0	[2]
dotriacontane	17	13.62016	-2.69535*	0.61098	0*	[2]
hexatriacontane	5	11.88946	-2.91297*	0.558964	0*	[2]
branches alkanes						
2-methylpentane	11	5.48339	-0.939309	0.242462	0	[2]
3-methylpentane	16	6.73866	-1.00518	0.2319	0	[2, 47]
2,3-dimethylbutane	33	7.96452	-0.910161	0.240922	0.007822	[2]
2,2-dimethylbutane	56	8.73179	-1.12644	0.110321	0.062379	[2, 47]
2,2,3-trimethylbutane	21	3.63862	-1.4852	0	0.098556	[2]
squalane	4	3.37134	-2.13197*	0.862028	0.01357	[2]
cycloalkane						
cyclopentane	29	4.81718	-0.568273	0.30396	0	[2]
methylcyclopentane	4	2.55453	-0.446176*	0.372999	0*	[2]
cyclohexane	234	6.94828	-0.473953	0.447734	0	[2, 35, 41, 46, 48–50]
methylcyclohexane	22	13.63526	-0.390612	0.356212	0	[2]
cycloheptane	14	9.80803	-0.462425*	0.462149	0	[2]
cyclooctane	17	6.56597	-0.517903*	0.500629	0*	[2]
cyclopropane	3	0.00002	-0.806019	0.034239	0.030604	[2]
aromatics						
benzene	484	4.38855	-0.428269	0.340303	0	[2, 35, 36, 48, 49, 51–56]

Continued on next page

Table – continued from previous page

Name	points	AAD / %	a	b	c	Literature
toluene #	170	13.75738	-0.899845	0	0.075585	[2, 36]
1,3-Dimethylbenzen	5	4.10389	-0.575211*	0	0.096895	[2]
1,4-Dimethylbenzen	5	5.7079	-0.564577*	0	0.08369	[2]
1,2-Dimethylbenzen	6	4.83319	-0.559817*	0	0.10963	[2]
1,3,5-trisopropylbenzene	10	7.67369	-1.1407*	0.678947	0*	[2]
1,2-Diphenylbenzen #	34	8.81846	-1.16348*	0	0.345011	[2]
1,3,5-Trimethylbenzene	15	2.07777	-0.695017*	0.356664	0.002324	[57]
ether						
dimethylether	40	6.67935	-0.590694	0.191117	0	[2]
diethylether	6	2.24814	-0.667945	0.133717	0.039341	[2]
1,2-dimethoxyethane	11	9.59809	-0.944915	0.320998	0	[2]
esters						
methylacetate	4	3.54001	-0.569309*	0.414841	0*	[2]
ethylacetate	5	2.36024	-0.658813*	0.455688	0*	[2]
butylacetate	8	8.03415	-0.80252*	0.496374	0*	[2]
hexylacetate	9	5.79824	-0.95616*	0.419028	0.056691	[2]
octylacetate	8	1.83714	-1.13189*	0.608988	0	[2]
decylacetate	9	2.44908	-1.43226*	0.532508	0.068141	[2]
ketones						
acetone	48	4.55735	-0.965214	0	0.070927	[2]
2-pentanone	7	9.35567	-0.599634*	0.327866	0*	[2]
2-hexanone	8	2.89959	-0.677032*	0.076925	0.122646	[2]
2-heptanone	8	4.0099	-0.765583*	0.008247	0.16411	[2]
2-octanone	8	5.47309	-0.883669*	0.306242	0.068987	[2]
alcohols						
methanol #	140	9.16137	-0.243496	0.063881	0.005532	[2, 53, 58-63]
ethanol	217	7.21353	-0.775611	0	0.049007	[2, 41, 53, 60, 62-64]

Continued on next page

Table – continued from previous page

Name	points	AAD / %	a	b	c	Literature
1-propanol	147	5.14875	-0.963904	0.263424	0.022822	[2, 41, 64, 65]
2-propanol	68	4.34816	-1.06308	0.384243	0.033524	[2]
1-butanol	27	6.84122	-0.83861*	0.501015	0	[2, 41, 66, 67]
1,3-propanediol	4	9.27352	-0.423929*	0.313828	0*	[68]
1,2-propanediol	8	31.18197	-0.602287*	0.411092	0*	[68, 69]
2-pentanol	39	6.23039	-1.32381	0.277296	0.159301	[2]
3-pentanol	45	16.82831	-0.675806	0.357618	0.152856	[2]
1-pentanol	177	5.48718	-1.17636	0.369508	0.030086	[2, 70]
1,4-butanediol	4	8.71776	-0.80708*	0.56869	0*	[68]
1,3-butanediol	9	6.68043	-0.671183*	0	0.091508	[2]
1-hexanol	11	5.6718	-0.867189*	0.4149	0.033776	[2, 67]
1-octanol	19	19.31287	-1.18074*	0.62459	0.006478	[2]
1,2-Ethanediol	6	15.67712	-0.672275*	0.720735	0*	[58]
2-methylpropan-2-ol	18	6.47892	-0.883456*	0.41696	0.148739	[2]
1,2,3-Propantriol #	60	17.51393	-0.697687*	0	0.110202	[2]
acids						
aceticacid	13	6.77951	-0.059792*	0	0.008492	[2]
nonanoicacid	6	4.02945	-1.01206*	0.379112	0*	[2]
stearicacid	18	11.38945	-1.97968*	0.622352	0*	[2]
substances containing nitrogen						
acetonitrile	53	10.98829	-0.383798*	0.35019	0*	[2]
trimethylamine	49	8.63583	-0.803661	0.242877	0	[2]
nitromethane	15	7.06299	-0.44138*	0.31524	0*	[2, 71]
pyridine	33	9.56692	-0.405766	0.259048	0.018519	[2, 72]
triethylamine	8	6.92184	-0.613208*	0.436488	0*	[2]
methylamine	45	7.13949	-0.537177	0.057107	0.007773	[2]
methanamid	4	10.97567	-0.266397*	0.160719	0*	[2]

Continued on next page

Table – continued from previous page

Name	points	AAD / %	a	b	c	Literature
aniline	12	19.67536	-0.219746*	0	0.023121	[2]
ammonia	113	6.15429	-0.315485	0	0.015077	[2, 73, 74]
nitrogenoxide	27	2.59214	-0.703519	0.578423*	0*	[17]
dinitrogenmonoxide	24	2.39435	-0.289499	0.215533*	0*	[17]
methylformamide #	23	12.88391	-0.18135*	0	0.018167	[2, 75]
others						
water # +	687	12.93466	-0.258783*	0.021673*	0.000007*	[2, 76–78]
tetrahydrofuran	14	9.06722	-1.30295	0	0.040764	[2]
propylenecarbonate #	6	3.16298	-0.616238*	0.390562	0*	[2, 79]
ethylene	296	6.913	-0.18411	0.159554	0	[2, 17]
cyclopentene	4	7.02714	-0.947096	0.180243	0	[2]
substances containing sulfur						
hydrogensulfide	8	5.63206	-0.319891	0.149439	0	[2]
carbondsulfide	19	4.95109	-0.205193*	0.131513	0	[2]
dimethylsulfoxide	24	7.86498	-0.54716*	0.363001	0*	[2, 79]
thiophene	18	9.35884	-0.29069	0.3198	0	[2]
substances containing silicium						
decamethylcyclopentasiloxane	7	6.25431	-1.3573*	1.142582	0*	[2]
decamethyltetrasiloxane	11	9.91619	-1.3515*	0.790291	0	[80]
dodecamethylpentasiloxane	10	10.63144	-1.54045*	0.777861	0	[80]
hexamethyldisiloxane	11	6.86424	-0.800422*	0.58906	0	[80]
octamethylcyclotetrasiloxane	62	7.56125	-1.90923	0.794534	0	[2]
octamethyltrisiloxane	10	8.17522	-1.08866*	0.707551	0	[80]
substances containing halogenes						
dichloromethane	90	7.03603	-0.718947	0.238182	0	[2, 72]
tert-butylchloride	61	20.72755	0.281189	0.506539	0	[2, 81]
fluorobenzene	19	2.22101	-0.663053	0.271987	0	[2]

Continued on next page

Table – continued from previous page

Name	points	AAD / %	a	b	c	Literature
1,2-dichloroethane	32	9.03629	-0.403982	0.347764	0	[2]
chlorobenzene	22	23.47613	-0.612624	0.000001	0.074444	[2]
chloroform	110	8.0461	-0.839754	0.227165	0	[2]
hexafluorobenzene	90	6.31652	-0.609186	0.622003	0	[2]
hydrogenchloride	37	13.68542	-0.036395	0.140215	0	[2]
fluorine	6	4.67196	-0.373237	0	0.027204	[2]
trimethylchlorosilane	16	16.74724	-0.499587*	0.418979	0	[2]
trifluoroaceticacid	5	5.44787	-0.245954*	0.152816	0	[2]
bromobenzene	16	4.33135	-0.671511	0.232141	0	[2]
1,2-dibromoethane	20	3.41704	-0.317837*	0.251511	0	[2]
iodobenzene	18	1.69873	-0.743727	0.142231	0.021033	[2]
1,2-dibromotetrafluoroethane	52	4.62508	-1.50821	0.05055	0.07271	[2]
substances with data in gas phase						
hydrogen	81	6.32052	-0.140289	0.134984	0	[2]
neon	79	3.22571	0.221854	0.056496	0	[1, 2]
argon	214	7.86227	-0.022454	0.105345	0	[1–13]
krypton	208	8.02107	-0.015216	0.102235	0	[2, 14]
xenon	197	5.40039	-0.025539	0.083192	0.002669	[1, 2, 15, 16]
nitrogen	57	1.3888	-0.079515	0.124514*	0*	[2, 17, 18]
oxygen	32	2.0051	-0.030615	0.115892*	0*	[2, 17]
carbonmonoxide	60	2.37101	-0.046786	0.130567	0	[2, 17]
carbondioxide	305	6.93725	-0.471826	0.504955	0	[2, 11, 19, 20]
nitrogenoxide	27	2.59214	-0.703519	0.578423*	0*	[17]
ammonia	113	6.15429	-0.315485	0	0.015077	[2, 73, 74]
dinitrogenmonoxide	24	2.39435	-0.289499	0.215533*	0*	[17]
methane	624	6.33889	-0.036578	0.09581	0	[2, 11, 17, 21–30]
ethane	145	11.23427	-0.336378	0.132181	0	[2, 17, 22, 26, 31]

Continued on next page

Table – continued from previous page

Name	points	AAD / %	a	b	c	Literature
cyclohexane	234	6.94828	-0.473953	0.447734	0	[2, 35, 41, 46, 48–50]
ethylene	296	6.913	-0.18411	0.159554	0	[2, 17]
benzene	484	4.38855	-0.428269	0.340303	0	[2, 35, 36, 48, 49, 51–56]
toluene #	170	13.75738	-0.899845	0	0.075585	[2, 36]
methanol #	140	9.16137	-0.243496	0.063881	0.005532	[2, 53, 58–63]
water # +	687	12.93466	-0.258783	0.021673	0.000007	[2, 76–78]

substances with data at subcooled liquid conditions, but here evaluated with correlation

(3) and without these subcooled data;

+ water evaluated with correlation 5, but without data at subcooled liquid conditions;

* Parameter (A, B or C) not adjusted, but taken from parameter rules.

B.2.1 Substances with Data at subcooled liquid conditions

Resulting parameters a - d for all substances with data at subcooled liquid conditions available, using $D^{ref} = D^{CE}$ and correlation Eq. (3.5).

Name	points	AAD / %	a	b	c	d
substances with data in subcooled liquid phase						
toluene	199	12.76085	-0.631865	0.273994	0.000003	3.20588
1,2-Diphenylbenzen	57	8.64850	-1.02116	0.758291	0.00004	4.30653
propylenecarbonate	39	15.92851	-0.616238*	0.337466	0.00014	3.03404
methylformamide	37	27.59869	-0.18135*	0.000001	0.037107	0.830585
methanol	168	13.67245	-0.311107	0.071712	0.00004	1.85105
1,2,3-Propantriol	99	10.97084	-1.50843	0	0.107731	1.01724
water	804	17.58077	-0.258783	0.021673	0.000007	2.70092

* Parameter A not adjusted, but taken from parameter rules.

B.3 Diagram for reference self-diffusion coefficients

Diagram for all references given in Table 3.1 in the manuscript, which were not shown in Figure 3.1.

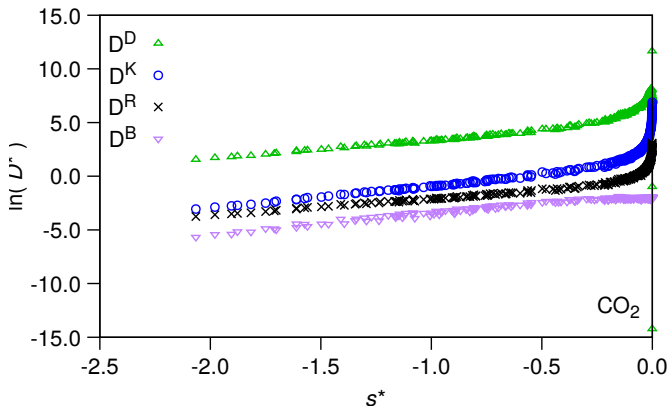


Figure B.2: Logarithmic reduced self diffusion $\ln(D^{exp}/D^{ref})$ over reduced residual entropy s^* with $D^{ref} \in \{D^R, D^K, D^D, D^B\}$ for CO_2 .

Bibliography

- [1] J. Kestin, K. Knierim, E. A. Mason, B. Najafi, S. T. Ro, and M. Waldman, "Equilibrium and transport properties of the noble gases and their mixtures at low density," *Journal of Physical and Chemical Reference Data*, vol. 13, no. 1, pp. 229–303, 1984.
- [2] O. Suárez-Iglesias, I. Medina, M. de los Ángeles Sanz, C. Pizarro, and J. L. Bueno, "Self-diffusion in molecular fluids and noble gases: Available data," *Journal of Chemical & Engineering Data*, vol. 60, no. 10, pp. 2757–2817, 2015.
- [3] A. Saarnak and C. Hansen, "Löslighetsparametrar karaktärisering av färgbindemedel och polymerer," *Research Rep.*, 1982.
- [4] D. O'Reilly and E. Peterson, "Self-diffusion of liquid hydrogen and deuterium," *J.Chem.Phys.*, vol. 66, pp. 934 – 937, 1977.
- [5] E. Winn, "The temperature dependence of the self-diffusion coefficients of argon, neon, nitrogen, oxygen, carbon dioxide, and methane," *Phys.Rev.*, vol. 80, pp. 1024 – 1027, 1950.
- [6] K. Al'zhanov and K. Musenov, "Bayandamalary kazak," *Resp. Ul'tyik Gylym Akadem*, pp. 32–38, 2003.
- [7] M. D. Paz, B. Turi, and M. Klein, "New self diffusion measurements in argon gas," *Physica*, vol. 36, no. 1, pp. 127–135, 1967.
- [8] J. Naghizadeh and S. A. Rice, "Kinetic theory of dense fluids. x. measurement and interpretation of self-diffusion in liquid Ar, Kr, Xe, and CH₄," *The Journal of Chemical Physics*, vol. 36, no. 10, pp. 2710–2720, 1962.
- [9] S. Raman, R. Paul, and W. W. Watson, "Thermal diffusion factor of argon from column operation," *The Journal of Chemical Physics*, vol. 46, no. 10, pp. 3916–3920, 1967.
- [10] P. Zandveld, C. Andriesse, J. Bregman, A. Hasman, and J. V. Loeff, "Temperature dependence of the atomic self-motion in liquid argon," *Physica*, vol. 50, no. 4, pp. 511–523, 1970.
- [11] E. B. Winn, "The temperature dependence of the self-diffusion coefficients of argon, neon, nitrogen, oxygen, carbon dioxide, and methane," *Physical Review*, vol. 80, no. 6, pp. 1024–1027, 1950.

- [12] F. Hutchinson, "Self-diffusion in argon," *The Journal of Chemical Physics*, vol. 17, no. 11, pp. 1081–1086, 1949.
- [13] G. Cini-Castagnoli and F. P. Ricci, "Self-diffusion in liquid argon," *The Journal of Chemical Physics*, vol. 32, no. 1, pp. 19–20, 1960.
- [14] M. Bohdanecky, "On the structure and properties of vinyl polymers and their models. xiii. viscometrically determined polyvinyl chloride-solvent interaction parameters," *Collect. Czech. Chem. Commun.*, vol. 34, pp. 2065 – 2073, 1969.
- [15] R. E. Benenson, K. Rimawi, M. Chaitin, S. Goldenberg, and D. Kaplan, "Self-diffusion experiment using a neutron generator," *American Journal of Physics*, vol. 44, no. 11, pp. 1089–1093, 1976.
- [16] D. Hesse, "Selbstdiffusion von gasen durch kapillaren," *Zeitschrift für Physikalische Chemie*, vol. 81, no. 1-4, pp. 113–134, 1972.
- [17] A. Boushehri, J. Bzowski, J. Kestin, and E. A. Mason, "Equilibrium and transport properties of eleven polyatomic gases at low density," *Journal of Physical and Chemical Reference Data*, vol. 16, no. 3, pp. 445–466, 1987.
- [18] H. Vugts, A. Boerboom, and J. Los, "Diffusion coefficients of isotopic mixtures of CO and N₂," *Physica*, vol. 50, no. 4, pp. 593–605, 1970.
- [19] P. Etesse, J. A. Zega, and R. Kobayashi, "High pressure nuclear magnetic resonance measurement of spin-lattice relaxation and self-diffusion in carbon dioxide," *The Journal of Chemical Physics*, vol. 97, no. 3, pp. 2022–2029, 1992.
- [20] T. Groß, J. Buchhauser, and H.-D. Lüdemann, "Self-diffusion in fluid carbon dioxide at high pressures," *The Journal of Chemical Physics*, vol. 109, no. 11, pp. 4518–4522, 1998.
- [21] T. E. Mistler, G. R. Correll, and J. O. Mingle, "Gaseous diffusion in the transition pressure range," *AIChE Journal*, vol. 16, no. 1, pp. 32–37, 1970.
- [22] C. R. Mueller and R. W. Cahill, "Mass spectrometric measurement of diffusion coefficients," *The Journal of Chemical Physics*, vol. 40, no. 3, pp. 651–654, 1964.
- [23] T. Shinji and I. Hiroji, "Evaluation and correlation of diffusion coefficient data : the most probable values of the self-diffusion coefficients of gaseous methane," *The Review of Physical Chemistry of Japan*, vol. 46, no. 2, pp. 88–94, 1976.

- [24] H. Vugts, A. Boerboom, and J. Los, "Diffusion coefficients of isotopic methane mixtures and of methane-rare-gas mixtures," *Physica*, vol. 51, no. 2, pp. 311–318, 1971.
- [25] S. Weissman and G. A. DuBro, "Diffusion coefficients for $\text{CO}_2\text{-CH}_4$," *The Journal of Chemical Physics*, vol. 54, no. 5, pp. 1881–1883, 1971.
- [26] A. Greiner-Schmid, S. Wappmann, M. Has, and H.-D. Lüdemann, "Self-diffusion in the compressed fluid lower alkanes: Methane, ethane, and propane," *The Journal of Chemical Physics*, vol. 94, no. 8, pp. 5643–5649, 1991.
- [27] C. R. Mueller and R. W. Cahill, "Mass spectrometric measurement of diffusion coefficients," *The Journal of Chemical Physics*, vol. 40, no. 3, pp. 651–654, 1964.
- [28] K. Harris, "The density dependence of the self-diffusion coefficient of methane at -50° , 25° and 50°C ," *Physica A: Statistical Mechanics and its Applications*, vol. 94, no. 3-4, pp. 448–464, 1978.
- [29] K. Harris and N. Trappeniers, "The density dependence of the self-diffusion coefficient of liquid methane," *Physica A: Statistical Mechanics and its Applications*, vol. 104, no. 1-2, pp. 262–280, 1980.
- [30] H. Vugts, A. Boerboom, and J. Los, "Diffusion coefficients of isotopic methane mixtures and of methane-rare-gas mixtures," *Physica*, vol. 51, no. 2, pp. 311–318, 1971.
- [31] M. Helbæk, B. Hafskjold, D. K. Dysthe, and G. H. Sørland, "Self-diffusion coefficients of methane or ethane mixtures with hydrocarbons at high pressure by NMR," *Journal of Chemical & Engineering Data*, vol. 41, no. 3, pp. 598–603, 1996.
- [32] G. Panchenkov and V. Erchenkov, "Temperature variation of the coordination number and diffusion coefficient in a liquid," *Russ.J.Phys.Chem.*, vol. 36, pp. 455 – 457, 1962.
- [33] M. Iwahashi, Y. Yamaguchi, Y. Ogura, and M. Suzuki, "Dynamical structures of normal alkanes, alcohols, and fatty acids in the liquid state as determined by viscosity, self-diffusion coefficient, infrared spectra, and cnmr spin-lattice relaxation time measurements," *Bull.Chem.Soc.Japan*, vol. 63, pp. 2154 – 2158, 1990.
- [34] D. Douglass and D. McCall, "Diffusion in paraffin hydrocarbons," *J.Phys.Chem.*, vol. 62, pp. 1102 – 1107, 1958.
- [35] D. W. McCall, D. C. Douglass, and E. W. Anderson, "Diffusion in liquids," *The Journal of Chemical Physics*, vol. 31, no. 6, pp. 1555–1557, 1959.

- [36] M. Awan and J. Dymond, "Transport properties of nonelectrolyte liquid mixtures. xi. mutual diffusion coefficients for toluene + n-hexane and toluene + acetonitrile at temperatures from 273 to 348 k and at pressures up to 25 mpa," *Int.J.Thermophys.*, vol. 22, pp. 679 – 700, 2001.
- [37] C. D'Agostino, M. Mantle, L. Gladden, and G. Moggridge, "Prediction of binary diffusion coefficients in non-ideal mixtures from nmr data: Hexane-nitrobenzene near its consolute point," *Chem.Eng.Sci.*, vol. 66, pp. 3898 – 3906, 2011.
- [38] D. McCall, D. Douglass, and E. Anderson, "Self-diffusion in liquids: Paraffin hydrocarbons," *Phys.Fluids*, vol. 2, pp. 87 – 91, 1959.
- [39] K. R. Harris, "Temperature and density dependence of the self-diffusion coefficient of n-hexane from 223 to 333 k and up to 400 MPa," *Journal of the Chemical Society, Faraday Transactions 1: Physical Chemistry in Condensed Phases*, vol. 78, no. 7, p. 2265, 1982.
- [40] G. Panchenkov, N. Borisenko, and V. Erchenkov, "Self-diffusion of n-paraffins in a wide temperature range," *Zh. Fiz. Khim*, vol. 43, pp. 2369–2370, 1969.
- [41] P. Tofts, D. Lloyd, C. Clark, G. Barker, G. Parker, P. McConville, C. Baldock, and J. Pope, "Test liquids for quantitative mri measurements of self-diffusion coefficient in vivo," *Magnetic Resonance in Medicine*, vol. 43, no. 3, pp. 368–374, 2000.
- [42] G. Panchenkov and V. Erchenkov, "Temperature variation of the coordination number and diffusion coefficient in a liquid," *Russ. J. Phys. Chem.(Engl. Transl.)*, vol. 36, p. 455, 1962.
- [43] M. Iwahashi, Y. Yamaguchi, Y. Ogura, and M. Suzuki, "Dynamical structures of normal alkanes, alcohols, and fatty acids in the liquid state as determined by viscosity, self-diffusion coefficient, infrared spectra, and ^{13}C nmr spin-lattice relaxation time measurements," *Bulletin of the Chemical Society of Japan*, vol. 63, no. 8, pp. 2154–2158, 1990.
- [44] D. C. Douglass and D. W. McCall, "Diffusion in paraffin hydrocarbons," *The Journal of Physical Chemistry*, vol. 62, no. 9, pp. 1102–1107, 1958.
- [45] H. Walderhaug and K. D. Knudsen, "Aqueous mixtures of a trisiloxane surfactant and oil studied by SANS and NMR self-diffusion: Effect of temperature and oil concentration," *Journal of Solution Chemistry*, vol. 41, no. 2, pp. 367–379, 2012.
- [46] M. Holz, S. R. Heil, and A. Sacco, "Temperature-dependent self-diffusion coefficients of water and six selected molecular liquids for calibration in

- accurate 1h NMR PFG measurements,” *Physical Chemistry Chemical Physics*, vol. 2, no. 20, pp. 4740–4742, 2000.
- [47] D. W. McCall, D. C. Douglass, and E. W. Anderson, “Self-diffusion in liquids: Paraffin hydrocarbons,” *Physics of Fluids*, vol. 2, no. 1, p. 87, 1959.
- [48] R. Freer and J. N. Sherwood, “Diffusion in organic liquids. part 1. - appraisal of a gel sectioning technique and its application to self-diffusion in benzene and cyclohexane,” *Journal of the Chemical Society, Faraday Transactions 1: Physical Chemistry in Condensed Phases*, vol. 76, no. 0, p. 1021, 1980.
- [49] R. Freer and J. N. Sherwood, “Diffusion in organic liquids. part 2. - isotope-mass effects in self-diffusion in benzene and cyclohexane,” *Journal of the Chemical Society, Faraday Transactions 1: Physical Chemistry in Condensed Phases*, vol. 76, no. 0, p. 1030, 1980.
- [50] M. McCool and L. Woolf, “Self-diffusion measurements under pressure with a diaphragm cell. theory of the method and experimental results for cyclohexane,” *High Temp-High Press*, vol. 4, pp. 85–95, 1972.
- [51] L. M. d. J. B. M. M. J.B., “Vapor-liquid equilibria for the binary systems isobutanol with m-xylene, o-xylene and p-xylene at 101.3 kpa,” *J.Chem.Eng.Data*, vol. 44, pp. 869 – 872, 1999.
- [52] H. Hiroyuki, O. Jiro, and J. Wasaburo, “Self-diffusion of benzene and diffusions of sulfur and iodine in benzene under pressure,” *The Review of Physical Chemistry of Japan*, vol. 28, pp. 52–60, 1958.
- [53] P. A. Johnson and A. L. Babb, “Self-diffusion in liquids. 1. concentration dependence in ideal and non-ideal binary solutions,” *The Journal of Physical Chemistry*, vol. 60, no. 1, pp. 14–19, 1956.
- [54] H. J. Parkhurst and J. Jonas, “Dense liquids. i. the effect of density and temperature on self-diffusion of tetramethylsilane and benzene-d₆,” *The Journal of Chemical Physics*, vol. 63, no. 6, pp. 2698–2704, 1975.
- [55] M. A. McCool, A. F. Collings, and L. A. Woolf, “Pressure and temperature dependence of the self-diffusion of benzene,” *Journal of the Chemical Society, Faraday Transactions 1: Physical Chemistry in Condensed Phases*, vol. 68, no. 0, p. 1489, 1972.
- [56] A. F. Collings and L. A. Woolf, “Self-diffusion in benzene under pressure,” *Journal of the Chemical Society, Faraday Transactions 1: Physical Chemistry in Condensed Phases*, vol. 71, no. 0, p. 2296, 1975.

- [57] A. J. Easteal and L. A. Woolf, "Freezing pressures, p , v , t , and self-diffusion data at 298 and 313 k and pressures up to 300 MPa for 1, 3, 5-trimethylbenzene," *International Journal of Thermophysics*, vol. 8, no. 1, pp. 71–79, 1987.
- [58] G. H. Vogel, *Transporteigenschaften reiner Flüssigkeiten und binärer Mischungen*. PhD thesis, 1982.
- [59] X. Chen, R. Hu, H. Feng, L. Chen, and H.-D. Lüdemann, "Intradiffusion, density, and viscosity studies in binary liquid systems of acetylacetone + alkanols at 303.15 k," *Journal of Chemical & Engineering Data*, vol. 57, no. 9, pp. 2401–2408, 2012.
- [60] G. Guevara-Carrion, C. Nieto-Draghi, J. Vrabec, and H. Hasse, "Prediction of transport properties by molecular simulation: Methanol and ethanol and their mixture," *The Journal of Physical Chemistry B*, vol. 112, no. 51, pp. 16664–16674, 2008.
- [61] H. Hiroyuki, I. Yasushi, O. Jiro, and J. Wasaburo, "Self-diffusion of methanol under pressure," *The Review of Physical Chemistry of Japan*, vol. 28, no. 2, pp. 61–63, 1958.
- [62] N. Karger, T. Vardag, and H.-D. Lüdemann, "Temperature dependence of self-diffusion in compressed monohydric alcohols," *The Journal of Chemical Physics*, vol. 93, no. 5, pp. 3437–3444, 1990.
- [63] R. L. Hurlle, A. J. Easteal, and L. A. Woolf, "Self-diffusion in monohydric alcohols under pressure. methanol, methan(2h)ol and ethanol," *Journal of the Chemical Society, Faraday Transactions 1: Physical Chemistry in Condensed Phases*, vol. 81, no. 3, p. 769, 1985.
- [64] S. Meckl and M. Zeidler, "Self-diffusion measurements of ethanol and propanol," *Molecular Physics*, vol. 63, no. 1, pp. 85–95, 1988.
- [65] X. Chen, R. Hu, H. Feng, L. Chen, and H.-D. Lüdemann, "Intradiffusion, density, and viscosity studies in binary liquid systems of acetylacetone + alkanols at 303.15 k," *Journal of Chemical & Engineering Data*, vol. 57, no. 9, pp. 2401–2408, 2012.
- [66] X. Chen, R. Hu, H. Feng, L. Chen, and H.-D. Lüdemann, "Intradiffusion, density, and viscosity studies in binary liquid systems of acetylacetone + alkanols at 303.15 k," *Journal of Chemical & Engineering Data*, vol. 57, no. 9, pp. 2401–2408, 2012.
- [67] K. P. Das, A. Ceglie, and B. Lindman, "Microstructure of formamide microemulsions from NMR self-diffusion measurements," *The Journal of Physical Chemistry*, vol. 91, no. 11, pp. 2938–2946, 1987.

- [68] M. N. Rodnikova, Z. S. Idiyatullin, and I. A. Solonina, "Mobility of molecules of liquid diols in the temperature range of 303-318 k," *Russian Journal of Physical Chemistry A*, vol. 88, no. 8, pp. 1442-1444, 2014.
- [69] M. Mitchell and H. J. V. Tyrrell, "Diffusion of benzene, phenol and resorcinol in propane-1, 2-diol, and the validity of the stokes-einstein equation," *Journal of the Chemical Society, Faraday Transactions 2*, vol. 68, p. 385, 1972.
- [70] N. Karger, S. Wappmann, N. Shaker-Gaafar, and H.-D. Lüdemann, "The p, t - dependence of self diffusion in liquid 1-, 2- and 3-pentanol," *Journal of Molecular Liquids*, vol. 64, no. 3, pp. 211-219, 1995.
- [71] W. S. Price, H. Ide, and Y. Arata, "Translational and rotational motion of isolated water molecules in nitromethane studied using ^{17}O NMR," *The Journal of Chemical Physics*, vol. 113, no. 9, pp. 3686-3689, 2000.
- [72] D. E. O'Reilly, E. M. Peterson, and E. L. Yasaitis, "Self-diffusion coefficients and rotational correlation times in polar liquids. IV. dichloromethane and pyridine," *The Journal of Chemical Physics*, vol. 57, no. 2, pp. 890-894, 1972.
- [73] D. W. McCall, D. C. Douglass, and E. W. Anderson, "Self-diffusion in liquid ammonia," *Physics of Fluids*, vol. 4, no. 10, p. 1317, 1961.
- [74] D. E. O'Reilly, E. M. Peterson, and C. E. Scheie, "Self-diffusion in liquid ammonia and deuterioammonia," *The Journal of Chemical Physics*, vol. 58, no. 10, pp. 4072-4075, 1973.
- [75] L. Chen, T. Groß, and H.-D. Lüdemann, "T, p-dependence of self-diffusion in the lower n-methylsubstituted amides," *Zeitschrift für Physikalische Chemie*, vol. 214, no. 2, 2000.
- [76] H. Walderhaug and K. D. Knudsen, "Aqueous mixtures of a trisiloxane surfactant and oil studied by SANS and NMR self-diffusion: Effect of temperature and oil concentration," *Journal of Solution Chemistry*, vol. 41, no. 2, pp. 367-379, 2012.
- [77] K. T. Gillen, D. C. Douglass, and M. J. R. Hoch, "Self-diffusion in liquid water to -31°C ," *The Journal of Chemical Physics*, vol. 57, no. 12, pp. 5117-5119, 1972.
- [78] H. R. Pruppacher, "Self-diffusion coefficient of supercooled water," *The Journal of Chemical Physics*, vol. 56, no. 1, pp. 101-107, 1972.
- [79] M. N. Rodnikova, F. M. Samigullin, I. A. Solonina, and D. A. Sirotkin, "Molecular mobility and the structure of polar liquids," *Journal of Structural Chemistry*, vol. 55, no. 2, pp. 256-262, 2014.

- [80] D. W. McCall, E. W. Anderson, and C. M. Huggins, "Self-diffusion in linear dimethylsiloxanes," *The Journal of Chemical Physics*, vol. 34, no. 3, pp. 804–808, 1961.
- [81] D. E. O'Reilly, E. M. Peterson, C. E. Scheie, and E. Seyfarth, "Proton, deuterium, and chlorine-35 nuclear magnetic resonance of solid and liquid t -butyl chloride," *The Journal of Chemical Physics*, vol. 59, no. 7, pp. 3576–3584, 1973.

C Supporting Information for Chapter 4: Thermal Conductivity via Entropy Scaling: An Approach that Captures the Effect of Intramolecular Degrees of Freedom

This Supporting Information details (1) the AADs for the investigated approaches, the quality of the underlying approach for D^s , as well as the number of available data for all investigated substances. Further, (2) parameters A - D for the group of simple molecules using λ^{CE} are given, and (3) parameters A - D for all considered substances using the new model $\lambda^{\text{ref},\rho^D}$ are listed, and (4) parameters A - D using the formerly published model $\lambda^{\text{ref},\alpha}$ are provided for all substances not considered in the Supporting Information of Hopp and Gross 2017.

C.1 Comparison of Averaged Absolute Deviations

Table C.1: Averaged absolute deviations (AAD) for the investigated approaches (λ^{CE} and $\lambda^{\text{ref},\rho\text{D}}$), and the quality of the underlying approach for D^{s} as well as the amount of available data for all substances with reduced internal degrees of freedom.

name	Self-diffusion D^{s}		Thermal conductivity λ		
	points	AAD/%	points	AAD/%(λ^{CE})	AAD/%($\lambda^{\text{ref},\rho\text{D}}$)
substances with reduced internal degrees of freedom					
Hydrogen	81	6.321	2378	6.878	8.382
Neon	79	3.226	686	1.221	1.221
Carbon monoxide	60	2.371	204	5.600	3.644
Nitrogen	57	1.389	2333	6.245	4.558
Oxygen	32	2.005	1393	5.043	4.255
Hydrogen chloride	37	13.685	53	4.115	3.969
Argon	214	7.862	4526	5.781	5.606
Krypton	208	8.021	320	4.455	4.403
Xenon	197	5.400	421	6.041	5.072

Table C.2: Averaged absolute deviations (AAD) for the investigated approaches ($\lambda^{\text{ref},\alpha}$ and $\lambda^{\text{ref},\rho}$), and the quality of the underlying approach for D^s as well as the amount of available data for all substances with many internal degrees of freedom, grouped by chemical family and sorted by molecular mass.

name	Self-diffusion D^s		Thermal conductivity λ		
	points	AAD/%	points	AAD/% ($\lambda^{\text{ref},\alpha}$) AAD/% ($\lambda^{\text{ref},\rho}$)	
<i>n</i> -alkanes					
Methane	624	6.346	3215	8.025	10.115
Ethane	145	11.575	1495	7.803	13.805
Propane	70	10.332	3013	7.598	10.853
<i>n</i> -Butane	25	15.633	2941	5.148	8.599
<i>n</i> -Pentane	73	11.343	487	2.571	7.425
<i>n</i> -Hexane	197	19.843	646	3.243	7.999
<i>n</i> -Heptane	134	16.545	1330	3.786	8.302
<i>n</i> -Octane	115	8.590	495	3.022	4.365
<i>n</i> -Nonane	104	8.228	533	3.209	5.911
<i>n</i> -Decane	113	6.220	755	2.891	5.045
<i>n</i> -Undecane	36	6.055	451	2.876	5.170
<i>n</i> -Dodecane	61	4.945	365	4.061	4.585
<i>n</i> -Tridecane	56	2.349	613	2.795	4.284
<i>n</i> -Tetradecane	48	5.374	474	2.451	5.077
<i>n</i> -Pentadecane	56	8.238	368	1.965	3.279
<i>n</i> -Hexadecane	66	4.620	466	2.117	2.919
<i>n</i> -Heptadecane	27	4.590	352	4.117	3.863
<i>n</i> -Octadecane	22	5.370	369	3.736	3.402
<i>n</i> -Nonadecane	4	0.244	327	2.466	3.127

Continued on next page

name	Self-diffusion D^s		points	Thermal conductivity λ	
	AAD/%	%		AAD/%($\lambda^{\text{ref},\alpha}$)	%($\lambda^{\text{ref},\beta}$)
<i>n</i> -Eicosane	17	4.348	55	0.862	2.647
<i>n</i> -Heneicosane	6	1.969	48	0.390	1.387
<i>n</i> -Tricosane	4	1.056	42	0.321	0.979
<i>n</i> -Tetracosane	18	9.127	55	1.769	1.934
branched alkanes					
2-Methylpentane	11	5.483	17	0.776	1.586
3-Methylpentane	16	6.739	20	1.629	3.704
2,3-Dimethylbutane	33	7.963	81	1.947	3.453
2,2-Dimethylbutane	56	8.732	17	0.771	1.803
2,2,3-Trimethylbutane	21	3.639	16	0.630	1.739
cyclic alkanes					
Cyclopentane	29	4.817	142	1.508	4.271
Cyclohexane	234	6.948	642	4.761	6.205
Methylcyclopentane	4	2.555	16	2.406	2.028
Cycloheptane	14	9.808	16	1.121	1.104
Methylcyclohexane	22	13.635	1398	6.549	9.673
Cyclooctane	17	6.566	16	1.140	1.158
alkenes					
Ethylene	296	6.913	530	6.099	6.645
Cyclopentene	4	7.027	15	2.746	2.544
aromatics					
Benzene	484	4.389	952	3.152	5.436
Toluene	170	13.757	3418	8.927	9.850
<i>m</i> -Xylene	5	4.104	487	3.144	5.110

Continued on next page

name	Self-diffusion D^s		Thermal conductivity λ	
	points	AAD/%	points	AAD/%
<i>p</i> -Xylene	5	5.708	506	1.962
<i>o</i> -Xylene	6	4.833	553	1.963
1,3,5-Trimethylbenzene	15	2.078	82	1.615
1,3,5-Trisopropylbenzene	10	7.674	4	0.105
<i>o</i> -Terphenyl	34	8.818	30	1.268
ethers				
Dimethyl ether	40	6.679	347	4.009
Diethyl ether	6	2.248	210	5.548
1,2-Dimethoxyethane	11	9.598	165	0.968
esters				
Methyl acetate	4	3.540	243	7.409
Ethyl acetate	5	2.360	253	8.083
Butyl acetate	8	8.034	200	7.914
Hexyl acetate	9	5.798	202	3.171
ketones				
Acetone	48	4.557	373	6.806
2-Pentanone	7	9.356	174	2.415
2-Hexanone	8	2.900	103	6.090
2-Heptanone	8	4.010	11	0.488
2-Octanone	8	5.473	30	1.012
alcohols				
Methanol	140	9.161	935	6.995
Ethanol	217	7.214	880	6.729
1-Propanol	147	5.149	407	8.017

Continued on next page

name	Self-diffusion D^s		Thermal conductivity λ	
	points	AAD/%	points	AAD/%
2-Propanol	68	4.348	440	10.541
1,2-Ethanediol	6	15.677	175	2.480
tert-Butanol	18	6.479	174	3.958
1-Butanol	27	6.841	251	4.630
1,3-Propanediol	4	9.274	10	0.250
1,2-Propanediol	8	31.182	51	2.942
2-Pentanol	39	6.230	63	13.248
1-Pentanol	177	5.487	132	2.686
1,4-Butanediol	4	8.718	26	2.496
1,3-Butanediol	9	6.680	15	10.025
Glycerol	60	17.514	164	2.204
1-Hexanol	11	5.672	256	2.447
1-Octanol	19	19.313	211	3.295
substances containing nitrogen				
Ammonia	113	6.154	678	7.461
Methylamine	45	7.139	130	4.299
Acetonitrile	53	10.988	147	6.877
Dinitrogen monoxide	24	2.394	297	5.762
Formamide	4	10.976	8	1.081
Nitromethane	15	7.063	15	2.486
Pyridine	33	9.567	9	1.036
Aniline	12	19.675	24	4.337
Triethylamine	8	6.922	20	3.375
substances containing sulfur				
Carbon disulfide	19	4.951	22	4.696
				5.270
				Continued on next page

name	Self-diffusion D^s		Thermal conductivity λ	
	points	AAD/%	points	AAD/%
Dimethyl sulfoxide	24	7.865	12	4.204
substances containing silicon				
Hexamethyldisiloxane	11	6.864	142	1.552
Octamethyltrisiloxane	10	8.175	132	2.658
Octamethylcyclotetrasiloxane	62	7.561	149	0.679
Decamethyltetrasiloxane	11	9.916	135	2.085
Decamethylcyclopentasiloxane	7	6.254	150	1.679
substances containing halogens				
Dichloromethane	90	7.036	120	3.859
Fluorobenzene	19	2.221	67	5.323
1,2-Dichloroethane	32	9.036	34	2.527
Chlorobenzene	22	23.476	316	7.600
Chloroform	110	8.046	95	6.603
Bromobenzene	16	4.331	185	4.762
Iodobenzene	18	1.699	70	5.905
1,2-Dibromotetrafluoroethane	52	4.625	188	3.269
others				
Water	768	8.964	2923	6.015
Carbon dioxide	305	6.937	1480	7.216
Tetrahydrofuran	14	9.067	14	2.594
Propylene carbonate	6	3.163	10	0.058

C.2 Correlation Parameters (A - D) using λ^{CE}

Table C.3: Resulting parameters A - C for small molecules, using $\lambda^{\text{ref}} = \lambda^{\text{CE}}$ and correlation eq. (8). Parameter $D = 0$ for all substances.

Name	A	B	C
Hydrogen	0.23209	-0.32186	0.42259
Neon	0.72998	-0.61907	-0.23657
Carbon monoxide	-0.11169	-0.99112	0.20000
Nitrogen	-0.04265	-0.82004	0.56479
Oxygen	0.03040	-0.65868	0.80000
Hydrogen chloride	-0.53094	-0.46931	2.53559
Argon	0.04324	-0.67168	0.80000
Krypton	0.01696	-0.67866	0.70000
Xenon	0.09167	-0.63999	0.90000

C.3 Correlation Parameters (A - D) using $\lambda^{\text{ref},\rho D}$

Table C.4: Resulting parameters A - C for all considered substances, using $\lambda^{\text{ref}} = \lambda^{\text{ref},\rho D}$ and correlation eq. (8). Parameter $D = 0$ for all substances.

Name	A	B	C
substances with reduced internal degrees of freedom			
Hydrogen	-0.0385647	-0.361742	0.364126
Neon	0.729981	-0.619072	-0.236569
Carbon monoxide	-0.388307	-0.958583	0.48679
Nitrogen	-0.334107	-0.843768	0.686544
Oxygen	-0.273984	-0.717138	0.826418
Hydrogen chloride	-0.735913	-0.543197	2.4507
Argon	0.0432413	-0.671675	0.815049
Krypton	0.0169564	-0.678659	0.707473
Xenon	0.0916715	-0.639993	0.859133
<i>n</i>-alkanes			
Methane	0.0136239	-0.808409	0.134873
Ethane	-0.410971	-0.684542	1.0939
Propane	-0.308257	-0.73244	0.71376
<i>n</i> -Butane	-0.284511	-0.826233	0.482184
<i>n</i> -Pentane	-0.262682	-0.895853	0.328476
<i>n</i> -Hexane	-0.468875	-1.05194	0.271688

Continued on next page

Name	A	B	C
<i>n</i> -Heptane	-0.414816	-1.05972	0.274945
<i>n</i> -Octane	-0.338099	-1.05783	0.372046
<i>n</i> -Nonane	-0.342122	-1.1815	0.0978659
<i>n</i> -Decane	-0.289395	-1.17631	0.13146
<i>n</i> -Undecane	-0.367551	-1.23996	0.127574
<i>n</i> -Dodecane	-0.242025	-1.14659	0.246314
<i>n</i> -Tridecane	-0.210867	-0.967633	0.641818
<i>n</i> -Tetradecane	0.00535809	-1.07397	0.163684
<i>n</i> -Pentadecane	-0.338484	-0.96308	0.838663
<i>n</i> -Hexadecane	-0.183214	-0.948473	0.751468
<i>n</i> -Heptadecane	0	-1.02515	0.408964
<i>n</i> -Octadecane	0	-0.954305	0.62634
<i>n</i> -Nonadecane	0	-0.93796	0.68418
<i>n</i> -Eicosane	0	-1.00373	0.539784
<i>n</i> -Heneicosane	0	-0.829871	0.937068
<i>n</i> -Tricosane	0	-0.792383	1.08506
<i>n</i> -Tetracosane	0	-0.702336	1.32024
branched alkanes			
2-Methylpentane	0	-1.1487	-0.435662
3-Methylpentane	0	-1.11201	-0.319699
2,3-Dimethylbutane	0	-0.7361	0.49319
2,2-Dimethylbutane	-0.201804	-1.05418	0.0412796
2,2,3-Trimethylbutane	0	-0.991329	0.00728835
cyclic alkanes			
Cyclopentane	-0.467151	-1.0708	0.224043
Cyclohexane	-0.368088	-1.2796	-0.29934
Methylcyclopentane	0	-0.904084	0.175254
Cycloheptane	0	-0.767833	0.574978
Methylcyclohexane	-0.410295	-1.73487	-1.6089
Cyclooctane	0	-0.870873	0.331772
alkenes			
Ethylene	-0.444341	-0.970826	0.522175
Cyclopentene	0	-0.857725	0.310791
aromatics			
Benzene	-0.413808	-1.24472	-0.224109
Toluene	0.0935592	-0.92621	-0.183475
<i>m</i> -Xylene	-0.354715	-1.36054	-0.735157
<i>p</i> -Xylene	-0.100694	-1.47084	-1.31022
<i>o</i> -Xylene	-0.356566	-1.35461	-0.747444
1,3,5-Trimethylbenzene	0	-0.970106	-0.00343622
1,3,5-Triisopropylbenzene	0	-0.0180583	2.52682

Continued on next page

Name	A	B	C
<i>o</i> -Terphenyl	-0.212795	-0.839684	0.836726
ethers			
Dimethyl ether	-0.530215	-0.956802	0.492884
Diethyl ether	-0.412114	-1.08453	0.125775
1,2-Dimethoxyethane	0	-0.986998	-0.00656905
esters			
Methyl acetate	-0.539855	-1.17226	0.139868
Ethyl acetate	-0.469874	-1.30782	-0.200368
Butyl acetate	-0.5226	-1.09229	0.376112
Hexyl acetate	0	-1.43885	-0.832925
ketones			
Acetone	-0.495796	-0.909893	0.562554
2-Pentanone	0	-1.58972	-1.5641
2-Hexanone	-0.395547	-1.14552	0.046352
2-Heptanone	0	-1.20831	-0.541898
2-Octanone	0	-0.921778	0.170031
alkoholes			
Methanol	-0.577769	-0.444281	0.65699
Ethanol	-0.629536	-0.392423	1.12456
1-Propanol	-0.623286	-0.307419	1.54148
2-Propanol	-0.775603	-0.0621844	2.22113
1,2-Ethanediol	0	-0.389889	0.936802
tert-Butanol	-0.853675	-0.149604	2.01654
1-Butanol	-0.703853	-0.383845	1.55549
1,3-Propanediol	0	-0.495968	0.601228
1,2-Propanediol	0	-0.446829	0.707382
2-Pentanol	-0.18277	-0.743178	0.116134
1-Pentanol	0	-0.456113	0.704217
1,4-Butanediol	0	-0.5731	0.293121
1,3-Butanediol	0	-0.649379	0.06103
Glycerol	0	-0.244229	1.81303
1-Hexanol	-0.616124	-0.534051	1.32983
1-Octanol	-0.618861	-0.469871	1.71615
substances containing nitrogen			
Ammonia	-0.406549	-0.414155	1.71024
Methylamine	-0.390111	-0.67105	0.569273
Acetonitrile	-1.17399	-0.983277	1.20763
Dinitrogen monoxide	-0.799749	-1.92352	-0.712021
Formamide	0	-0.541641	0.675736
Nitromethane	-1.09895	-0.885087	1.33897
Pyridine	-0.687692	-0.634098	1.5861

Continued on next page

Name	A	B	C
Aniline	0	-0.661675	-0.114741
Triethylamine	-0.608185	-0.915426	0.854797
substances containing sulfur			
Carbon disulfide	-0.404886	-0.675285	1.16649
Dimethyl sulfoxide	0	-0.53047	1.00509
substances containing silicium			
Hexamethyldisiloxane	0	-2.13617	-1.93543
Octamethyltrisiloxane	0	-1.66757	-0.720411
Octamethylcyclotetrasiloxane	0	-1.08334	0.713325
Decamethyltetrasiloxane	0	-1.43177	-0.0432925
Decamethylcyclopentasiloxane	0	-1.43947	0.164515
substances containing halogene			
Dichloromethane	-0.822704	-0.542931	1.94646
Fluorobenzene	0	-1.4612	-1.24927
1,2-Dichloroethane	-0.628083	-0.699104	1.32618
Chlorobenzene	0.21289	-0.991176	-0.598055
Chloroform	-0.614795	-0.504153	1.9554
Bromobenzene	0.143338	-0.965435	-0.225121
Iodobenzene	0	-0.869472	0.165407
1,2-Dibromotetrafluoroethane	-0.129939	-0.66311	0.985682
others			
Water	-0.590097	-0.212420	2.34572
Carbon dioxide	-1.02373	-0.925011	1.53124
Tetrahydrofuran	-0.446277	-0.725381	1.11212
Propylene carbonate	0	-0.751502	0.371064

Parameter A was set to zero if no data in gas phase was available.

C.4 Correlation Parameters (A - D) using $\lambda^{\text{ref},\alpha}$

Table C.5: Resulting parameters A - D for all considered substances except small molecules, using $\lambda^{\text{ref}} = \lambda^{\text{ref},\alpha}$ and correlation eq. (8). Parameter $D = 0$ for all substances.

Name	A	B	C
<i>n</i> -Dodecane	0.18665	-0.56835	1.20290
Cyclopentane	-0.10034	-0.62298	1.17083
Cyclohexane	0.10628	-0.45107	1.37964
Methylcyclopentane	0	-0.53081	1.30301
Cycloheptane	0	-0.45591	1.51588
Methylcyclohexane	0.18938	-0.70452	0.61014
Cyclooctane	0	-0.40137	1.67433
Cyclopentene	0	-0.61227	1.12518
1,3,5-Trimethylbenzene	0	-0.50394	1.38095
1,2-Diphenylbenzen	0.34427	-0.39754	1.34106
Diethyl ether	-0.02886	-0.65402	1.01314
1,2-Dimethoxyethane	0	-0.60166	1.06793
Ethyl acetate	-0.07439	-0.60293	1.05213
2-Propanol	-0.54005	0.09756	2.43825
1,2-Ethanediol	0	-0.37467	0.98748
2-Methylpropan-2-ol	-0.52710	0.12445	2.34169
1,3-Propanediol	0	-0.43732	0.84274
1,2-Propanediol	0	-0.39551	0.89848
2-Pentanol	0.05494	-0.49356	0.47878
1,4-Butanediol	0	-0.52573	0.44630
1,3-Butanediol	0	-0.56790	0.37259
1,2,3-Propantriol	0	-0.20412	1.97516
Ammonia	-0.20679	-0.30825	2.05821
Methylamine	-0.12784	-0.44642	1.23780
Acetonitrile	-0.94064	-0.67807	1.79279
Dinitrogen monoxide	-0.71002	-1.17198	0.70512
Methanamid	0	-0.45104	1.09275
Nitromethane	-0.79959	-0.67888	1.62863
Pyridine	-0.18798	-0.38376	1.83946
Aniline	0	-0.37318	1.48068
Triethylamine	0.00422	-0.50180	1.44242
Water	-0.39559	-0.13893	2.62775
Carbon dioxide	-0.96390	-0.44418	2.39597
Tetrahydrofuran	-0.31434	-0.53138	1.62466
Propylene carbonate	0	-0.62242	0.79043

Continued on next page

Name	A	B	C
Carbon disulfide	-0.30030	-0.48576	1.82625
Dimethyl sulfoxide	0	-0.33187	1.62564
Hexamethyldisiloxane	0	-0.73376	1.25056
Octamethyltrisiloxane	0	-0.33793	2.15186
Octamethylcyclotetrasiloxane	0	-0.44101	2.10391
Decamethyltetrasiloxane	0	-0.29929	2.38454
Decamethylcyclopentasiloxane	0	-0.48809	2.22375
Dichloromethane	-0.76397	-0.42276	2.27770
Fluorobenzene	0	-0.58639	1.12271
1,2-Dichloroethane	-0.32339	-0.48484	1.66366
Chlorobenzene	0.51772	-0.55534	0.58294
Chloroform	-0.62244	-0.31271	2.56795
Bromobenzene	0.40182	-0.53629	0.87805
Iodobenzene	0	-0.42536	1.66110
1,2-Dibromotetrafluoroethane	-0.29923	-0.42716	1.92808

Parameter A was set to zero if no data in gas phase was available.

D Supporting Information for Chapter 5: Thermal Conductivity from Entropy Scaling: A Group-Contribution Method

This supporting Information details...

1. the definition of AAD.
2. the resulting group-contribution parameters $A_\alpha - C_\alpha$ for thermal conductivities based on GC PCP-SAFT.
3. the full legend of Fig. 5.1 of the manuscript.
4. diagrams supplementing Fig. 5.3 of the manuscript.
5. the list of components shown in Fig. 5.6 of the manuscript.
6. results of the full GC method for substances containing two or more functional groups.
7. the AADs for the individual approach using PCP-SAFT and the full GC method using GC PCP-SAFT, as well as the number of available data for all investigated substances.
8. the individual correlation parameters $A-D$ for PCP-SAFT for all investigated components, for which no parameters were published yet,
9. as well as the according individual PCP-SAFT parameters.
10. group decomposition of all considered substances.

D.1 Definition of AAD

The averaged absolute deviations (AAD) is defined as

$$AAD\% = \frac{100}{N_{\text{data}}} \sum_i^{N_{\text{data}}} \left(\frac{|\lambda_{i,\text{calc}} - \lambda_{i,\text{exp}}|}{\lambda_{i,\text{exp}}} \right)$$

D.2 resulting gc parameters $A_\alpha - C_\alpha$

functional group α	A_α	B_α	C_α
<i>n</i> -alkanes			
$-\text{CH}_3$	-0.022767	-0.271017	0.631023
$-\text{CH}_2-$	0.023790	-0.000372	-0.000737
$\text{H}_3\text{C}-\text{CH}_3$	-0.171653	-0.395063	1.884401
CH_4	0.083389	-0.525218	1.144751
branched alkanes			
$-\text{CH} <$	0.073479	0.268006	-0.715219
$> \text{C} <$	0.137522	0.432011	-1.603643
cyclic alkanes			
$-\text{CH}_2- (C_5)$	-0.023861	-0.125883	0.233695
$-\text{CH} < (C_5)$	1.569517	0.030302	-2.415547
$-\text{CH}_2- (C_6)$	0.021505	-0.098933	0.171388
$-\text{CH} < (C_6)$	0.081725	-0.001426	-0.962725
alkenes			
$\text{H}_2\text{C} =$	0.118742	-0.212624	0.603502
$-\text{HC} =$	-0.149712	-0.100910	-0.053894
$> \text{C} =$	-0.040429	0.281085	-0.591450
aldehydes			
$-\text{CH} = \text{O}$	0.108913	-0.536623	-0.229006
aromatics			
$-\text{CH}- (\text{aromatic})$	0.020046	-0.083404	0.208123
$> \text{C}- (\text{aromatic})$	0.152283	0.115018	-0.756362
esters			
$\text{HCOO}-$	0.139924	-0.390715	0.141069
$-\text{COO}-$	-0.047422	-0.094117	-0.217276
ethers*			
$-\text{O}-\text{CH}_3$	0.013269	0.037753	0.077359
$-\text{O}-\text{CH}_2-$	-0.279392	-0.455717	0.458677
$-\text{O}-$	-0.900976	0.253726	1.716688
ketones			
$> \text{C} = \text{O}$	-0.209035	0.052247	0.226533
alcohols**			
$-\text{OH}$	0.095944	0.227526	1.182451
CH_3OH	-0.558730	-0.434812	0.894255
others			
$-\text{NH}_2$	0.260570	-0.062493	0.661768
$> \text{NH}$	0.185228	0.238233	0.393120
CO_2	-0.577272	-0.515448	1.671248
H_2O	-0.392458	-0.120720	2.717849
$\text{HC} \equiv \text{CH}$	-0.088542	-0.666847	-0.673819

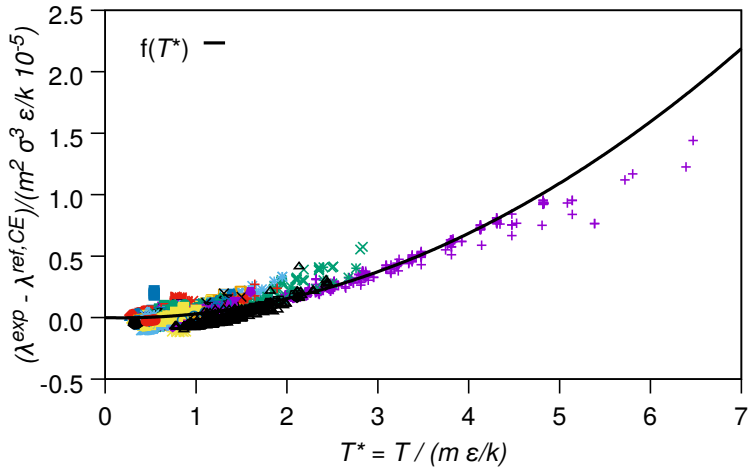
*: for ethers, use $-\text{O}-\text{CH}_3$ group, if possible.

Otherwise use $-\text{O}-\text{CH}_2-$ group, if possible.

Otherwise use $-\text{O}-$ group (for branched ethers).

** : $D_{\text{OH}} = D_{\text{CH}_3\text{OH}} = 0.0038$

D.3 Full Legend of Fig. 5.1



- | | | | | | |
|------------------------|---|-------------------------------|---|----------------------------|---|
| Methane | + | Butyraldehyde | ○ | Diisopropylether | ◇ |
| Ethane | × | 3-Methylbutyraldehyde | ● | Triethylamine | ◆ |
| Propane | × | 2-Methylpropanal | + | Trimethylamine | ○ |
| n-Butane | □ | Toluene | × | Nitromethane | ● |
| Pentane | ■ | Ethylbenzene | * | Pyridine | + |
| Hexane | ○ | Propylbenzene | □ | Propionitrile | × |
| Heptane | ● | Isopropylbenzene | ■ | Acetonitrile | × |
| Octane | ▲ | m-Xylene | ○ | Cyclopentanone | □ |
| Nonane | ▲ | o-Xylene | ● | Phthalicaciddimethylester | ■ |
| Decane | ▼ | o-Terphenyl | ▲ | Tetrahydrofuran | ○ |
| n-Undecane | ▼ | m-Terphenyl | ▲ | N,N-Dimethylformamide(DMF) | ● |
| Dodecane | ◇ | p-Terphenyl | ▼ | Ethyleneoxide | ▲ |
| Tridecane | ◇ | Acetone | ▼ | Furfural | ▲ |
| Tetradecane | ○ | 2-Butanone | ◇ | Phthalicacidpropylester | ▼ |
| Pentadecane | ● | 2-Hexanone | ◆ | Phthalicaciddiethylester | ▼ |
| Hexadecane | + | 4-Heptanone | ○ | Phthalicacidbutylester | ◆ |
| 2,2,4-Trimethylpentane | × | Propanoicacidethylester | ● | Di-n-hexylphthalate | ◇ |
| Ethylene | × | Ethylbutyrate | + | Methanol | ○ |
| 1,3-Butadiene | □ | Formicacidmethylester | × | Ethanol | ● |
| trans-2-Butene | ■ | Formicacidethylester | * | 1-Propanol | + |
| Cyclopentane | ○ | Aceticacidisobutylester | □ | 2-Propanol | × |
| Cyclohexane | ● | Formicacidpropylester | ■ | 1-Butanol | × |
| Methylcyclohexane | ▲ | Formicacidoctylester | ○ | 2-Butanol | □ |
| Ethylcyclohexane | ▲ | Butylacetate | ● | 2-Pentanol | ■ |
| n-Propylcyclohexane | ▼ | Aceticacid3-methylbutylester | ▲ | 1-Hexanol | ○ |
| Benzene | ▼ | Ethylacetate | ▲ | 1-Heptanol | ● |
| Biphenyl | ◇ | Methylpropanoate | ▼ | 1-Octanol | ▲ |
| Carbondsulfide | ◇ | Propanoicacidbutylester | ▼ | 2-Octanol | ▲ |
| 2-Methylbutane | ● | Formicacidbutylester | ◇ | 1-Nonanol | ▼ |
| 2-Methylpropane | ○ | Aceticacidpentylester | ◆ | 1-Decanol | ▼ |
| Propylene | + | Formicacidpentylester | ○ | tert-Butanol | ◇ |
| 1-Butene | × | Methylacetate | ● | 3-Methyl-1-butanol | ◇ |
| 1-Pentene | * | Di-n-propylether | + | 2-Methyl-1-butanol | ○ |
| 1-Hexene | □ | Diethyleneglycoldimethylether | × | 3-Methyl-2-butanol | ● |
| 1-Heptene | ■ | Dimethylether | * | Butyricacid | + |
| 1-Octene | ○ | Dibutylether | □ | Octanoicacid | × |
| 1-Nonene | ● | Methylethylether | ■ | Hexanoicacid | * |
| 1-Decene | ▲ | Methylpropylether | ○ | N,N-Diethylamine | ■ |
| 1-Undecene | ▲ | Diethylether | ● | Dimethylamine | ■ |
| Isobutylene | ▼ | Methylbutylether | ▲ | Methylamine | ○ |
| cis-2-Butene | ▼ | Ethylpropylether | ▲ | 2-Propen-1-ol | ● |
| Isoprene | ◇ | Ethylbutylether | ▼ | Ammonia | ▲ |
| Acetaldehyde | ◆ | Dipentylether | ▼ | f(T*) | — |

D.4 Additions to Fig. 5.3

As an addition to Fig. 5.3, we give here the diagrams for a rather small molecule, Methane, as well. Furthermore, deviations over the range of reduced residual entropy are given for the substances of Fig. 5.3 and Methane. The high deviations in the gas phase result from the definition of deviation.

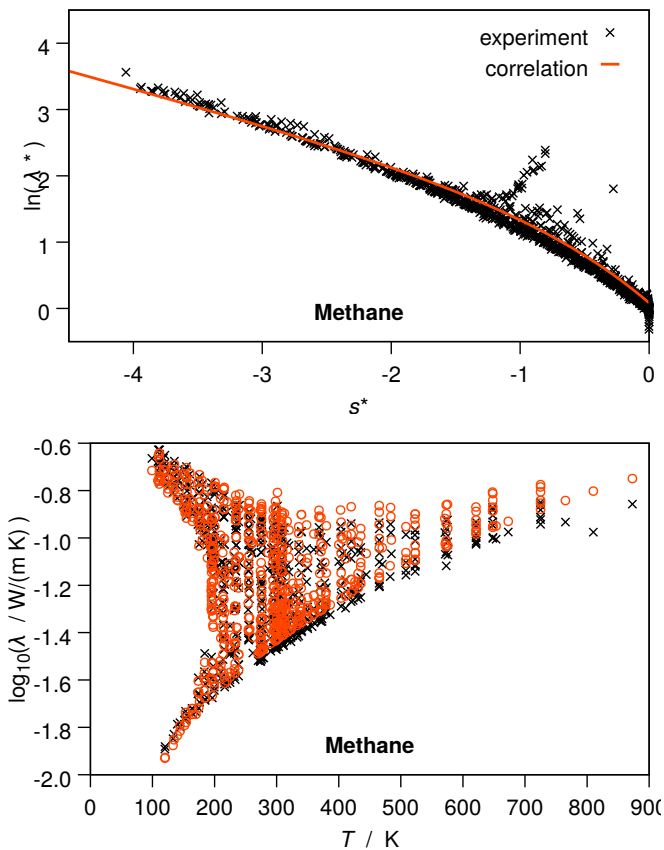


Figure D.1: Thermal conductivity of methane. Left diagrams show the logarithmic reduced thermal conductivity $\ln(\lambda_*)$ versus reduced residual entropy s^* . Right diagrams give thermal conductivities for varying temperature. Comparison of the proposed group-contribution entropy scaling model (red line and red circles) to experimental data (black crosses).

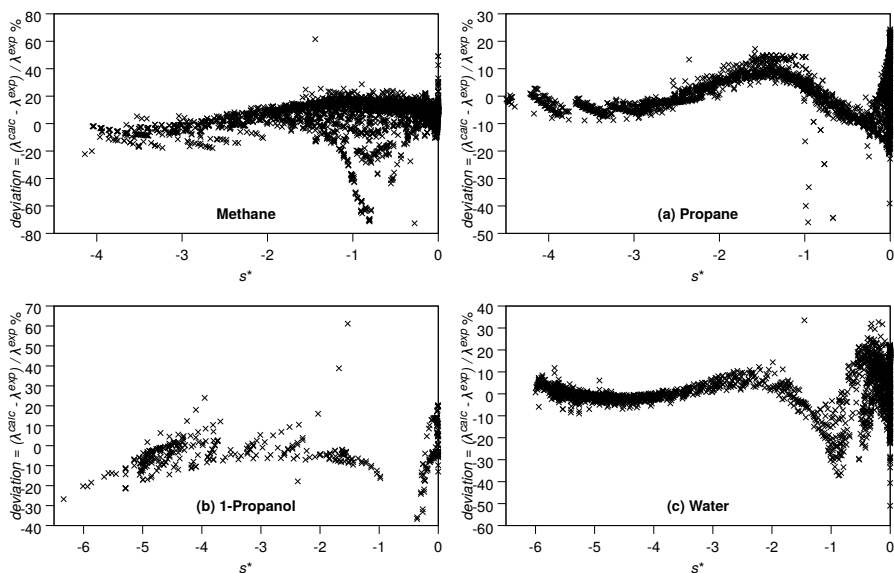


Figure D.2: Deviations of calculated to experimental thermal conductivity of methane, n-propane, 1-propanol and water.

D.5 Components of Fig. 5.6

Table D.1:

#	group	number of functional groups	number of points	AAD / %	name
1	Cyclo	4	2	6.091	Bicyclopentyl
2	Cyclo	4	2	23.690	Bicyclohexyl
3	Cyclo	6	2	25.892	Dicyclohexylmethane
4	Cyclo	5	2	17.854	1,1-Dicyclohexylheptane
5	Aromatic	37	2	27.326	Biphenyl
6	Aromatic	26	2	12.489	Diphenylmethane
7	Aromatic	53	2	10.508	Ditolylmethane
8	Aromatic	24	2	11.925	Isopropylbiphenyl
9	Aromatic	37	2	11.981	Bis(isopropylphenyl)methane
10	Aromatic	28	3	11.753	o-Terphenyl
11	Aromatic	22	3	22.234	m-Terphenyl
12	Aromatic	12	3	28.730	p-Terphenyl
13	Ester	256	2	27.520	Diethylsuccinate
14	Ester	171	2	30.384	Dipropylsuccinate
15	Ester	73	2	21.035	Decanedioicacididibutylester
16	Ester	159	2	15.690	Di-n-hexyladipate
17	Ester	201	2	24.320	Diisobutylsebacate
18	Ester	173	2	14.467	Di-n-heptyladipate

Continued on next page

Table – continued from previous page

#	group	number of functional groups	number of points	AAD / %	name
19	Ester	4	2	4.920	Di(2-ethylhexyl)adipate
20	Ester	186	2	13.839	Hexanedioicaciddioctylester
21	Ester	180	2	15.150	Succinicaciddinonylester
22	Ether	185	2	30.990	Dimethoxymethane
23	Ether	165	2	30.870	1,2-Dimethoxyethane
24	Ether	7	2	23.761	1,2-Diethoxyethane
25	Ether	10	2	8.405	Dibutoxymethane
26	Ether	6	2	11.375	Ethyleneglycoldi-n-butylether
27	Ether	14	3	13.964	Diethyleneglycoldimethylether
28	Ether	43	3	15.787	Diethyleneglycoldiethylether
29	Ether	42	3	6.156	Diethyleneglycoldibutylether
30	Ether	5	4	28.516	Triethyleneglycoldimethylether
31	Ether	4	5	26.780	Tetraethyleneglycoldimethylether

functional groups	Alcohol	Aldehyde	Alkene	Aromatic	Ester	Cyclic
Contains Nitrogen	1 18 68.79	1 8 17.83		1 24 20.79		2 7 16.70
Ketone				2 23 49.10	1 6 27.01	2 25 24.83
Ether	6 160 9.53				3 286 62.88	
Ester			5 549 22.25	4 621 16.81		
Cyclic	2 20 38.31		3 95 62.89			
Aromatic	3 37 6.11	1 9 13.82	1 14 26.92			
Alkene	2 18 16.86	1 5 79.69				

Table D.2: Average absolute deviations for substances containing two different functional groups (AAD in %, as bottom values of cells), the corresponding number of substances (top left) and number of experimental data points (top right).

D.6 Substances with different functional groups

Results for substances that contain two different functional groups are presented in Table D.2. The table reports averaged absolute deviations of predicted thermal conductivities from experimental values. Each cell in the table represents a sub-group of substances that all have a certain combination of functional groups. The table states averaged absolute deviations for a sub-group (as the bottom-value of the cell), the number of considered substances (top left), and the number of available data points (top right). For empty cells, no experimental data of thermal conductivity were found for substances falling into this sub-group. For most of the considered substances the model gives surprisingly good predictions, considering that substances with multiple functional groups are a particularly demanding test case for group-contribution approaches. Considering substances with different functional groups, where any functional group can occur more than once (not explicitly shown here), we saw that combinations from esters, alkenes and aromatics (in addition to normal and branched alkane functional groups) lead to good predictive results (18 substances, 1412 pts, AAD 15.65%).

D.7 Averaged Absolute Deviations

Averaged absolute deviations of all considered substances, for the individual approach with PCP-SAFT and the full GC approach with GC PCP-SAFT. Components are sorted by chemical families. Here, an additional identifier "SI-Symbol" is introduced, which is used in the table stating the group decomposition at the end of the Supporting Information. s_{crit}^* calculated from GC PCP-SAFT, resulting in arithmetic mean $\bar{s}_{\text{crit}}^* = -0,491$.

Table D.3:

name	SI-Symbol	number of points	s_{crit}^*	AAD / %	
				full GC method	individual method
Alkanes					
Methane	A-1	3215	-0.070	10.899	8.025
Ethane	A-2	1486	-0.079	14.874	7.803
Propane	A-3	2888	-0.080	6.168	7.598
Butane	A-4	2931	-0.089	4.936	5.148
Pentane	A-5	487	-0.098	4.678	2.571
Hexane	A-6	650	-0.106	4.000	3.243
Heptane	A-7	1332	-0.113	4.959	3.786
Octane	A-8	495	-0.121	5.992	3.022
Nonane	A-9	533	-0.128	4.755	3.209
Decane	A-10	755	-0.134	4.097	2.891
Undecane	A-11	453	-0.141	4.336	2.876
Dodecane	A-12	365	-0.148	4.533	4.061
Tridecane	A-13	613	-0.154	3.120	2.795
Tetradecane	A-14	474	-0.160	3.336	2.451
Pentadecane	A-15	368	-0.166	3.076	1.965
Hexadecane	A-16	466	-0.172	3.122	2.117
Heptadecane	A-17	352	-0.178	3.333	4.117
Octadecane	A-18	369	-0.183	3.436	3.736
Nonadecane	A-19	327	-0.189	3.873	2.466
Eicosane	A-20	55	-0.194	4.994	0.862
Heneicosane	A-21	48	-0.199	5.744	0.390
Docosane	A-22	54	-0.205	5.719	1.276

Continued on next page

Table – continued from previous page

name	SI-Symbol	number of points	s_{crit}^*	AAD / % full GC method	AAD / % individual method
Tricosane	A-23	42	-0.210	6.206	0.321
Tetracosane	A-24	55	-0.215	6.041	1.769
Branched Alkanes					
2-Methylpropane	B-1	1714	-0.255	6.421	5.707
2-Methylbutane	B-2	67	-0.280	3.271	1.993
2-Methylpentane	B-3	17	-0.305	1.881	0.776
2,2-Dimethylbutane	B-4	17	-0.269	1.728	0.771
2,3-Dimethylbutane	B-5	81	-0.296	4.444	1.947
3-Methylpentane	B-6	20	-0.305	2.377	1.629
2,4-Dimethylpentane	B-7	17	-0.320	2.535	0.486
2,2,3-Trimethylbutane	B-8	16	-0.286	6.477	0.630
3,3-Dimethylpentane	B-9	16	-0.294	2.269	0.315
2,3-Dimethylpentane	B-10	27	-0.320	5.675	0.423
3-Methylhexane	B-11	26	-0.327	1.821	0.255
2,2-Dimethylpentane	B-12	15	-0.294	0.414	0.285
2-Methylhexane	B-13	16	-0.327	1.764	0.308
3-Ethylpentane	B-14	16	-0.327	3.522	0.227
2,2,4-Trimethylpentane	B-15	338	-0.310	3.889	2.421
2,3,4-Trimethyl pentane	B-16	15	-0.334	8.790	0.216
3-Methylheptane	B-17	16	-0.349	2.467	0.385
2-Methylheptane	B-18	16	-0.349	1.599	0.256
Alkene					
Ethylene	C-1	493	-0.108	8.578	6.099
Propylene	C-2	351	-0.117	7.888	6.035

Continued on next page

Table – continued from previous page

name	SI-Symbol	number of points	s_{crit}^*	AAD / % full GC method	AAD / % individual method
1-Butene	C-3	31	-0.130	8.251	9.085
Isobutylene	C-4	65	-0.143	18.612	18.677
cis-2-Butene	C-5	20	-0.140	10.802	6.574
trans-2-Butene	C-6	23	-0.140	11.357	5.838
2-Methylbuta-1,3-dien	C-7	38	-0.152	16.704	3.284
1-Pentene	C-8	32	-0.143	7.972	1.983
2,3-Dimethyl-1-butene	C-9	18	-0.163	2.589	0.143
2,3-Dimethyl-2-butene	C-10	18	-0.187	6.265	0.265
1-Hexene	C-11	312	-0.156	3.932	3.464
1-Heptene	C-12	415	-0.167	4.212	2.986
2-Heptene	C-13	34	-0.176	7.395	1.178
1-Octene	C-14	430	-0.178	5.226	4.230
1-Nonene	C-15	335	-0.189	6.727	3.454
1-Decene	C-16	304	-0.199	5.949	2.264
1-Undecene	C-17	257	-0.210	3.671	2.255
1-Dodecene	C-18	290	-0.219	3.101	2.327
1-Tridecene	C-19	246	-0.229	1.892	2.290
1-Tetradecene	C-20	271	-0.238	1.962	2.313
1-Pentadecene	C-21	249	-0.247	1.855	2.468
1-Hexadecene	C-22	249	-0.256	2.277	2.600
Cyclic Alkanes					
Cyclopentane	D-1	142	-0.297	1.542	1.508
Cyclohexane	D-2	642	-0.298	6.312	4.932
Methylcyclohexane	D-3	1398	-0.313	6.153	6.967

Continued on next page

Table – continued from previous page

name	SI-Symbol	number of points	s_{crit}^*	AAD / %	
				full GC method	individual method
Ethylcyclohexane	D-4	333	-0.338	5.855	3.498
cis-1,2-Dimethylcyclohexane	D-5	21	-0.327	12.365	0.334
trans-1,4-Dimethylcyclohexane	D-6	50	-0.327	8.197	0.722
cis-1,3-Dimethyl cyclohexane	D-7	44	-0.327	7.851	0.663
trans-1,2-Dimethylcyclohexane	D-8	36	-0.327	7.933	1.032
n-Propyl cyclohexane	D-9	668	-0.363	3.809	1.837
Methylcyclopentane	D-10	16	-0.307	2.358	-
1,2-Dimethylcyclohexane	D-11	4	-0.327	16.727	-
Aldehydes					
Butyraldehyde	E-1	80	-0.180	6.650	3.889
2-Methylpropanal	E-2	67	-0.175	5.249	5.045
Pentanal	E-3	8	-0.191	5.096	0.192
3-Methylbutyraldehyde	E-4	54	-0.187	3.389	2.292
Heptanal	E-5	12	-0.214	3.659	0.421
Decanal	E-6	21	-0.247	6.499	1.250
Dodecanal	E-7	16	-0.268	13.704	1.515
Aromatics					
Benzene	F-1	947	-0.187	7.692	3.152
Toluene	F-2	3435	-0.198	3.923	8.927
Ethylbenzene	F-3	560	-0.213	6.195	2.686
p-Xylene	F-4	506	-0.210	2.513	1.962
m-Xylene	F-5	485	-0.210	5.558	3.144
o-Xylene	F-6	552	-0.210	4.140	1.963
Propylbenzene	F-7	94	-0.228	3.137	1.973

Continued on next page

Table – continued from previous page

name	SI-Symbol	number of points	s_{crit}^*	full GC method	individual method
1,3,5-Trimethylbenzene	F-8	82	-0.221	8.172	1.615
1,2,3-Trimethylbenzene	F-9	18	-0.221	3.399	0.259
1,2,4-Trimethylbenzene	F-10	117	-0.221	4.586	1.478
Isopropylbenzene	F-11	358	-0.223	2.961	16.422
Butylbenzene	F-12	98	-0.241	8.228	2.011
1,2-Diethylbenzene	F-13	11	-0.238	1.422	0.751
sec-Butylbenzene	F-14	11	-0.237	2.067	0.544
tert-Butylbenzene	F-15	104	-0.216	5.019	1.614
1,3,5-Triisopropylbenzene	F-16	4	-0.286	19.743	0.105
Ketones					
Acetone	G-1	373	-0.171	11.664	6.806
2-Butanone	G-2	334	-0.179	5.859	4.718
2-Pentanone	G-3	174	-0.189	3.522	2.415
3-Pentanone	G-4	22	-0.189	4.184	1.515
4-Methyl-2-pentanone	G-5	9	-0.196	0.810	0.119
3-Hexanone	G-6	163	-0.200	2.566	1.994
2-Hexanone	G-7	103	-0.200	10.769	6.090
3-Heptanone	G-8	175	-0.212	4.876	1.765
2-Heptanone	G-9	11	-0.212	4.996	0.488
4-Heptanone	G-10	86	-0.212	7.407	7.505
2-Octanone	G-11	30	-0.223	3.996	1.012
5-Nonanone	G-12	168	-0.234	2.409	1.326
6-Undecanone	G-13	184	-0.255	3.223	1.084
2-Decanone	G-14	170	-0.245	2.976	-

Continued on next page

Table – continued from previous page

name	SI-Symbol	number of points	s_{crit}^*	full GC method	AAD / % individual method
2-Undecanone	G-15	171	-0.255	2.975	-
3-Dodecanone	G-16	172	-0.266	3.655	-
7-Tridecanone	G-17	11	-0.276	7.380	-
6,10-Dimethyl-2-undecanone	G-18	6	-0.269	8.574	-
Ester					
Formic acid methyl ester	H-1	11	-0.099	16.536	0.613
Formic acid ethyl ester	H-2	148	-0.103	12.635	8.853
Formic acid propyl ester	H-3	201	-0.110	12.095	5.433
Formic acid butyl ester	H-4	135	-0.116	5.622	3.018
Formic acid pentyl ester	H-5	194	-0.123	6.559	4.289
Formic acid heptyl ester	H-6	10	-0.136	3.610	2.930
Formic acid octyl ester	H-7	57	-0.143	8.864	10.058
Acetic acid methyl ester	H-8	222	-0.104	8.920	7.409
Acetic acid ethyl ester	H-9	253	-0.109	8.176	8.063
Acetic acid 1-methyl-ethyl ester	H-10	21	-0.113	3.874	1.232
Acetic acid butyl ester	H-11	198	-0.122	8.254	7.914
Acetic acid 2-methyl-propyl ester	H-12	125	-0.120	7.410	4.740
Acetic acid pentyl ester	H-13	154	-0.129	15.877	10.337
Acetic acid 3-methyl-butyl ester	H-14	95	-0.126	16.462	9.629
Acetic acid hexyl ester	H-15	202	-0.135	5.716	3.171
Acetic acid heptyl ester	H-16	207	-0.141	3.531	3.130
Acetic acid 2-ethyl-hexyl ester	H-17	125	-0.146	4.091	0.907
Butanoic acid ethyl ester	H-18	218	-0.122	4.386	3.648
Propanoic acid methyl ester	H-19	99	-0.109	7.195	6.955

Continued on next page

Table – continued from previous page

name	SI-Symbol	number of points	s_{crit}^*	AAD / %	
				full GC method	individual method
Propanoic acid butyl ester	H-20	131	-0.129	7.402	2.920
Octadecanoic acid butyl ester	H-21	13	-0.214	6.724	0.267
Formic acid 1-methyl-ethyl ester	H-22	87	-0.107	6.968	-
Formic acid 3-methyl-butyl ester	H-23	97	-0.121	7.635	-
Formic acid hexyl ester	H-24	213	-0.130	4.133	-
Formic acid 4-methyl-pentyl ester	H-25	144	-0.127	13.520	-
Acetic acid octadecyl ester	H-26	5	-0.204	12.956	-
Butanoic acid 1-methyl-ethyl ester	H-27	16	-0.126	4.837	-
Butanoic acid pentyl ester	H-28	10	-0.141	5.129	-
Butanoic acid 3-methyl-butyl ester	H-29	98	-0.139	6.729	-
Butanoic acid heptyl ester	H-30	159	-0.154	5.492	-
Propanoic acid pentyl ester	H-31	120	-0.135	4.835	-
Propanoic acid 3-methyl-butyl ester	H-32	126	-0.133	8.293	-
Propanoic acid hexyl ester	H-33	12	-0.141	5.441	-
Propanoic acid heptyl ester	H-34	93	-0.148	7.069	-
Propanoic acid octyl ester	H-35	98	-0.154	5.221	-
Pentanoic acid methyl ester	H-36	16	-0.122	5.480	-
Pentanoic acid pentyl ester	H-37	154	-0.148	8.023	-
Pentanoic acid 3-methyl-butyl ester	H-38	141	-0.146	5.852	-
Hexanoic acid methyl ester	H-39	292	-0.129	4.982	-
Hexanoic acid ethyl ester	H-40	160	-0.135	3.740	-
Hexanoic acid propyl ester	H-41	109	-0.141	2.886	-
Hexanoic acid butyl ester	H-42	144	-0.148	2.445	-
Hexanoic acid pentyl ester	H-43	151	-0.154	2.149	-

Continued on next page

Table – continued from previous page

name	SI-Symbol	number of points	s_{crit}^*	AAD / %	
				full GC method	individual method
Hexanoic acid hexyl ester	H-44	147	-0.160	2.064	-
Hexanoic acid heptyl ester	H-45	147	-0.166	2.082	-
Hexanoic acid octyl ester	H-46	125	-0.171	2.695	-
Hexanoic acid nonyl ester	H-47	132	-0.177	3.443	-
Octanoic acid methyl ester	H-48	247	-0.141	15.340	-
Hexadecanoic acid butyl ester	H-49	9	-0.204	5.460	-
Octadecanoic acid methyl ester	H-50	8	-0.199	9.293	-
Alcohols					
Methanol	K-1	931	-0.684	11.851	6.995
Ethanol	K-2	876	-0.388	8.456	6.729
1-Propanol	K-3	402	-0.372	7.662	8.017
2-Propanol	K-4	396	-0.369	4.643	10.529
1-Butanol	K-5	251	-0.367	5.319	4.630
2-Butanol	K-6	76	-0.363	4.251	2.083
1-Pentanol	K-7	132	-0.372	4.028	2.686
2-Pentanol	K-8	55	-0.367	2.874	13.248
1-Hexanol	K-9	256	-0.382	4.047	2.447
1-Heptanol	K-10	267	-0.396	4.745	3.481
1-Octanol	K-11	211	-0.412	5.550	3.295
2-Octanol	K-12	36	-0.405	5.847	1.779
1-Nonanol	K-13	182	-0.429	4.025	2.161
1-Decanol	K-14	286	-0.447	5.630	3.990
1-Undecanol	K-15	92	-0.465	3.257	2.069
1-Dodecanol	K-16	94	-0.483	6.993	2.081

Continued on next page

Table – continued from previous page

name	SI-Symbol	number of points	s_{crit}^*	full GC method	individual method
1-Tetradecanol	K-17	14	-0.518	5.680	1.098
1-Hexadecanol	K-18	4	-0.553	9.026	1.073
1-Octadecanol	K-19	13	-0.587	3.075	1.188
2-Methyl-2-propanol	K-20	94	-0.336	26.264	3.958
2-Methyl-1-propanol	K-21	43	-0.363	4.701	4.974
2-Methyl-1-butanol	K-22	27	-0.367	11.485	2.674
3-Methyl-1-butanol	K-23	64	-0.367	5.599	9.162
3,3-Dimethyl-2-butanol	K-24	8	-0.340	8.815	-
2-Methyl-2-pentanol	K-25	42	-0.346	8.664	-
2,3-Dimethyl-2-butanol	K-26	36	-0.340	6.481	-
2-Methyl-2-hexanol	K-27	35	-0.359	9.070	-
5-Methyl-1-hexanol	K-28	11	-0.390	4.967	-

Ethers

Dimethyl ether	L-1	347	-0.229	5.089	4.009
Methyl propyl ether	L-2	146	-0.268	7.587	5.834
Diethyl ether	L-3	210	-0.257	7.072	5.548
Methyl tert-butyl ether	L-4	7	-0.252	2.944	0.074
Di-n-propyl ether	L-5	142	-0.291	6.827	2.412
Ethyl butyl ether	L-6	9	-0.291	9.116	2.459
Dibutyl ether	L-7	262	-0.325	4.873	4.695
Dipentyl ether	L-8	242	-0.358	7.046	5.138
Diphenyl ether	L-9	37	-0.336	2.497	2.020
Propyl butyl ether	L-10	2	-0.308	16.344	-
Diisopentyl ether	L-11	8	-0.347	3.912	-

Continued on next page

Table – continued from previous page

name	SI-Symbol	number of points	s_{crit}^*	AAD / % full GC method	AAD / % individual method
Dihexyl ether	L-12	101	-0.389	9.621	-
Diheptylether	L-13	9	-0.418	8.306	-
Di-n-octyl ether	L-14	74	-0.447	9.646	-
Eugenol	L-15	7	-0.330	4.515	-
contains Nitrogen					
Methylamine	M-1	131	-0.240	6.618	4.282
Isopropylamine	M-2	5	-0.244	3.509	0.439
N,N-Diethylamine	M-3	10	-0.263	12.348	5.825
Hexylamine	M-4	4	-0.306	14.524	0.958
1-Octanamine	M-5	4	-0.343	13.310	1.479
Dibutylamine	M-6	4	-0.338	6.657	1.143
Diisopropylamine	M-7	4	-0.286	5.263	-
Others					
Ethyne	N-1	29	-0.893	6.655	10.705
Water	N-2	2923	-0.880	5.735	6.015
Carbon dioxide	N-3	1460	-0.861	5.972	9.307
multiple functional groups					
1,2-Ethanediol	O-1	175	-1.434	27.146	2.480
1,3-Propanediol	O-2	10	-1.468	12.759	0.250
1,2-Propanediol	O-3	51	-1.441	16.436	2.942
1,3-Butanediol	O-4	15	-1.495	11.136	10.025
1,4-Butanediol	O-5	26	-1.525	9.563	2.496
2,2-Dimethyl-1,3-propanediol	O-6	5	-1.416	18.795	-
1,5-Pentanediol	O-7	7	-1.596	3.396	0.612

Continued on next page

Table – continued from previous page

name	SI-Symbol	number of points	s_{crit}^*	full GC method	individual method
1,6-Hexanediol	O-8	7	-1.674	1.825	0.129
1,8-Octanediol	O-9	8	-1.839	5.834	-
1,9-Nonanediol	O-10	7	-1.923	7.974	-
1,10-Decanediol	O-11	7	-2.006	11.680	0.258
Glycerol	O-12	164	-1.392	33.983	2.204
2-(Hydroxymethyl)-2-methyl-1,3-propanediol	O-13	1	-1.416	27.779	-
2-Ethyl-2-hydroxymethyl-1,3-propanediol	O-14	3	-1.511	2.679	-
Biphenyl	O-15	37	-1.043	27.326	2.671
Diphenylmethane	O-16	26	-1.192	12.489	0.658
Ditolylmethane	O-17	53	-1.395	10.508	-
Isopropylbiphenyl	O-18	24	-1.390	11.925	-
Bis (isopropylphenyl) methane	O-19	37	-1.808	11.981	-
O-Terphenyl	O-20	28	-1.621	11.753	1.268
m-Terphenyl	O-21	22	-1.621	22.234	1.085
p-Terphenyl	O-22	12	-1.621	28.730	2.486
Bicyclopentyl	O-23	4	-0.859	6.091	-
Bicyclohexyl	O-24	4	-1.014	23.690	0.164
Dicyclohexylmethane	O-25	6	-1.155	25.892	-
1,1-Dicyclohexylheptane	O-26	5	-1.842	17.854	-
Diethyl succinate	O-27	256	-1.340	27.520	5.331
Dipropyl succinate	O-28	171	-1.616	30.384	-
Decanedioic acid dibutyl ester	O-29	73	-2.488	21.035	1.509
Di-n-hexyladipate	O-30	159	-2.488	15.690	-
Diisobutyl sebacate	O-31	201	-2.429	24.320	-

Continued on next page

Table – continued from previous page

name	SI-Symbol	number of points	s_{crit}^*	AAD / %	
				full GC method	individual method
Di-n-heptyl adipate	O-32	173	-2.669	14.467	-
Di(2-ethylhexyl) adipate	O-33	4	-2.787	4.920	1.725
Hexanedioic acid dioctyl ester	O-34	186	-2.840	13.839	-
Succinic acid dimonyl ester	O-35	180	-2.840	15.150	-
Dimethoxymethane	O-36	185	-0.499	30.990	1.473
1,2-Dimethoxyethane	O-37	165	-0.711	30.870	0.968
1,2-Diethoxyethane	O-38	7	-0.903	23.761	0.494
Dibutoxymethane	O-39	10	-1.358	8.405	-
Ethylene glycol di-n-butyl ether	O-40	6	-1.492	11.375	-
Diethylene glycol dimethyl ether	O-41	14	-1.230	13.964	1.540
Diethylene glycol diethyl ether	O-42	43	-1.367	15.787	-
Diethylene glycol dibutyl ether	O-43	42	-1.876	6.156	-
Triethylene glycol dimethyl ether	O-44	5	-1.666	28.516	-
Tetraethylene glycol dimethyl ether	O-45	4	-2.046	26.780	8.541
mixed functional groups, each group only once					
3,7,11,15-Tetramethyl-1-hexadecen-3-ol	P-1	6	-0.846	27.863	-
Phenol	P-2	22	-0.511	4.675	0.659
Benzyl alcohol	P-3	4	-0.537	1.578	0.178
3-Methylphenol	P-4	11	-0.526	10.615	0.526
Cyclopentanol	P-5	5	-0.504	20.363	-
Cyclohexanol	P-6	15	-0.495	44.295	0.817
2-Methoxyethanol	P-7	10	-0.586	10.086	3.123
2-Ethoxyethanol	P-8	45	-0.581	14.440	1.072
2-Butoxyethanol	P-9	50	-0.613	6.812	5.082

Continued on next page

Table – continued from previous page

name	SI-Symbol	number of points	s_{crit}^*	AAD / %	
				full GC method	individual method
Diethylene glycol monomethyl ether	P-10	43	-0.651	8.152	5.026
2-Phenoxy-ethanol	P-11	6	-0.611	14.038	-
Ethylene glycol monohexyl ether	P-12	6	-0.658	4.432	0.182
2-Ethylpropenal	P-13	5	-0.116	79.692	-
Benzaldehyde	P-14	9	-0.266	13.819	0.744
Cyclopentene	P-15	15	-0.125	70.791	2.746
Cyclohexene	P-16	76	-0.170	62.046	2.192
1-Methylcyclohexene	P-17	4	-0.292	49.234	-
Styrene	P-18	14	-0.523	26.925	0.242
Amyl salicylate	P-19	69	-0.735	11.492	-
Vinyl acetate	P-20	5	-0.485	4.261	1.026
trans-2-Butenoic acid methyl ester	P-21	70	-0.543	25.739	-
Methacrylic acid methyl ester	P-22	8	-0.551	8.761	1.286
trans-2-Butenoic acid ethyl ester	P-23	71	-0.566	69.476	-
Methyl oleate	P-24	395	-0.947	13.647	-
Benzoic acid methyl ester	P-25	137	-0.562	62.980	0.871
Ethyl benzoate	P-26	277	-0.615	2.187	1.394
Salicylic acid methyl ester	P-27	66	-0.623	10.788	2.633
Propyl benzoate	P-28	141	-0.649	3.533	1.117
Carbonic acid dimethyl ester	P-29	19	-0.531	12.060	0.439
Ethylene glycol acetate monomethyl ether	P-30	127	-0.567	68.180	-
Carbonic acid diethyl ester	P-31	140	-0.567	64.960	1.031
Ethyleneglycol mono(2-ethylbutyl) ether	P-32	6	-0.649	9.500	-
2-Hydroxyacetophenone	P-33	8	-0.603	69.557	5.858

Continued on next page

Table – continued from previous page

name	SI-Symbol	number of points	s_{crit}^*	AAD / %	
				full GC method	individual method
Acetophenone	P-34	15	-0.342	39.677	18.951
p-Methylacetophenone	P-35	8	-0.382	66.760	-
Cyclopentanone	P-36	18	-0.215	18.195	3.394
Cyclohexanone	P-37	7	-0.247	41.884	5.152
Acetic anhydride	P-38	6	-0.272	27.010	12.500
Monoethanolamine	P-39	18	-0.403	68.793	7.685
Formamide	P-40	8	-0.457	17.826	1.081
Aniline	P-41	24	-0.473	20.792	4.336
Piperidine	P-42	2	-0.430	32.470	-
Cyclohexylamine	P-43	5	-0.453	10.384	4.741
mixed functional groups, each group maximum twice					
2-Phenylphenol	Q-1	5	-0.495	5.734	-
Diethylene glycol	Q-2	87	-0.444	5.424	1.348
Diethylene glycol ethyl ether	Q-3	7	-0.518	15.131	4.786
Triethylene glycol	Q-4	116	-0.518	3.504	1.078
Diethylene glycol monobutyl ether	Q-1	7	-0.554	8.994	0.338
2,2'-Diethanolamine (DEA)	Q-2	13	-0.379	41.851	0.471
(Z)-2-Butenedioic acid dihexyl ester	Q-3	128	-0.738	14.705	-
(Z,Z)-9,12-Octadecadienoic acid methyl ester	Q-4	350	-0.760	21.513	-
Dihexyl maleate	Q-1	131	-0.776	15.204	-
Diethyl maleate	Q-2	129	-0.813	12.553	-
(Z)-2-Butenedioic acid dimonyl ester	Q-3	264	-0.849	12.414	-
Dimethyl terephthalate	Q-4	22	-0.567	16.081	0.810
Phthalic acid dimethyl ester	Q-1	133	-0.567	15.169	2.582

Continued on next page

Table – continued from previous page

name	SI-Symbol	number of points	s_{crit}^*	AAD / %	
				full GC method	individual method
Phthalic acid diethyl ester	Q-2	30	-0.612	14.434	2.921
Phthalic acid dipropyl ester	Q-3	29	-0.655	23.968	1.378
Phthalic acid diisopropyl ester	Q-4	16	-0.640	8.795	-
Phthalic acid dibutyl ester	Q-1	42	-0.696	12.647	4.043
Diisobutyl terephthalate	Q-2	17	-0.682	11.250	-
Terephthalic acid dibutyl ester	Q-3	29	-0.696	8.194	-
Phthalic acid diisobutyl ester	Q-4	16	-0.682	5.831	-
Di-n-hexylphthalate	Q-1	17	-0.775	26.382	4.301
Phthalic acid diheptyl ester	Q-2	20	-0.812	15.654	-
Bis(2-ethylhexyl) phthalate	Q-3	16	-0.835	4.792	0.349
Phthalic acid dioctyl ester	Q-4	23	-0.848	11.689	-
Diallyl ether	Q-1	89	-0.452	65.765	-
1,3-Benzenedimethanamine	Q-2	4	-0.435	56.063	-
1,3-Cyclopentadiene	Q-3	5	-0.355	84.320	0.702
1,3-Cyclohexadiene	Q-4	18	-0.379	77.387	0.238
1,4-Cyclohexadiene	Q-1	18	-0.379	79.306	0.263
mixed functional groups, some groups three times or more					
Tetraethylene glycol	R-1	67	-0.211	8.192	3.159
Pentaethylene glycol	R-2	30	-0.236	11.054	-
Hexaethyleneglycol	R-3	32	-0.261	14.419	-
Heptaethyleneglycol	R-4	26	-0.284	16.598	-
6,10-Dimethyl-3,5,9-undecatrien-2-one	R-5	6	-0.239	20.214	-
segments missing in GC PCP-SAFT					
Diisopropyl ether	S-1	143	-	-	1.347

Continued on next page

Table – continued from previous page

name	SI-Symbol	number of points	s_{crit}^*	AAD / % full GC method	AAD / % individual method
Triethylamine	S-2	20		-	3.375
Hydrazine	S-3	77		-	3.085
1-Nitropropane	S-4	4		-	0.823
Nitromethane	S-5	15		-	2.486
Nitroethane	S-6	165		-	3.900
2-Nitropropane	S-7	14		-	2.267
Nitrobenzene	S-8	40		-	6.832
m-Nitrotoluene	S-9	12		-	0.219
Pyridine	S-10	9		-	1.036
Benzonitrile	S-11	11		-	0.137
Propionitrile	S-12	66		-	1.387
Acrylonitrile	S-13	94		-	2.585
Butanenitrile	S-14	65		-	0.592
1,4-Dicyanobutane	S-15	4		-	0.805
Methacrylonitrile	S-16	135		-	2.010
Acetonitrile	S-17	149		-	6.955
N,N-Diethylethanamine	S-18	6		-	0.470
Triethanolamine	S-19	7		-	0.223
Methyldiethanolamine (MDEA)	S-20	6		-	0.538
Tripropylene glycol	S-21	7		-	1.792
Dinitrogen monoxide	S-22	297		-	5.762
Hexamethyl disiloxane	S-23	146		-	1.578
Octamethyltrisiloxane	S-24	132		-	2.658
Propylene carbonate	S-25	10		-	0.058

Continued on next page

Table – continued from previous page

name	SI-Symbol	number of points	s_{crit}^*	full GC method	AAD / %	individual method	AAD / %
Tetrahydrofuran	S-26	14		-			2.594
Tetrahydrothiophene	S-27	4		-			1.073
1,4-Dioxane	S-28	31		-			2.458
Sulfolane	S-29	5		-			0.207
N,N-Dimethylacetamide	S-30	15		-			4.051
Decamethyltetrasiloxane	S-31	135		-			2.085
Cycloheptane	S-32	16		-			1.121
Cyclooctane	S-33	16		-			1.140
Diethyl sulfide	S-34	4		-			0.670
cis-Decahydronaphthalene	S-35	13		-			7.191
trans-Decahydronaphthalene	S-36	10		-			0.077
Decamethylcyclopentasiloxane	S-37	150		-			1.679
Octamethylcyclohexasiloxane	S-38	149		-			0.678
Dimethyl sulfoxide	S-39	12		-			4.204
N,N-Dimethylformamide (DMF)	S-40	52		-			4.368
Tetramethoxysilane	S-41	6		-			0.293
Carbon disulfide	S-42	22		-			4.696
Ammonia	S-43	728		-			8.165
Tetraethoxysilane	S-44	9		-			5.290
1-Methylnaphthalene	S-45	68		-			1.378
Naphthalene	S-46	82		-			0.522
2-Methylnaphthalene	S-47	63		-			0.491
Furfural	S-48	41		-			2.090
Ozone	S-49	4		-			0.689

D.8 Parameters (A - D) for individual Entropy-Scaling with PCP-SAFT

Correlation parameters A - C for individual entropy scaling for all components, for which no parameters were published yet. D is set to zero for all substances, since its influence is neglectable in the individual approach.

Table D.4:

Name	A	B	C
Alkenes			
Isobutylene	0.07483	1.55986	4.42680
2,3-Dimethyl-1-butene	0.0	-0.64795	0.99169
2,3-Dimethyl-2-butene	0.0	-0.66721	0.94891
2-Heptene	0.0	-0.60426	1.27720
2-Methylbuta-1,3-diene	-0.05766	-0.46053	1.56562
Cyclic Alkanes			
Bicyclohexyl	0.0	-0.21067	2.26358
Ethylcyclohexane	0.07477	-0.58273	1.11457
Propylcyclohexane	0.26614	-0.52649	1.01660
cis-1,2-Dimethylcyclohexane	0.0	-0.61586	1.09147
cis-1,3-Dimethyl-cyclohexane	0.0	-0.49817	1.37660
trans-1,2-Dimethylcyclohexane	0.0	-0.48908	1.44026
trans-1,4-Dimethylcyclohexane	0.0	-0.49929	1.40414
Aromatics			
Diphenylmethane	0.0	-0.36671	1.80936
1,2-Diethylbenzene	0.0	-0.55567	1.27650
m-Terphenyl	0.35096	-0.34288	1.50011
p-Terphenyl	0.36378	-0.54675	1.04831
Biphenyl	0.19102	-0.48255	1.30469
Esters			
Di(2-ethylhexyl)adipate	0.0	-0.50860	2.41211
Ethylbutyrate	0.15395	-0.61105	1.04292
Methylformate	-0.55994	-0.30040	2.39540
Decanedioicacid dibutylester	0.0	-0.47736	1.82906
Formicacid ethylester	-0.04841	-0.48800	1.33416
Formicacid propylester	0.03880	-0.59708	0.98757
Heptylformate	0.0	-0.78237	-0.05382
Formicacid octylester	0.51843	-0.56844	1.06385
Aceticacid 3-methylbutylester	0.32853	-0.82454	0.14052
n-Butyloctadecanoate	0.0	-0.21795	2.37847
Methylpropanoate	-0.31767	-0.20512	2.26115
Propanoicacid butylester	-0.14575	-0.36734	1.80521

Continued on next page

Table – continued from previous page

Name	A	B	C
Formicacidbutylester	0.08838	-0.48238	1.26000
Formicacidpentylester	0.10577	-0.62602	0.99201
Alcohols			
2-Butanol	-0.57052	-0.19717	1.79621
2-Octanol	-0.25125	-0.33457	1.62121
3-Methyl-1-butanol	-0.39999	-0.43079	1.30483
2-Methyl-1-butanol	-0.45581	-0.34331	1.43463
2-Methyl-1-propanol	0.0	-0.46590	0.48784
1,5-Pentanediol	0.0	-0.87989	-0.29278
1,6-Hexanediol	0.0	-0.45765	1.03512
1,10-Decanediol	0.0	-0.32088	1.61150
Ethers			
Diethyleneglycol-dimethyl-ether	-0.15647	-0.70176	1.19390
Tetraethylene-glycol-dimethyl-ether	0.0	-0.32949	2.95300
1,2-Diethoxyethane	0.0	-0.58180	1.24999
Substances Containing Nitrogen			
N,N-Diethylamine	-0.01033	-0.33882	1.83741
Hexylamine	0.0	-0.30369	1.88478
1-Octanamine	0.0	-0.34512	1.93194
Dibutylamine	0.0	-0.43847	1.60757
Isopropylamine	0.0	-0.33714	1.49995
Hydrazine	0.0	-0.42140	-1.14552
1-Nitropropane	0.0	-0.52611	1.15864
Nitroethane	0.0	-0.72350	0.43799
2-Nitropropane	0.0	-0.70527	0.63157
Nitrobenzene	0.0	-0.67647	0.85533
m-Nitrotoluene	0.0	-0.55611	1.18943
Benzonitrile	0.0	-0.64666	0.81844
Propionitrile	-0.72209	-0.85776	0.96149
Acrylonitrile	0.0	-0.96103	0.05925
Butanenitrile	0.0	-0.71644	0.61715
1,4-Dicyanobutane	0.0	-0.43635	1.47591
Methacrylonitrile	0.0	-0.58559	1.16137
mixed or multiple functional groups			
Styrene	0.0	-0.47130	1.45773
Benzylalcohol	0.0	-0.36037	1.26410
2,2'-Diethanolamine(DEA)	0.0	-0.36881	1.20300
3-Methylphenol	0.0	-0.25866	1.65310
1,3-Cyclopentadiene	0.0	-0.73773	0.86798
1,3-Cyclohexadiene	0.0	-0.55739	1.23206

Continued on next page

Table – continued from previous page

Name	A	B	C
Cyclohexene	0.0	-0.56174	1.20478
1,4-Cyclohexadiene	0.0	-0.57565	1.17366
Cyclohexanol	0.0	-0.36784	0.93080
Cyclohexylamine	0.0	-0.92392	-3.21031
Phenol	0.0	-0.24971	1.55312
Dimethoxymethane	0.0	-0.70530	0.77078
2-Methoxyethanol	0.0	-0.02641	4.12898
2-Ethoxyethanol	0.0	-0.30698	1.71812
2-Butoxyethanol	0.0	-0.31303	1.68689
Bis(2-ethylhexyl)phthalate	0.0	-0.28142	1.96326
2-Hydroxyacetophenone	0.0	0.68198	9.51775
SalicylicAcidMethylEster	0.0	-0.20864	2.22601
DimethylTerephthalate	0.0	-0.39441	1.74184
PhthalicAcidDimethylEster	0.64855	-0.50552	0.69637
PhthalicAcidDipropylEster	0.73382	-0.57136	0.52599
Monoethanolamine	0.0	-0.07430	1.93077
Propylbenzoate	0.0	-0.43802	1.60054
Diethyleneglycol	0.0	-0.17036	1.80066
Triethyleneglycol	0.0	-0.21463	2.03870
Tetraethyleneglycol	0.0	-0.62460	0.82295
Benzoicacid	0.0	-0.42349	0.84263
MethacrylicAcidMethylEster	0.0	-0.72089	0.79990
PhthalicAcidDiethylEster	0.60034	-0.43004	0.87411
PhthalicAcidDibutylEster	0.88843	-0.52239	0.44660
Di-n-hexylphthalate	1.22863	-0.95217	-0.88821
BenzoicAcidMethylEster	0.0	-0.49896	1.32812
EthylBenzoate	0.0	-0.44218	1.54692
CarbonicAcidDimethylEster	0.0	-0.68107	0.88489
CarbonicAcidDiethylEster	0.0	-0.57309	1.17265
DiethyleneGlycolMonomethylEther	0.0	-0.28079	1.90593
DiethyleneGlycolEthylEther	0.0	-0.36247	1.68142
EthyleneGlycolMonohexylEther	0.0	-0.30912	2.08880
DiethyleneGlycolMonobutylEther	0.0	-0.25675	1.93055
AceticAnhydride	0.0	-0.54045	1.22262
N,N-Diethylethanolamine	0.0	-0.35543	1.84286
Triethanolamine	0.0	-0.28919	1.63469
Methyldiethanolamine(MDEA)	0.0	-0.24657	1.72045
Tripropyleneglycol	0.0	-1.98013	-4.21886
others			
Ethyne	-0.62228	-0.88697	0.70596

Continued on next page

Table – continued from previous page

Name	A	B	C
Diethylsuccinate	0.0	-0.32907	1.83649
Sulfur#	0.0	0.00011	3.32920
Phosphorus#	0.0	0.89489	11.24345
Tetrahydrothiophene	0.0	-0.56469	1.16793
1,4-Dioxane	-0.16754	-0.46607	1.61009
Sulfolane	0.0	-0.71859	0.68120
N,N-Dimethylacetamide	0.0	-0.78081	0.49268
Diethylsulfide	0.0	-0.47011	1.53832
cis-Decahydronaphthalene	0.0	-0.34063	1.98674
trans-Decahydronaphthalene	0.0	-0.41576	1.94955
N,N-Dimethylformamide(DMF)	-0.69680	-0.25376	2.45183
Tetramethoxysilane	0.0	-0.38773	2.03337
Tetraethoxysilane	0.0	-0.10868	2.63396
1-Methylnaphthalene	0.0	-0.40001	1.62722
Naphthalene	0.0	-0.48828	1.45158
2-Methylnaphthalene	0.0	-0.47613	1.49981
Furfural	0.30286	-0.13491	1.80407
Ozone	0.0	-0.27412	2.21961

: $\lambda^{\text{ref}} = \lambda^{\text{CE}}$; A = 0.0: no data in gas phase;

D.9 PCP-SAFT Parameters

Individual PCP-SAFT parameters (not GC PCP-SAFT) for all components, for which no parameters were published yet.

Table D.5:

Name	Molar Mass g/mol	m	σ \AA	ϵ/k K	κ^{AB} -	ϵ^{AB} K	DM Debye
Alkenes							
Isobutylene	56.1063	2.2514801	3.6636166	223.21650498	0	0	0.50006493
2,3-Dimethyl-1-butene	84.1595	2.77363944	3.83803055	241.08309141	0	0	0
2,3-Dimethyl-2-butene	84.1595	3.03149114	3.69217841	243.58924632	0	0	0
2-Heptene	98.1861	3.06331045	3.90136805	257.01882569	0	0	0.30638538
Isoprene(2-Methylbuta-1,3-dien)	68.117	2.46974796	3.69796414	244.79228133	0	0	0.24999788
Cyclo							
Bicyclohexyl	166.303	3.61372396	4.19405735	321.34290579	0	0	0
Ethylcyclohexane	112.213	3.009034	3.99798409	283.7907283	0	0	0
Propylcyclohexane	126.239	3.38128662	4.00163107	280.93141198	0	0	0
cis-1,2-Dimethylcyclohexane	112.213	2.8691387	4.05104792	290.04064501	0	0	0
cis-1,3-Dimethyl-cyclohexane	112.213	2.93001148	4.06046489	278.28569333	0	0	0
trans-1,2-Dimethylcyclohexane	112.213	2.80217091	4.11195764	288.20666564	0	0	0
trans-1,4-Dimethylcyclohexane	112.213	2.8485207	4.10613168	281.96517035	0	0	0
Aromatics							
Diphenylmethane	168.234	4.23409987	3.83678585	316.18261029	0	0	0.7704603
1,2-Diethylbenzene	134.218	3.75757274	3.82705757	284.55602682	0	0	0.58999571
m-Terphenyl	230.304	5.52509921	3.82240602	332.3654902	0	0	0.199995993
p-Terphenyl	230.304	5.77865185	3.75664023	330.44128948	0	0	0.59958
Biphenyl	154.208	3.95976327	3.77834207	324.36855579	0	0	0
Esters							

Continued on next page

Table – continued from previous page

Name	Molar Mass g/mol	m	σ Å	ϵ/k K	κ^{AB} -	ϵ^{AB} K	DM Debye
Di(2-ethylhexyl)adipate	370.566	3.56405279	5.57530614	421.97001554	0	0	0.90533658
Ethylbutyrate	116.158	3.45927023	3.70591314	256.97838446	0	0	1.8107316
Methylformate	60.052	2.65742833	3.08961748	237.33483908	0	0	1.768761
Decanedioicacid dibutylester	314.46	9.09341665	3.72397083	251.63179216	0	0	2.4792633
Formicacid ethylester	74.0785	2.8658349	3.30613454	241.08580789	0	0	1.9306476
Formicacid propylester	88.1051	3.22145209	3.40507259	243.60394881	0	0	1.9096623
Heptylformate	144.211	0.60817724	7.7028527	776.6007853	0	0	1.8706896
Formicacid octylester	158.238	3.29938703	4.2537604	313.37177763	0	0	1.8736875
Aceticacid 3-methylbutylester	130.185	4.03482216	3.66721468	247.41677742	0	0	1.79874
n-Butyloctadecanoate	340.584	10.58845881	3.72454132	228.30411105	0	0	1.8796833
Methylpropanoate	88.1051	3.43630567	3.31449171	235.23467086	0	0	1.70310699
Propanoicacid butylester	130.185	4.69407187	3.47220558	231.73533363	0	0	1.79998413
Formicacid butylester	102.132	3.54129976	3.48984779	245.90599605	0	0	2.0295783
Formicacid pentylester	116.158	3.9795426	3.53028854	245.90974728	0	0	1.9006686
Alcohols							
2-Butanol	74.1216	4.42069067	3.01505586	205.18076274	0.03	1718.048839	1.6608366
2-Octanol	130.228	5.75454115	3.35447019	220.90183533	0.03	1721.386902	1.648845
3-Methyl-1-butanol	88.1482	4.37793433	3.22224391	213.80019455	0.03	2119.118265	1.8497043
2-Methyl-1-butanol	88.148	4.02143507	3.30692459	215.91462536	0.03	2231.564115	1.8796833
2-Methyl-1-propanol	74.1216	4.27710154	3.06044221	211.92588912	0.03	1810.490952	1.6398513
1,5-Pentanediol	104.148	4.58496158	3.00071149	137.99632955	0.03	5630.302108	2.3713389
1,6-Hexanediol	118.174	4.02505454	3.48543691	248.15550428	0.03	3776.660105	2.5002486
1,10-Decanediol	174.28	6.96136504	3.36923606	256.76352149	0.03	2452.260779	2.1434985
Ethers							
Diethyleneglycol-dimethyl-ether	134.174	4.22816112	3.57222113	258.40783543	0	0	1.96998305
Tetraethyleneglycol-dimethyl-ether	222.279	0.57395438	8.95115925	1043.08768009	0	0	2.4702696

Continued on next page

Table – continued from previous page

Name	Molar Mass g/mol	m	σ Å	ϵ/k K	κ^{AB} -	ϵ^{AB} K	DM Debye
1,2-Diethoxyethane	118.174	4.54815039	3.42012194	221.69115044	0	0	1.648845
Substances Containing Nitrogen							
N,N-Diethylamine	73.1368	1.36880311	4.72622953	295.21357872	0.03	1547.442233	0.9203553
Hexylamine	101.19	3.94342351	3.5462531	247.46742376	0.03	82.510822	1.588887
1-Octanamine	129.243	1.93493766	4.97206083	315.30460049	0.03	2476.987864	1.4210046
Dibutylamine	129.243	4.34732354	3.74368162	246.66446311	0.03	0	0.9803133
Isopropylamine	59.1103	2.43967047	3.56086161	234.27553689	0.03	945.013082	1.4509836
Hydrazine	32.0452	1.20733663	3.43503629	368.76910462	0.03	2073.007202	1.7507736
1-Nitropropane	89.0932	3.02852671	3.43398085	269.95816973	0	0	3.657438
Nitroethane	75.0666	2.95444798	3.21587938	252.86240319	0	0	3.657438
2-Nitropropane	89.0932	2.93864229	3.47387916	262.93119463	0	0	3.717396
Nitrobenzene	123.109	3.19056277	3.59606986	318.02757086	0	0	4.227039
m-Nitrotoluene	137.136	3.17444905	3.78491342	337.14991874	0	0	4.227039
Benzonitrile	103.121	3.1939634	3.57760237	302.7820018	0	0	4.167081
Propionitrile	55.0785	2.81089271	3.24759465	226.58975362	0	0	4.017186
Acrylonitrile	53.0626	2.30326522	3.38761506	229.02795427	0	0	3.867291
Butanenitrile	69.1051	2.95655209	3.43498587	249.08315527	0	0	4.06994904
1,4-Dicyanobutane	108.141	3.3299288	3.69309216	388.97468328	0	0	3.747375
Methacrylonitrile	67.0892	2.15598833	3.76307068	275.20795813	0	0	3.687417
mixed or multiple functional groups							
Styrene	104.149	3.131905	3.69608667	293.27444694	0	0	0.12980907
Benzylalcohol	108.138	3.51285899	3.49547545	303.81055124	0.03	1834.407547	1.708803
2,2'-Diethanolamine(DEA)	105.136	3.9598349	3.26101631	276.63374264	0.03	3680.50848	0.8514036
3-Methylphenol	108.138	3.17702169	3.62964521	315.13990196	0.03	1858.132747	1.588887
1,3-Cyclopentadiene	66.1011	1.8547324	3.8645386	301.98919274	0	0	0.419706
1,3-Cyclohexadiene	80.1277	2.42045264	3.7445737	288.83934228	0	0	0.4406913

Continued on next page

Table – continued from previous page

Name	Molar Mass g/mol	m	σ Å	ϵ/k K	κ^{AB} -	ϵ^{AB} K	DM Debye
Cyclohexene	82.1436	2.53906421	3.75108247	281.42712214	0	0	0.329769
1,4-Cyclohexadiene	80.1277	2.65134014	3.60816561	281.75205483	0	0	0.13010886
Cyclohexanol	100.159	4.49560245	3.18261124	242.25182955	0.03	1728.040538	1.858698
Cyclohexylamine	99.1741	0.85206251	5.71782654	217.58102338	0.03	3253.518793	1.30998937
Phenol	94.1112	3.6777636	3.23412092	294.06152162	0.03	1318.262979	1.4509836
Dimethoxymethane	76.0944	3.24596977	3.23390382	218.23374636	0	0	0.7404813
2-Methoxyethanol	76.0944	0.4952167	6.53702801	516.17573831	0.03	515.015956	2.128509
2-Ethoxyethanol	90.121	2.32096647	3.90742255	299.17683923	0.03	1841.624211	2.0805426
2-Butoxyethanol	118.174	3.07135251	3.93570877	285.50637769	0.03	1876.646646	2.0805426
Bis(2-ethylhexyl)phthalate	390.556	11.90875431	3.59775216	236.11529738	0	0	2.8390113
2-Hydroxyacetophenone	136.148	0.92643131	5.84976709	255.58730946	0.03	3740.091592	3.277732
SalicylicAcidMethylEster	152.147	3.09911529	3.93694269	331.37472745	0.03	1512.082156	2.4699788
DimethylTerephthalate	194.184	4.75630429	3.65524239	310.93632276	0	0	2.2993893
PhthalicAcidDimethylEster	194.184	5.04147081	3.58874891	302.17337401	0	0	2.7790533
PhthalicAcidDipropylEster	250.29	7.17228722	3.57711055	264.7644404	0	0	2.8390113
Monoethanolamine	61.0831	3.34229525	2.95467693	289.20390047	0.03	2117.367832	0.7764561
Propylbenzoate	164.201	4.01945666	3.83697794	303.78618704	0	0	1.828719
Diethyleneglycol	106.12	4.788631	3.06825596	286.60113351	0.03	1993.243659	2.5212339
Triethyleneglycol	150.173	4.62798909	3.48916318	308.73186594	0.03	2127.906068	2.9889063
Tetraethyleneglycol	194.226	5.41866735	3.46250924	187.38768182	0.03	5696.270095	3.237732
Benzoicacid	122.121	3.37273168	3.55568744	287.48230113	0.03	3363.255554	1.0012986
MethacrylicAcidMethylEster	100.116	3.68291747	3.35231994	238.58829744	0	0	1.6698303
PhthalicAcidDiethylEster	222.237	6.67017833	3.47750418	266.28869668	0	0	2.7310869
PhthalicAcidDibutylEster	278.343	7.53141171	3.68549871	269.00881584	0	0	2.8210239
Di-n-hexylphthalate	334.45	9.58331851	3.66527404	254.77418556	0	0	2.8989693
BenzoicAcidMethylEster	136.148	3.83508455	3.57592247	294.8660173	0	0	2.5302276

Continued on next page

Table – continued from previous page

Name	Molar Mass g/mol	m	σ Å	ϵ/k K	κ^{AB} -	ϵ^{AB} K	DM Debye
EthylBenzoate	150.175	3.97230232	3.69661406	296.49764136	0	0	1.9995993
CarbonicAcidDimethylEster	90.0779	3.19032943	3.26480345	257.35885798	0	0	0.89937
CarbonicAcidDiethylEster	118.131	4.17867589	3.36894758	237.97766745	0	0	1.1002293
DiethyleneGlycolMonomethylEther	120.147	2.58790973	4.04619048	309.58597837	0.03	2322.249958	2.7490743
DiethyleneGlycolEthylEther	134.174	3.54992886	3.80475544	289.37938958	0.03	1844.421706	2.7790533
EthyleneGlycolMonohexylEther	146.227	2.81201639	4.4097601	329.31286074	0.03	1821.781926	2.2604166
DiethyleneGlycolMonobutylEther	162.227	4.98877552	3.64722193	263.44573266	0.03	1706.006709	2.3503536
AceticAnhydride	102.089	3.83220077	3.22150598	257.78962735	0	0	2.788047
N,N-Diethylethanamine	117.189	2.5552308	4.20861965	332.34140138	0.03	1136.09683	2.4312969
Triethanolamine	149.188	4.64139259	3.45882853	286.31112929	0.03	4162.659234	1.079244
Methyldiethanolamine(MDEA)	119.162	3.70434864	3.57214045	306.53730855	0.03	2356.764602	2.85997561
Tripropyleneglycol	192.253	2.3815648	4.54938426	148.67790408	0.03	5597.843775	0.4107123
others							
Ethylene	26.0373	2.20861083	2.87818336	166.59289875	0	0	0
Diethylsuccinate	174.194	5.76145969	3.41354079	246.32890419	0	0	2.158488
Sulfur	32.065	0.63306661	4.09390397	1466.93256859	0	0	0
Phosphorus	30.9738	0.64702792	3.69405265	1126.69713766	0	0	0
Tetrahydrothiophene	88.1713	2.45170595	3.67444801	320.99500352	0	0	1.9006686
1,4-Dioxane	88.1051	2.92000477	3.39150021	278.66950724	0	0	0
Sulfolane	120.17	2.86051137	3.68506182	391.76465804	0	0	4.676724
N,N-Dimethylacetamide	87.1204	3.19866606	3.43920404	288.81233199	0	0	3.80997115
Diethylsulfide	90.1872	2.77904847	3.71596675	372.0531904	0	0	1.5409206
cis-Decalhydronaphthalene	138.25	3.15413326	4.09603387	220.92703412	0	0	0
trans-Decalhydronaphthalene	138.25	3.07457283	4.16609677	318.17249179	0	0	0
N,N-Dimethylformamide(DMF)	73.0938	3.30912449	3.1886783	266.95684695	0	0	3.807333
Tetramethoxysilane	152.221	4.19027756	3.58332069	229.84460391	0	0	1.738782

Continued on next page

Table – continued from previous page

Name	Molar Mass g/mol	m -	σ Å	ϵ/k K	κ^{AB} -	ϵ^{AB} K	DM Debye
Tetraethoxysilane	208.328	5.54511524	3.75470377	219.06905963	0	0	1.6998093
1-Methylnaphthalene	142.197	3.48553908	3.86177511	341.34296748	0	0	0.509643
Naphthalene	128.171	3.00816136	3.90259784	353.60396054	0	0	0
2-Methylnaphthalene	142.197	3.20991022	4.00157139	354.531572	0	0	0.419706
Furfural	96.0841	3.38699475	3.24163083	279.87127678	0	0	3.59748
Ozone	47.9982	1.82614457	2.92208738	159.86641923	0	0	0.539622

The quadropol moment is zero for all listed substances.

D.10 Group Decomposition

Substances, which are represented as single segment:

- Methane: CH_4
- Ethane: $\text{H}_3\text{C}-\text{CH}_3$
- Methanol: CH_3OH
- Ethyne: $\text{HC}\equiv\text{CH}$
- Water: H_2O
- Carbon Dioxide: CO_2

Group compositions for all other considered substances are given in the following table. n^t is the total number of groups. To fit all columns on one page, we use the internal identifier "SI-Symbols" here, which is defined in table D.3, in section *Averaged Absolute Deviations*.

Table D.6:

SI-Symbol	n^t	CH^δ	CH^γ	CH	$\text{C} <$	$\text{H}^\delta\text{C} =$	$\text{HC} =$	$\text{C} <$	$\text{O} = \text{C} <$	$\text{O} = \text{CH}$	OH	HN^γ	$\text{HN} <$	HCOOH	COO	$\text{CH}_2 - (\text{C}^6)$	$\text{CH} > (\text{C}^6)$	$\text{CH}_2 - (\text{C}^5)$	$\text{CH} > (\text{C}^5)$	$\text{CH} - (\text{aromatic})$	$\text{C} - (\text{aromatic}) >$	$\text{CH}_3 - \text{O}$	$\text{O} - \text{CH}_2$	O	
A-3	3	2	1	0	0	0	0	0	0	0	0	0	0	0	0	0	0	0	0	0	0	0	0	0	
A-4	4	2	2	0	0	0	0	0	0	0	0	0	0	0	0	0	0	0	0	0	0	0	0	0	0
A-5	5	2	3	0	0	0	0	0	0	0	0	0	0	0	0	0	0	0	0	0	0	0	0	0	0
A-6	6	2	4	0	0	0	0	0	0	0	0	0	0	0	0	0	0	0	0	0	0	0	0	0	0
A-7	7	2	5	0	0	0	0	0	0	0	0	0	0	0	0	0	0	0	0	0	0	0	0	0	0
A-8	8	2	6	0	0	0	0	0	0	0	0	0	0	0	0	0	0	0	0	0	0	0	0	0	0
A-9	9	2	7	0	0	0	0	0	0	0	0	0	0	0	0	0	0	0	0	0	0	0	0	0	0
A-10	10	2	8	0	0	0	0	0	0	0	0	0	0	0	0	0	0	0	0	0	0	0	0	0	0
A-11	11	2	9	0	0	0	0	0	0	0	0	0	0	0	0	0	0	0	0	0	0	0	0	0	0
A-12	12	2	10	0	0	0	0	0	0	0	0	0	0	0	0	0	0	0	0	0	0	0	0	0	0
A-13	13	2	11	0	0	0	0	0	0	0	0	0	0	0	0	0	0	0	0	0	0	0	0	0	0
A-14	14	2	12	0	0	0	0	0	0	0	0	0	0	0	0	0	0	0	0	0	0	0	0	0	0
A-15	15	2	13	0	0	0	0	0	0	0	0	0	0	0	0	0	0	0	0	0	0	0	0	0	0
A-16	16	2	14	0	0	0	0	0	0	0	0	0	0	0	0	0	0	0	0	0	0	0	0	0	0
A-17	17	2	15	0	0	0	0	0	0	0	0	0	0	0	0	0	0	0	0	0	0	0	0	0	0
A-18	18	2	16	0	0	0	0	0	0	0	0	0	0	0	0	0	0	0	0	0	0	0	0	0	0
A-19	19	2	17	0	0	0	0	0	0	0	0	0	0	0	0	0	0	0	0	0	0	0	0	0	0
A-20	20	2	18	0	0	0	0	0	0	0	0	0	0	0	0	0	0	0	0	0	0	0	0	0	0
A-21	21	2	19	0	0	0	0	0	0	0	0	0	0	0	0	0	0	0	0	0	0	0	0	0	0
A-22	22	2	20	0	0	0	0	0	0	0	0	0	0	0	0	0	0	0	0	0	0	0	0	0	0
A-23	23	2	21	0	0	0	0	0	0	0	0	0	0	0	0	0	0	0	0	0	0	0	0	0	0

Continued on next page

Table – continued from previous page

SI-Symbmol	n^t	^6CH	^7CH	$>\text{C}<$	$\text{H}^7\text{C}=\text{H}$	$=\text{HC}$	$=\text{C}<$	$\text{O}=\text{C}<$	$\text{O}=\text{CH}$	HO	^7HN	$\text{HN}>$	HCOO	COO	$^6\text{CH}_2$	$>\text{C}^{(6)}$	$^6\text{CH}_2$	$^6\text{CH}_2$	$^6\text{CH}_2$	$\text{CH}^{(6)}$	$>\text{C}^{(6)}$	$\text{CH}^{(6)}$	$>\text{C}^{(aromatic)}$	$\text{CH}^{(aromatic)}$	$\text{O}-\text{CH}_3$	$\text{O}-\text{CH}_2$	O												
A-24	24	2	2	0	0	0	0	0	0	0	0	0	0	0	0	0	0	0	0	0	0	0	0	0	0	0	0	0	0										
Branched Alkanes																																							
B-1	4	3	0	1	0	0	0	0	0	0	0	0	0	0	0	0	0	0	0	0	0	0	0	0	0	0	0	0	0										
B-2	5	3	1	1	0	0	0	0	0	0	0	0	0	0	0	0	0	0	0	0	0	0	0	0	0	0	0	0	0	0									
B-3	6	3	2	1	0	0	0	0	0	0	0	0	0	0	0	0	0	0	0	0	0	0	0	0	0	0	0	0	0	0	0								
B-4	6	4	1	0	1	0	0	0	0	0	0	0	0	0	0	0	0	0	0	0	0	0	0	0	0	0	0	0	0	0	0	0							
B-5	6	4	0	2	0	0	0	0	0	0	0	0	0	0	0	0	0	0	0	0	0	0	0	0	0	0	0	0	0	0	0	0	0						
B-6	6	3	2	1	0	0	0	0	0	0	0	0	0	0	0	0	0	0	0	0	0	0	0	0	0	0	0	0	0	0	0	0	0	0					
B-7	7	4	1	2	0	0	0	0	0	0	0	0	0	0	0	0	0	0	0	0	0	0	0	0	0	0	0	0	0	0	0	0	0	0	0				
B-8	7	5	0	1	1	0	0	0	0	0	0	0	0	0	0	0	0	0	0	0	0	0	0	0	0	0	0	0	0	0	0	0	0	0	0	0			
B-9	7	4	2	0	1	0	0	0	0	0	0	0	0	0	0	0	0	0	0	0	0	0	0	0	0	0	0	0	0	0	0	0	0	0	0	0	0		
B-10	7	4	1	2	0	0	0	0	0	0	0	0	0	0	0	0	0	0	0	0	0	0	0	0	0	0	0	0	0	0	0	0	0	0	0	0	0		
B-11	7	3	3	1	0	0	0	0	0	0	0	0	0	0	0	0	0	0	0	0	0	0	0	0	0	0	0	0	0	0	0	0	0	0	0	0	0	0	
B-12	7	4	2	0	1	0	0	0	0	0	0	0	0	0	0	0	0	0	0	0	0	0	0	0	0	0	0	0	0	0	0	0	0	0	0	0	0	0	0
B-13	7	3	3	1	0	0	0	0	0	0	0	0	0	0	0	0	0	0	0	0	0	0	0	0	0	0	0	0	0	0	0	0	0	0	0	0	0	0	0
B-14	7	3	3	1	0	0	0	0	0	0	0	0	0	0	0	0	0	0	0	0	0	0	0	0	0	0	0	0	0	0	0	0	0	0	0	0	0	0	0
B-15	8	5	1	1	1	0	0	0	0	0	0	0	0	0	0	0	0	0	0	0	0	0	0	0	0	0	0	0	0	0	0	0	0	0	0	0	0	0	0
B-16	8	5	0	3	0	0	0	0	0	0	0	0	0	0	0	0	0	0	0	0	0	0	0	0	0	0	0	0	0	0	0	0	0	0	0	0	0	0	0
B-17	8	3	4	1	0	0	0	0	0	0	0	0	0	0	0	0	0	0	0	0	0	0	0	0	0	0	0	0	0	0	0	0	0	0	0	0	0	0	0
B-18	8	3	4	1	0	0	0	0	0	0	0	0	0	0	0	0	0	0	0	0	0	0	0	0	0	0	0	0	0	0	0	0	0	0	0	0	0	0	0
Alkene																																							
C-1	2	0	0	0	0	0	0	0	0	0	0	0	0	0	0	0	0	0	0	0	0	0	0	0	0	0	0	0	0	0	0	0	0	0	0	0	0	0	
C-2	3	1	0	0	0	1	0	0	0	0	0	0	0	0	0	0	0	0	0	0	0	0	0	0	0	0	0	0	0	0	0	0	0	0	0	0	0	0	0

Continued on next page

Table – continued from previous page

SI-Symbmol	n^t	CH_3	CH_2	CH	$>\text{C}$	$\text{H}^{\text{C}}\text{C}=\text{H}$	$\text{HC}=\text{C}$	$\text{C}=\text{C}$	$>\text{C}=\text{O}$	$\text{O}=\text{CH}$	HO	HN	HN	HCOO	COO	CH_2	CH	$>\text{C}$	CH	$>\text{C}$	CH	O	CH_3	CH_2	O		
D-3	7	1	0	0	0	0	0	0	0	0	0	0	0	0	0	5	1	0	0	0	0	0	0	0	0	0	
D-4	8	1	1	0	0	0	0	0	0	0	0	0	0	0	0	5	1	0	0	0	0	0	0	0	0	0	
D-5	8	2	0	0	0	0	0	0	0	0	0	0	0	0	0	4	2	0	0	0	0	0	0	0	0	0	
D-6	8	2	0	0	0	0	0	0	0	0	0	0	0	0	0	4	2	0	0	0	0	0	0	0	0	0	
D-7	8	2	0	0	0	0	0	0	0	0	0	0	0	0	0	4	2	0	0	0	0	0	0	0	0	0	
D-8	8	2	0	0	0	0	0	0	0	0	0	0	0	0	0	4	2	0	0	0	0	0	0	0	0	0	
D-9	9	1	2	0	0	0	0	0	0	0	0	0	0	0	0	5	1	0	0	0	0	0	0	0	0	0	
D-10	6	1	0	0	0	0	0	0	0	0	0	0	0	0	0	0	0	0	0	0	0	0	0	0	0	0	
D-11	8	2	0	0	0	0	0	0	0	0	0	0	0	0	0	4	2	0	0	0	0	0	0	0	0	0	
Aldehydes																											
E-1	4	1	2	0	0	0	0	0	0	1	0	0	0	0	0	0	0	0	0	0	0	0	0	0	0	0	
E-2	4	2	0	1	0	0	0	0	0	1	0	0	0	0	0	0	0	0	0	0	0	0	0	0	0	0	
E-3	5	1	3	0	0	0	0	0	0	1	0	0	0	0	0	0	0	0	0	0	0	0	0	0	0	0	
E-4	5	2	1	1	0	0	0	0	0	1	0	0	0	0	0	0	0	0	0	0	0	0	0	0	0	0	
E-5	7	1	5	0	0	0	0	0	0	1	0	0	0	0	0	0	0	0	0	0	0	0	0	0	0	0	
E-6	10	1	8	0	0	0	0	0	0	1	0	0	0	0	0	0	0	0	0	0	0	0	0	0	0	0	
E-7	12	1	10	0	0	0	0	0	0	1	0	0	0	0	0	0	0	0	0	0	0	0	0	0	0	0	
Aromatics																											
F-1	6	0	0	0	0	0	0	0	0	0	0	0	0	0	0	0	0	0	0	0	0	0	0	0	0	0	
F-2	7	1	0	0	0	0	0	0	0	0	0	0	0	0	0	0	0	0	0	0	0	0	0	0	0	0	
F-3	8	1	1	0	0	0	0	0	0	0	0	0	0	0	0	0	0	0	0	0	0	0	0	0	0	0	
F-4	8	2	0	0	0	0	0	0	0	0	0	0	0	0	0	0	0	0	0	0	0	0	0	0	0	0	
F-5	8	2	0	0	0	0	0	0	0	0	0	0	0	0	0	0	0	0	0	0	0	0	0	0	0	0	

Continued on next page

Table – continued from previous page

SI-Symbmol	n^t	CH_3	CH_2	CH	$>\text{C}$	$\text{H}_2\text{C}=\text{C}=\text{H}$	$\text{HC}=\text{C}=\text{H}$	$>\text{C}=\text{C}=\text{H}$	$>\text{C}=\text{O}$	$\text{O}=\text{C}=\text{O}$	$\text{O}=\text{CH}$	HO	NH_2	HN	HCOOH	COOH	CH_2 - (C_6)	CH - (C_6)	CH_2 - (C_5)	CH - (C_5)	CH - (aromatic)	$>\text{C}$ - (aromatic)	$\text{O}-\text{CH}_3$	$\text{O}-\text{CH}_2$	O
F-6	8	2	0	0	0	0	0	0	0	0	0	0	0	0	0	0	0	0	0	0	2	0	0	0	
F-7	9	1	2	0	0	0	0	0	0	0	0	0	0	0	0	0	0	0	0	0	1	0	0	0	
F-8	9	3	0	0	0	0	0	0	0	0	0	0	0	0	0	0	0	0	0	0	3	0	0	0	
F-9	9	3	0	0	0	0	0	0	0	0	0	0	0	0	0	0	0	0	0	0	3	0	0	0	
F-10	9	3	0	0	0	0	0	0	0	0	0	0	0	0	0	0	0	0	0	0	3	0	0	0	
F-11	9	2	0	1	0	0	0	0	0	0	0	0	0	0	0	0	0	0	0	0	3	1	0	0	
F-12	10	1	3	0	0	0	0	0	0	0	0	0	0	0	0	0	0	0	0	0	5	1	0	0	
F-13	10	2	2	0	0	0	0	0	0	0	0	0	0	0	0	0	0	0	0	0	5	1	0	0	
F-14	10	2	1	1	0	0	0	0	0	0	0	0	0	0	0	0	0	0	0	0	4	2	0	0	
F-15	10	3	0	1	0	0	0	0	0	0	0	0	0	0	0	0	0	0	0	0	5	1	0	0	
F-16	15	6	0	3	0	0	0	0	0	0	0	0	0	0	0	0	0	0	0	0	3	3	0	0	
Ketones																									
G-1	3	2	0	0	0	0	0	1	0	0	0	0	0	0	0	0	0	0	0	0	0	0	0	0	
G-2	4	2	1	0	0	0	0	1	0	0	0	0	0	0	0	0	0	0	0	0	0	0	0	0	
G-3	5	2	2	0	0	0	0	1	0	0	0	0	0	0	0	0	0	0	0	0	0	0	0	0	
G-4	5	2	2	0	0	0	0	1	0	0	0	0	0	0	0	0	0	0	0	0	0	0	0	0	
G-5	6	3	1	1	0	0	0	1	0	0	0	0	0	0	0	0	0	0	0	0	0	0	0	0	
G-6	6	2	3	0	0	0	0	1	0	0	0	0	0	0	0	0	0	0	0	0	0	0	0	0	
G-7	6	2	3	0	0	0	0	1	0	0	0	0	0	0	0	0	0	0	0	0	0	0	0	0	
G-8	7	2	4	0	0	0	0	1	0	0	0	0	0	0	0	0	0	0	0	0	0	0	0	0	
G-9	7	2	4	0	0	0	0	1	0	0	0	0	0	0	0	0	0	0	0	0	0	0	0	0	
G-10	7	2	4	0	0	0	0	1	0	0	0	0	0	0	0	0	0	0	0	0	0	0	0	0	
G-11	8	2	5	0	0	0	0	1	0	0	0	0	0	0	0	0	0	0	0	0	0	0	0	0	

Continued on next page

Table – continued from previous page

SI-Symbol	n^t	^6CH	^7CH	$>\text{C}<$	$\text{H}^7\text{C}=\text{H}$	$-\text{HC}=\text{H}$	$=\text{C}<$	$>\text{C}=\text{O}$	$\text{CH}=\text{O}$	HO	^7HN	$\text{HN}>$	$-\text{HCOO}$	$-\text{COO}$	$^6\text{CH}_2-\text{C}^{(6)}$	$-\text{CH}^{(6)}$	$^6\text{CH}_2-\text{C}^{(6)}$	$-\text{CH}^{(6)}$	$>\text{C}^{(6)}$	$-\text{CH}^{(6)}$	$>\text{C}^{(6)}$	$-\text{CH}^{(6)}$	$>\text{C}^{(6)}$	$-\text{CH}^{(6)}$	$>\text{C}^{(6)}$	$-\text{CH}^{(6)}$	$-\text{O}$	
G-12	9	2	6	0	0	0	0	1	0	0	0	0	0	0	0	0	0	0	0	0	0	0	0	0	0	0	0	
G-13	11	2	8	0	0	0	0	1	0	0	0	0	0	0	0	0	0	0	0	0	0	0	0	0	0	0	0	
G-14	10	2	7	0	0	0	0	1	0	0	0	0	0	0	0	0	0	0	0	0	0	0	0	0	0	0	0	
G-15	11	2	8	0	0	0	0	1	0	0	0	0	0	0	0	0	0	0	0	0	0	0	0	0	0	0	0	
G-16	12	2	9	0	0	0	0	1	0	0	0	0	0	0	0	0	0	0	0	0	0	0	0	0	0	0	0	
G-17	13	2	10	0	0	0	0	1	0	0	0	0	0	0	0	0	0	0	0	0	0	0	0	0	0	0	0	
G-18	13	4	6	2	0	0	0	1	0	0	0	0	0	0	0	0	0	0	0	0	0	0	0	0	0	0	0	
Ester																												
H-1	2	1	0	0	0	0	0	0	0	0	0	0	1	0	0	0	0	0	0	0	0	0	0	0	0	0	0	0
H-2	3	1	1	0	0	0	0	0	0	0	0	0	1	0	0	0	0	0	0	0	0	0	0	0	0	0	0	0
H-3	4	1	2	0	0	0	0	0	0	0	0	0	1	0	0	0	0	0	0	0	0	0	0	0	0	0	0	0
H-4	5	1	3	0	0	0	0	0	0	0	0	0	1	0	0	0	0	0	0	0	0	0	0	0	0	0	0	0
H-5	6	1	4	0	0	0	0	0	0	0	0	0	1	0	0	0	0	0	0	0	0	0	0	0	0	0	0	0
H-6	8	1	6	0	0	0	0	0	0	0	0	0	1	0	0	0	0	0	0	0	0	0	0	0	0	0	0	0
H-7	9	1	7	0	0	0	0	0	0	0	0	0	1	0	0	0	0	0	0	0	0	0	0	0	0	0	0	0
H-8	3	2	0	0	0	0	0	0	0	0	0	0	0	1	0	0	0	0	0	0	0	0	0	0	0	0	0	0
H-9	4	2	1	0	0	0	0	0	0	0	0	0	0	1	0	0	0	0	0	0	0	0	0	0	0	0	0	0
H-10	5	3	0	1	0	0	0	0	0	0	0	0	0	1	0	0	0	0	0	0	0	0	0	0	0	0	0	0
H-11	6	2	3	0	0	0	0	0	0	0	0	0	0	1	0	0	0	0	0	0	0	0	0	0	0	0	0	0
H-12	6	3	1	1	0	0	0	0	0	0	0	0	0	1	0	0	0	0	0	0	0	0	0	0	0	0	0	0
H-13	7	2	4	0	0	0	0	0	0	0	0	0	0	1	0	0	0	0	0	0	0	0	0	0	0	0	0	0
H-14	7	3	2	1	0	0	0	0	0	0	0	0	0	1	0	0	0	0	0	0	0	0	0	0	0	0	0	0
H-15	8	2	5	0	0	0	0	0	0	0	0	0	0	1	0	0	0	0	0	0	0	0	0	0	0	0	0	0

Continued on next page

Table – continued from previous page

SI-Symbmol	n^t	${}^6\text{HC}$	${}^7\text{HC}$	$>C<$	$=\text{CH}$	$=\text{C}<$	$\text{O}=\text{C}<$	$\text{O}=\text{CH}$	HO	${}^7\text{HN}$	$\text{HN}<$	$-\text{OOH}$	$-\text{OO}$	${}^{(6)}\text{CH}_2-$	$>{}^{(6)}\text{CH}$	${}^{(5)}\text{CH}_2-$	$>{}^{(5)}\text{CH}$	$-\text{CH}$ (aromatic)	$>C-$ (aromatic)	${}^6\text{HC}$	$-\text{O}-\text{CH}_3$	$-\text{O}-\text{CH}_2$	$-\text{O}$
H-16	9	2	6	0	0	0	0	0	0	0	0	0	1	0	0	0	0	0	0	0	0	0	0
H-17	10	3	5	0	0	0	0	0	0	0	0	0	1	0	0	0	0	0	0	0	0	0	0
H-18	6	2	3	0	0	0	0	0	0	0	0	0	1	0	0	0	0	0	0	0	0	0	0
H-19	4	2	1	0	0	0	0	0	0	0	0	0	1	0	0	0	0	0	0	0	0	0	0
H-20	7	2	4	0	0	0	0	0	0	0	0	0	1	0	0	0	0	0	0	0	0	0	0
H-21	22	2	19	0	0	0	0	0	0	0	0	0	1	0	0	0	0	0	0	0	0	0	0
H-22	4	2	0	1	0	0	0	0	0	0	0	1	0	0	0	0	0	0	0	0	0	0	0
H-23	6	2	2	1	0	0	0	0	0	0	0	1	0	0	0	0	0	0	0	0	0	0	0
H-24	7	1	5	0	0	0	0	0	0	0	0	1	0	0	0	0	0	0	0	0	0	0	0
H-25	7	2	3	1	0	0	0	0	0	0	0	1	0	0	0	0	0	0	0	0	0	0	0
H-26	20	2	17	0	0	0	0	0	0	0	0	0	1	0	0	0	0	0	0	0	0	0	0
H-27	7	3	2	1	0	0	0	0	0	0	0	0	1	0	0	0	0	0	0	0	0	0	0
H-28	9	2	6	0	0	0	0	0	0	0	0	0	1	0	0	0	0	0	0	0	0	0	0
H-29	9	3	4	1	0	0	0	0	0	0	0	0	1	0	0	0	0	0	0	0	0	0	0
H-30	11	2	8	0	0	0	0	0	0	0	0	0	1	0	0	0	0	0	0	0	0	0	0
H-31	8	2	5	0	0	0	0	0	0	0	0	0	1	0	0	0	0	0	0	0	0	0	0
H-32	8	3	3	1	0	0	0	0	0	0	0	0	1	0	0	0	0	0	0	0	0	0	0
H-33	9	2	6	0	0	0	0	0	0	0	0	0	1	0	0	0	0	0	0	0	0	0	0
H-34	10	2	7	0	0	0	0	0	0	0	0	0	1	0	0	0	0	0	0	0	0	0	0
H-35	11	2	8	0	0	0	0	0	0	0	0	0	1	0	0	0	0	0	0	0	0	0	0
H-36	6	2	3	0	0	0	0	0	0	0	0	0	1	0	0	0	0	0	0	0	0	0	0
H-37	10	2	7	0	0	0	0	0	0	0	0	0	1	0	0	0	0	0	0	0	0	0	0
H-38	10	3	5	1	0	0	0	0	0	0	0	0	1	0	0	0	0	0	0	0	0	0	0

Continued on next page

Table – continued from previous page

SI-Symbol	n^t	CH_3	CH_2	CH	$>\text{C}$	$\text{H}_2\text{C}=\text{C}=\text{H}$	$\text{HC}=\text{C}=\text{H}$	$\text{C}=\text{C}$	$>\text{C}=\text{O}$	$\text{CH}=\text{O}$	HO	NH_2	HN	HCOO	COO	CH_2 - (C_6)	CH - (C_6)	CH_2 - (C_5)	CH - (C_5)	CH - (aromatic)	$>\text{C}$ - (aromatic)	$\text{O}-\text{CH}_3$	$\text{O}-\text{CH}_2$	O	
L-6	6	2	3	0	0	0	0	0	0	0	0	0	0	0	0	0	0	0	0	0	0	0	0	0	
L-7	8	2	5	0	0	0	0	0	0	0	0	0	0	0	0	0	0	0	0	0	0	0	1	0	0
L-8	10	2	7	0	0	0	0	0	0	0	0	0	0	0	0	0	0	0	0	0	0	0	1	0	0
L-9	13	0	0	0	0	0	0	0	0	0	0	0	0	0	0	0	0	0	0	10	2	0	0	1	0
L-10	7	2	4	0	0	0	0	0	0	0	0	0	0	0	0	0	0	0	0	0	0	0	1	0	0
L-11	10	4	3	2	0	0	0	0	0	0	0	0	0	0	0	0	0	0	0	0	0	0	1	0	0
L-12	12	2	9	0	0	0	0	0	0	0	0	0	0	0	0	0	0	0	0	0	0	0	1	0	0
L-13	14	2	11	0	0	0	0	0	0	0	0	0	0	0	0	0	0	0	0	0	0	0	1	0	0
L-14	16	2	13	0	0	0	0	0	0	0	0	0	0	0	0	0	0	0	0	0	0	0	1	0	0
L-15	12	1	1	0	0	1	1	0	0	0	1	0	0	0	0	0	0	0	0	3	3	0	0	1	0
contains Nitrogen																									
M-1	2	1	0	0	0	0	0	0	0	0	0	1	0	0	0	0	0	0	0	0	0	0	0	0	0
M-2	4	2	0	1	0	0	0	0	0	0	0	1	0	0	0	0	0	0	0	0	0	0	0	0	0
M-3	5	2	2	0	0	0	0	0	0	0	0	1	0	0	0	0	0	0	0	0	0	0	0	0	0
M-4	7	1	5	0	0	0	0	0	0	0	0	1	0	0	0	0	0	0	0	0	0	0	0	0	0
M-5	9	1	7	0	0	0	0	0	0	0	0	1	0	0	0	0	0	0	0	0	0	0	0	0	0
M-6	9	2	6	0	0	0	0	0	0	0	0	0	1	0	0	0	0	0	0	0	0	0	0	0	0
M-7	7	4	0	2	0	0	0	0	0	0	0	0	1	0	0	0	0	0	0	0	0	0	0	0	0
multiple functional groups																									
O-1	4	0	2	0	0	0	0	0	0	0	2	0	0	0	0	0	0	0	0	0	0	0	0	0	0
O-2	5	0	3	0	0	0	0	0	0	0	2	0	0	0	0	0	0	0	0	0	0	0	0	0	0
O-3	5	1	1	1	0	0	0	0	0	0	2	0	0	0	0	0	0	0	0	0	0	0	0	0	0
O-4	6	1	2	1	0	0	0	0	0	0	2	0	0	0	0	0	0	0	0	0	0	0	0	0	0

Continued on next page

Table – continued from previous page

SI-Symbol	n^t	CH_3	CH_2	CH	$>\text{C}$	$\text{H}_2\text{C}=\text{C}=\text{H}$	$\text{HC}=\text{C}=\text{H}$	$\text{C}=\text{C}$	$>\text{C}=\text{O}$	$\text{CH}=\text{O}$	HO	NH_2	HN	HCOO	COO	CH_2 - (C_6)	CH - (C_6)	CH_2 - (C_5)	CH - (C_5)	CH - (aromatic)	$>\text{C}$ - (aromatic)	$\text{O}-\text{CH}_3$	$\text{O}-\text{CH}_2$	O	
O-28	10	2	6	0	0	0	0	0	0	0	0	0	0	0	2	0	0	0	0	0	0	0	0	0	
O-29	18	2	14	0	0	0	0	0	0	0	0	0	0	0	2	0	0	0	0	0	0	0	0	0	0
O-30	18	2	14	0	0	0	0	0	0	0	0	0	0	0	2	0	0	0	0	0	0	0	0	0	0
O-31	18	4	10	2	0	0	0	0	0	0	0	0	0	0	2	0	0	0	0	0	0	0	0	0	0
O-32	20	2	16	0	0	0	0	0	0	0	0	0	0	0	2	0	0	0	0	0	0	0	0	0	0
O-33	22	4	14	2	0	0	0	0	0	0	0	0	0	0	2	0	0	0	0	0	0	0	0	0	0
O-34	22	2	18	0	0	0	0	0	0	0	0	0	0	0	2	0	0	0	0	0	0	0	0	0	0
O-35	22	2	18	0	0	0	0	0	0	0	0	0	0	0	2	0	0	0	0	0	0	0	0	0	0
O-36	3	0	1	0	0	0	0	0	0	0	0	0	0	0	0	0	0	0	0	0	0	0	0	0	0
O-37	4	0	2	0	0	0	0	0	0	0	0	0	0	0	0	0	0	0	0	0	0	0	0	0	0
O-38	6	2	2	0	0	0	0	0	0	0	0	0	0	0	0	0	0	0	0	0	0	0	0	0	0
O-39	9	2	5	0	0	0	0	0	0	0	0	0	0	0	0	0	0	0	0	0	0	0	0	0	0
O-40	10	2	6	0	0	0	0	0	0	0	0	0	0	0	0	0	0	0	0	0	0	0	0	0	0
O-41	6	0	3	0	0	0	0	0	0	0	0	0	0	0	0	0	0	0	0	0	0	0	2	1	0
O-42	8	2	3	0	0	0	0	0	0	0	0	0	0	0	0	0	0	0	0	0	0	0	0	3	0
O-43	12	2	7	0	0	0	0	0	0	0	0	0	0	0	0	0	0	0	0	0	0	0	0	3	0
O-44	8	0	4	0	0	0	0	0	0	0	0	0	0	0	0	0	0	0	0	0	0	0	2	2	0
O-45	10	0	5	0	0	0	0	0	0	0	0	0	0	0	0	0	0	0	0	0	0	0	2	3	0
mixed functional groups, each group only once																									
P-1	21	5	9	3	1	1	1	0	0	0	1	0	0	0	0	0	0	0	0	0	0	0	0	0	0
P-2	7	0	0	0	0	0	0	0	0	0	1	0	0	0	0	0	0	0	0	0	0	5	1	0	0
P-3	8	0	1	0	0	0	0	0	0	0	1	0	0	0	0	0	0	0	0	0	0	5	1	0	0
P-4	8	1	0	0	0	0	0	0	0	0	1	0	0	0	0	0	0	0	0	0	4	2	0	0	0

Continued on next page

Table – continued from previous page

SI-Symbmol	n^t	ϵ CH	τ CH	<CH	>C<	H τ C=	=CH-	=C<	O=C<	O=CH-	HO	τ HN-	HN<	-OOH	-OO-	τ CH $_2$ -(C^6)	CH-(C^6)>	τ CH $_2$ -(C^5)	CH-(C^5)>	(aromatic)CH-	>C-(aromatic)	ϵ CH $_3$ -O-	τ CH $_2$ -O-	-O-
P-5	6	0	0	0	0	0	0	0	0	0	1	0	0	0	0	0	0	4	1	0	0	0	0	0
P-6	7	0	0	0	0	0	0	0	0	0	1	0	0	0	0	0	0	0	0	0	0	0	0	0
P-7	4	0	2	0	0	0	0	0	0	0	1	0	0	0	0	0	0	0	0	0	0	1	0	0
P-8	5	1	2	0	0	0	0	0	0	0	1	0	0	0	0	0	0	0	0	0	0	0	1	0
P-9	7	1	4	0	0	0	0	0	0	0	1	0	0	0	0	0	0	0	0	0	0	0	1	0
P-10	6	0	3	0	0	0	0	0	0	0	1	0	0	0	0	0	0	0	0	0	0	1	0	0
P-11	9	0	1	0	0	0	0	0	0	0	1	0	0	0	0	0	0	0	0	0	5	1	0	0
P-12	9	1	6	0	0	0	0	0	0	0	1	0	0	0	0	0	0	0	0	0	0	0	1	0
P-13	5	1	1	0	1	1	0	0	0	1	0	0	0	0	0	0	0	0	0	0	0	0	1	0
P-14	7	0	0	0	0	0	0	0	0	1	0	0	0	0	0	0	0	0	0	0	5	1	0	0
P-15	5	0	0	0	0	0	2	0	0	0	0	0	0	0	0	0	0	3	0	0	0	0	0	0
P-16	6	0	0	0	0	0	2	0	0	0	0	0	0	0	0	4	0	0	0	0	0	0	0	0
P-17	7	1	1	0	0	0	0	1	0	0	0	0	0	0	0	0	0	4	0	0	0	0	0	0
P-18	8	0	0	0	0	1	6	0	0	0	0	0	0	0	0	0	0	0	0	0	5	1	0	0
P-19	13	1	4	0	0	0	0	0	0	0	1	0	0	0	1	0	0	0	0	0	4	2	0	0
P-20	4	1	0	0	0	1	1	0	0	0	0	0	0	0	0	0	0	0	0	0	0	0	0	0
P-21	5	2	0	0	0	0	2	0	0	0	0	0	0	0	1	0	0	0	0	0	0	0	0	0
P-22	5	2	0	0	0	1	0	1	0	0	0	0	0	0	1	0	0	0	0	0	0	0	0	0
P-23	6	1	2	0	0	0	2	0	0	0	0	0	0	0	1	0	0	0	0	0	0	0	0	0
P-24	19	2	14	0	0	0	2	0	0	0	0	0	0	0	1	0	0	0	0	0	0	0	0	0
P-25	8	1	0	0	0	0	0	0	0	0	0	0	0	0	1	0	0	0	0	0	4	2	0	0
P-26	9	1	1	0	0	0	0	0	0	0	0	0	0	0	1	0	0	0	0	0	5	1	0	0
P-27	9	1	1	0	0	0	0	0	0	0	1	0	0	0	1	0	0	0	0	0	4	2	0	0

Continued on next page

Table – continued from previous page

SI-Symbmol	n^t	CH_3	CH_2	CH	$>\text{C}$	$\text{HC}=\text{C}$	$\text{HC}=\text{C}$	$\text{H}_2\text{C}=\text{C}$	$\text{H}_2\text{C}=\text{C}$	HO	HN	HCOO	COO	CH_2 - (C_6)	CH - (C_6)	CH_2 - (C_5)	CH - (C_5)	CH - (aromatic)	$>\text{C}$ - (aromatic)	$\text{O}-\text{CH}_3$	$\text{O}-\text{CH}_2$	O
P-28	10	1	2	0	0	0	0	0	0	0	0	0	1	0	0	0	0	1	0	0	0	0
P-29	3	1	0	0	0	0	0	0	0	0	0	1	0	0	0	0	0	0	0	0	0	0
P-30	5	1	2	0	0	0	0	0	0	0	0	0	1	0	0	0	0	0	0	0	1	0
P-31	5	1	2	0	0	0	0	0	0	0	0	0	1	0	0	0	0	0	0	0	1	0
P-32	9	2	4	1	0	0	0	0	0	1	0	0	0	0	0	0	0	0	0	0	1	0
P-33	9	1	0	0	0	0	0	0	0	1	0	0	0	0	0	0	0	0	0	0	1	0
P-34	8	1	0	0	0	0	0	0	0	0	0	0	0	0	0	0	0	0	0	0	0	0
P-35	9	2	0	0	0	0	0	0	0	0	0	0	0	0	0	0	0	0	0	0	0	0
P-36	5	0	0	0	0	0	0	0	0	0	0	0	0	0	0	0	0	0	0	0	0	0
P-37	6	0	0	0	0	0	0	0	0	0	0	0	0	0	0	4	0	0	0	0	0	0
P-38	4	2	0	0	0	0	0	0	0	0	0	0	1	0	0	0	0	0	0	0	0	0
P-39	4	0	2	0	0	0	0	0	0	1	0	0	0	0	0	0	0	0	0	0	0	0
P-40	2	0	0	0	0	0	0	0	0	1	0	0	0	0	0	0	0	0	0	0	0	0
P-41	7	0	0	0	0	0	0	0	0	0	1	0	0	0	0	0	0	0	0	0	0	0
P-42	6	0	0	0	0	0	0	0	0	0	0	0	0	0	0	0	0	0	0	0	0	0
P-43	7	0	0	0	0	0	0	0	0	0	1	0	0	0	0	0	0	0	0	0	0	0
mixed functional groups, each group maximum twice																						
Q-1	13	0	0	0	0	0	0	0	0	1	0	0	0	0	0	0	0	0	3	0	0	0
Q-2	6	0	3	0	0	0	0	0	0	2	0	0	0	0	0	0	0	0	0	0	1	0
Q-3	7	1	3	0	0	0	0	0	0	1	0	0	0	0	0	0	0	0	0	0	2	0
Q-4	8	0	4	0	0	0	0	0	0	2	0	0	0	0	0	0	0	0	0	0	2	0
Q-1	9	1	5	0	0	0	0	0	0	1	0	0	0	0	0	0	0	0	0	0	2	0
Q-2	7	0	4	0	0	0	0	0	0	2	0	0	0	0	0	0	0	0	0	0	0	0

Continued on next page

Table – continued from previous page

SI-Symbol	n^t	H^3	CH_2^3	CH^3	CH^2	HN^2	HN^3	HO^2	$\text{O}=\text{CH}^2$	$\text{O}=\text{C}^2$	$\text{O}=\text{C}^3$	H^2C^2	H^2C^3	C^2	C^3	CH^2	CH^3	CH_2^2	CH_2^3	CH^2	CH^3	CH_2^2	CH_2^3	CH^2	CH^3	CH_2^2	CH_2^3	CH^2	CH^3
Q-3	16	2	10	0	0	0	0	0	0	0	0	0	0	0	0	0	0	0	0	0	0	0	0	0	0	0	0	0	0
Q-4	19	2	12	0	0	0	0	0	0	0	0	0	0	0	0	0	0	0	0	0	0	0	0	0	0	0	0	0	0
Q-1	18	2	12	0	0	0	0	0	0	0	0	0	0	0	0	0	0	0	0	0	0	0	0	0	0	0	0	0	0
Q-2	20	2	14	0	0	0	0	0	0	0	0	0	0	0	0	0	0	0	0	0	0	0	0	0	0	0	0	0	0
Q-3	22	2	16	0	0	0	0	0	0	0	0	0	0	0	0	0	0	0	0	0	0	0	0	0	0	0	0	0	0
Q-4	10	2	0	0	0	0	0	0	0	0	0	0	0	0	0	0	0	0	0	0	0	0	0	0	0	0	0	0	0
Q-1	10	2	0	0	0	0	0	0	0	0	0	0	0	0	0	0	0	0	0	0	0	0	0	0	0	0	0	0	0
Q-2	12	2	2	0	0	0	0	0	0	0	0	0	0	0	0	0	0	0	0	0	0	0	0	0	0	0	0	0	0
Q-3	14	2	4	0	0	0	0	0	0	0	0	0	0	0	0	0	0	0	0	0	0	0	0	0	0	0	0	0	0
Q-4	14	4	0	2	0	0	0	0	0	0	0	0	0	0	0	0	0	0	0	0	0	0	0	0	0	0	0	0	0
Q-1	16	2	6	0	0	0	0	0	0	0	0	0	0	0	0	0	0	0	0	0	0	0	0	0	0	0	0	0	0
Q-2	16	4	2	2	0	0	0	0	0	0	0	0	0	0	0	0	0	0	0	0	0	0	0	0	0	0	0	0	0
Q-3	16	2	6	0	0	0	0	0	0	0	0	0	0	0	0	0	0	0	0	0	0	0	0	0	0	0	0	0	0
Q-4	16	4	2	2	0	0	0	0	0	0	0	0	0	0	0	0	0	0	0	0	0	0	0	0	0	0	0	0	0
Q-1	20	2	10	0	0	0	0	0	0	0	0	0	0	0	0	0	0	0	0	0	0	0	0	0	0	0	0	0	0
Q-2	22	2	12	0	0	0	0	0	0	0	0	0	0	0	0	0	0	0	0	0	0	0	0	0	0	0	0	0	0
Q-3	24	4	10	2	0	0	0	0	0	0	0	0	0	0	0	0	0	0	0	0	0	0	0	0	0	0	0	0	0
Q-4	24	2	14	0	0	0	0	0	0	0	0	0	0	0	0	0	0	0	0	0	0	0	0	0	0	0	0	0	0
Q-1	6	0	1	0	0	0	0	0	0	0	2	0	0	0	0	0	0	0	0	0	0	0	0	0	0	0	0	0	0
Q-2	10	0	2	0	0	0	0	0	0	0	0	0	0	0	0	0	0	0	0	0	0	0	0	0	0	0	0	0	0
Q-3	5	0	0	0	0	0	0	0	0	0	0	0	0	0	0	0	0	0	0	0	0	0	0	0	0	0	0	0	0
Q-4	6	0	0	0	0	0	0	0	0	0	0	0	0	0	0	0	0	0	0	0	0	0	0	0	0	0	0	0	0
Q-1	6	0	0	0	0	0	0	0	0	0	0	0	0	0	0	0	0	0	0	0	0	0	0	0	0	0	0	0	0

Continued on next page

